AWARD NUMBER: W81XWH-18-1-0078

TITLE: Development and Testing of New Noninvasive Monitoring Tools for Prolonged Field Care Goal-Directed Therapy

PRINCIPAL INVESTIGATOR: Kevin Ward, MD

CONTRACTING ORGANIZATION: University of Michigan, Ann Arbor, MI

REPORT DATE: July 2022

TYPE OF REPORT: Final

PREPARED FOR: U.S. Army Medical Research and Development Command
Fort Detrick, Maryland 21702-5012

REPORT DOCUMENTATION PAGE

Form Approved
OMB No. 0704-0188

1. REPORT DATE	2. REPORT TYPE	3. DATES COVERED
July 2022	Final	01Apr2018-31Mar2022

4. TITLE AND SUBTITLE

Development and Testing of New Noninvasive Monitoring Tools for Prolonged Field Care Goal-Directed Therapy

5a. CONTRACT NUMBER

W81XWH-18-1-0078

5b. GRANT NUMBER

DM160294

5c. PROGRAM ELEMENT NUMBER

6. AUTHOR(S)

Kevin Ward, MD: keward@umich.edu
Mohamad H. Tiba, MD : tibam@med.umich.edu

5d. PROJECT NUMBER

5e. TASK NUMBER

5f. WORK UNIT NUMBER

7. PERFORMING ORGANIZATION NAME(S) AND ADDRESS(ES)

University of Michigan
Michigan Center for Integrative Research in Critical Care
2800 Plymouth Road, NCRC
Building 10, Room A107
Ann Arbor, Michigan 48109-2800

8. PERFORMING ORGANIZATION REPORT NUMBER

9. SPONSORING / MONITORING AGENCY NAME(S) AND ADDRESS(ES)

U.S. Army Medical Research and Development Command
Fort Detrick, Maryland 21702-5012

10. SPONSOR/MONITOR'S ACRONYM(S)

11. SPONSOR/MONITOR'S REPORT NUMBER(S)

12. DISTRIBUTION / AVAILABILITY STATEMENT

Approved for Public Release; Distribution Unlimited

13. SUPPLEMENTARY NOTES

14. ABSTRACT

Management of the polytrauma patient with or without TBI in the prolonged field care (PFC) setting especially when prolonged damage control resuscitation (pDCR) is required represents an extraordinary challenge. While there is a desire to develop new therapeutic agents to improve survival and mitigate tissue injury and organ failure, we have not yet developed tools which assist in helping providers maximize use of supportive treatments such blood transfusion, volume expansion, vasopressor use, etc. in a precision manner for goal directed therapy (GDT). The use of goal GDT has been demonstrated to be life saving for both surgical and medical populations with severe hemodynamic compromise but is difficult to implement with current invasive and noninvasive tools because of their lack of precision or form factor and expense. This proposal will scale testing of two novel noninvasive measures that could allow for real-time use of GDT in the PFC/pDCR setting.

These include: 1) Resonance Raman Spectroscopy (RRS) to measure tissue hemoglobin oxygen saturation (StO2) of the buccal mucosa as a substitute for central or mixed venous hemoglobin oxygen saturation (ScvO2) and potentially lactate, and 2) Dynamic Respiratory Impedance Volume Evaluation (DRIVE) of the limb as a substitute for ultrasound of the inferior/superior vena cava and central venous pressure (CVP). RRS-StO2 uses a special wavelength of light to determine how much oxygen a tissue is receiving. DRIVE uses a small amount of electricity passed through tissue to measure blood volume moving in and out of the tissue during breathing.

Hypothesis: The use of noninvasive RRS-StO2 and DRIVE will provide information of sufficient value in complex surgical patients regarding tissue oxygenation and intravascular volume to allow consideration of their use for GDT in PFC and pDCR.

Specific Aims/Objectives:

1) Test and compare RRS-StO2 with other measures and surrogates of tissue oxygenation including lactate and ScvO2 in polytrauma and complex operative and post-operative surgical patients.

2) Test and compare DRIVE to other measures and surrogates of intravascular volume monitoring including ultrasound of the IVC and SVC, CVP, and stroke volume variation (SVV) (when measured) in polytrauma and complex operative and post-operative surgical patients.

3) Compare time series measurement RRS-StO2 and DRIVE to patient outcomes including mortality and organ failure in order to support future clinical intervention trials.

This is a clinical research study examining two prototype noninvasive devices (RRS-StO2 and DRIVE) to compare their performance to a range of standard invasive and noninvasive monitoring that may not be suitable for PFC and pDCR. Trauma and surgical critical care patients undergoing invasive monitoring (CVP, ScvO2 stroke volume variation (SVV), etc.) and noninvasive or minimally invasive monitoring (IVC ultrasound, TEE, etc.) will have these measures compared to RRS-StO2 and DRIVE over time. Responses to treatment such as transfusion, volume loading, vasoactive medication administration, mechanical ventilation, etc. will be tracked and compared. Additional data such as lactate levels, injury severity scores, surgical interventions, organ failure scores, and finally outcome will be compared to understand how DRIVE and RRS-StO2 perform compared to other traditional measures. An attempt will be made to enroll 200-300 subjects.

15. SUBJECT TERMS

Tissue Oxygenation, Resonance Raman Spectroscopy, Bioimpedance, Intravascular Volume, Hemodynamics, Goal Directed Therapy

16. SECURITY CLASSIFICATION OF:			**17. LIMITATION OF ABSTRACT**	**18. NUMBER OF PAGES**	**19a. NAME OF RESPONSIBLE PERSON**
					USAMRDC
a. REPORT	**b. ABSTRACT**	**c. THIS PAGE**	Unclassified	116	**19b. TELEPHONE NUMBER** *(include area code)*
Unclassified	Unclassified	Unclassified			

Table of Contents

Page

1. INTRODUCTION:

Trauma frequently leads to a state of shock usually through significant hemorrhage. Hemorrhage continues to be the leading cause of death on the battlefield. The ability is lacking to both quickly determine the severity of hypoperfusion and tissue hypoxia after injury as well as during resuscitation as a means to guide therapy and optimally resuscitate victims early in their care and between echelons of care. Cellular dysfunction, organ damage, coagulopathy and death are known to occur proportional to the degree of shock. Early goal directed therapy (GDT) is a resuscitation strategy developed over the last decade based on the physiologic principle of reversing tissue dysoxia and restoring basic oxygen transport metrics to a level that meets the body's oxygen demands in an early and individualized targeted fashion. Management of the polytrauma patient with or without TBI in the prolonged field care (PFC) setting especially when prolonged damage control resuscitation (pDCR) is required represents an extraordinary challenge. While there is a desire to develop new therapeutic agents to improve survival and mitigate tissue injury and organ failure, we have not yet developed tools which assist in helping providers maximize use of supportive treatments such blood transfusion, volume expansion, vasopressor use, etc. in a precision manner for GDT. The use of goal GDT has been demonstrated to be life saving for both surgical and medical populations with severe hemodynamic compromise, but is difficult to implement with current invasive and noninvasive tools because of their lack of precision or form factor and expense. This proposal will scale testing of two novel noninvasive measures that could allow for real-time use of GDT in the PFC/pDCR setting. These include:

1) Resonance Raman Spectroscopy (RRS) to measure tissue hemoglobin oxygen saturation (StO_2) of the buccal mucosa as a substitute for central or mixed venous hemoglobin oxygen saturation ($ScvO_2$) and potentially lactate
2) Dynamic Respiratory Impedance Volume Evaluation (DRIVE) of the limb as a substitute for ultrasound of the inferior/superior vena cava and central venous pressure (CVP).

RRS-StO2 uses a special wavelength of light to determine how much oxygen a tissue is receiving. DRIVE and NICVP use a small amount of electricity passed through tissue to measure blood volume moving in and out of the tissue during breathing.

2. KEYWORDS:

Tissue Oxygenation, Resonance Raman Spectroscopy, Bioimpedance, Intravascular Volume, Hemodynamics, Shock, Resuscitation, Central Venous Pressure, Goal Directed Therapy

3. ACCOMPLISHMENTS:

3.1. What were the major goals of the project?

- **Major Task 1:** Test and compare RRS-StO_2 with other measures and surrogates of tissue oxygenation including lactate and $ScvO_2$ in polytrauma and complex operative and post-operative surgical patients. Months 0-36
- **Major Task 2**: Test and compare DRIVE to other measures and surrogates of intravascular volume monitoring including ultrasound of the IVC and SVC, transthoracic echo, CVP, and SVV in polytrauma and complex operative and post-operative surgical patients. Months 0-36
- **Major Task 3:** Compare time series measurement RRS-StO_2 and DRIVE to patient outcomes including mortality and organ failure in order to support future clinical intervention trials. Months 6-36

This table is adapted from the approved statement of work

Specific Aim 1(specified in proposal)	Timeline	Progress
Major Task 1: Test and compare RRS-StO2 with other measures and surrogates of tissue oxygen including lactate and ScvO2 in polytrauma and complex operative and post-operative surgical patients.		
Subtask 1: Local/Institutional IRB approval	0	Completed
Subtask 2: HRPO/ACURO Approval	2-3	Completed
Subtask 3: Obtain equipment, hire and train study personnel	2	Completed

Subtask 4: Begin enrollment of 200-300 polytrauma and complex operative-postoperative surgical patients. Blindly compare RRS-StO2 to lactate and ScvO2/SmvO2 values. Quarterly enrollment targets 20-25 subjects	3-36	Completed
Milestone Achieved: Local IRB/Approval	0	Completed
Milestone Targeted: HRPO/ACURO Approval	2-3	Completed
Milestone Targeted: quarterly enrolment targets met	3-36	Completed
Milestone Targeted: One or more peer reviewed publications/year	12-36	Tiba MH, et al. Resonance Raman Spectroscopy Derived Tissue Hemoglobin Oxygen Saturation in Critically Ill and Injured Patients. Shock. 2021 Jul 1;56(1):92-97. PMID: 33208679.
Milestone Targeted: Work with industry (Pendar Technologies and New Vital Signs on technology transition plan	12-36	In progress
Major Task 2: Test and compare DRIVE to other measures and surrogates of intravascular volume monitoring including ultrasound of the IVC and SVC, CVP, and stroke volume variation (SVV) in polytrauma and complex operative and post-operative surgical patients.		
Subtask 1: Local/Institutional IRB approval	0	Completed
Subtask 2: HRPO/ACURO Approval	2-3	Completed
Subtask 3: Obtain equipment, hire and train study personnel	2	Completed
Subtask 4: Begin enrollment of 200-300 polytrauma and complex operative-postoperative surgical patients. Blindly compare DRIVE values to other measures of volume endpoints including IVC and SVC collapsibility index, CVP, SVV etc. Quarterly enrollment targets 20-25 subjects	3-36	Due to unforeseen circumstances and COVID pandemic, we needed to pivot from DRIVE measurement to noninvasive measurements of central venous pressure (NICVP)
Milestone Achieved: Local IRB/Approval	0	Completed
Milestone Targeted: HRPO/ACURO Approval	2-3	Completed
Milestone Targeted: quarterly enrolment targets met	3-36	Completed
Milestone Targeted: One or more peer reviewed publications/year	12-36	In progress. Manuscript is in preparation
Milestone Targeted: Work with industry (Pendar Technologies and New Vital Signs on technology transition plan	12-36	In progress. Working with Triple Ring Technologies to refine NICVP device and measurements
Major Task 3: Compare time series measurement RRS-StO2 and DRIVE to patient outcomes including mortality and organ failure in order to support future clinical intervention trials.		
Subtask 1: Local/Institutional IRB approval	0	Completed
Subtask 2: HRPO/ACURO Approval	2-3	Completed
Subtask 3: Comparison and analysis of time series RRS-StO2 and DRIVE measures to concurrent outcomes including mortality, organ failure, treatments, etc.	6-36	On going
Milestone Achieved: Local IRB/Approval	0	Completed
Milestone Targeted: HRPO/ACURO Approval	2-3	Completed
Milestone Targeted: quarterly enrolment targets met	3-36	---
Milestone Targeted: One or more peer reviewed publications/year	12-36	In progress
Milestone Targeted: Work with industry (Pendar Technologies and New Vital Signs on technology transition plan	12-36	In progress

3.2. What was accomplished under these goals?

Major Task 1: Test and compare RRS-StO_2 with other measures and surrogates of tissue oxygenation including lactate and $ScvO_2$ in polytrauma and complex operative and post-operative surgical patients. Months 0-36

Specific objectives:

Protocol: A-20596
Title: Development and Testing of New Noninvasive Monitoring Tools for Prolonged Field Care Goal Directed Therapy
Target required for clinical significance: 275
Target approved for clinical significance: 1500

a) IRB approval January 22, 2013
b) HRPO approval November 15, 2017
c) Patient recruitment: 19 additional patients were recruited since last quarterly report

One hundred and seventy-one patients were recruited from multiple intensive care units across the University of Michigan's hospital. The patients had a mean (Standard Deviation) age and weight of 60 (15) years and 97.3 (30) kg respectively. One hundred and seventeen (68%) of the patients were recruited from the cardiovascular ICU, nine (5%) from the Critical Care Medicine Unit, twenty-seven (16%) from Emergency Department and the Emergency Critical Care Center (EC3), and the rest are from the Cath lab, trauma and burn ICU, Cardiac ICU, and the surgical ICU. The RRS probe was covered in a sterile sleeve and placed on the buccal mucosa of the patient. Data were collected for 20 minutes. Both sides of the buccal mucosa were tested independently. Near the end of testing, 3cc of mixed venous blood was collected from the pulmonary artery port of the central line and the reading from the Raman spectrophotometer was recorded for comparison. Blood was tested for $ScvO_2$ and compared to tissue oxygen saturation (StO_2) as measured by RRS.

Significant results:

Preliminary Data analysis: Descriptive statistics are expressed as means and standard deviations. Linear regression was used to quantify the relationships between RRS-StO_2 and $ScvO_2$. Summary statistics using receiver operating characteristic (ROC) and area under the curve (AUC) values were used for pooled data to assess performance of RRS-StO_2 at different thresholds of $ScvO_2$.

There was a significant correlation between StO_2 and $ScvO_2$ ($r=0.614$, $p < 0.0001$) (Figure 1). A paired *t-test* revealed no significant difference between RRS-StO_2 and $ScvO_2$ with a mean(SD) of the difference between RRS-StO_2 and $ScvO_2$ of 0.95 (8.6)% (95%CI: -3.1, 2.2%, p=0.281). ROC analysis yielded a mean area under the curve for RRS-StO_2 of 0.81(95% CI: 0.74, 0.87. $p<0.0001$) at different thresholds of $ScvO_2$ (60%, 65%, and 70%) (Figure 2).

Since StO_2 and $ScvO_2$ are not identical measures, we are experimenting with various means to compare the two since being fundamentally different, utilization of such techniques Clarke Error Grid was constructed to quantify the clinical accuracy of R-StO_2 when compared to the gold standard ($ScvO_2$). The plot places the data into different zones (A, B, C, D, and E) based on their utility. Zones A represent values that are considered accurate (difference is less than 7%) in this study. Zone B represent acceptable values that will not lead to change in management. Zone C could be viewed to represent false positive values that might lead to unnecessary corrections (normal $ScvO_2$ and low R-StO_2). Zone D may be viewed to represent false negatives as failure to detect low $ScvO_2$ (low $ScvO_2$ but normal R-StO_2) resulting in failure to address tissue hypoxia. And finally, zone E represent erroneous measurement. The Clarke Error Grid showed significant clinical accuracy of R-StO_2 with 83% of the data residing within the accurate and acceptable grids (A and B), 11% in the false positive grid (C), and 6% in the false negative grid (D) (Figure 3).

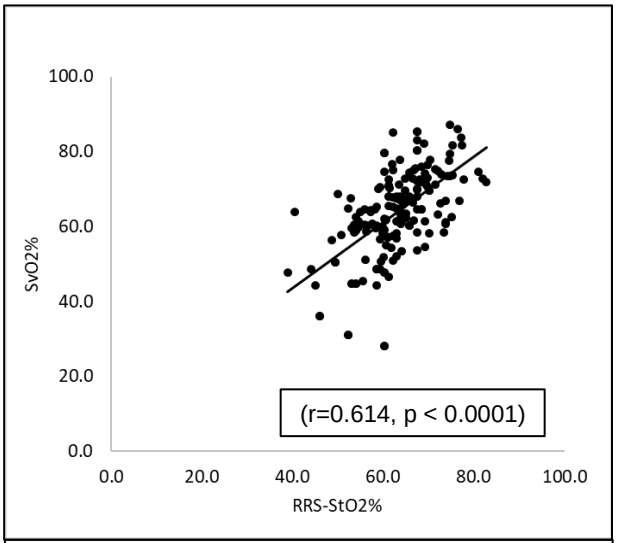

Figure 1: Linear regression model demonstrating the relationship between RRS-StO_2 and $ScvO_2$.

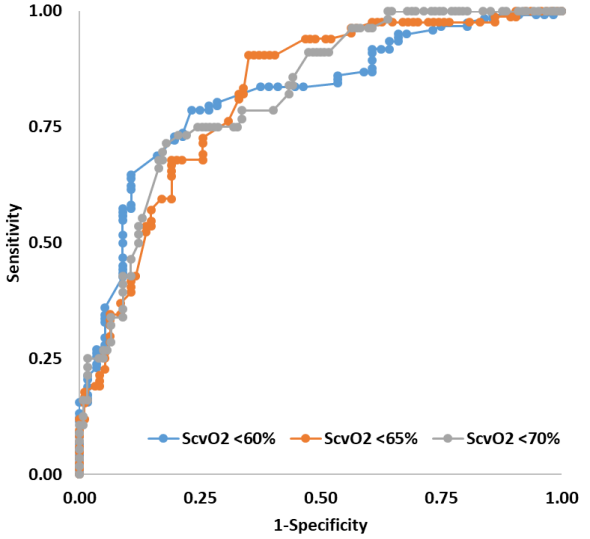

Figure 2: Receiver operator characteristics and area under the curve values for RRS-StO_2 at different thresholds of $ScvO_2$ (60%, 65%, and 70%). RRS-StO_2

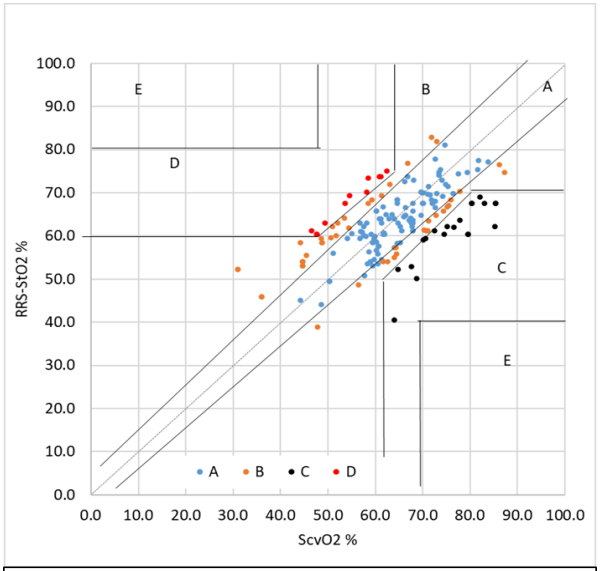

Figure 3: Modified Clarke's Error Grid

Major Task 2: *Test and compare DRIVE and NICVP to other measures and surrogates of intravascular volume monitoring including ultrasound of the IVC and SVC, transthoracic echo, CVP, and SVV in polytrauma and complex operative and post-operative surgical patients. Months 0-36*

Specific objectives:

a. IRB approval January 22, 2013
b. HRPO approval November 15, 2017
c. Patient recruitment: 18 patients were recruited since last quarterly report

Initial Testing of DRIVE

The objective of the Dynamic Respiratory Impedance Volume Estimation (DRIVE) technology is to noninvasively assess intravascular volume status using limb bioimpedance. Bioimpedance represents the cumulative effect of individual bodily tissues on externally induced electrical current. Blood has a unique and distinct effect on the bioimpedance signal. Blood is a relatively good conductor, and the volume of blood in a localized area such as the limb varies with respiration and the cardiac cycle. Patients who were admitted to the University of Michigan trauma ICU, emergency department, or emergency critical care center were consented and enrolled into the study. Subjects underwent an abdominal ultrasound to

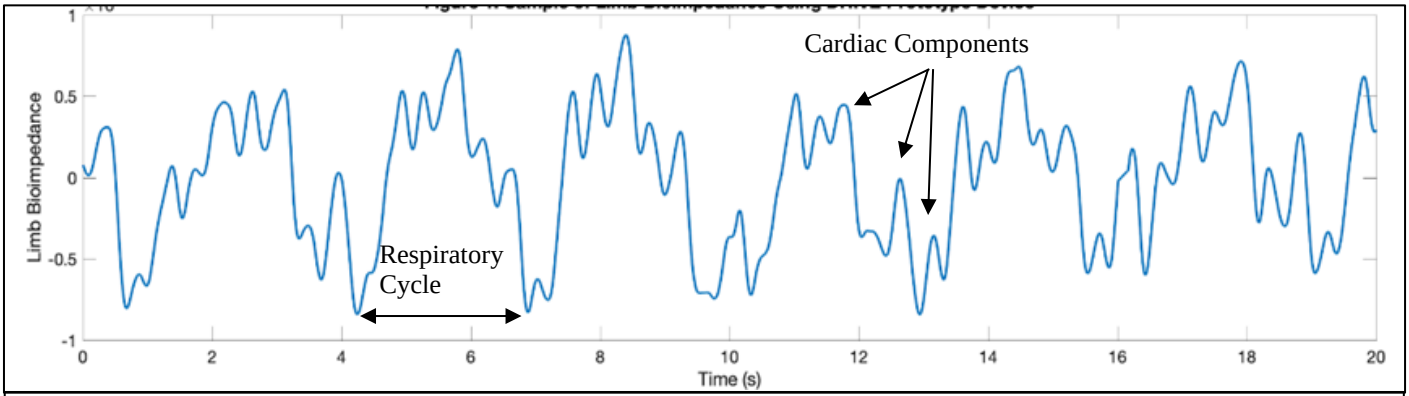

Figure 4: Sample bioimpedance waveform. Note the prevalent respiratory cycle (low frequency) and the higher-frequency cardiac component. This sample signal was obtained from a human subject using the prototype device.

measure changes in IVC diameter during normal tidal breathing as well as during respiratory maneuvers such as deep breathing and sniff. Of these patients, a small subset was selected for bioimpedance monitoring with a new portable prototype device. These subjects were monitored using the prototype for 15-30 minutes, using a bipolar electrode array. The amplitude of the cardiac and respiratory components (Figure 4) of the bioimpedance signal was quantified and compared to changes in IVC diameter as measured by ultrasound. The bioimpedance signal, comprised of distinct cardiac and respiratory components, was quantified by taking the ratio of the amplitude of these components.

Significant results

During testing, we have identified the tetrapolar array to provide the most consistent high-quality signal. This arrangement also allows indexing of the respiratory-induced signal changes to a baseline level of impedance. Bioimpedance "nb_normalized_dz" was calculated as the respiratory variability during a maneuver (sniff in the leftmost panel, or deep breathing on the right) divided by the respiratory variability during a normal spontaneous breath. With the exception of the right-handed outliers, the correlation between our bioimpedance measure and dIVC is moderate- to high (Figure 5). We are currently investigating the cause of these outliers to understand why they deviate so far from the trend.

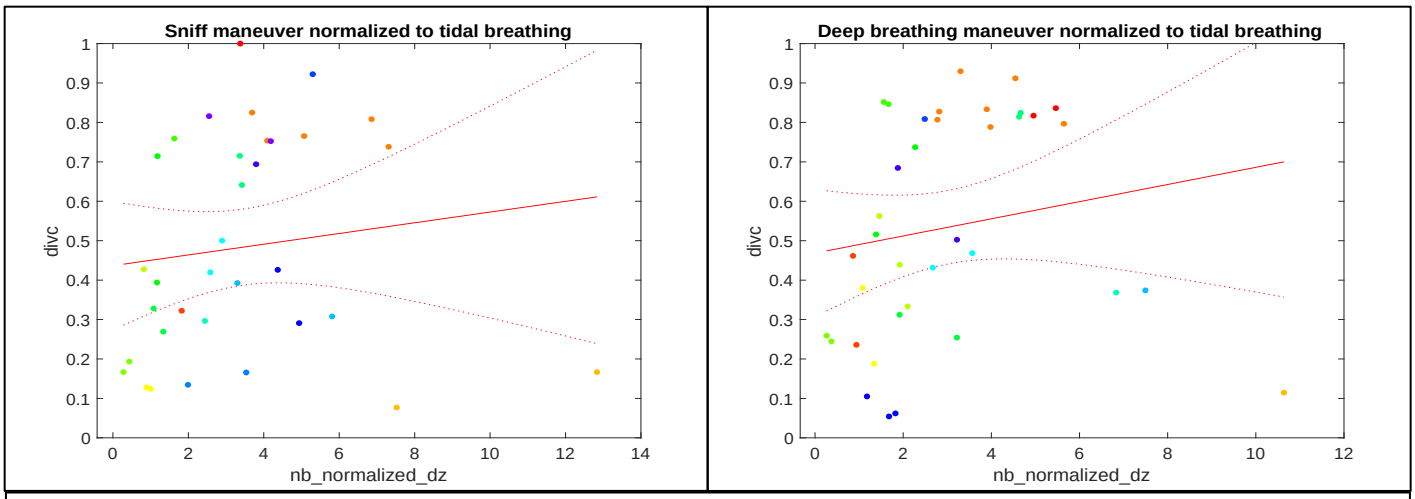

Figure 5: Bioimpedance vs. dIVC during a sniff and deep breathing maneuvers

Additionally, we examined optimal electrode placement sites ranging from whole arm to upper arm to forearm. As delineated above, these metrics are compared to inferior vena cava (IVC) collapsibility index (dIVC) as a gold standard of volume status. The IVC is visualized longitudinally via B-mode ultrasound by a trained emergency medicine physician. IVC collapsibility during such a maneuver is believed to be indicative of volume status and responsiveness. The minimum and maximum diameter of the IVC during the exercise is recorded by the physician, and the collapsibility index (dIVC) is described as the relative change in IVC diameter during these respiratory maneuvers. In addition, we continue to explore how these respiratory maneuvers may be standardized across patients. One technique we have investigated is to index the impedance change noted during the respiratory maneuver to a baseline measurement taken moments prior. Preliminary data supports that using a dIVC of 50% may produce DRIVE values that are more consistent with critical decision making. We have noted significant noise in the impedance signal especially when subjects repeat the maneuvers of deep breathing. Due to this noise, we have been challenged in using the impedance signal to track breathing patterns of subjects prior to the breathing maneuver. We believe this variability plays a significant role in the impedance signal variability of the outliers. In an attempt to reduce noise, add critical redundancy, and preserve the value of the venous component of the impedance signal, we added a photoplethysmographic (PPG) signal to the impedance methodology. Figure 6 demonstrates compressed PPG signals (beat to beat) during various respiratory maneuvers. The PPG signal capture both arterial and venous components of volume whereas changes in impedance are mainly reflective of changes in venous volume. Our plan in future studies is to combine the two signals to increase the fidelity of the venous signal in order to

match changes in dIVC. Simultaneous use of the PPG will assist in developing noise mitigation/cancellation strategies and understanding patient breathing patterns during and in between maneuvers.

Figure 6: PPG pattern during breathing that will compliment changes in impedance signal

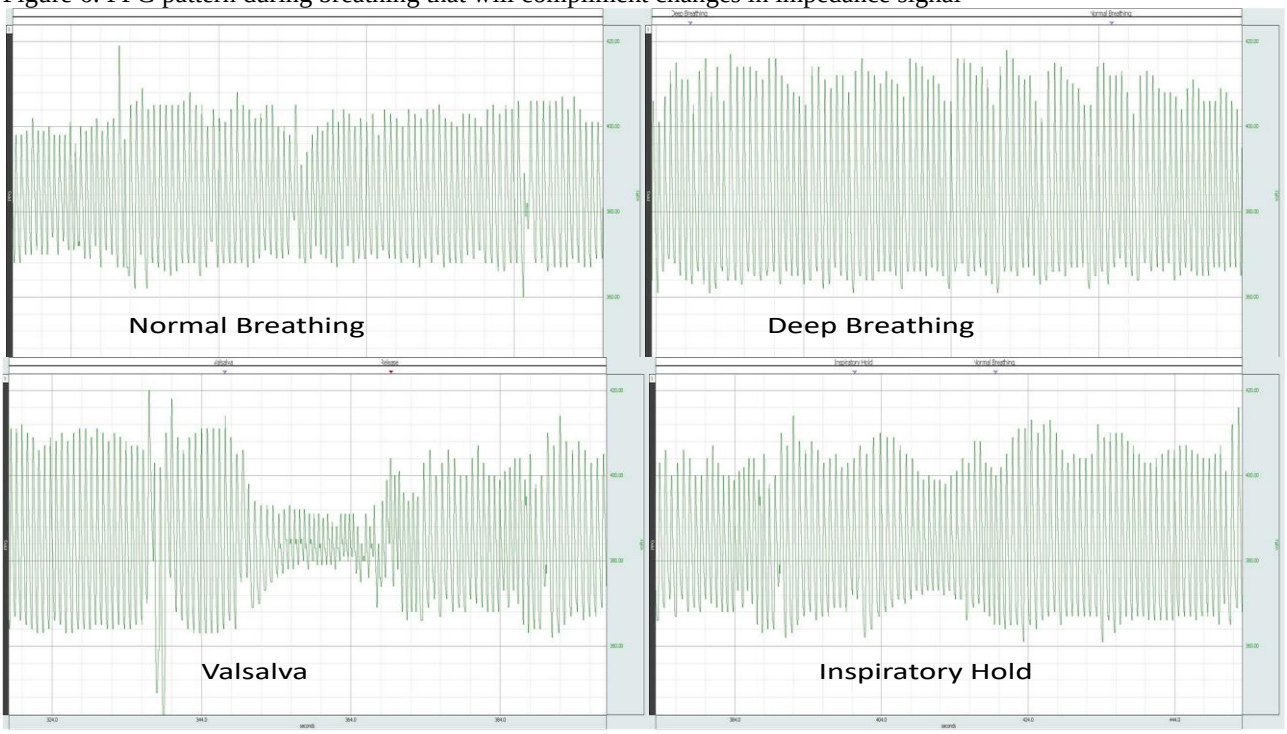

We unfortunately encountered several setbacks during DRIVE testing including noisy signal, unexplained outliers, difficulty recruiting patient and then COVID-19 pandemic. For the remainder of the grant, by agreement of the grant administrators and officers, we have, pivoted to using bioimpedance to measure Central venous pressure

Using bioimpedance to measure NICVP

We have previously developed an impedance based noninvasive method of central venous pressure (NICVP) monitoring. This NICVP method shares many important features with DRIVE. Its combination with DRIVE would allow a unique static and dynamic measure if intravascular volume. Central venous pressure (CVP) is static measure of central circulatory volume. While controversial, it has recently enjoyed a renaissance demonstrating value in assessing critically ill and injured patients and in reducing the incidence of acute renal failure. Figure 7 demonstrates how this technology works along with data from a previously published study by Ward et al. (Shock 33(3): 269-273, 2010. PM19487978) demonstrating the ability of the technology to potentially replace invasively

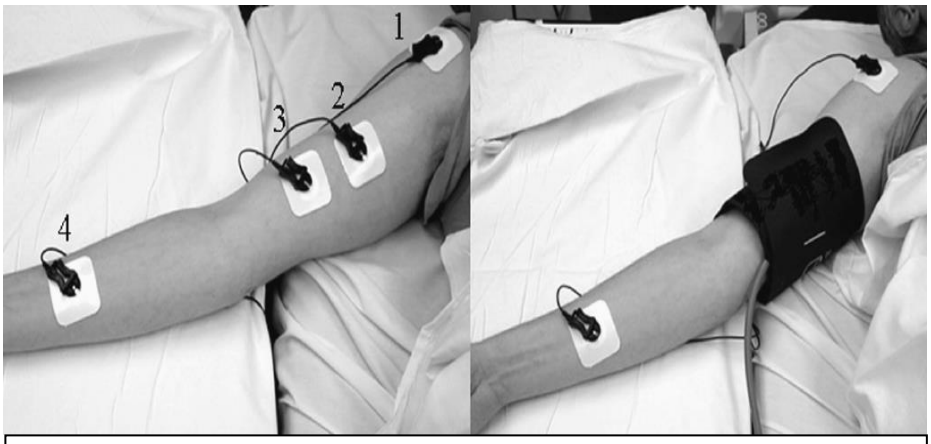

Figure 7: Orientation of electrodes used for tetra-polar impedance plethysmography. Electrodes 1 and 4 inject current toward electrodes 2 and 3, respectively. Ward et al 2010.

1- Ward KR, Tiba MH, Draucker GT, Proffitt EK, Barbee RW, Gunnerson KJ, Reynolds PS, Spiess BD: A novel noninvasive impedance-based technique for central venous pressure measurement Shock 33(3): 269-273, 2010. PM19487978"
2- Irwin Gratz, Vinay Kudur, Francis Spitz, Smith Jean, Isabel Elaine Allen, Julia E. Seaman and Edward Deal. Comparison of Invasive vs. Noninvasive CVP Monitoring in Patients Undergoing Major Intra-Abdominal Surgery: A Prospective Comparative Pilot Study. J Anesth Clin Res 2018, 9:11. DOI:10.4172/2155-6148.1000866

We now have the new prototype (Figure 8). The new prototype will allow the combined measure of both DRIVE and NICVP with no additional need for extra personnel or significant change in workflow or protocol. We anticipate the addition of NICVP will provide significant value to the volume assessment of critically ill and injured patients. As indicated in the last report the underlying theory involves a well-founded and studied method incorporating impedance plethysmography. Specifically, a small amount of current, 400 µA @ 28 kHz sine wave is applied to the patient's arm through standard ECG electrodes. A blood pressure cuff on the patient's arm is inflated to ~40 mm Hg, blocking venous return but below diastolic arterial pressure. After 45-60 sec, the pressure is rapidly deflated for a period of approximately 30 seconds and the impedance is measured by the processing unit while simultaneously measuring the pressure in the cuff. Changes in bioimpedance, resulting from the changes in volume and velocity of blood in the arm are directly related to the pressure within the large veins of the upper arm. Pressures in these veins are essentially the same as pressures in the large central veins in which they empty into. Maximum blood volume changes in the upper arm detected by impedance are matched to the pressure in the blood pressure cuff during deflation.

Figure 8: Prototype device to measure central venous pressure non-invasively using bioimpedance

The pressure in the blood pressure cuff at this time is pressure within the large vein in the upper arm and this pressure is substituted for CVP. The NICVP device measures impedance in ohms over time (Figure 9-1). The initial change in

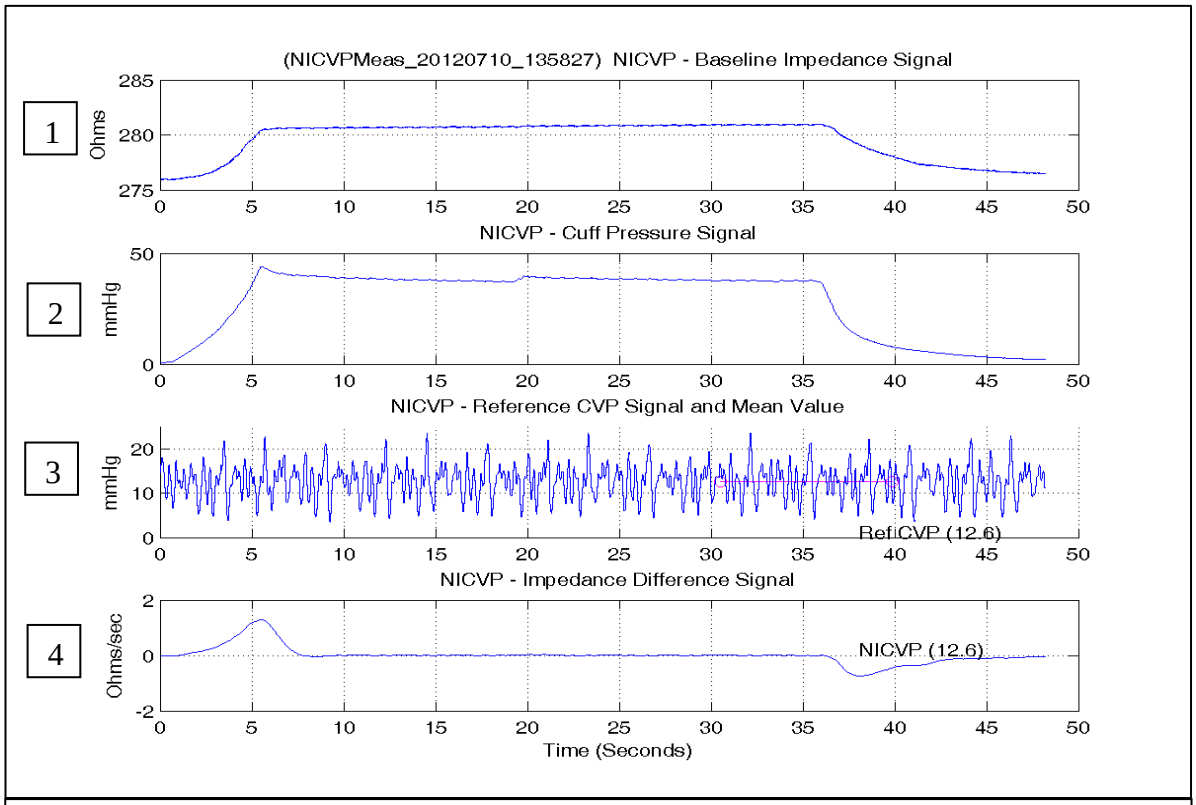

Figure 9: Early prototype device to measure central venous pressure non-invasively using bioimpedance. *Shock 33(3): 269-273, 2010. PM19487978*

impedance seen in Figure 9-1 is due to the arm filling with blood when venous return is impeded by the cuff. The change in impedance over time is calculated by the processing unit and a waveform is generated (Figure 9-4). This waveform of the rate of change in impedance over time is an indirect measurement of blood flow under the blood pressure cuff. The cuff pressure, graphed in (Figure 9-2), that is observed at the minimum point in this delta impedance waveform has been found to correlate to the patient's CVP, as measured with a catheter (9-3). The cuff pressure reading is reported as the NICVP parameter value by the device.

Significant results

Fifty-seven patients have been recruited from different ICUs across the University of Michigan's Hospital. The patients had a mean (Standard Deviation) age and weight of 62 (12.6) years and 88.32 (22.6) kg respectively. Forty-three patients have been recruited from the Cardiovascular Center ICU and nine patients have been recruited from other ICUs (Surgical, critical care ICU, and Burn and Trauma ICU). Patients' NICVP was measured as described above while their CVP was recorded at the same time of NICVP measurement. Each patient's NICVP was measured 3 to 4 times. The measurements were averaged and compared to corresponding CVP. Patients NICVP has been shown to be highly correlated with their CVP ($r = 0.611$, $p < 0.0001$) (Figure 10). A paired t-test yielded no significant difference between CVP and NICVP ($p=0.16$). A Bland-Altman analysis showed a bias (average of the differences between each NICVP and CVP reading) of 0.57 mmHg with a standard deviation of 2.47 mmHg (Figure 11). Such low bias provides a strong indication that the two reading might be exchangeable.

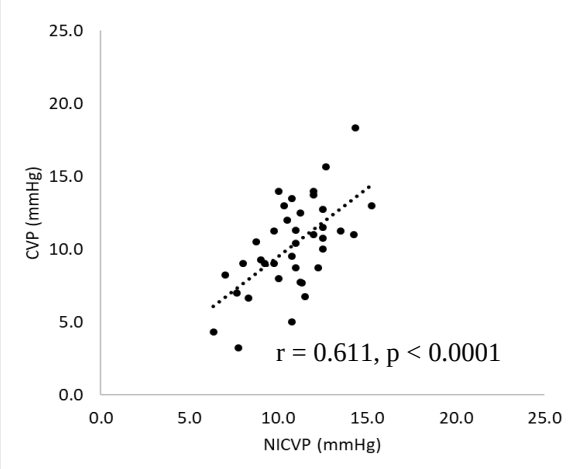

Figure 10: Correlation between NIVCP and CVP

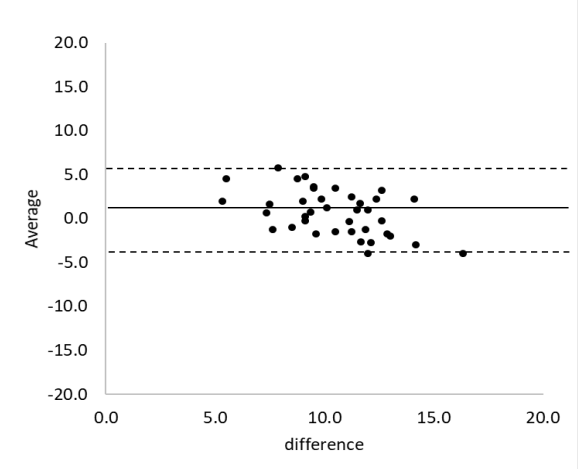

Figure 11: Bland-Altman plot. Average vs. difference

Furthermore, we have constructed a modified Clark's Error Grid to quantify the clinical accuracy of NICVP when compared to the gold standard (CVP). The plot places the data into different zones (A, B, C, D, and E) based on their utility. Zone A represent values that are considered accurate (difference is less than 4 mmHg) in this study. Zone B represent acceptable values that will not lead to change in management. Zone C could be viewed to represent false positive values (normal CVP and high NICVP) leading to unnecessary correction. Zone D may be viewed to represent false negatives as failure to detect high CVP (high CVP but normal NICVP). And finally, zone E represent erroneous measurement. The Clarke's Error Grid showed significant clinical accuracy of NICVP with 100% of the data residing within the accurate and acceptable grids (A and B) (87% in zone A and 13% in zone B). In this dataset there was no false positive grid (C) or false negative grid (D) (Figure 12).

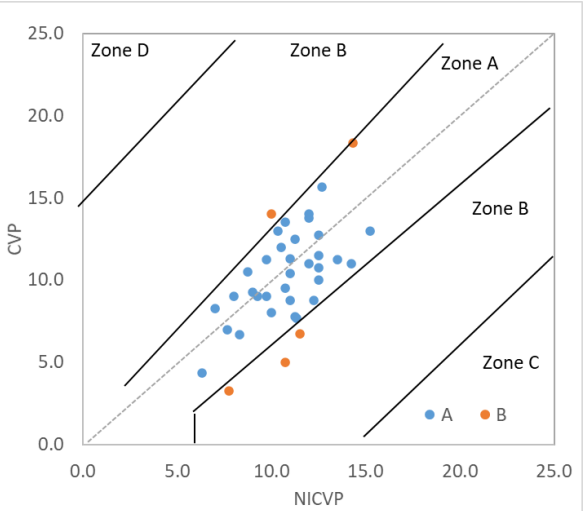

Figure 12: Clarke's Error Grid for NIVCP

To further advance this technology, we are currently working with Triple Ring Technologies to investigate additional signal collection and processing techniques.

Major Task 3: *Compare time series measurement RRS-StO_2 and DRIVE to patient outcomes including mortality and organ failure in order to support future clinical intervention trials.*

Still in progress through data analysis

4. OTHER ACHIEVEMENTS

Development of a reduced size device prototype with a handheld tablet in collaboration with New Vital Signs (NVS). The unit is currently being tested alongside Biopac. This prototype has received positive feedback from patients for comfort and ease of application. This prototype will be used during patients testing in conjunction with Biopac system. We will work with New Vital Signs to discuss licensing and incorporation of the NICVP method into the DRIVE technology.

4.1. What opportunities for training and professional development has the project provided?

Providing opportunities to several undergraduate students to participate in RRS and NICVP portions of this project as a part of university Undergraduate Research Opportunity Program (UROP) The student helped with data collection and presented posters to their peers at the annual UROP Symposium. See below for detailed list

- Isabella Sperry, Carmen I. Colmenero Mahmood, Hakam Tiba. Novel Noninvasive Impedance-based Technique, for Central Venous Pressure Measurement. 2022 UROP Symposium

4.2. How were the results disseminated to communities of interest?

- A peer reviewed publication has resulted from the data collected by this award. See below for detail.
- Several conference abstracts were submitted and accepted for presentation. See below for detailed list.

4.3. What do you plan to do during the next reporting period to accomplish the goals?

The activities and all major tasks of this award have been completed. However, we plan to continue development of both technologies through other future funding opportunities. Using the data collected from this project, we will continue refining signal processing techniques and validating other bioimpedance methodologies to measure CVP. Data and results will continue to be presented at scientific meetings both locally at the University of Michigan and nationally at the MHSRS and Shock Society meetings. Additional peer reviewed manuscripts covering all major results of this award will be prepared and submitted high impact journals. We will continue development of the devices in collaboration with industry partners such as Pendar Medical, New Vital Signs, and Triple ring Technologies, who will further the translation of the technology towards clinical applications and patient care. In addition, we are currently developing a strategy to engage the FDA in a pre-submission meeting. We will continue to utilize new data capture platform to compare Raman and NICVP values to other patient physiologic parameters. Additional developing new IP for NICVP monitoring with potential licensing implications to New Vital Signs

5. IMPACT:

5.1. What was the impact on the development of the principal discipline(s) of the project?

This award enriched our understanding of bioimpedance properties, characteristics, and its relation to body fluid volume. This award allowed us to explore other impedance methodologies to assess fluid volume through the noninvasive measurement of central venous pressure. We are currently working closely with New Vital Signs and Triple Rings Technologies to develop other impedance techniques to measure CVP that considers the unique features of impedance signal. In the same token, this award allowed us to collect precious data related to tissue oxygenation in critically ill patients. We will utile this data for further development of the device, add additional measurement of cytochrome oxidase and possible submission to the FDA for a phase one trials.

5.2. What was the impact on other disciplines?

Nothing to report at this time, but we feel that in the future that the biomedical engineering and data science disciplines will also be impacted

5.3. What was the impact on technology transfer?

The RRS technology has been licensed to Pendar Technologies. RRS data and the performance of the device is being shared with Pendar to allow for continuous improvement and to develop regulatory approval and commercialization strategies. We anticipate starting working with Pendar Medical towards scheduling pre-submission meetings with the FDA to develop a rapid regulatory approval pathway that will place the technology on a path towards commercialization. The NICVP technology will be licensed to New Vital Signs and is undergoing new prototyping by Triple Ring Technologies. NICVP data and performance of the prototype device is being utilized to support continuous improvement of the technology and approaches to develop regulatory approval and commercialization strategies.

5.4. What was the impact on society beyond science and technology?

While there has been no direct societal impact of the project to date, the *long-term* impact of this research is expected to result in the development and deployment of technologies that noninvasively measure tissue oxygenation and volume status at earlier points of care that may:

- Allow for rapid point of care diagnostic indicators of compensated shock states allowing for significantly earlier intervention in more far forward echelons of care.
- Allow for improved therapeutic allocations by helping to drive therapy to objective measurable endpoints thus optimizing use of important resources such as resuscitation fluids including blood.
- Allow for a greater uninterrupted continuum of care as casualties move from lower to higher levels of care including en-route care.
- Allow for improved outcomes by preventing the early under or over-resuscitation of casualties.
- Reducing iatrogenic and nosocomial complications associated with invasive monitoring.
- Allow for improved resource allocation by providing indications for invasive monitoring.
- Allow earlier termination of the use of invasive monitoring (when they are indicated) by transitioning invasive monitoring for noninvasive monitoring.
- Allow for additional diagnostic and therapeutic end-points for casualties in intermediate care settings.
- Allow for the eventual development of simpler closed-loop and decision assist algorithms and devices for early and late echelon of care settings including en-route care.

6. CHANGES/PROBLEMS:

6.1. Changes in approach and reasons for change

We expanded our impedance-based knowledge and technology to allow incorporation of a very similar technology we have previously developed to allow noninvasive measurement of central venous pressure (NICVP) to complement the dynamic impedance signals measured by DRIVE. This will provide both an important static measure of volume status monitoring which is now enjoying a renaissance.

6.2. Actual or anticipated problems or delays and actions or plans to resolve them

The University of Michigan clinical research office has approved our request to reactivate the study as tier 2 while applying some restrictions that aim to mitigate the spread of COVID-19 disease. Necessary amendments with IRB have been reviewed and approved by the IRB. To help mitigating the spread of COVID-19 among susceptible population, research staff were not allowed to approach the following populations for recruitment purposes:

- Patients 65 years or older (restriction left on September 30th, 2020).
- Immunocompromised patients.

These restrictions resulted in a decreased pool of eligible subjects, hence a decrease in recruited subjects for the study.

6.3. Changes that had a significant impact on expenditures
The COVID-19 pandemic has moderately effected expenditures. We have requested and has been granted a no-cost extension for one year.

6.4. Significant changes in use or care of human subjects, vertebrate animals, biohazards, and/or select agents: None to report

6.5. Significant changes in use or care of human subjects: None to report

6.6. Significant changes in use or care of vertebrate animals: None to report

6.7. Significant changes in use of biohazards and/or select agents: None to report

7. PRODUCTS:

7.1. Publications, conference papers, and presentations

7.1.1. Journal publications.

- Tiba MH, Awad AB, Pennington A, Fung CM, Napolitano LM, Park PK, Machado-Aranda DA, Gunnerson KJ, Romfh P, Ward KR. Resonance Raman Spectroscopy Derived Tissue Hemoglobin Oxygen Saturation in Critically Ill and Injured Patients. Shock. 2021 Jul 1;56(1):92-97. doi: 10.1097/SHK.0000000000001696. PMID: 33208679.

7.1.2. Books or other non-periodical, one-time publications. Nothing to report

7.1.3. Other publications, conference papers, and presentations.

- Abstract # MHSRS-19-01948: Amanda J. Pennington, Mohamad Hakam Tiba, Brandon C. Cummings, Varisha Essani, Claire Roberge, Kyle Gunnerson, Kevin R. Ward. Novel monitoring of tissue microvasculature oxygenation using resonance Raman spectroscopy. Military Health System Research Symposium (MHSRS), August 2019, Kissimmee, Florida. Accpepted for poster presentation
- Abstract # MHSRS-20-01069**:** Abdelrahman Awad, MD; Varisha Essani; Claire Roberge; Kyle Gunnerson, MD; Mohamad Hakam Tiba, MD, MS; Kevin Ward, MD, Monitoring of Tissue Microvasculature Oxygenation Using Resonance Raman Spectroscopy. **2020** Military Health System Research Symposium (MHSRS. Due to COVID-19, the conference has been cancelled, however the abstract will still be published**.**
- Abstract # MHSRS-21-02936: Mohamad H. Tiba, MD, MS, Abdelrahman B. Awad, MD, Christopher M. Fung, MD, Lena M. Napolitano, MD, Pauline K. Park, MD, David A. Machado-Aranda, MD, Kyle J. Gunnerson, MD, Padraic Romfh, BS, MBA, Kevin R. Ward, MD. Resonance Raman Spectroscopy-Derived Tissue Hemoglobin Oxygen Saturation for the Management of the Critically Ill and Injured Patients. 2021 Military Health System Research Symposium (MHSRS). Due to COVID-19, the conference has been cancelled, however the abstract will still be published
- Abstract # MHSRS-22-05939: Mohamad Hakam Tiba, Carmen I. Colmenero Mahmood, Kevin R. Ward. Impedance-based noninvasive technique for central venous pressure measurement. 2022 Military Health System Research Symposium (MHSRS). Accepted for poster presentation.
- Student Claire Roberge, Varisha Essani, Amanda Pennington, Brandon Cummings, Kevin Ward, Mohamad H Tiba, MD, MS. Novel Monitoring of Tissue Microvasculature Oxygenation Using Resonance Raman Spectroscopy. Poster presentation at the 2019 UROP Symposium
- Student Isabella Sperry, Carmen I. Colmenero Mahmood, Hakam Tiba. Novel Noninvasive Impedance-based Technique, for Central Venous Pressure Measurement. Poster presentation at the 2022 UROP Symposium

7.1.4. **Website(s) or other Internet site(s)**
https://weilinstitute.med.umich.edu/product-portfolio/microvascular-tissue-oximetry?rq=RAMAN

https://weilinstitute.med.umich.edu/product-portfolio/drive?rq=DRIVE

7.1.5. Technologies or techniques
The new DRIVE RMS and noise/movement detection analysis is new and will be reviewed soon for their potential/need for intellectual property protection. Discussion regarding these analytic techniques will take place with New Vital Signs in order to consider their incorporation into the DRIVE prototypes. We are actively exploring the addition of the impedance based NICVP technology for noninvasive evaluation of volume status. The new RRS clip will continue to be utilized and evaluated for ease of use. These were designed and 3-D printed by our team. Their final utilization and incorporation into the RRS system will be discussed with Pendar Technologies.

7.1.6. Inventions, patent applications, and/or licenses.
- United States Patent 7,113,814: Ward KR, R. RW, Terner J, Ivatury RR, Hawkridge F. Tissue Interrogation Spectroscopy
- United States Patent 14/445,926: Ward KR, Tiba MH, Blum M. Evaluating cardiovascular health using intravascular volume.

7.1.7. Other Products
Nothing to report

7.1.8. Research material (e.g., Germplasm; cell lines, DNA probes, animal models);
Nothing to report

8. PARTICIPANTS & OTHER COLLABORATING ORGANIZATIONS

8.1. What individuals have worked on the project?

Name:	***Kevin Ward, MD***
Project Role:	*PI*
Researcher Identifier (e.g. ORCID ID):	
Nearest person month worked:	*8*
Contribution to Project:	*Oversight of data collection and analysis*
Funding Support:	

Name:	***Mohamad Hakam Tiba, MD, MS***
Project Role:	*Co-I*
Researcher Identifier (e.g. ORCID ID):	
Nearest person month worked:	*8*
Contribution to Project:	*Oversight of data collection and analysis*
Funding Support:	

Name:	***Kyle Gunnerson, MD***
Project Role:	*Co-I*

Researcher Identifier (e.g. ORCID ID):	
Nearest person month worked:	*8*
Contribution to Project:	*medical consultation*
Funding Support:	

Name:	***Lena Napolitano, MD***
Project Role:	*Co-I*
Researcher Identifier (e.g. ORCID ID):	
Nearest person month worked:	*6*
Contribution to Project:	*medical consultation*

Name:	***Pauline Park, MD***
Project Role:	*Co-I*
Researcher Identifier (e.g. ORCID ID):	
Nearest person month worked:	*6*
Contribution to Project:	*medical consultation*

Name:	***Nik Theyyunni, MD***
Project Role:	*Co-I*
Researcher Identifier (e.g. ORCID ID):	
Nearest person month worked:	*5*
Contribution to Project:	*Perform ultrasounds*
Funding Support:	

Name:	***Christopher Fung, MD***
Project Role:	*Co-I*
Researcher Identifier (e.g. ORCID ID):	
Nearest person month worked:	*5*
Contribution to Project:	*Perform ultrasounds*
Funding Support:	

Name:	***Michael Cover, MD***
Project Role:	*Co-I*
Researcher Identifier (e.g. ORCID ID):	
Nearest person month worked:	*5*
Contribution to Project:	*Perform ultrasounds*
Funding Support:	

Name:	***Joseph Blackmer***

Project Role:	*Research Staff*
Researcher Identifier (e.g. ORCID ID):	
Nearest person month worked:	*12*
Contribution to Project:	*Data analysis*
Funding Support:	

Name:	***Christopher Gillies, PhD***
Project Role:	*Data Scientist*
Researcher Identifier (e.g. ORCID ID):	
Nearest person month worked:	*27*
Contribution to Project:	*data analysis*
Funding Support:	

Name:	***Guan Wang, MS, ME***
Project Role:	*Application programmer / Analyst*
Researcher Identifier (e.g. ORCID ID):	
Nearest person month worked:	*8*
Contribution to Project:	*Software engineering and system administration*
Funding Support:	

Name:	***Jonathan Motyka***
Project Role:	*Data scientist*
Researcher Identifier (e.g. ORCID ID):	
Nearest person month worked:	*1*
Contribution to Project:	*Data analysis*
Funding Support:	

Name:	***Brandon Cummings, BS***
Project Role:	*Research Staff*
Researcher Identifier (e.g. ORCID ID):	
Nearest person month worked:	*40*
Contribution to Project:	*Data analysis*
Funding Support:	

Name:	***Nicholas Greer, BS***
Project Role:	*Research Staff*
Researcher Identifier (e.g. ORCID ID):	
Nearest person month worked:	*5*
Contribution to Project:	*data analysis*

Funding Support:	

Name:	***Denise Poirier***
Project Role:	*Administrative Staff*
Researcher Identifier (e.g. ORCID ID):	
Nearest person month worked:	*8*
Contribution to Project:	*Scheduling of meetings*
Funding Support:	

Name:	***Amanda Pennington, MS***
Project Role:	*Clinical Research Project Manager*
Researcher Identifier (e.g. ORCID ID):	
Nearest person month worked:	*8*
Contribution to Project:	*Subject screening and enrollment, regulatory and compliance management, data collection*
Funding Support:	

Name:	***Abdelrahman Awad***
Project Role:	*Clinical Coordinator*
Researcher Identifier (e.g. ORCID ID):	
Nearest person month worked:	*14*
Contribution to Project:	*Screening and consenting patients, data collection*
Funding Support:	

Name:	***Carmen Colmenero-Mahmood***
Project Role:	*Clinical Coordinator*
Researcher Identifier (e.g. ORCID ID):	
Nearest person month worked:	*9*
Contribution to Project:	*Screening and consenting patients, regulatory and compliance management, data collection*
Funding Support:	

Name:	***Nicholas Sautter, BS***
Project Role:	*Research Staff*
Researcher Identifier (e.g. ORCID ID):	
Nearest person month worked:	*4*
Contribution to Project:	*Screening and consenting patients, data collection*
Funding Support:	

Name:	***Erin Bisco, BS***
Project Role:	*Research Staff*
Researcher Identifier (e.g. ORCID ID):	
Nearest person month worked:	*7*
Contribution to Project:	*Screening and consenting patients, data collection*
Funding Support:	

Name:	***Anne Weitzel, BS***
Project Role:	*Research Staff*
Researcher Identifier (e.g. ORCID ID):	
Nearest person month worked:	*7*
Contribution to Project:	*Data analysis*
Funding Support:	

Name:	***Justin Massey, BS***
Project Role:	*Research Staff*
Researcher Identifier (e.g. ORCID ID):	
Nearest person month worked:	*1*
Contribution to Project:	*Screening and consenting patients, data collection*
Funding Support:	

Name:	***Negar Farzaneh***
Project Role:	*Research Staff*
Researcher Identifier (e.g. ORCID ID):	
Nearest person month worked:	*6*
Contribution to Project:	*data analysis*
Funding Support:	

Name:	***Sarah Coderre***
Project Role:	*Research Staff*
Researcher Identifier (e.g. ORCID ID):	
Nearest person month worked:	*1*
Contribution to Project:	*Screening and consenting patients, data collection*
Funding Support:	

8.2. Has there been a change in the active other support of the PD/PI(s) or senior/key personnel since the last reporting period?
Nothing to report

8.3. What other organizations were involved as partners?

Pendar Technologies and New Vital Signs as manufacturers and commercial partners in developing the RRS and DRIVE technologies respectively.

8.4. Other.
Nothing to report

9. SPECIAL REPORTING REQUIREMENTS

9.1. COLLABORATIVE AWARDS:
None

9.2. QUAD CHARTS: Included with this report before the appendices

10. APPENDICES:

10.1. Journal publications.

Tiba MH, Awad AB, Pennington A, Fung CM, Napolitano LM, Park PK, Machado-Aranda DA, Gunnerson KJ, Romfh P, Ward KR. Resonance Raman Spectroscopy Derived Tissue Hemoglobin Oxygen Saturation in Critically Ill and Injured Patients. Shock. 2021 Jul 1;56(1):92-97. doi: 10.1097/SHK.0000000000001696. PMID: 33208679.

10.2. Abstracts, conference papers, and presentations.

Abstract # MHSRS-19-01948: Amanda J. Pennington, Mohamad Hakam Tiba, Brandon C. Cummings, Varisha Essani, Claire Roberge, Kyle Gunnerson, Kevin R. Ward. Novel monitoring of tissue microvasculature oxygenation using resonance Raman spectroscopy. Military Health System Research Symposium (MHSRS), August 2019, Kissimmee, Florida. Accpepted for poster presentation

Abstract # MHSRS-20-01069**:** Abdelrahman Awad, MD; Varisha Essani; Claire Roberge; Kyle Gunnerson, MD; Mohamad Hakam Tiba, MD, MS; Kevin Ward, MD, Monitoring of Tissue Microvasculature Oxygenation Using Resonance Raman Spectroscopy. **2020** Military Health System Research Symposium (MHSRS. Due to COVID-19, the conference has been cancelled, however the abstract will still be published**.**

Abstract # MHSRS-21-02936: Mohamad H. Tiba, MD, MS, Abdelrahman B. Awad, MD, Christopher M. Fung, MD, Lena M. Napolitano, MD, Pauline K. Park, MD, David A. Machado-Aranda, MD, Kyle J. Gunnerson, MD, Padraic Romfh, BS, MBA, Kevin R. Ward, MD. Resonance Raman Spectroscopy-Derived Tissue Hemoglobin Oxygen Saturation for the Management of the Critically Ill and Injured Patients. 2021 Military Health System Research Symposium (MHSRS). Due to COVID-19, the conference has been cancelled, however the abstract will still be published

Abstract # MHSRS-22-05939: Mohamad Hakam Tiba, Carmen I. Colmenero Mahmood, Kevin R. Ward. Impedance-based noninvasive technique for central venous pressure measurement. 2022 Military Health System Research Symposium (MHSRS). Accepted for poster presentation.

Student Claire Roberge, Varisha Essani, Amanda Pennington, Brandon Cummings, Kevin Ward, Mohamad H Tiba, MD, MS. Novel Monitoring of Tissue Microvasculature Oxygenation Using Resonance Raman Spectroscopy. Poster presentation at the 2019 UROP Symposium

Student Isabella Sperry, Carmen I. Colmenero Mahmood, Hakam Tiba. Novel Noninvasive Impedance-based Technique, for Central Venous Pressure Measurement. Poster presentation at the 2022 UROP Symposium

10.3. Patents

United States Patent 7,113,814: Ward KR, R. RW, Terner J, Ivatury RR, Hawkridge F. Tissue Interrogation Spectroscopy

United States Patent 14/445,926: Ward KR, Tiba MH, Blum M. Evaluating cardiovascular health using intravascular volume.

Development and Testing of New Noninvasive Monitoring Tools for Prolonged Field Care Goal Directed Therapy

DM160225 Prolonged Field Care Research Award

PI: Kevin R. Ward, MD **Org:** University of Michigan **Award Amount:** $2,998,209

Study/Product Aim(s)

- Test and compare resonance Raman spectroscopy tissue oxygenation (RRS StO2) with other measures of tissue oxygen in polytrauma and complex surgical patients.
- Test and compare dynamic respiratory impedance volume evaluation(DRIVE) to other measures and surrogates of intravascular volume monitoring in polytrauma and complex surgical patients.
- Compare time series measurement RRS StO2 and DRIVE to patient outcomes including mortality and organ failure in order to support future trials supporting their use in PFC and pRDC.

Approach

We will compare two newly developed noninvasive hemodynamic monitoring technologies to traditional hemodynamic monitoring in surgical patients for their suitability in goal directed therapy for potential future use in PFC and pRDC.

Comparing CVP, ScvO2 and IVC Ultrasound monitoring to

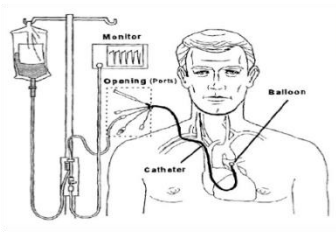

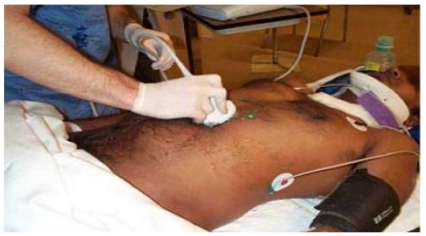

DRIVE and RRS StO2 monitoring for GDT in PFC

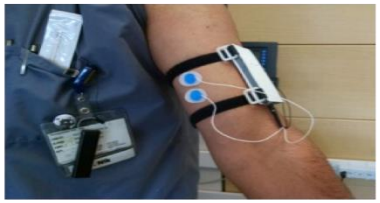

Clinical comparison of newly developed DRIVE and RRS StO2 buccal mucosa monitoring to traditional CVP, ScVO2, IVC ultrasound and other measures for potential in goal directed therapy in PFC

Timeline and Cost

Activities	CY18	CY19	CY20
Enroll 200-300Subjects			
Data comparisons to gold standard monitoring			
Monitoring comparisons to outcomes and interventions			
Estimated Budget ($K)	**$967,249**	**$1,003,281**	**$1,027,679**

Goals/Milestones

CY18Goal –

✓ Patient recruitment

✓ Comparison of new tools to standard measures

CY19 Goals –

✓ Additional patient recruitment

✓ Comparison of new tools to standard measures

✓ Begin comparisons of monitoring to outcomes and interventions

CY20 Goal – Production readiness

✓ Complete patient enrollment

✓ Complete data comparisons of monitors and comparisons to outcomes and interventions

✓ Work with industry partners on commercialization, trialing and scaling strategies

Comments/Challenges/Issues/Concerns. COVID-19.

Budget Expenditure to Date: $2,998,209

SHOCK, Vol. 56, No. 1, pp. 92–97, 2021

RESONANCE RAMAN SPECTROSCOPY DERIVED TISSUE HEMOGLOBIN OXYGEN SATURATION IN CRITICALLY ILL AND INJURED PATIENTS

Mohamad H. Tiba,[*†] Abdelrahman B. Awad,[*†] Amanda Pennington,[*†] Christopher M. Fung,[*†] Lena M. Napolitano,[†‡] Pauline K. Park,[†‡] David A. Machado-Aranda,[†‡] Kyle J. Gunnerson,[*†] Padraic Romfh,[§] and Kevin R. Ward[*†‖]

[*]Department of Emergency Medicine, University of Michigan, Ann Arbor, Michigan; [†]Michigan Center for Integrative Research in Critical Care, University of Michigan, Ann Arbor, Michigan; [‡]Department of Surgery, University of Michigan, Ann Arbor, Michigan; [§]Pendar Technologies, LLC, Cambridge, Massachusetts; and [‖]Department of Biomedical Engineering, University of Michigan, Ann Arbor, Michigan

Received 2 Oct 2020; first review completed 19 Oct 2020; accepted in final form 11 Nov 2020

ABSTRACT—**Background:** In this study, we examined the ability of resonance Raman spectroscopy to measure tissue hemoglobin oxygenation (R-StO_2) noninvasively in critically ill patients and compared its performance with conventional central venous hemoglobin oxygen saturation ($ScvO_2$). **Methods:** Critically ill patients (n = 138) with an indwelling central venous or pulmonary artery catheter in place were consented and recruited. R-StO_2 measurements were obtained by placing a sensor inside the mouth on the buccal mucosa. R-StO_2 was measured continuously for 5 min. Blood samples were drawn from the distal port of the indwelling central venous catheter or proximal port of the pulmonary artery catheter at the end of the test period to measure $ScvO_2$ using standard co-oximetry analyzer. A regression algorithm was used to calculate the R-StO_2 based on the observed spectra. **Results:** Mean (SD) of pooled R-StO_2 and $ScvO_2$ were 64(7.6) % and 65(9.2) % respectively. A paired *t* test showed no significant difference between R-StO_2 and $ScvO_2$ with a mean(SD) difference of −1(7.5) % (95% CI: −2.2, 0.3%) with a Clarke Error Grid demonstrating 84.8% of the data residing within the accurate and acceptable grids. Area under the receiver operator curve for R-StO_2's was 0.8(0.029) (95% CI: 0.7, 0.9 $P < 0.0001$) at different thresholds of $ScvO_2$ (≤60%, ≤65%, and ≤70%). Clinical adjudication by five clinicians to assess the utility of R-StO_2 and $ScvO_2$ yielded Fleiss' Kappa agreement of 0.45 ($P < 0.00001$). **Conclusions:** R-StO_2 has the potential to predict $ScvO_2$ with high precision and might serve as a faster, safer, and noninvasive surrogate to these measures.

KEYWORDS—Central venous oxygen saturation, hemoglobin, noninvasive monitoring, resonance Raman spectroscopy, tissue hemoglobin oxygen saturation

INTRODUCTION

Ensuring adequate oxygen delivery and preventing tissue hypoxia in the care of the critically ill and injured continues to be of paramount importance (1). However, identifying imbalances in the delivery and consumption of oxygen through measurement and monitoring of tissue oxygenation continues to be a challenge with no clearly established and adopted technologies allowing for continuous or point-of-care measurement. While the use of lactate monitoring is of significant value in identifying oxygen delivery dependent states of oxygen consumption, it changes relatively late and cannot be used as a continuous measure (1–3).

While central venous oxygen saturation ($ScvO_2$) can play a significant role in the management of critically ill and injured patients as a means to assess the adequacy of whole body oxygen delivery, $ScvO_2$ measurements are invasive and thus difficult to use as a screening or point-of-care tool in the early care of patients (4–6). In an attempt to overcome these issues, optical-based noninvasive technologies such as near infrared spectroscopy (NIRS) have been developed as a means to measure tissue hemoglobin oxygen saturation (StO_2) as an indicator of tissue oxygenation as well as a surrogate to $ScvO_2$ (7–10). The basis for such approaches is that 70% to 80% of blood volume in tissue is venous and thus aggregate measures of blood hemoglobin oxygenation in a target tissue predominately represent the post-extraction compartment, and thus may mirror the balance of oxygen delivery and consumption similar to $ScvO_2$ (10, 11). However, techniques like NIRS are not without challenges related to the presence of interfering chromophores such as myoglobin from muscle tissue which have a vastly different P50 limiting its clinical utility as a surrogate of more established measures like $ScvO_2$ (10, 12, 13).

To overcome some of these barriers we have developed a StO_2-measurement modality that utilizes the principles of resonance Raman spectroscopy (RRS) (14–16). RRS uses the well-established phenomenon of Raman inelastic scattering of light (17). Inelastic scattering is the result of photons interacting with the molecule and exciting it to a new vibrational state which cause the photon to lose or gain energy. The

Address reprint requests to Kevin R. Ward, MD, Department of Emergency Medicine, Michigan Center for Integrative Research in Critical Care, University of Michigan, 2800 N. Plymouth Road, North Campus Research Complex Building 10-A103, Ann Arbor, MI 48109. E-mail: keward@umich.edu

KRW and PR have intellectual property on Raman spectroscopy. The technology is licensed to Pendar Technologies, LLC, where PR is a Co-Founder and Director of Clinical Business Development.

This work has been supported by a grant award from the Department of Defense Joint Program Committee 6 (JPC-6) Combat Casualty Care (CCC) Research (W81XWH-18-1-0078). The study sponsor did not have any role in the study design, in the collection, analysis and interpretation of data; in the writing of the manuscript; and in the decision to submit the manuscript for publication. KRW is a LTC in the US Army Reserve MC. His views do not necessarily reflect the view of the US Army or Department of Defense.

The rest of authors report no conflict of interest.

DOI: 10.1097/SHK.0000000000001696

resulting shift in the scattered photon's wavelength gives a signature spectrum for the excited molecule (17–19). The Raman spectroscopic basis of our determination of StO_2 (R-StO_2) lies in the resonance vibrational enhancement of hemoglobin and deoxy-hemoglobin in the near ultraviolet region (15–20). This allows for simultaneous identification of the proportion of oxy and deoxy-hemoglobin in a concentration-dependent manner using a single wavelength of light which creates a spectral fingerprint of both species of hemoglobin (Fig. 1) (17, 19, 20). In this study, we explored R-StO_2 measurements obtained from the buccal mucosa in critically ill adult ICU patients and compared them to spot measures of $ScvO_2$ values. We hypothesized that R-StO_2 could potentially be a noninvasive surrogate of $ScvO_2$ as an indicator of tissue oxygenation.

PATIENTS AND METHODS

This prospective, noninterventional observational study was conducted under approval of the University of Michigan Institutional Review Board ((HUM00067675). Patients or their legally authorized representatives were consented for the study.

Study Population

One hundred thirty-eight patients were recruited from multiple intensive care units across Michigan Medicine (formerly the University of Michigan Health System). The hospital serves as a major quaternary care facility for the state of Michigan for critically ill and injured patients. Patients had a mean (SD) age of 62(13) years old and weight of 90(26) kg. There were 93(68%) males and 45(32%) females with racial makeup of White (88%), Black (11%), and Asian (1%). Units included surgical (cardiovascular, surgical, trauma-burn) (86%), medical (11%), and emergency department (5%)). Inclusion criteria included adults 18 years and older critically ill ICU patients while patients under 18 years old, pregnant women, and prisoners were excluded. Seventy-six (55%) of the patients had central venous catheter (CVC) in place at the time of testing, while 62 (45%) patients had pulmonary artery catheter (PAC).

Tissue Oxygen Saturation Measurements and Data Collection

R-StO_2 measurements were performed by placing a small sensor fitted with a clip inside the mouth on the buccal mucosa. The sensor is connected to an experimental microvascular oximeter (Pendar Technologies, LLC, Cambridge, Mass). The microvascular oximeter uses a 405 nm, 4 mW laser to illuminates an area of tissue that is approximately 12 mm^2. The laser light excites both oxyhemoglobin and deoxy-hemoglobin in the interrogated tissue's microvasculature into distinct vibrational states causing differential wavelength shift of the scattered light (15). The spectrum of the scattered light is then used by a regression algorithm to calculate R-StO_2 as the relative ratio of concentration of oxygenated hemoglobin to that of total hemoglobin based on a library of known hemoglobin spectra. The oximeter calculates StO_2 every 1 s based on a running average of spectra from the previous 30 to 180 s. The buccal mucosa was the chosen tissue site of interrogation since light at a wavelength of 405 nm penetrates only 2 to 3 mm (15). At this depth enough microvasculature and thus blood is encountered to derive an RRS signal for calculation of StO_2. In addition, the mucosa is largely void of other potentially contaminating chromophores such as skin pigment and myoglobin. Lastly the oral mucosa is known to be sensitive to changes in tissue perfusion (15, 21–23) and is relatively insensitive to environmental temperature, unlike skin. R-StO_2 was collected and measured continuously over 15 to 20 min. An average R-StO_2 over 5 min at the time of blood sample acquisition (below) was used to compare R-StO_2 to the value of $ScvO_2$.

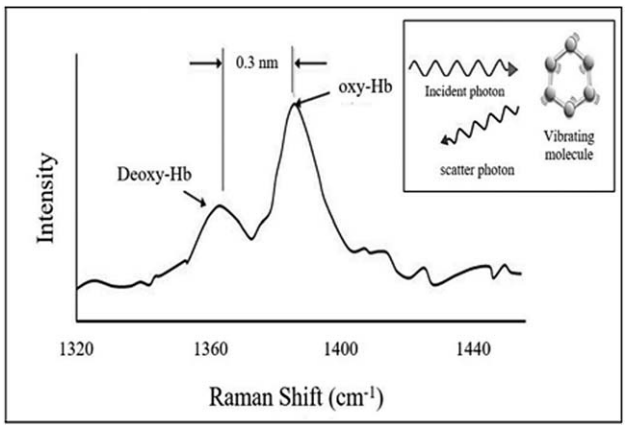

FIG. 1. **Example of a molecule being interrogated by RRS depicting the Raman vibrational spectroscopy phenomena. Deoxy-Hb indicates Deoxy-hemoglobin; Oxy-Hb, Oxy-hemoglobin.**

Central Venous Blood Gas Samples

At the conclusion of each testing session, a blood sample was collected from the distal port of the central venous catheter or the proximal port of the pulmonary artery catheter using standard clinical protocols and collected in blood gas syringes for measurement of $ScvO_2$. Blood hemoglobin oxygen saturation was directly measured in the Michigan Medicine's critical care clinical laboratories using a multiwavelength co-oximeter (GEM Premier 5000: Instrumentation laboratory, Bedford, Mass).

Statistical Analysis

Descriptive statistics are expressed as means and standard deviations. Linear regression was used to quantify the relationships between R-StO_2 and $ScvO_2$. A modified Clarke Error Grid was constructed to quantify the clinical accuracy of R-StO_2 when compared to the gold standard ($ScvO_2$) (24). Summary statistics using receiver operator characteristic (ROC) and area under the curve (AUC) values were used for pooled data to assess performance of R-StO_2 at different thresholds of $ScvO_2$. Clinical utility of R-StO_2 and $ScvO_2$ was conducted by asking five blinded medical and surgical intensivists to indicate if they would consider changing management of a theoretical patient to increase oxygen delivery based on R-StO_2 and $ScvO_2$ values provided to them. R-StO_2 and $ScvO_2$ values were randomly presented (blinded to source). Percentage of agreement or disagreement between paired R-StO_2 and $ScvO_2$ for management decisions was calculated for each rater individually. In addition, Fleiss' Kappa (25) was calculated to test overall agreement between the five raters. Data analysis was performed on GraphPad Prizm8 (GraphPad Software, Inc, La Jolla, Calif). Statistical significance was set at $\alpha < 0.05$.

RESULTS

Table 1 lists descriptive statistics of R-StO_2, $ScvO_2$, and the difference between the two (R-StO_2 – $ScvO_2$). Mean(SD) of pooled R-StO_2 and $ScvO_2$ were 64(7.6) and 65(9.2)% respectively. A linear regression of the type ($ScvO_2 = \beta_0 + \beta_1 * S$-

TABLE 1. **Descriptive statistics.**

	R-StO_2 (%)	$ScvO_2$ (%)	Difference (R-StO_2-$ScvO_2$) (%)
Number of values	138	138	138
Mean	64	65	−1
Std. deviation	7.6	9.2	7.5
Std. error of mean	0.65	0.78	0.64
95% CI of the mean	63, 66	64, 67	−2.2, 0.3
Minimum	39	44	−19
25% Percentile	60	59	−7
Median	64	65	−2
75% Percentile	69	72	5
Maximum	83	87	15

Descriptive statistics of R-StO_2, $ScvO_2$ and the difference between the two.
95% CI indicates 95% confidence intervals; R-StO_2, resonance Raman spectroscopy-tissue oxygen saturation; $ScvO_2$, central venous oxygen saturation.

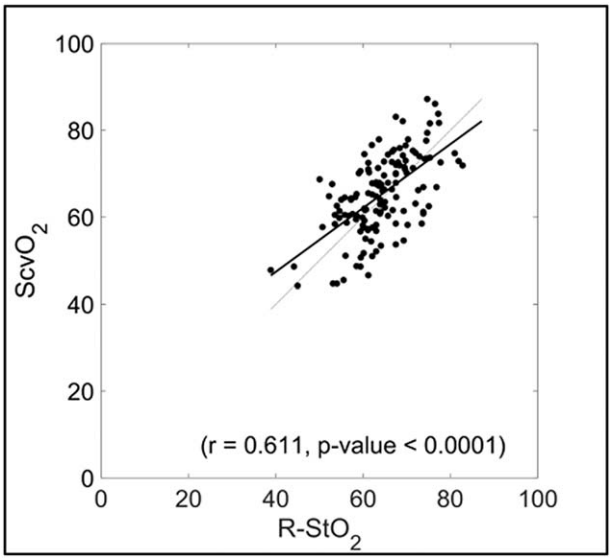

Fig. 2. **Linear regression model demonstrating the relationship between R-StO2 and $ScvO_2$. R-StO2 indicates resonance Raman spectroscopy-tissue hemoglobin oxygen saturation; ScvO2, central or mixed venous hemoglobin oxygen saturation.**

$StO_2 + \gamma$) showed a significant correlation between StO_2 and $ScvO_2$ ($r = 0.611$, $P < 0.0001$) (Fig. 2). A paired t test revealed no significant difference between R-StO_2 and $ScvO_2$ with a mean(SD) of the difference between R-StO_2 and $ScvO_2$ of $-1(7.5)$ % (95% CI: -2.2, 0.3%, $P = 0.11$). The Clarke Error Grid showed significant clinical accuracy of R-StO_2 with 84.8% of the data residing within the accurate and acceptable grids (A and B), 8% in the false-positive grid (C), and 7.2% in the false-negative grid (D) (Fig. 3).

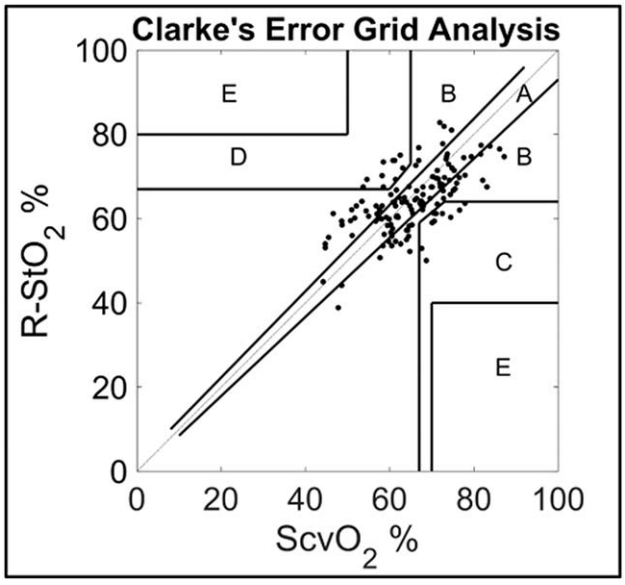

Fig. 3. **Clarke Error Grid plot to quantify clinical accuracy of estimated R-StO_2. Zone A, Accurate values within clinically acceptable difference; Zone B, acceptable values; Zone C, represent potential of unnecessary treatment or false-positive values; Zone D, represent failure to detect and treat or false-negative values; And zone E, represent erroneous measurements. See results and discussion section for details.**

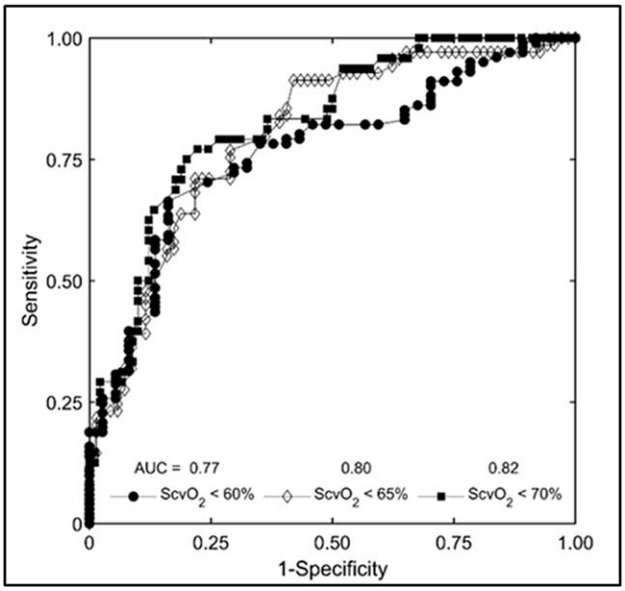

Fig. 4. **Receiver operator characteristics and area under the curve values for R-StO_2 at different thresholds of $ScvO_2$ (60%, 65%, and 70%). R-StO_2 indicates resonance Raman spectroscopy-tissue hemoglobin oxygen saturation; $ScvO_2$, central or mixed venous hemoglobin oxygen saturation.**

ROC analysis yielded a mean(SD) area under the curve for R-StO_2 of 0.8(0.029) (95% CI: 0.7, 0.9 $P < 0.0001$) at different thresholds of $ScvO_2$ ($\leq$60%, $\leq$65%, and $\leq$70%) (Fig. 4). These $ScvO_2$ thresholds were examined as general examples of ''actionability'' in the setting of critical illness and injury assuming actions would be taken or not taken above or below these thresholds to increase oxygen delivery.

The blinded critical care physicians clinically adjudicated the values of R-StO_2 and $ScvO_2$ regarding management of patients based on saturation values. For each value of R-StO_2 or $ScvO_2$, the raters answered the question of ''would you change your management plan based on such value'' by yes or no. Overall agreement between all five raters was highly significant (Fleiss' Kappa 0.45, $P < 0.00001$). In addition, agreement between R-StO_2 and $ScvO_2$ utility to management decision was performed for each rater separately. Post-adjudication pairing of each of the raters' assessments yielded a mean(SD) a (yes, no) agreement of 0.73(0.045) for all raters with a range of 0.69 to 0.81.

DISCUSSION

Management strategies for critically ill and injured patients continue to evolve. Prevention of tissue hypoxia continues to be a fundamental principle in the initial resuscitation and ongoing care of patients to limit further accumulation of oxygen debt in sepsis, trauma, heart failure, complex surgeries, and others (1, 26–30). However, assessment of the adequacy of tissue oxygenation in critically ill patients remains a challenge, especially in the early phases of emergency and critical care. The value of $ScvO_2$ monitoring is likely highest when used early and may find greater value when coupled with lactate measures (3, 31–35).

Implementation of $ScvO_2$ monitoring, however, can be challenging especially in early echelons of care, in part, due to the invasive nature of the measure. Even when used, in many institutions (including ours) the use of catheters capable of continuous oximetry measurement is inconsistent and clinical management varies with experience and levels of training, and therefore, at best, only intermittent $ScvO_2$ measurements are available which may not provide adequate information to carefully titrate fluid/blood infusions and inotropic/vasopressor support. In addition, invasive $ScvO_2$ monitors require accurate placement of the catheter, calibration, and bedside clinical validation, all of which can result in delays of intervention. In contrast, noninvasive methodologies, which could be easily applied and allow for point-of-care or continuous monitoring of tissue oxygen saturation as a surrogate to $ScvO_2$, would potentially be of significant value in the management of the critically ill.

In this study, R-StO_2 was measured from the buccal mucosa and predicted $ScvO_2$ with moderately high precision of statistical and clinical significance. Our data shows that R-StO_2 and $ScvO_2$ are highly correlated with no significant difference when compared using a paired *t* test. Furthermore, the ROC analysis using $ScvO_2$ as a gold standard revealed a high predictive performance of R-StO_2 at different levels of $ScvO_2$ with high area under the curve enforcing its potential as a clinical metric to guide management. Although, as shown in Figure 2, the correlation coefficient might appear to be moderate, it gives a good indication regarding the positive relationship between the two measurements and when combined with the more rigorous statistics such as a *t* test (interchangeability and equality of means), Clark's error grid (strength and accuracy of our measurement) and the Receiver Operator Characteristic curve (predictive performance of our measurement), it gives an additional indication of the robustness of our measurement of tissue oxygenation.

To assess the clinical accuracy of the R-StO_2 measurement, we constructed a modified Clarke Error Grid plot (24). The plot places the data into different zones (A, B, C, D, and E) based on their utility. Zone A represents values that are considered accurate (difference is less than 7%) in this study. Zone B represents acceptable values that will not lead to change in management. Zone C could be viewed to represent false-positive values that might lead to unnecessary corrections (normal $ScvO_2$ and low R-StO_2). Zone D may be viewed to represent false negatives as failure to detect low $ScvO_2$ (low $ScvO_2$ but normal R-StO_2) resulting in failure to address tissue hypoxia. And finally, zone E represents erroneous measurement. Of note is that 84.8% of out R-StO_2 data resides in zones A and B showing the accuracy of clinical utility of the RRS measurement. In addition, the low false-positive measurements in zone C (8% of readings) and the low false-negative measurements in zone D (7.2% of readings) indicate a high specificity and sensitivity of the measurement. It is interesting to consider zone C where R-StO_2 values are lower than $ScvO_2$ values by 13% to 27%. Such differences could indicate that R-StO_2 is identifying tissue hypoxia earlier than $ScvO_2$. Studies using video microscopy of the oral microcirculation have demonstrated changes indicating tissue hypoperfusion prior to changes in traditional oxygen transport metrics and despite (21, 22, 36). Such change is closely dependent on the type of circulatory shock (sepsis, cardiogenic, hemorrhagic) and is related to changes in the buccal mucosa's microcirculatory blood flow. However, such changes are usually an early indication and reflective of global hypoperfusion (37, 38).

To further assess and understand the utility of the R-StO_2 measure to clinically differentiate between physiologic states requiring intervention, we solicited the *post-hoc* clinical judgement of critical care and subject matter experts to adjudicate the influence of both R-StO_2 and $ScvO_2$ over the clinicians' management decision. The five raters individually rated the measures based on their potential to indicate the need for therapies that would increase oxygen delivery. All five raters had high agreement between R-StO_2 and $ScvO_2$.

Examining the utility of a tissue oxygenation in this manner when comparing to more established measures may be helpful in understanding both the limits of the measure and how it could be used. For example, an R-StO_2 level of 70% and a $ScvO_2$ level of 85% may be significantly different from a statistical standpoint but neither of these levels is likely to invoke a change in therapy to increase oxygen delivery. Similarly, an R-StO_2 value of 40% and a $ScvO_2$ level of 55% while significantly different would likely result in similar changes in management to increase oxygen delivery.

This study is important as it indicates significant correlation between R-StO_2 and $ScvO_2$ in adult ICU patients. Thus, it may be capable of providing early detection of tissue hypoperfusion providing intensivists and emergency physicians with an opportunity to improve perfusion and potentially improve patient outcomes. The results also align with our previous work in small and large animals as well *in-vitro* testing demonstrating the validity of R-StO_2 over a wide range of clinically relevant hemoglobin oxygen saturation levels (15, 16, 20). Interestingly, the findings of this study are in contrast to the findings of a pilot study in 16 neonates which reported R-StO_2 was safe and feasible, but reported no correlation between buccal or plantar R-StO_2 with umbilical vein hemoglobin oxygen saturation as a surrogate of $ScvO_2$. However, as indicated in that study, the timing of sample pairing was sometimes different by up to 4 h and the microcirculation of neonates especially those that are premature is complex (39).

This study has several limitations. First, while the study is a prospective comparison of R-StO_2 and $ScvO_2$, patients were only tested at one point in time during their care without repeated measures of both $ScvO_2$ and R-StO_2 to assess trends, responses to various treatments, or outcomes. Despite this, the investigation represents a necessary first step in the evaluation of RRS utility to measure tissue oxygenation and begin to place it in context to a better-known body oxygenation measure ($ScvO_2$). Further studies will be conducted to assess R-StO_2 performance over a longer period of time with more frequent comparisons to $ScvO_2$ as well as other noninvasive measures such as NIRS to assess its ability to detect changes in response to therapies and to drive patient management. Second, comparison of R-StO_2 and $ScvO_2$ may be over simplified, given that R-StO_2 is a peripheral mixed measure (tissue blood contains arterial, capillary, and venous components) from a single tissue

bed and $ScvO_2$ is an aggregate central measure of pure venous blood reflecting contributions from the entire body. The source and composition of the sample is a reason why a traditional Bland-Altman analysis is not appropriate in this case (40). As such, we have used the Clarke-Error Grid as more appropriate measure of the R-StO_2 clinical utility (24). Lastly, we restricted sampling and comparison to $ScvO_2$ and not mixed venous hemoglobin oxygen saturation. While the values from these two sites are similar, we chose to limit our measurement and analysis to $ScvO_2$ which is likely more available in most institutions (5, 33, 41). In regard to this, the tip position of central venous catheter or the proximal port of a pulmonary artery catheter could impact $ScvO_2$ values (superior vena cava, right atrium, inferior vena cava) and thus its comparison to R-StO_2 (42). Too high and the sample may not be adequately mixed with blood from the inferior vena cava. In other cases, being too close to the coronary sinus or in the inferior vena cava can result in lower values. Comparison of R-StO_2 to mixed venous oxygen saturation from a pulmonary artery catheter may have yielded differing results. However, we plan in future studies to collect this data from diverse populations of patients which will allow us to better understand the value of R-StO_2 in this setting and its potential as a surrogate indicator to prevent under- or over-resuscitation of patients especially in the early phases of care. Future observational studies combining time series R-StO_2 measures in conjunction with lactate should further shed light regarding the utility of R-StO_2 as a reliable measure of tissue oxygenation capable of informing and guiding management and impacting clinical outcomes.

CONCLUSION

R-StO_2 local measurement from the buccal mucosa demonstrated significant agreement with $ScvO_2$ at levels that would potentially allow it to be used to guide clinical management. The use of R-StO_2 may have potential as a suitable noninvasive indicator of systemic oxygenation and as a surrogate metric to $ScvO_2$. Additional testing will be required to assess RRS's longitudinal ability to track changes in tissue oxygenation over time and in response to therapies.

ACKNOWLEDGMENTS

The authors thank Danielle Leander as well as the Michigan Center for Integrative Research in Critical Care and Michigan Medicine Intensive Care Units staff for their technical support.

REFERENCES

1. Barbee RW, Reynolds PS, Ward KR: Assessing shock resuscitation strategies by oxygen debt repayment. *Shock* 33(2):113–122, 2010.
2. Abramson D, Scalea TM, Hitchcock R, Trooskin SZ, Henry SM, Greenspan J: Lactate clearance and survival following injury. *J Trauma* 35(4):584–588, 1993.
3. Bisarya R, Shaath D, Pirzad A, Satterwhite L, He J, Simpson SQ: Serum lactate poorly predicts central venous oxygen saturation in critically ill patients: a retrospective cohort study. *J Intensive Care* 7:47, 2019.
4. Hosking C, Wilander P, Goosen J, Jacobson H, Moeng M, Boffard K, Bentzer P: Low central venous oxygen saturation in haemodynamically stabilized trauma patients is associated with poor outcome. *Acta Anaesthesiol Scand* 55(6):713–721, 2011.
5. el-Masry A, Mukhtar AM, el-Sherbeny AM, Fathy M, el-Meteini M: Comparison of central venous oxygen saturation and mixed venous oxygen saturation during liver transplantation. *Anaesthesia* 64(4):378–382, 2009.
6. Marx G, Reinhart K: Venous oximetry. *Curr Opin Crit Care* 12(3):263–268, 2006.
7. Hampton DA, Schreiber MA: Near infrared spectroscopy: clinical and research uses. *Transfusion* 53(suppl 1):52S–58S, 2013.
8. Peters J, Van Wageningen B, Hoogerwerf N, Tan E: Near-infrared spectroscopy: a promising prehospital tool for management of traumatic brain injury. *Prehosp Disaster Med* 32(4):414–418, 2017.
9. Seki T, Fujioka M, Fukushima H, Matsumori H, Maegawa N, Norimoto K, Okuchi K: Regional tissue oxygen saturation measured by near-infrared spectroscopy to assess the depth of burn injuries. *Int J Burns Trauma* 4(1):40–44, 2014.
10. Ward KR, Ivatury RR, Barbee RW, Terner J, Pittman R, Filho IP, Spiess B: Near infrared spectroscopy for evaluation of the trauma patient: a technology review. *Resuscitation* 68(1):27–44, 2006.
11. Shepherd JT. Circulation to Skeletal Muscle. Shepherd JT, Abboud FM, Geiger SR Editors, Vol. 3. Bethesda, MD: American Physiology Society, 1983, 319–370.
12. Tran TK, Sailasuta N, Kreutzer U, Hurd R, Chung Y, Mole P, Kuno S, Jue T: Comparative analysis of NMR and NIRS measurements of intracellular PO2 in human skeletal muscle. *Am J Physiol* 276(6 pt 2):R1682–R1690, 1999.
13. Nighswander-Rempel SP, Kupriyanov VV, Shaw RA: Relative contributions of hemoglobin and myoglobin to near-infrared spectroscopic images of cardiac tissue. *Appl Spectrosc* 59(2):190–193, 2005.
14. Ward KR, Torres Filho I, Barbee RW, Torres L, Tiba MH, Reynolds PS, Pittman RN, Ivatury RR, Terner J: Resonance Raman spectroscopy: a new technology for tissue oxygenation monitoring. *Crit Care Med* 34(3):792–799, 2006.
15. Tiba MH, Draucker GT, Barbee RW, Terner J, Torres Filho I, Romfh P, Vakhshoori D, Ward KR: Tissue oxygenation monitoring using resonance Raman spectroscopy during hemorrhage. *J Trauma Acute Care Surg* 76(2):402–408, 2014.
16. Torres Filho IP, Terner J, Pittman RN, Proffitt E, Ward KR: Measurement of hemoglobin oxygen saturation using Raman microspectroscopy and 532-nm excitation. *J Appl Physiol* 104(6):1809–1817, 2008.
17. Spiro TG, Li XY. Resonance Raman Spectroscopy of Metalloporphyrins and Heme Proteins. Spiro TG Editor: Vol. 3. New York, NY: Wiley, 1988, 1–38.
18. Spiro TG: Resonance Raman spectroscopy: a new structure probe for biological chromophores. *Accts Chem Res* 7:339–344, 1974.
19. Spiro TG: Resonance Raman spectroscopy as a probe of heme protein structure and dynamics. *Adv Protein Chem* 37:111–159, 1985.
20. Torres Filho IP, Terner J, Pittman RN, Somera LG, Ward KR: Hemoglobin oxygen saturation measurements using resonance Raman intravital microscopy. *Am J Physiol Heart Circ Physiol* 289(1):H488–H495, 2005.
21. De Backer D, Dubois MJ: Assessment of the microcirculatory flow in patients in the intensive care unit. *Curr Opin Crit Care* 7(3):200–203, 2001.
22. Marik PE: Sublingual capnography: a clinical validation study. *Chest* 120(3):923–927, 2001.
23. Vincent JL, De Backer D: Microcirculatory alterations in the critically ill. *Hosp Pract* 37(1):107–112, 2009.
24. Clarke WL: The original Clarke Error Grid Analysis (EGA). *Diabetes Technol Ther* 7(5):776–779, 2005.
25. Falotico R, Quatto P: Fleiss' kappa statistic without paradoxes. *Qual Quant* 49:463–470, 2015.
26. Shoemaker WC, Appel PL, Kram HB: Tissue oxygen debt as a determinant of lethal and nonlethal postoperative organ failure. *Crit Care Med* 16(11):1117–1120, 1988.
27. Shoemaker WC, Appel PL, Kram HB: Role of oxygen debt in the development of organ failure sepsis, and death in high-risk surgical patients. *Chest* 102(1):208–215, 1992.
28. Dunham CM, Fabian M, Siegel JH, Gettings L: Relationship of plasma amino acids to oxygen debt during hemorrhagic shock. *Circ Shock* 35(2):87–95, 1991.
29. Dunham CM, Siegel JH, Weireter L, Fabian M, Goodarzi S, Guadalupi P, Gettings L, Linberg SE, Vary TC: Oxygen debt and metabolic acidemia as quantitative predictors of mortality and the severity of the ischemic insult in hemorrhagic shock. *Crit Care Med* 19(2):231–243, 1991.
30. Siegel JH, Fabian M, Smith JA, Kingston EP, Steele KA, Wells MR, Kaplan LJ: Oxygen debt criteria quantify the effectiveness of early partial resuscitation after hypovolemic hemorrhagic shock. *J Trauma* 54(5):862–880, 2003.
31. Boulain T, Garot D, Vignon P, Lascarrou JB, Desachy A, Botoc V, Follin A, Frat JP, Bellec F, Quenot JP, et al.:, Clinical Research in Intensive Care and Sepsis Group. Prevalence of low central venous oxygen saturation in the first hours of intensive care unit admission and associated mortality in septic shock patients: a prospective multicentre study. *Crit Care* 18(6):609, 2014.
32. Lee YK, Hwang SY, Shin TG, Jo IJ, Suh GY, Jeon K: Prognostic value of lactate and central venous oxygen saturation after early resuscitation in sepsis patients. *PLoS One* 11(4):e0153305, 2016.
33. Rivers EP, Ander DS, Powell D: Central venous oxygen saturation monitoring in the critically ill patient. *Curr Opin Crit Care* 7(3):204–211, 2001.

34. Scalea TM, Holman M, Fuortes M, Baron BJ, Phillips TF, Goldstein AS, Sclafani SJ, Shaftan GW: Central venous blood oxygen saturation: an early, accurate measurement of volume during hemorrhage. *J Trauma* 28(6):725–732, 1988.
35. Shin TG, Jo IJ, Hwang SY, Jeon K, Suh GY, Choe E, Lee YK, Lee TR, Cha WC, Sim MS: Comprehensive interpretation of central venous oxygen saturation and blood lactate levels during resuscitation of patients with severe sepsis and septic shock in the emergency department. *Shock* 45(1):4–9, 2016.
36. Sakr Y, Dubois MJ, De Backer D, Creteur J, Vincent JL: Persistent microcirculatory alterations are associated with organ failure and death in patients with septic shock. *Crit Care Med* 32(9):1825–1831, 2004.
37. Tafner P, Chen FK, Rabello RF, Correa TD, Chaves RCF, Serpa AN: Recent advances in bedside microcirculation assessment in critically ill patients. *Rev Bras Ter Intensiva* 29(2):238–247, 2017.
38. Trzeciak S, Dellinger RP, Parrillo JE, Guglielmi M, Bajaj J, Abate NL, Arnold RC, Colilla S, Zanotti S, Hollenberg SM, Microcirculatory Alterations in Resuscitation and Shock Investigators. Early microcirculatory perfusion derangements in patients with severe sepsis and septic shock: relationship to hemodynamics, oxygen transport, and survival. *Ann Emerg Med* 49(1):88–98, 2007.
39. Iyengar A, Gaillardetz A, Tighiouart H, Castillo B, Romfh P, Davis JM: Direct measurement of tissue oxygenation in neonates via resonance Raman spectroscopy: a pilot study. *Neonatology* 112(2):137–142, 2017.
40. Bland JM, Altman DG: Measuring agreement in method comparison studies. *Stat Methods Med Res* 8(2):135–160, 1999.
41. Maddirala S, Khan A: Optimizing hemodynamic support in septic shock using central and mixed venous oxygen saturation. *Crit Care Clin* 26(2):323–333, 2010.
42. Brandt L, Mertzlufft F: [The meaningfulness of central venous blood samples. Central venous versus mixed venous O2 status]. *Anaesthesist* 40(3):131–144, 1991.

NOVEL MONITORING OF TISSUE MICROVASCULATURE OXYGENATION USING RESONANCE RAMAN SPECTROSCOPY

Amanda J. Pennington, MS[1,2], Mohamad Hakam Tiba, MD, MS[1,2], Brandon C. Cummings, BS[1,2], Varisha Essani[1,2], Claire Roberge[1,2], Kyle Gunnerson, MD[1,2], Kevin R. Ward, MD[1,2]

[1] Department of Emergency Medicine, University of Michigan. Ann Arbor Michigan.
[2] Michigan Center for Integrative Research in Critical Care (MCIRCC), University of Michigan, Ann Arbor, Michigan.

Introduction: The ability to monitor the critically ill patient noninvasively remains a challenge especially in settings outside the intensive care unit. Measurements of oxygenation at the level of a specific tissue might offer sensitive information to guide therapeutic modalities and decision making in the management of the critically ill. We examined the ability of Resonance Raman Spectroscopy (RRS) to monitor tissue hemoglobin oxygenation (StO_2) noninvasively in a post-surgery setting and compared its performance with conventional central venous hemoglobin oxygen saturation ($ScvO_2$). RRS is a novel optical technique capable of providing information on the vibrational and electronic properties of compounds, including oxy- and deoxyhemoglobin. RRS can be used to interrogate tissue hemoglobin levels (StO_2) by producing signals heavily dominated by venous blood. Thus, the resulting aggregate StO_2 is reflective of the post-extraction compartment of the tissue similar to $ScvO_2$.

Methods: Post-surgery patients who had a central venous catheter in place were consented and recruited. StO_2 measurements were obtained using RRS with a sensor placed on the buccal mucosa inside the mouth. Simultaneous blood samples were drawn from the indwelling central catheter. An algorithm that utilizes the spectral peaks was used to calculate the StO_2 which were compared to $ScvO_2$ measured by co-oximetry (gold standard).

Results: Eighteen patients with a mean(SD) age 64(15) years old were consented and recruited. Mean(SD) StO_2 and $ScvO_2$ were 64(11.1)% and 67(8.0)% respectively (*$r=0.57$, $p<0.013$*). A paired t-test showed no significant difference between the StO_2 and $ScvO_2$ with a mean(SD) difference of 4(10.3)% (*95%CI = [-1.3, 9], $p = 0.13$*). Receiver Operator Characteristic (ROC) curves for predicting $ScvO_2$ at thresholds of $ScvO_2$ above and below 65, and 70% demonstrated the high predictive power of StO_2 with areas under the curve of 0.74 and 0.83 respectively. Improvements to the clip are currently underway to allow the sensor to penetrate deeper into the tissue of the buccal mucosa.

Conclusions: RSS is showing promise as a non-invasive alternative to $ScvO_2$. StO_2 measurements taken using RSS are highly correlated with $ScvO_2$, which is an important measure of tissue oxygenation. Because of its non-invasive nature, RSS may serve as a faster, safer, and more cost-effective way to assess patient tissue oxygenation, aiding in the diagnosis and treatment of conditions such as sepsis, trauma, heart failure and other critical states.

Novel Monitoring of Tissue Microvasculature Oxygenation Using Resonance Raman Spectroscopy

Amanda Pennington, MS[1,2]; Hakam Tiba, MD, MS[1,2]; Brandon Cummings[1,2]; Varisha Essani[1,2]; Claire Roberge[1,2]; Kyle Gunnerson, MD[1,2]; Kevin Ward, MD[1,2]

[1] Department of Emergency Medicine, [2]Michigan Center for Integrative Research in Critical Care (MCIRCC)
University of Michigan, Ann Arbor, MI

CENTER FOR INTEGRATIVE RESEARCH IN CRITICAL CARE
UNIVERSITY OF MICHIGAN

DEPARTMENT OF EMERGENCY MEDICINE
UNIVERSITY OF MICHIGAN HEALTH SYSTEM

ABSTRACT

Introduction: The ability to monitor the critically ill patient noninvasively remains a challenge especially in settings outside the intensive care unit. Measurements of oxygenation at the level of a specific tissue might offer sensitive information to guide therapeutic modalities and decision making in the management of the critically ill. We examined the ability of Resonance Raman Spectroscopy (RRS) to monitor tissue hemoglobin oxygenation (StO_2) noninvasively in a post-surgery setting and compared its performance with conventional central venous hemoglobin oxygen saturation ($ScvO_2$). RRS is a novel optical technique capable of providing information on the vibrational and electronic properties of compounds, including oxy- and deoxyhemoglobin. RRS can be used to interrogate tissue hemoglobin levels (StO_2) by producing signals heavily dominated by venous blood. Thus, the resulting aggregate StO_2 is reflective of the post-extraction compartment of the tissue similar to $ScvO_2$.

Methods: Post-surgery patients who had a central venous catheter in place were consented and recruited. StO_2 measurements were obtained using RRS with a sensor placed on the buccal mucosa inside the mouth. Simultaneous blood samples were drawn from the indwelling central catheter. An algorithm that utilizes the spectral peaks was used to calculate the StO_2 which were compared to $ScvO_2$ measured by co-oximetry (gold standard).

Results: Eighteen patients with a mean(SD) age 64(15) years old were consented and recruited. Mean(SD) StO_2 and $ScvO_2$ were 64(11.1)% and 67(8.0)% respectively (*r=0.57, p<0.013*). A paired t-test showed no significant difference between the StO_2 and $ScvO_2$ with a mean(SD) difference of 4(10.3)% (*95%CI = [-1.3, 9], p = 0.13*). Receiver Operator Characteristic (ROC) curves for predicting $ScvO_2$ at thresholds of $ScvO_2$ above and below 65, and 70% demonstrated the high predictive power of StO_2 with areas under the curve of 0.74 and 0.83 respectively. Improvements to the clip are currently underway to allow the sensor to penetrate deeper into the tissue of the buccal mucosa.

Conclusions: RSS is showing promise as a non-invasive alternative to $ScvO_2$. StO_2 measurements taken using RSS are highly correlated with $ScvO_2$, which is an important measure of tissue oxygenation. Because of its non-invasive nature, RSS may serve as a faster, safer, and more cost-effective way to assess patient tissue oxygenation, aiding in the diagnosis and treatment of conditions such as sepsis, trauma, heart failure and other critical states.

INTRODUCTION

Resonance Raman Spectroscopy (RRS) is promising as a non-invasive method to monitor tissue oxygenation status

- Provide early diagnosis of shock
- Reduce oxygen debt and allow better treatment resources
- Increase patient comfort
- Decrease common problems associated with central venous catheters such as infection and injury to the vein

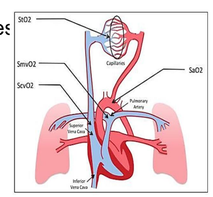

Approximately 70-80% of the blood in tissue resides in the venous system, making the hemoglobin oxygen saturation (StO_2) as measured by RRS a hopeful alternative to the invasively measured $ScvO_2$

INTRODUCTION

Changes in peripheral VO_2 resulting in lowering of StO_2 will parallel those of more central locations such as those used for $ScvO_2$ in the right atrium/superior vena cava or the $SmvO_2$ in the pulmonary artery.

Spectroscopic techniques produce hemoglobin signals that are heavily dominated by venous blood.

RRS provides information on the unique vibrational and electronic properties of compounds based on the well-defined and narrow Resonance Raman Spectral fingerprint of oxy and deoxy-hemoglobin and direct measurement of hemoglobin concentration in the illuminated volume.

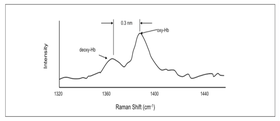

Interfering chemicals such as melanin, tissue composition or myoglobin will not affect the signal.

RRS in the near ultraviolet spectrum matches the electronic energy state of heme, allowing measurement of both the oxygenated and deoxygenated heme states.

METHODS

- This study is approved for human subjects research by the University of Michigan IRB HUM00067675
- Critically ill patients with a central venous catheter in place were recruited from the cardiovascular ICU as well as the catheterization lab.
- Informed consent was obtained prior to any testing.
- The RRS sensor was placed on the buccal mucosa and StO_2 measurements were obtained and collected for 15 minutes.
- At the conclusion of testing, a blood sample was collected from the distal port of the central catheter and the RRS measurement at that time was recorded.
- An algorithm that utilizes the spectral peaks was used in GraphPad Prism 6 statistical software to calculate the StO_2 which were compared to $ScvO_2$.

RESULTS

Eighteen patients with an average(SD) age of 64(15) y/o were tested

3 females, 15 males

All $StVO_2$ values are multiplied by 0.9

RESULTS

	StO2	ScvO2
Mean	63.8	67.7
Std. Deviation	11.0	11.3
Lower 95% CI of mean	58.3	62.1
Upper 95% CI of mean	69.3	73.3
Minimum	42.0	48.0
Maximum	78.0	96.0

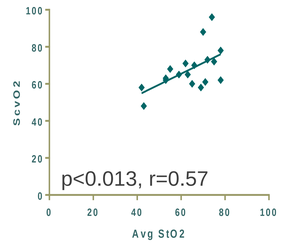

The scatter plot demonstrates the significant correlation between StO_2 and $ScvO_2$.

A paired t-test showed no significant difference between StO_2 and $ScvO_2$. Average(SD) difference of 4(10)% (*95%CI: 0.3% - 1.2%, p=0.128)*

Receiver operating characteristic (ROC) curve for StO_2 at thresholds of $ScvO_2$ between 65% and 70% have demonstrated high predictive power of StO_2 with area under the curve between 0.74 and 0.83 (*p < 0.006*).

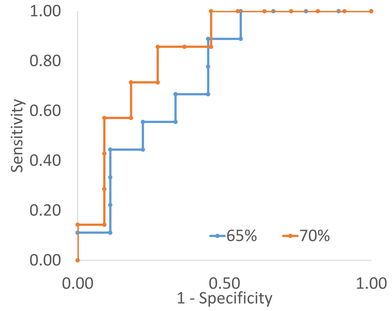

CONCLUSIONS

RRS is showing promise as a non-invasive alternative to $ScvO_2$.

StO_2 measurements taken using RRS are highly correlated with $ScvO_2$, which is an important measure of tissue oxygenation.

Because of its non-invasive nature, RRS may serve as a faster, safer, and more cost-effective way to assess patient tissue oxygenation, aiding in the diagnosis and treatment of conditions such as sepsis, trauma, heart failure and other critical states.

ACKNOWLEDGEMENT

This work has been supported by a grant award from the Department of Defense DM160294

Michigan Center for Integrative Research in Critical Care (MCIRCC)

MICHIGAN MEDICINE
UNIVERSITY OF MICHIGAN

MCIRCC

Monitoring of Tissue Microvasculature Oxygenation Using Resonance Raman Spectroscopy

Abdelrahman Awad, MD[1,3]; Varisha Essani[1,3]; Claire Roberge[1,3]; Kyle Gunnerson, MD[1,3]; Mohamad Hakam Tiba, MD, MS[1,3]; Kevin Ward, MD[1,2,3]

[1]Department of Emergency Medicine, University of Michigan, Ann Arbor, Michigan
[2]Department of Biomedical Engineering, University of Michigan, Ann Arbor, Michigan
[3]Michigan Center for Integrative Research in Critical Care (MCIRCC), University of Michigan, Ann Arbor, Michigan

Introduction: Management and treatment of critically ill patients remain a complicated process. Monitoring of the critically ill's tissue oxygenation status provides valuable insight into the effectiveness of their management plan. Current modalities to assess patients' oxygenation status is by obtaining a central venous blood gas sample ($ScvO_2$) which requires the presence of a central venous catheter (CVC) or a Pulmonary Artery Cather (PAC), which not only is considered invasive and non-continuous measurement but also has its own complications and challenges. Resonance Raman Spectroscopy (RRS) is a novel, non-invasive and effective measure to monitor and assess tissue oxygenation (StO_2) as a surrogate for $ScvO_2$. We have developed a portable monitor to measure StO_2 utilizing the well-defined and narrow Resonance Raman spectral fingerprint of oxy and deoxy-hemoglobin in the interrogated tissue. We present data for our investigation into the utility and effectiveness of our monitor comparing our SSR-StO_2 to blood gas measures of $ScvO_2$.
Hypothesis: We hypothesize that RRS-StO_2 will rack and predict patients' $ScvO_2$ with high precision.
Methods: Critically ill patients with a central venous catheter in place were recruited mainly from the cardiovascular ICU and other ICUs at Michigan Medicine. Informed consent was obtained from the patients or their legally authorized representatives prior to any testing. During the test, the RRS sensor was placed on the buccal mucosa for an average of 15 minutes and StO_2 measurements were obtained and collected. At the conclusion of testing, a blood sample was collected from the distal port of the central catheter to measure $ScvO_2$ and the RRS measurement at that time was marked and recorded. GraphPad Prism8 statistical software was used for data analysis to compare StO_2 to $ScvO_2$.
Results: Between 2015 and 2020, a total of 138 critically ill patients were recruited and tested. Average (standard deviation) of patients age and weight were 62(13) years, 90.3(26) kg respectively. Average (SD) of pooled StO_2 and $ScvO_2$ were 64(7.6) and 65.3 (9.1) respectively. There was significant correlation between StO_2 and $ScvO_2$ ($r=0.609$, $p < 0.0001$). A paired *t-test* showed no significant difference between StO_2 and $ScvO_2$ with an average (SD) difference of 1.04 (7.5) % (95%CI: 0.22- 2.3%). Receiver Operator Curve revealed an StO2 area under the curve > 0.8 (95% CI: 0.7 – 0.88. $p<0.0001$) at different thresholds of ScvO2 (60%, 65%, and 70%).
Conclusion: In this study, RRS is showing promise as a non-invasive alternative to $ScvO_2$. Because of its non-invasive nature, RRS may serve as a faster, safer, and more cost-effective way to assess patient tissue oxygenation, aiding in the diagnosis and treatment of conditions such as sepsis, trauma, heart failure and other critical states.

Disclaimer: This research project is supported by the Department of Defense – Combat Casualty Care grant award W81XWH-18-1-0078. KW is an inventor of the technology.

Learning Objectives:
Describe Resonance Raman Spectroscopy and its utility to interrogate tissue oxygenation
Describe current methodology to assess critically ill patients' oxygenation
Compare performance of RRS-StO_2 to measurements of central venous oxygen saturation.

Resonance Raman Spectroscopy-Derived Tissue Hemoglobin Oxygen Saturation for the Management of the Critically Ill and Injured Patients

Mohamad H. Tiba, MD, MS[1,4], Abdelrahman B. Awad, MD[1,4], Christopher M. Fung, MD[1,4], Lena M. Napolitano, MD[2,4], Pauline K. Park, MD[2,4], David A. Machado-Aranda, MD[2,4], Kyle J. Gunnerson, MD[1,4], Padraic Romfh, BS, MBA[5], Kevin R. Ward, MD[1,3,4]

1. Department of Emergency Medicine. University of Michigan, Ann Arbor, Michigan.
2. Department of Surgery. University of Michigan, Ann Arbor, Michigan.
3. Department of Biomedical Engineering. University of Michigan, Ann Arbor, Michigan.
4. Michigan Center for Integrative Research in Critical Care. University of Michigan, Ann Arbor, Michigan.
5. Pendar Technologies, LLC. Cambridge, Massachusetts

Introduction: Management and treatment of critically ill patients remain a challenging process. Monitoring of the critically ill's tissue oxygenation status provides valuable insight into the effectiveness of their management and prognosis. Current assessment of oxygenation status requires obtaining a central venous blood gas sample ($ScvO_2$) which requires the presence of a central venous catheter (CVC) or a Pulmonary Artery Cather (PAC), which not only is considered invasive and non-continuous measurement, but also has its own complications and challenges. In this study, we examined the ability of Resonance Raman Spectroscopy (RRS) to measure tissue hemoglobin oxygenation (R-StO_2) noninvasively in critically ill patients and compared its performance with conventional central venous hemoglobin oxygen saturation ($ScvO_2$)

Hypothesis: We hypothesized that R-StO_2 could potentially be a noninvasive surrogate of $ScvO_2$ as an indicator of tissue oxygenation.

Methods: Critically ill patients (n=138) with an indwelling central venous or pulmonary artery catheter in place were consented and recruited. R-StO_2 measurements were obtained by placing a sensor inside the mouth on the buccal mucosa. R-StO_2 was measured continuously for 5 minutes. Blood samples were drawn from the distal port of the indwelling central venous catheter or the proximal port of the pulmonary artery catheter at the end of the test period to measure $ScvO_2$ using a standard co-oximetry analyzer. A regression algorithm was used to calculate the R-StO_2 based on the observed spectra.

Results: Data is presented as mean and (Standard deviation). Mean (SD) of pooled R-StO_2 and $ScvO_2$ were 64%(7.6%) and 65% (9.2%) respectively. A paired t-test showed no significant difference between R-StO_2 and $ScvO_2$ with a mean(SD) difference of -1% (7.5%) (95% CI: -2.2, 0.3 %). A modified Clarke Error Grid showed significant clinical accuracy of R-StO_2 with 84.8% of the data residing within the accurate and acceptable grids (A and B), 8% in the false-positive grid (C), and 7.2% in the false-negative grid (D). Area under the receiver operator curve for R-StO_2's was 0.8 (0.029) (95% CI: 0.7, 0.9 $p<0.0001$) at different thresholds of $ScvO_2$ ($\leq$60%, $\leq$65%, and $\leq$70%). Five blinded critical care physicians clinically adjudicated the values of R-StO2 and ScvO2 regarding the management of patients based on saturation values. Overall agreement between all 5 raters was highly significant (Fleiss' Kappa 0.45, $p<0.00001$).

Conclusions: R-StO_2 local measurement from the buccal mucosa demonstrated significant agreement with $ScvO_2$ at levels that would potentially allow it to be used to guide clinical management. The use of R-StO_2 may have potential as a suitable noninvasive indicator of systemic oxygenation and as a surrogate metric to $ScvO_2$.

Disclaimer: This research project is supported by the Department of Defense – Combat Casualty Care grant award (W81XWH-18-1-0078). KRW is an inventor of the technology.

Learning Objectives:
Describe Resonance Raman Spectroscopy and its utility to interrogate tissue oxygenation
Describe current methodology to assess critically ill patients' oxygenation
Compare performance of R-StO_2 to measurements of central venous oxygen saturation.

Impedance-based noninvasive technique for central venous pressure measurement

Mohamad Hakam Tiba, MD, MS[1,3], Carmen I. Colmenero Mahmood, BS[1,3], Kevin R. Ward, MD[1,2,3]

[1]Department of Emergency Medicine, University of Michigan, Ann Arbor, Michigan
[2]Department of Biomedical Engineering, University of Michigan, Ann Arbor, Michigan
[3] The Max Harry Weil Institute for Critical Care Research and Innovation, University of Michigan, Ann Arbor, Michigan

Introduction: Monitoring and Knowledge of central venous pressure (CVP) can be valuable to aid with the diagnosis and management of a variety of critical illnesses and injuries, including trauma, burns, sepsis, congestive heart failure, cardiogenic shock, traumatic brain injury, kidney disease, and others. Current clinical practice guidelines call for the placement of an indwelling central venous catheter to measure CVP. However, this placement is often impractical as in an outpatient setting, and even when indicated, can be associated with significant risks. To mitigate such shortcomings, we tested a noninvasive method to measure CVP (NICVP) by monitoring upper arm blood flow changes as measured by impedance in response to externally applied circumferential pressure to the upper arm's veins.
Hypothesis: Impedance-based NICVP measurement can be performed with high accuracy over a wide range of CVP values.
Methods: Thirty-seven patients undergoing CVP monitoring as part of their clinical care had NICVP measured and compared with CVP. Blood volume changes were tracked in the upper arm by using tetra-polar impedance plethysmography underneath a blood pressure cuff. To perform the measurement, the cuff pressure is quickly inflated to 40-45 mmHg (a value higher than CVP but lower than the diastolic arterial pressure). The cuff is kept inflated at that pressure for 45 to 60 seconds. Because blood is a good conductor of electricity, the displacement of blood volume under the cuff causes the measured impedance to increase. Finally, the cuff is rapidly deflated at the end of the inflation hold period. NICVP was determined as the cuff pressure noted at the maximum slope of the impedance change during deflation. Measurements are usually repeated three to four times in each subject, and an average is calculated for NICVP and the corresponding CVP. In this investigation, averaged NICVP was compared with averaged CVP by appropriate statistical methodologies such as Bland-Altman analysis, Clarke's Error Grid, and the area under the receiver operator characteristic curve.
Results: A total of 140 trials (three or four per subject) were performed. The Bland-Altman analysis yielded a bias of 0.77 mmHg and a standard deviation of 2 mmHg with limits of agreement between -3.1 and 4.7 mmHg. A Clarke Error Grid showed significant clinical accuracy of NICVP with 84% of the data residing within the accurate grid A (difference of less than 3 mmHg), 8% of the measurements in the acceptable grid B (NICVP values that would not lead to inappropriate treatment), and 8% in the false-positive grid D (NICVP overestimates CVP). There were no values in the false-negative grid C (NICVP underestimating CVP). The area under the receiver operator characteristic curve for NICVP was (0.84, 95% CI: 0.7, 0.97, $p<0.0006$)) at CVP thresholds of 10.
Conclusion: NICVP as determined in this study may serve as a clinically useful substitute for traditional CVP measurement and may offer a tool for early diagnosis and treatment of acute states in which knowledge of CVP would be helpful.

Disclaimer:
This study is supported by a Department of Defense grant award W81XWH-18-1-0078.

Learning Objectives:

1- Describe the importance of central venous pressure during the management of critically ill and injured patients.
2- Describe the difficulties and complications associated with placement of indwelling catheter to measure CVP
3- Describe new and novel impedance-based non-invasive methodology to enable early and non-invasive measurement of CVP

Novel Monitoring of Tissue Microvasculature Oxygenation Using Resonance Raman Spectroscopy

Claire Roberge[1,2]; Varisha Essani[1,2]; Amanda Pennington, MS[1,2]; Brandon Cummings[1,2]; Kevin Ward, MD[1,2]; Mohamad H Tiba, MD, MS[1,2]

[1] Department of Emergency Medicine, [2]Michigan Center for Integrative Research in Critical Care (MCIRCC)
University of Michigan, Ann Arbor, MI

ABSTRACT

The Raman Resonance Spectroscopy (RRS) technology was developed in order to find an alternative and a potential surrogate to the measurements of mixed venous oxygen saturation (SmvO2) using a central line, which is an invasive way to monitor cardiac patients or other hospitalized patients. RRS is used through a light probe that is placed on the inner cheek of the patient. The StO2 values will be compared to a blood case sample. We utilized several statistical methods including Bland/Altman, t tests, and regression models that allow us to compare oxygen saturation in the blood versus the RRS tissue levels. Our data analysis already suggests that the RRS technology is very accurate and analogous to the SmvO2 measurements. The hope is that RRS can be incorporated into modern medicine in support of a central line as a noninvasive and safer alternative.

INTRODUCTION

Measuring oxygen saturation of mixed venous blood (SmvO2) is an important factor in monitoring critically ill patients, offering information essential to the prognosis and treatment management of these patients. In typical clinical settings, monitoring venous oxygenation can be an invasive process and carries the risk of complications. The use of non-invasive technology can help reduce the risk and make these measurements more accessible. Resonance Raman Spectroscopy (RRS) is a novel optical technique capable of providing information on the vibrational and electronic properties of compounds, including oxy- and deoxyhemoglobin.

INTRODUCTION

Spectroscopic techniques produce hemoglobin signals that are heavily dominated by venous blood. In this study, RRS was used to monitor tissues oxygen saturation (StO2) noninvasively in a post-surgical setting and compared to the mixed venous oxygen saturation standard. We hypothesize that StO2 will reflect changes in ScvO2 and act as a surrogate non-invasive measure. Thus, the resulting aggregate StO2 should be reflective of the post extraction compartment of the tissue similar to SmvO2.

METHODS

Critically ill patients with a central venous catheter were recruited from the Cardiovascular Center. Informed consent was obtained from each patient before beginning any measurements. The RRS was placed in both the right and left buccal for five minutes each, approximately ten minutes in totality. StO2 measurements were collected over this time period. At the end, a blood sample was obtained from the most distal port of the central line and a final RRS measurement was obtained at this time, as well. The StO2 values were compared to the ScvO2 values using various statistical analysis methods.

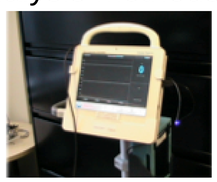

RESULTS

Twelve patients with an average(SD) age of 64(15) y/o were tested.
__ males and ___ females
All StO2 values are multiplied by 0.9.

RESULTS

	StO2	ScvO2
Mean	63.8	67.7
Std. Deviation	11.0	11.3
Lower 95% CI of mean	58.3	62.1
Upper 95% CI of mean	69.3	73.3
Minimum	42.0	48.0
Maximum	78.0	96.0

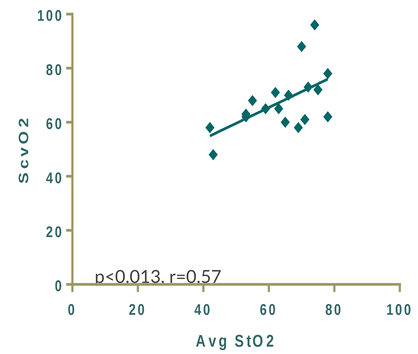

- The scatter plot demonstrates the significant correlation between StO_2 and $ScvO_2$.
- A paired t-test showed no significant difference between StO_2 and $ScvO_2$. Average(SD) difference of 4(10.)% (*95%CI: -1.2%, 9%, p=0.128)*
- Receiver operating characteristic (ROC) curve for StO_2 at thresholds of $ScvO_2$ between 65% and 70% have demonstrated high predictive power of StO_2 with area under the curve between 0.74 and 0.83 (*p < 0.006*).

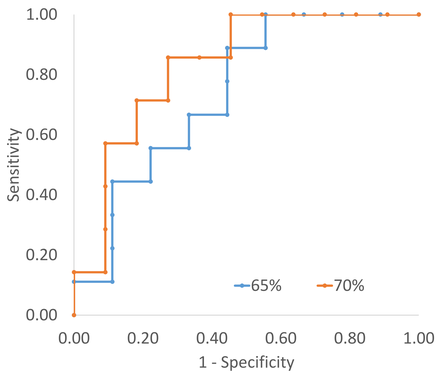

CONCLUSIONS

RRS is showing promise as a non-invasive alternative to ScvO2. StO2 measurements taken using RRS are highly correlated with ScvO2, which is an important measure of tissue oxygenation. Because of its non-invasive nature, RRS may serve as a faster, safer, and more cost effective way to assess patient tissue oxygenation, aiding in the diagnosis and treatment of conditions and critical states of health.

The Max Harry Weil Institute FOR CRITICAL CARE RESEARCH & INNOVATION

A Novel Noninvasive Impedance-based Technique for Central Venous Pressure Measurement

Isabella Sperry, Carmen I. Colmenero Mahmood, BS[1,2], Hakam Tiba, MD, MS[1,2]

[1]Department of Emergency Medicine, University of Michigan, Ann Arbor, Michigan, [2] The Max Harry Weil Institute for Critical Care Research and Innovation, University of Michigan, Ann Arbor, Michigan

MICHIGAN MEDICINE UNIVERSITY OF MICHIGAN

ABSTRACT

Introduction: The future of medicine is noninvasive, especially when monitoring high-risk trauma patients. The current standard for monitoring central venous pressure (CVP) requires invasive methods that might be associated with complications such as hemorrhage and infection.[1] We examined the ability of noninvasive central venous pressure (NICVP) to monitor CVP using bioimpedance. **Methods**: Patients were screened for the presence of a CVP line in the internal/external jugular or subclavian vein. Patients were monitored for a period of 5-10 minutes via a blood pressure cuff and four EKG stickers. The patient's CVP value was compared to the NICVP value during the monitoring period. **Results:** Analysis of a Bland-Altman plot gave a mean bias of 0.91 mmHg with a standard deviation of differences of 1.73 mmHg. The limits of agreement were -2.48 mmHg and 4.29 mmHg. **Conclusion:** NICVP may be an adequate substitute for CVP measurement and serve as a valuable tool for monitoring the critically ill and injured.[2]

INTRODUCTION

Central Venous Pressure

What is central venous pressure?

- Central venous catheters are used to monitor CVP invasively. CVP is an approximation of preload and right atrial pressure that assesses cardiac function and fluid status.[1]

Measuring central venous remains a challenge

- Using an indwelling catheter (gold standard) may be a poor indicator of fluid responsiveness, increasing the risk of clinical misdiagnosis and adverse outcomes.[1]
- Routine placement of central venous catheters is limited to hospitals and trained medical staff.
- CV line placements are associated with infection and failure.[2]

Electrobioimpedance

Bioimpedance measures the opposition to the electric current flowing through the tissues which can be used to measure blood volume (conductor of electricity).

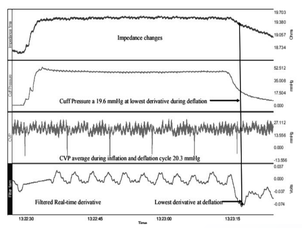

Figure 1: Multichannel view of CVP and NICVP measurement.

System operations

The outer electrodes on the shoulder and wrist inject a current, while the inner electrodes on the biceps receive the returned potential. During the measurements, the cuff pressure shows changes in impedance due to fluctuating blood volume. The lowest derivative point of impedance changes is aligned with the cuff pressure, as seen in Figure 1, which is ideally equal to CVP at the point.

Aim

In this study, we evaluate the efficacy of a noninvasive method to measure CVP utilizing bioimpedance. Non-invasive techniques for monitoring the critically ill and injured reduce the risk of complications such as infection and inaccurate values.

METHODS

Screening

Inclusion Criteria:	Exclusion Criteria:	University of Michigan Hospital Locations:
Aged 18+; jugular or subclavian vein placement of central line.	Pregnant women, prisoners, immunocompromisation, or Covid-19.	CVC, SICU, CCICU, Trauma and Burn.

Data Collection

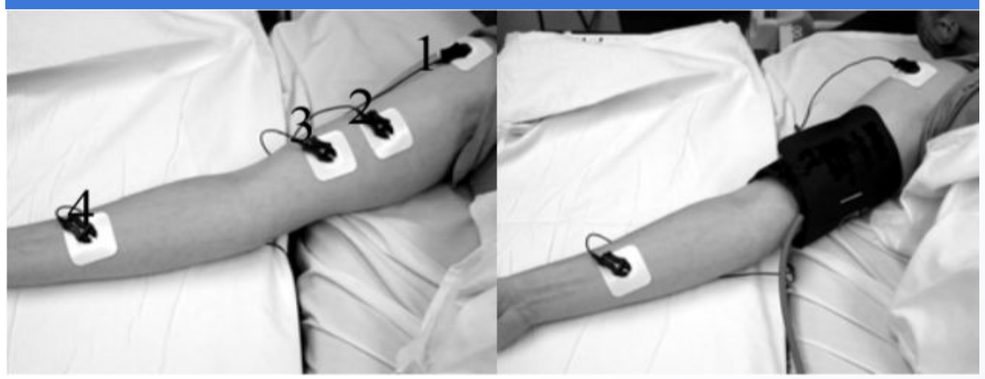

Figure 2: Four current-injecting EKG electrodes were placed in the arm, as seen in Figure 2 above, with a blood pressure cuff wrapped around the electrodes over the brachial-axillary vein system.[2]

RESULTS

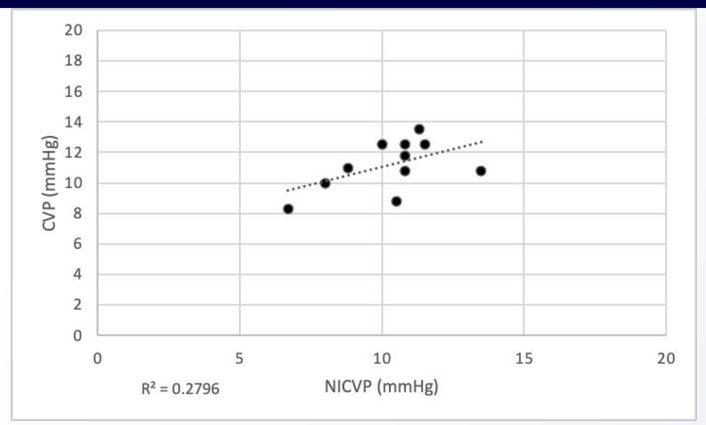

Figure 3: Pearson correlation of n=11 measures of NICVP with CVP. Correlation was 0.263.

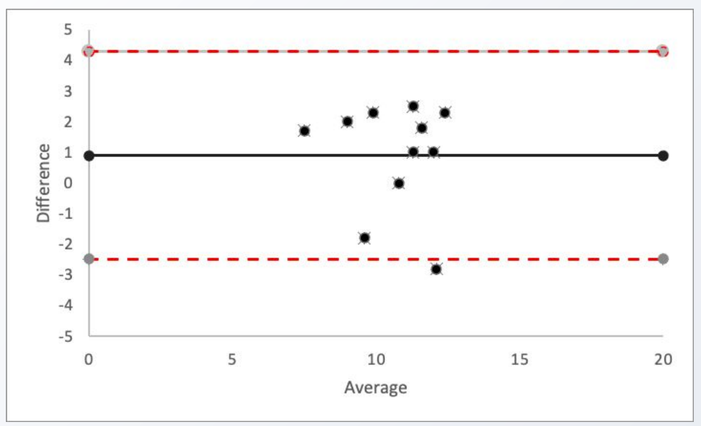

Figure 4: Bland-Altman plot of n=11 measures of NICVP with CVP.

CONCLUSIONS

Figure 3: CVP had an average of 10.25 mmHg with a 1.84 standard deviation, and NICVP had an average of 11.14 mmHg with a 1.63 standard deviation. CVP values ranged from 6.7 mmHg to 13.5 mmHg, and NICVP values ranged from 8.3 mmHg and 13.5 mmHg.

Figure 4: Bland-Altman plot of all 44 measures from 11 subjects (four measures per subject). The mean bias was 0.91 mmHg with a standard deviation of differences of 1.76 mmHg. The limits of agreement were -2.49 mmHg and 4.29 mmHg.

- Physicians have deemed that a pressure difference of 3 to 4 mmHg clinically acceptable without affecting the quality of care.
- On average, NICVP measurements tracked CVP measurements within the clinically acceptable range and showed a moderately strong correlation.
- **This small pool of data demonstrates that NICVP as determined by measuring impedance-based volume changes in the upper arm may have sufficiently small bias and limits of agreement to serve as an alternative method to measure CVP.**

Future Directions

Figure 5: Previous model of the NICVP Device

- We are still collecting data and working on analyzing the larger cohort of patients using statistical methodologies such as Clarke's Error Grid and regression models.
- This analysis supports the study hypothesis that NICVP may serve as a clinically useful substitute for traditional CVP measurement and may expand to other hospitals in the nation for further research.
- Hopefully, this information will be used to help patients and soldiers on the battlefield.

ACKNOWLEDGMENTS

Mentorship

Hakam Tiba, M.D., M.S.
Carmen Colmenero Mahmood, B.S.
Samara Kamal

Support

The Max Harry Weil Institute for Critical Care Research & Innovation
The U.S. Department of Defense

Isabella Sperry (left) and Carmen Colmenero Mahmood (right).

References

[1]Kornbau, C., Lee, K. C., Hughes, G. D., & Firstenberg, M. S. (2015). Central line complications. *International journal of critical illness and injury science*, *5*(3), 170–178. https://doi.org/10.4103/2229-5151.164940

[2]Ward KR, Tiba MH, Draucker GT, Proffitt EK, Barbee RW, Gunnerson KJ, Reynolds PS, Spiess BD. A novel noninvasive impedance-based technique for central venous pressure measurement. Shock. 2010 Mar;33(3):269-73. doi: 10.1097/SHK.0b013e3181ab9b9b. PMID: 19487978.

UROP UNIVERSITY OF MICHIGAN

US007113814B2

(12) **United States Patent**
Ward et al.

(10) **Patent No.: US 7,113,814 B2**
(45) **Date of Patent: Sep. 26, 2006**

(54) **TISSUE INTERROGATION SPECTROSCOPY**

(75) Inventors: **Kevin R. Ward**, Glen Allen, VA (US); **R. Wayne Barbee**, Richmond, VA (US); **James Terner**, Richmond, VA (US); **Rao R. Ivatury**, Richmond, VA (US); **Fred Hawkridge**, Glen Allen, VA (US)

(73) Assignee: **Virginia Commonwealth University**, Richmond, VA (US)

(*) Notice: Subject to any disclaimer, the term of this patent is extended or adjusted under 35 U.S.C. 154(b) by 277 days.

(21) Appl. No.: **10/332,613**

(22) PCT Filed: **Jul. 13, 2001**

(86) PCT No.: **PCT/US01/22187**

§ 371 (c)(1),
(2), (4) Date: **Jul. 29, 2003**

(87) PCT Pub. No.: **WO02/07585**

PCT Pub. Date: **Jan. 31, 2002**

(65) **Prior Publication Data**

US 2004/0039269 A1 Feb. 26, 2004

Related U.S. Application Data

(60) Provisional application No. 60/218,055, filed on Jul. 13, 2000.

(51) **Int. Cl.**
A61B 5/00 (2006.01)

(52) **U.S. Cl.** **600/310**; 600/476

(58) **Field of Classification Search** 600/310, 600/322, 323, 473, 476; 356/301, 303, 317–320; 250/341.1

See application file for complete search history.

(56) **References Cited**

U.S. PATENT DOCUMENTS

5,769,081 A 6/1998 Alfano et al.
5,991,653 A 11/1999 Richards-Kortum et al.

Primary Examiner—Eric F. Winakur
(74) *Attorney, Agent, or Firm*—Whitham, Curtis & Christofferson, PC

(57) **ABSTRACT**

In an emergency medicine patient, accurate measurement of change or lack thereof from non-shock, non-ischemic, non-inflammation, non-tissue injury, non-immune dysfunction conditions is important and is provided, as practical, real-time approaches for accurately characterizing a patient's condition, using Raman (**3**) and/or fluorescence (**30**) spectroscopy with a high degree of accuracy. Measurement times are on the order of seconds. High-accuracy measurement is achieved with Raman spectroscopy interrogation of tissue. Simultaneous interrogation by NADH fluorescence spectroscopy may he used. Measurements may be non-invasive to minimally invasive. Preclinical (ultra-early) states of shock can be detected (**5**), severity can be determined, effectiveness of various treatments can be determined.

70 Claims, 35 Drawing Sheets

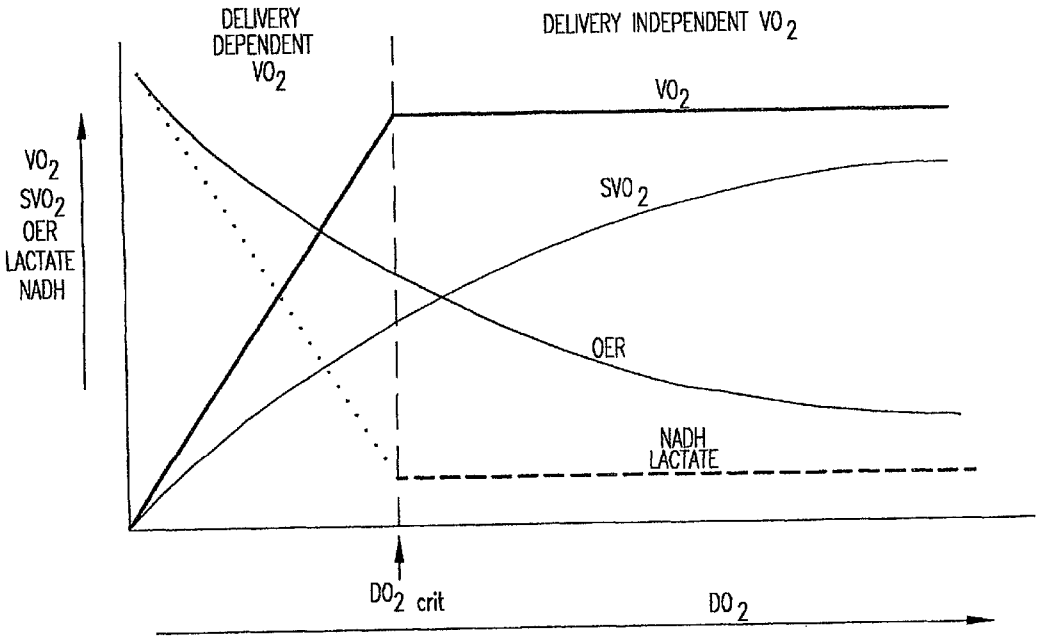

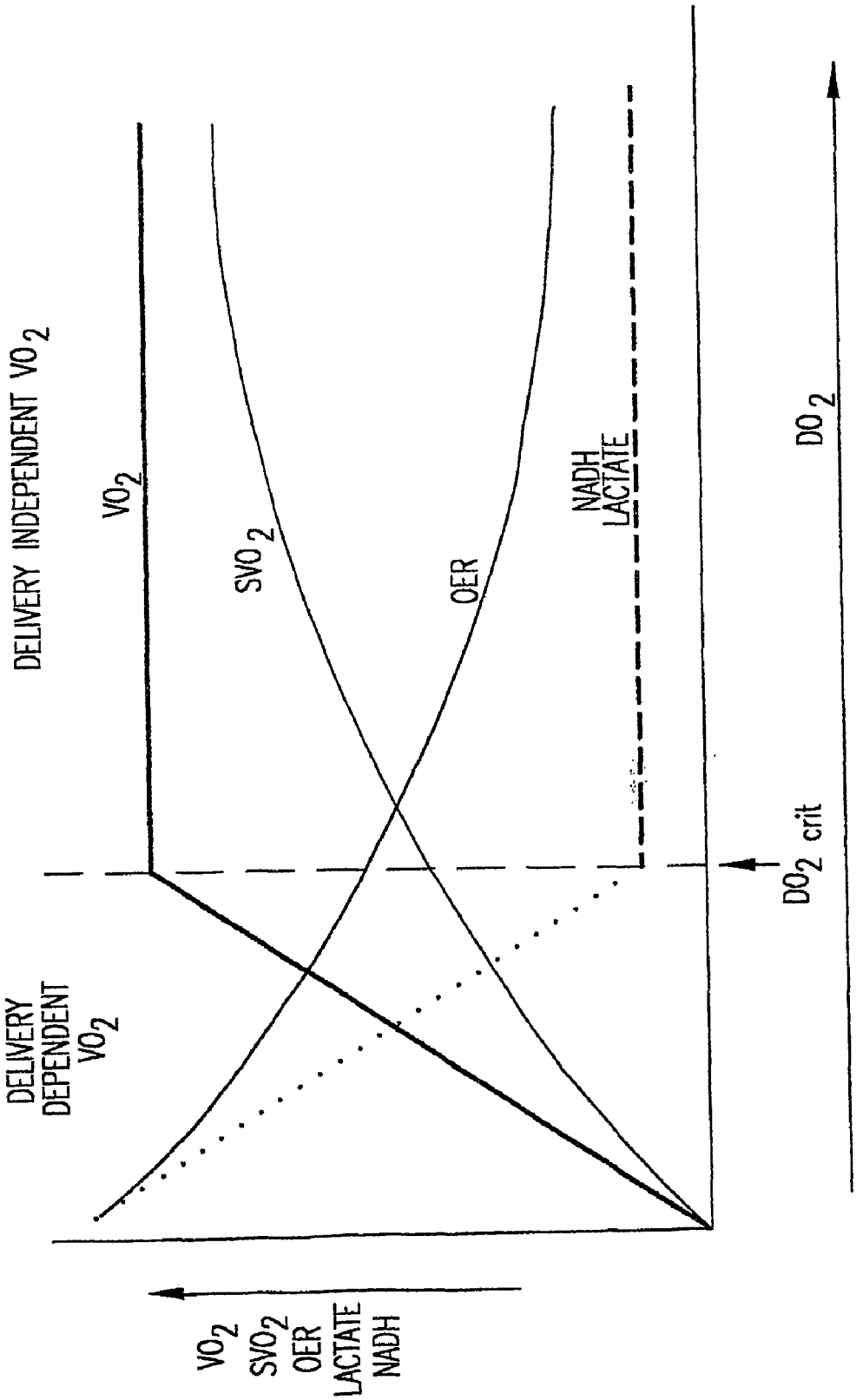
DELIVERY INDEPENDENT VO_2
VO_2
SVO_2
OER
NADH
LACTATE
DO_2
DO_2 crit
DELIVERY DEPENDENT VO_2
VO_2
SVO_2
OER
LACTATE
NADH

FIG. 1

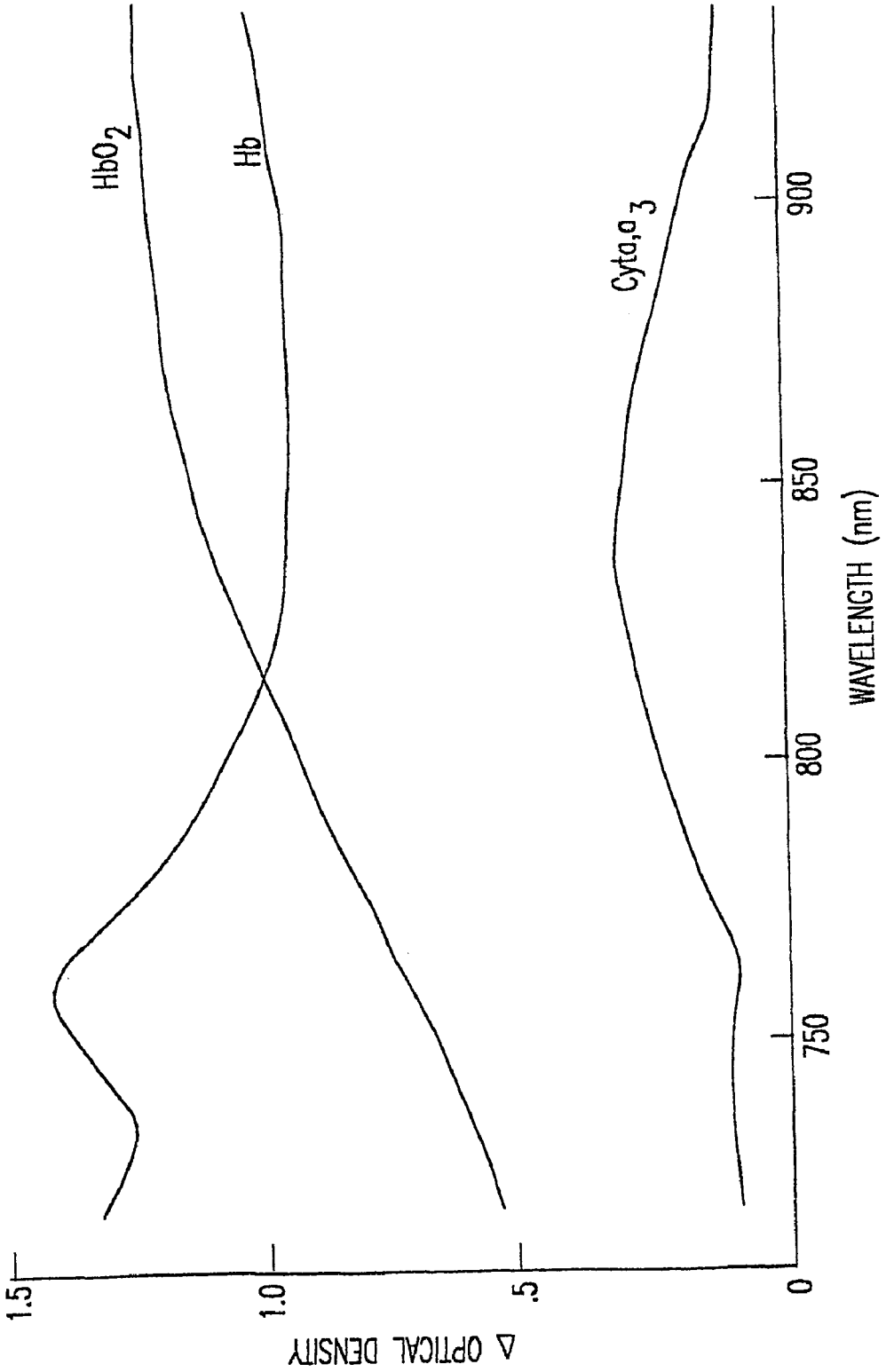
HbO_2
Hb
$Cyta,a_3$
1.5
1.0
.5
0
Δ OPTICAL DENSITY
750
800
850
900
WAVELENGTH (nm)

FIG.2

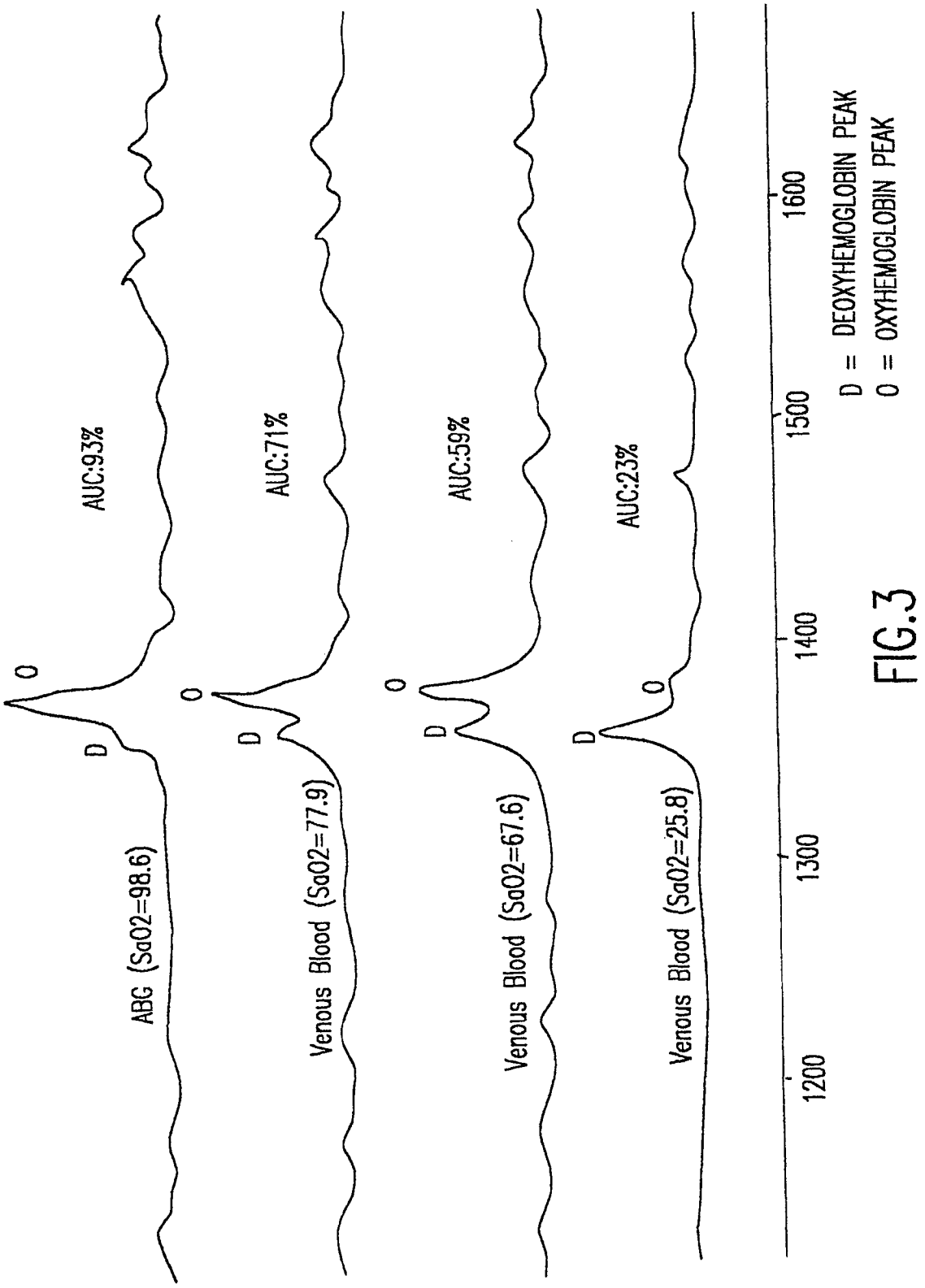
ABG (SaO2=98.6)
AUC:93%
Venous Blood (SaO2=77.9)
AUC:71%
Venous Blood (SaO2=67.6)
AUC:59%
Venous Blood (SaO2=25.8)
AUC:23%
D
O
1200
1300
1400
1500
1600
D = DEOXYHEMOGLOBIN PEAK
O = OXYHEMOGLOBIN PEAK

FIG.3

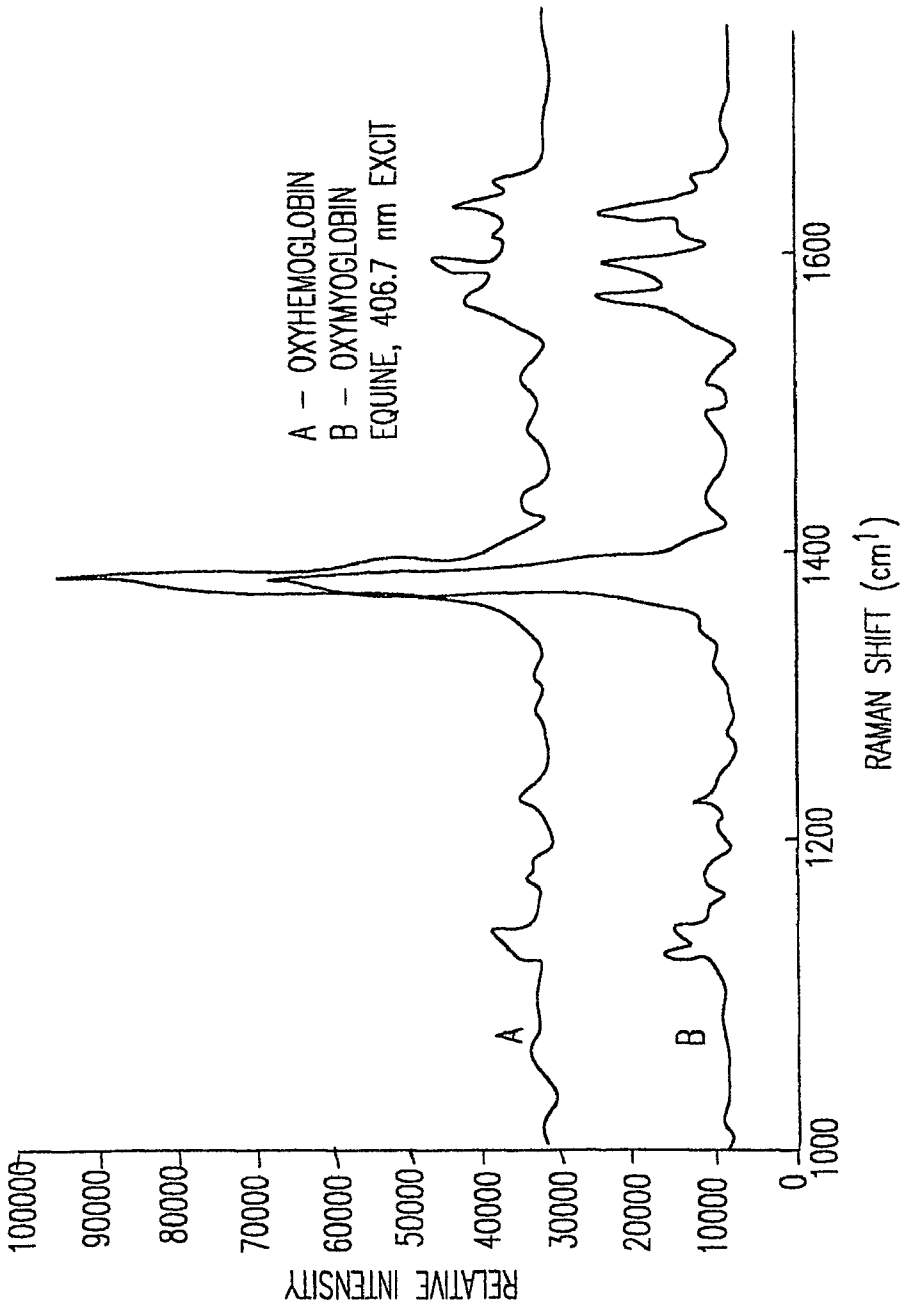
A – OXYHEMOGLOBIN
B – OXYMYOGLOBIN
EQUINE, 406.7 nm EXCIT
A
B
RELATIVE INTENSITY
100000
90000
80000
70000
60000
50000
40000
30000
20000
10000
0
1000
1200
1400
1600
RAMAN SHIFT (cm-1)

FIG.4

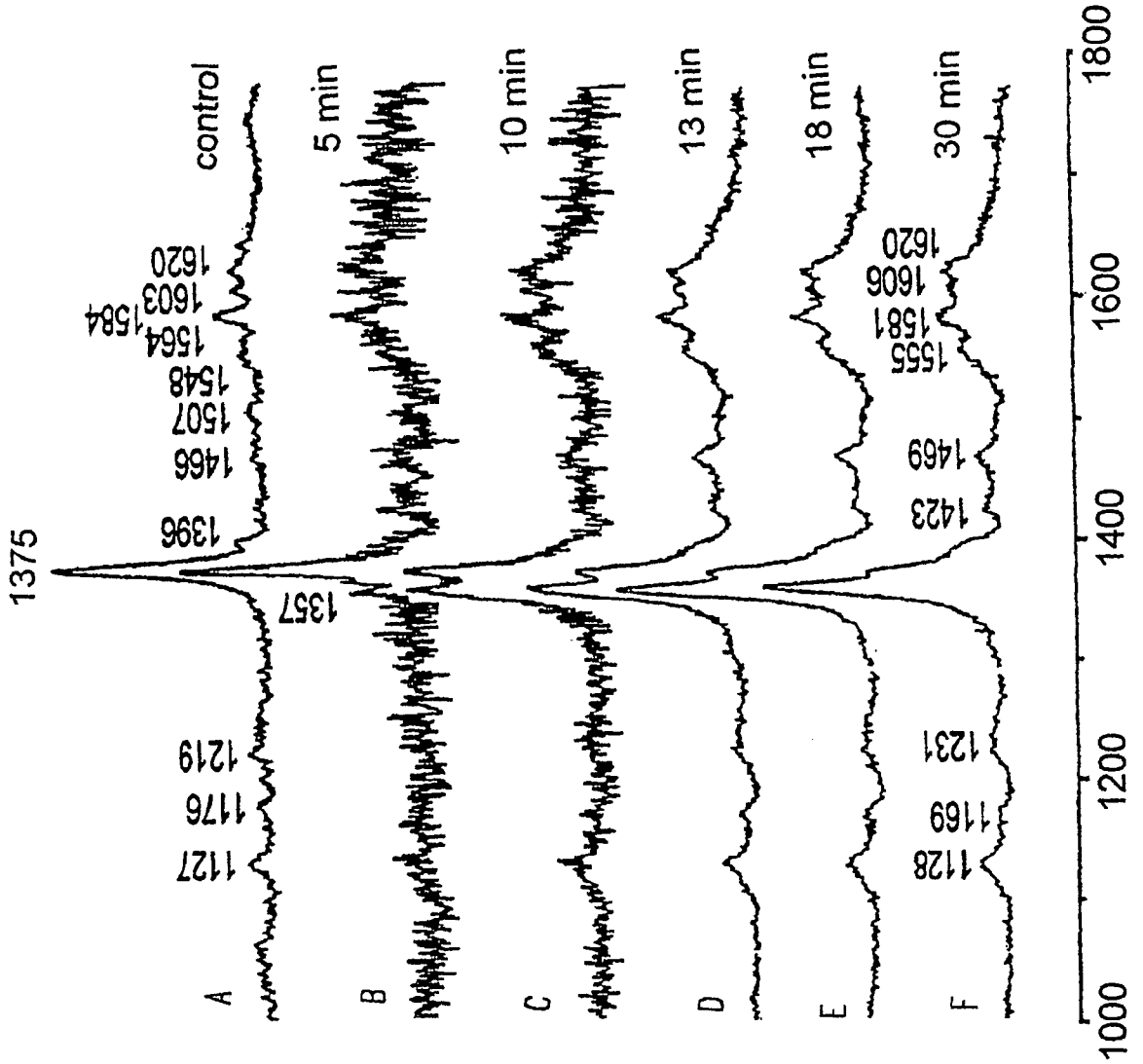
control
5 min
10 min
13 min
18 min
30 min
A
B
C
D
E
F
1375
1357
1396
1466
1507
1548
1564
1584
1603
1620
1219
1176
1127
1423
1469
1555
1581
1606
1620
1231
1169
1128
1000
1200
1400
1600
1800

FIG.5

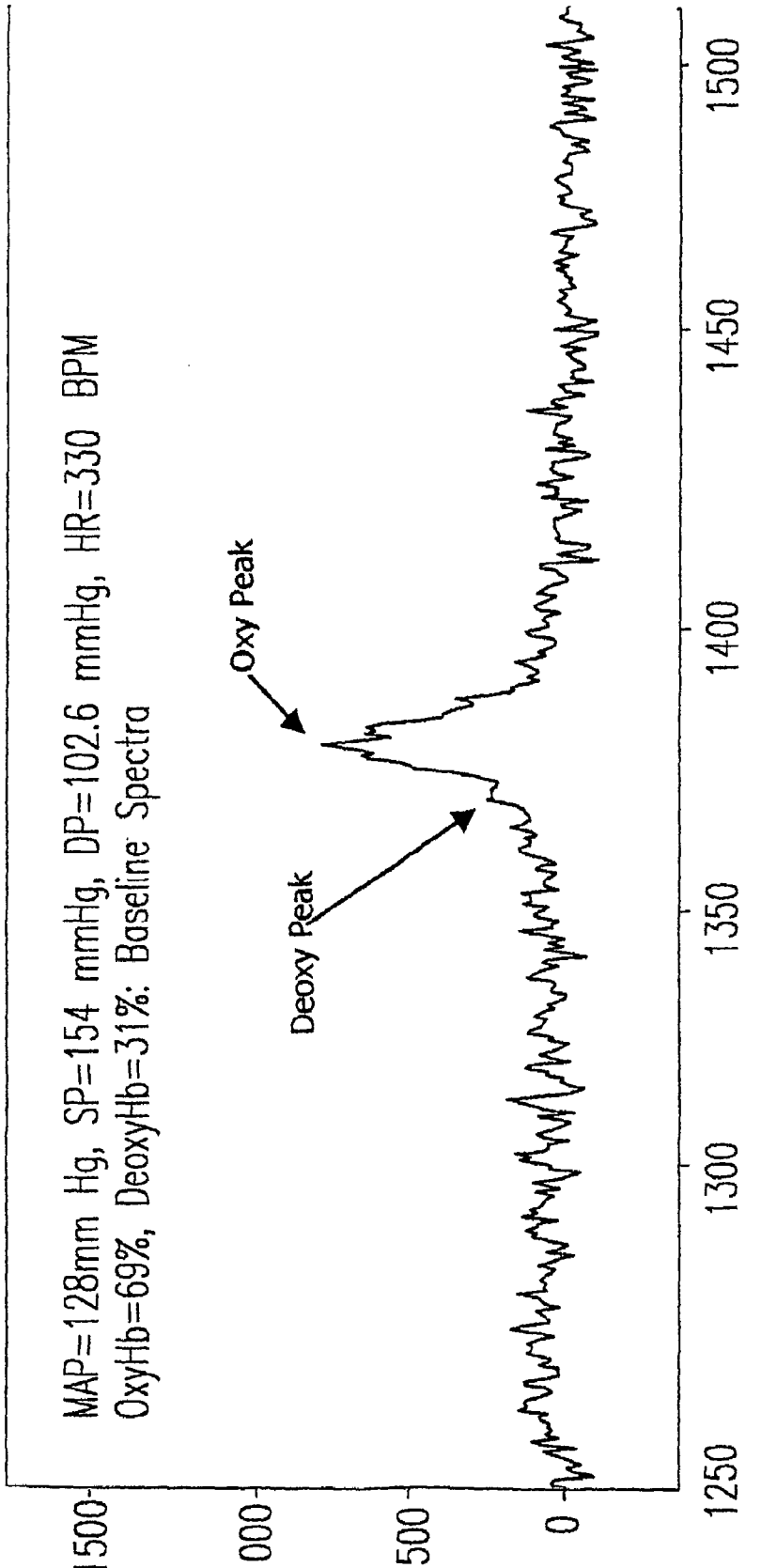
MAP=128mm Hg, SP=154 mmHg, DP=102.6 mmHg, HR=330 BPM
OxyHb=69%, DeoxyHb=31%: Baseline Spectra
Oxy Peak
Deoxy Peak
1500
1000
500
0
1250
1300
1350
1400
1450
1500

FIG.6

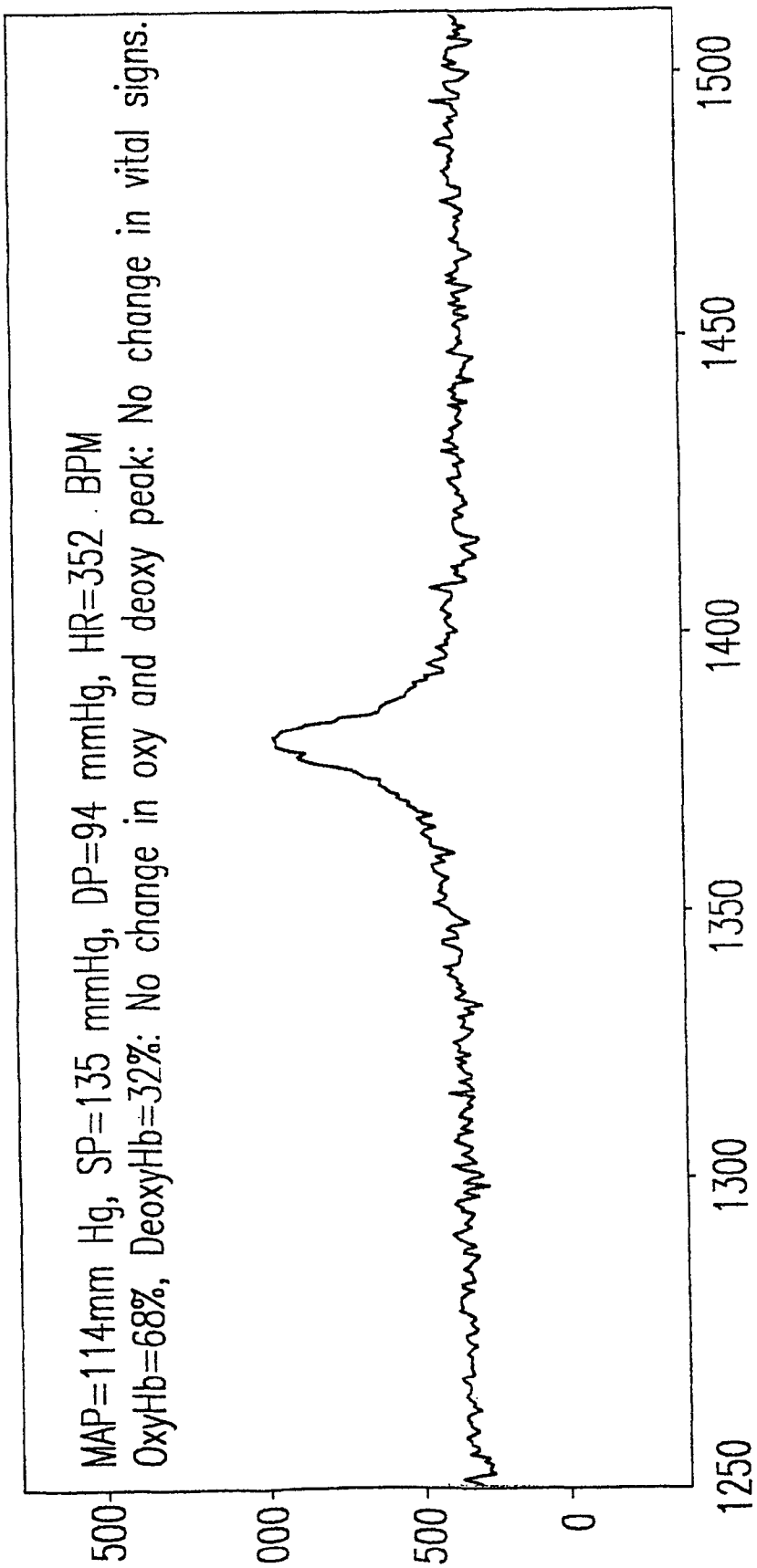
MAP=114mm Hg, SP=135 mmHg, DP=94 mmHg, HR=352 BPM
OxyHb=68%, DeoxyHb=32%: No change in oxy and deoxy peak: No change in vital signs.
1500
1000
500
0
1250
1300
1350
1400
1450
1500

FIG.7

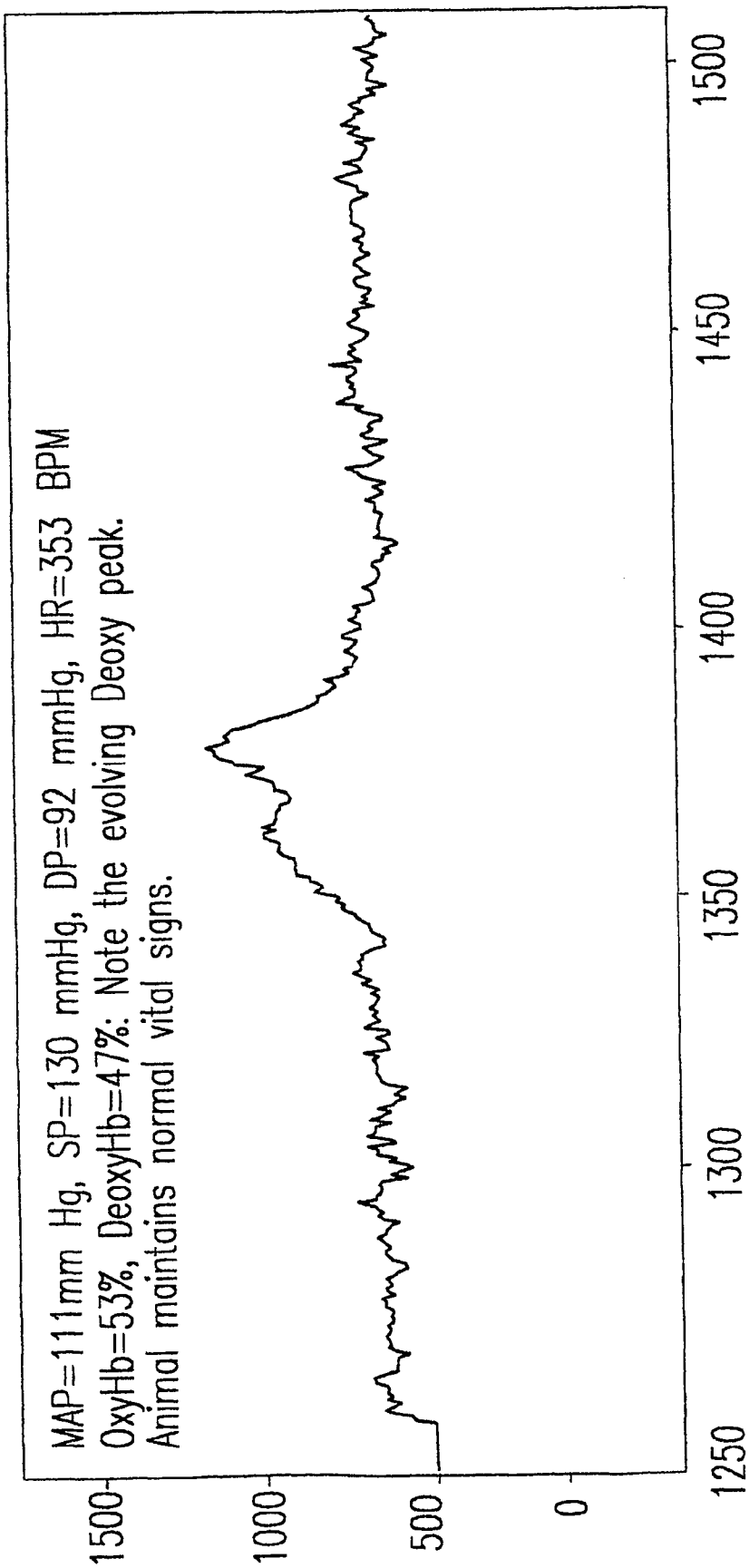
MAP=111mm Hg, SP=130 mmHg, DP=92 mmHg, HR=353 BPM
OxyHb=53%, DeoxyHb=47%: Note the evolving Deoxy peak.
Animal maintains normal vital signs.
1500
1000
500
0
1250
1300
1350
1400
1450
1500

FIG.8

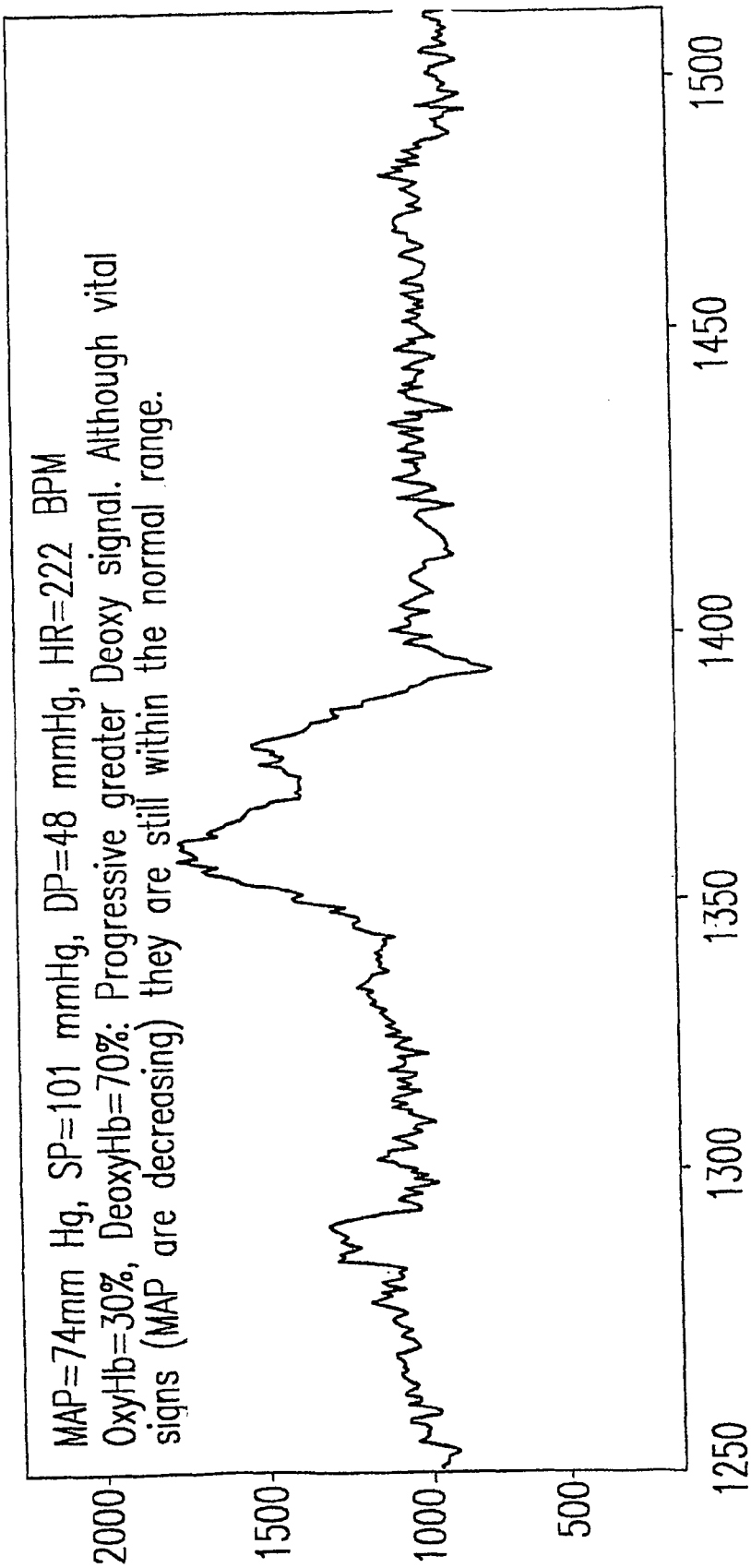
MAP=74mm Hg, SP=101 mmHg, DP=48 mmHg, HR=222 BPM
OxyHb=30%, DeoxyHb=70%: Progressive greater Deoxy signal. Although vital signs (MAP are decreasing) they are still within the normal range.
2000
1500
1000
500
1250
1300
1350
1400
1450
1500

FIG.9

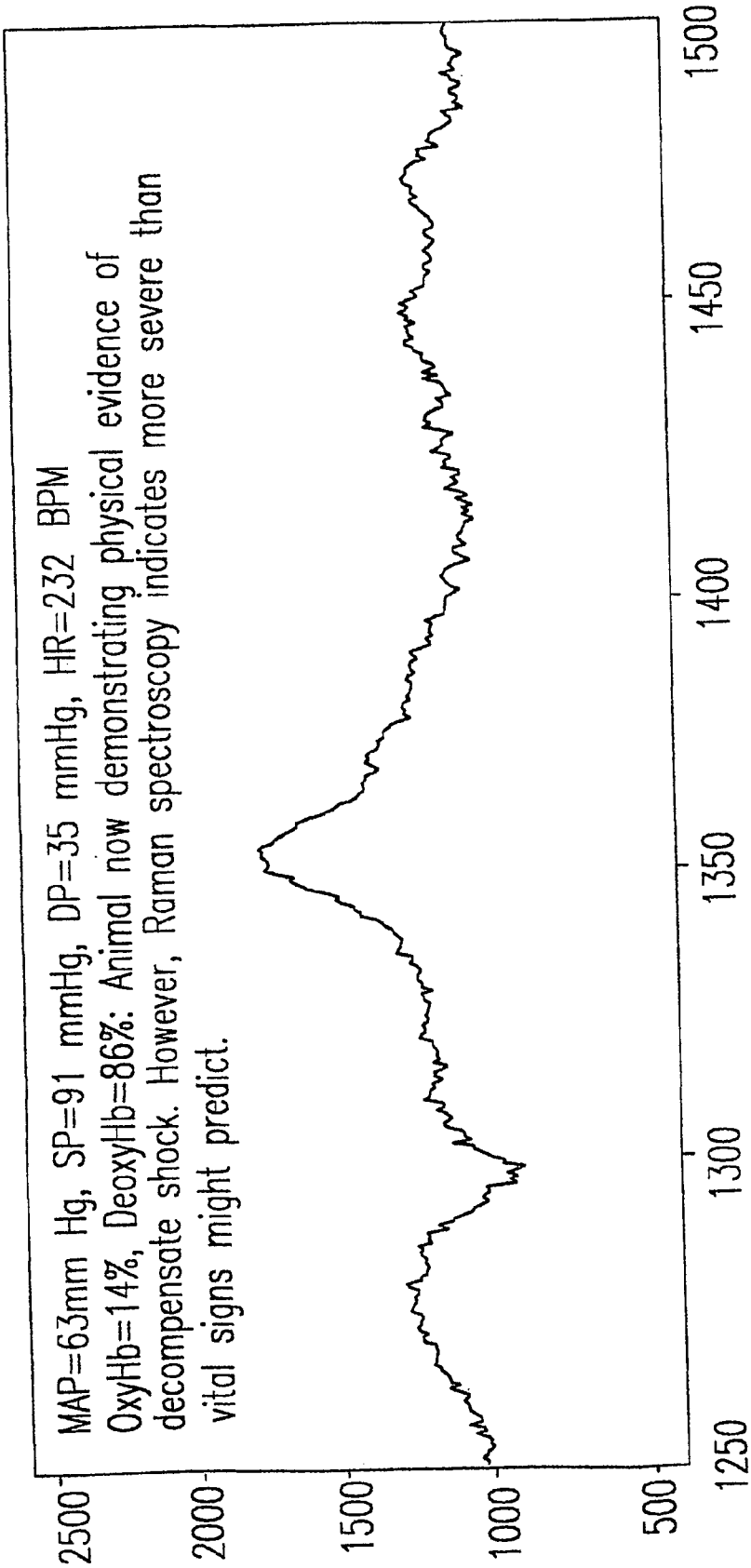
MAP=63mm Hg, SP=91 mmHg, DP=35 mmHg, HR=232 BPM
OxyHb=14%, DeoxyHb=86%: Animal now demonstrating physical evidence of decompensate shock. However, Raman spectroscopy indicates more severe than vital signs might predict.
2500
2000
1500
1000
500
1250
1300
1350
1400
1450
1500

FIG.10

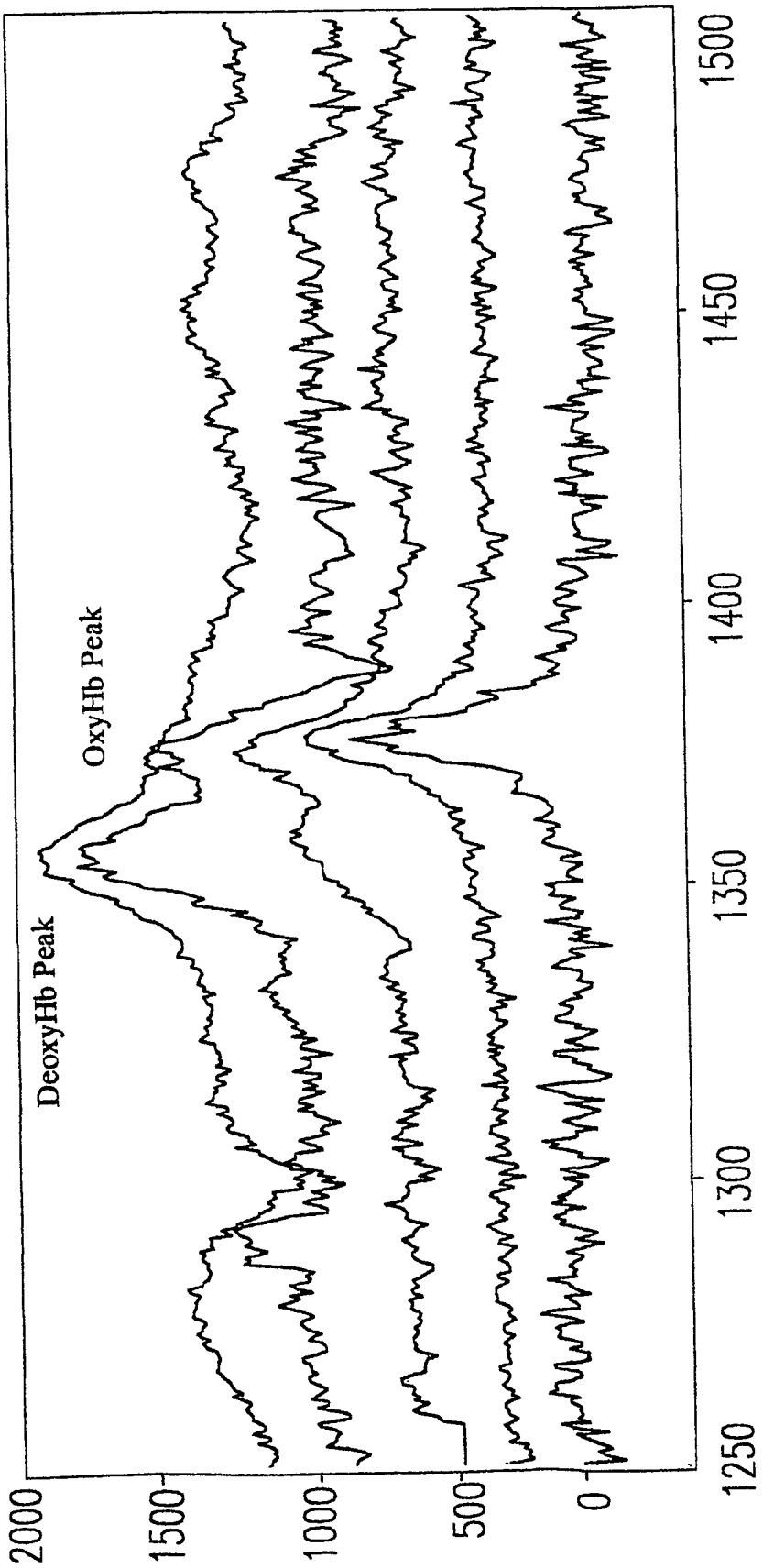
DeoxyHb Peak
OxyHb Peak
2000
1500
1000
500
0
1250
1300
1350
1400
1450
1500

FIG. 11

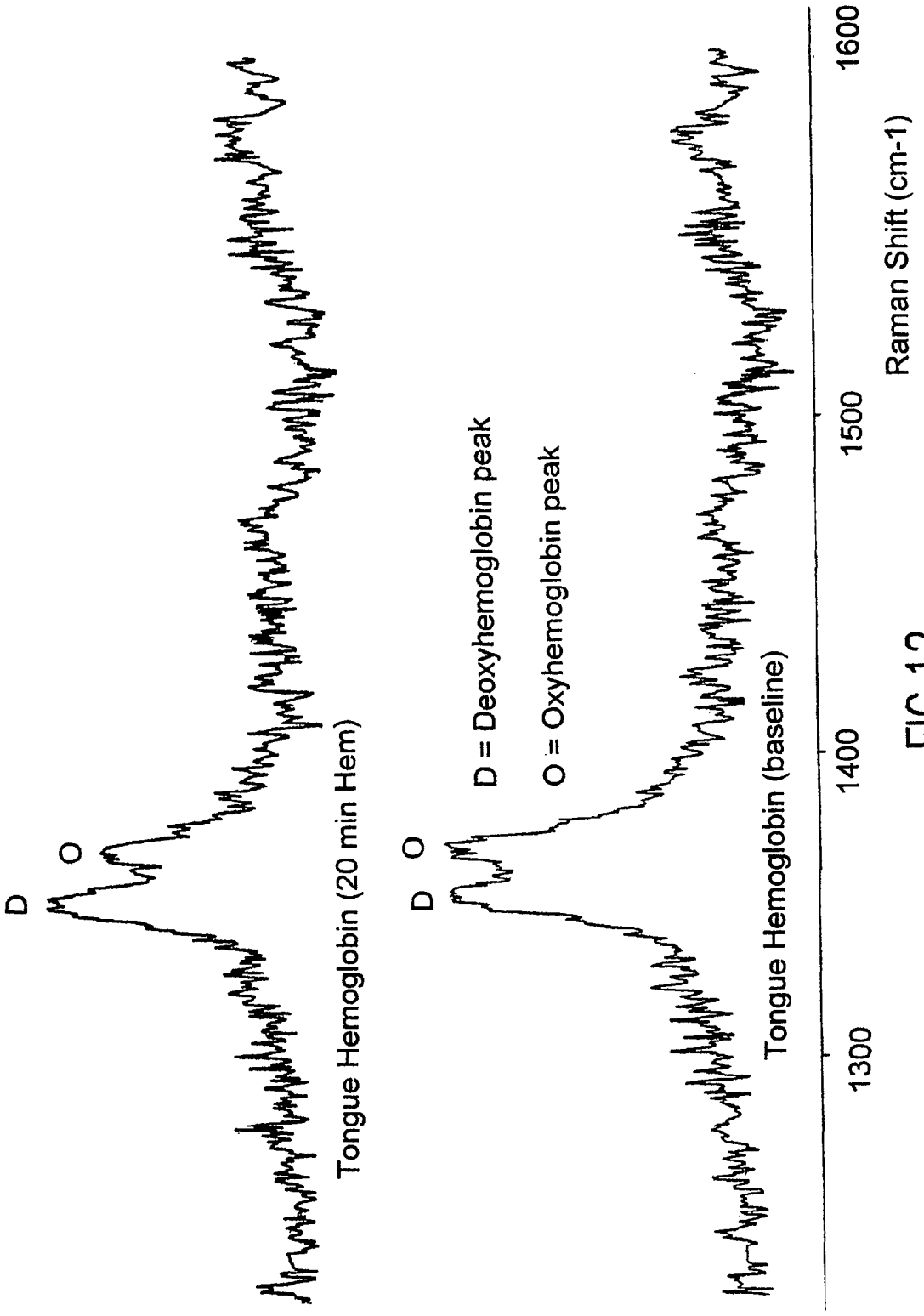
D
O
Tongue Hemoglobin (20 min Hem)
D
O
D = Deoxyhemoglobin peak
O = Oxyhemoglobin peak
Tongue Hemoglobin (baseline)
1300
1400
1500
1600
Raman Shift (cm-1)

FIG.12

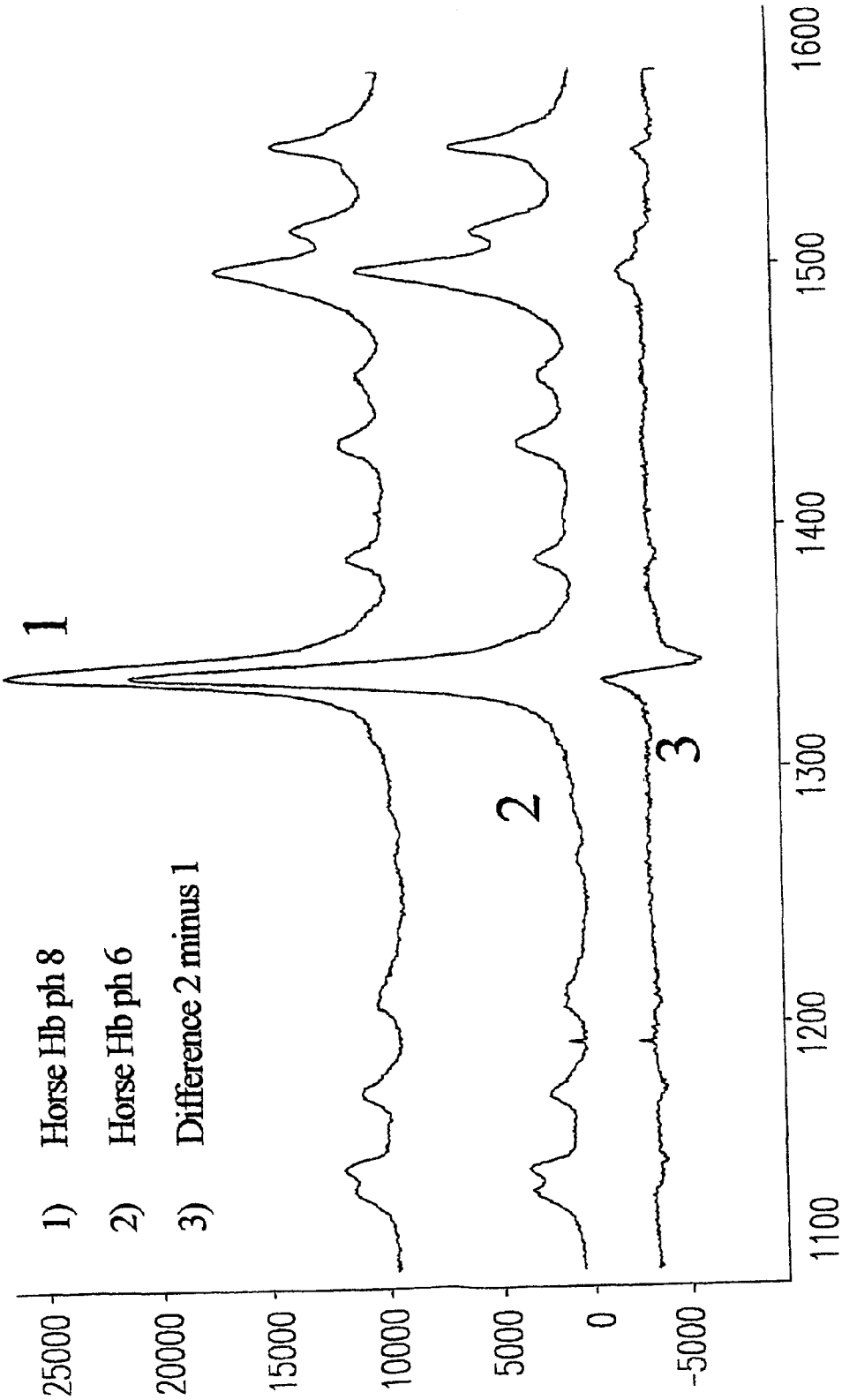
1) Horse Hb ph 8
2) Horse Hb ph 6
3) Difference 2 minus 1
1
2
3
25000
20000
15000
10000
5000
0
-5000
1100
1200
1300
1400
1500
1600

FIG.13

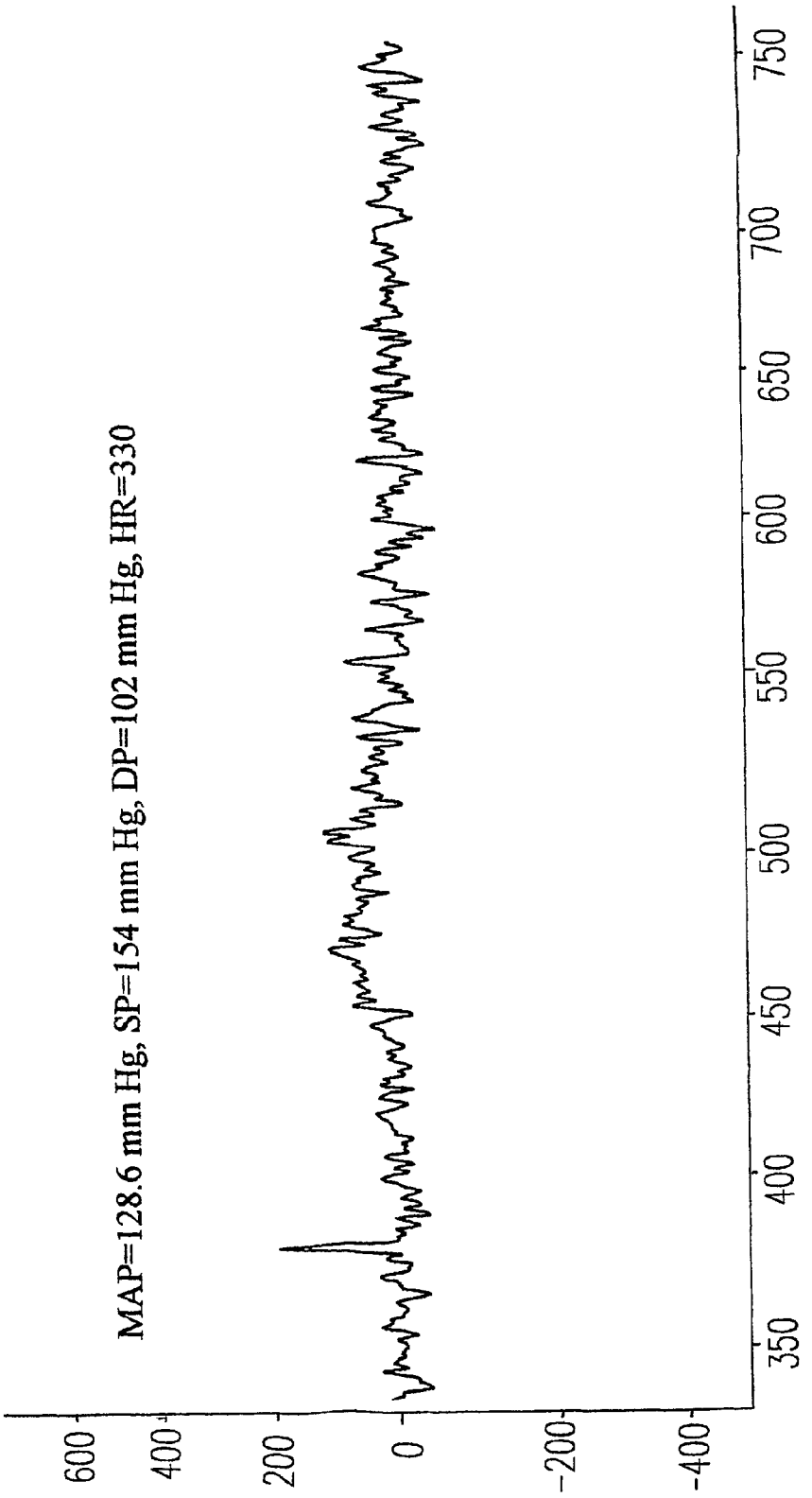
MAP=128.6 mm Hg, SP=154 mm Hg, DP=102 mm Hg, HR=330
600
400
200
0
-200
-400
350
400
450
500
550
600
650
700
750

FIG.14

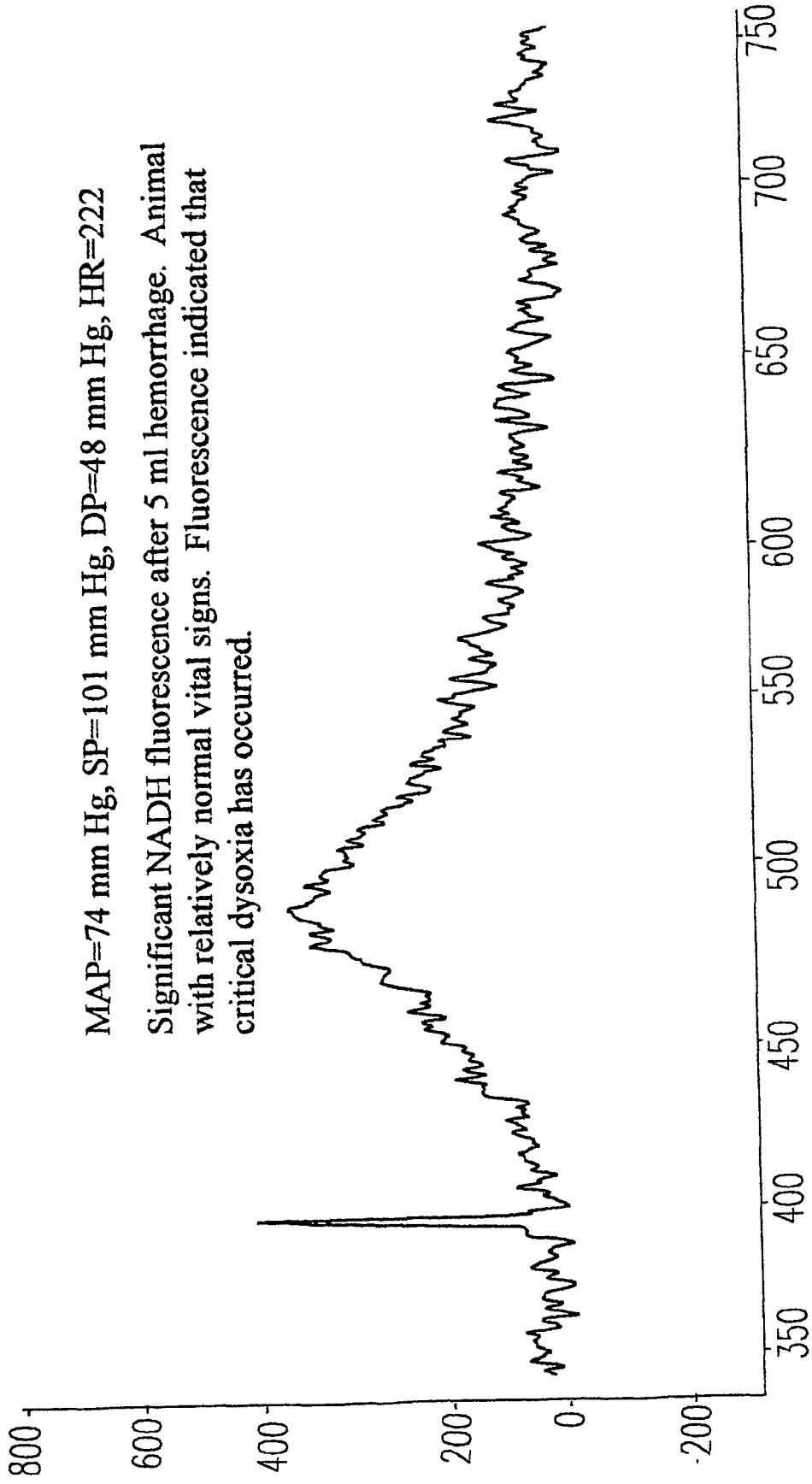
MAP=74 mm Hg, SP=101 mm Hg, DP=48 mm Hg, HR=222
Significant NADH fluorescence after 5 ml hemorrhage. Animal with relatively normal vital signs. Fluorescence indicated that critical dysoxia has occurred.
800
600
400
200
0
-200
350
400
450
500
550
600
650
700
750

FIG.15

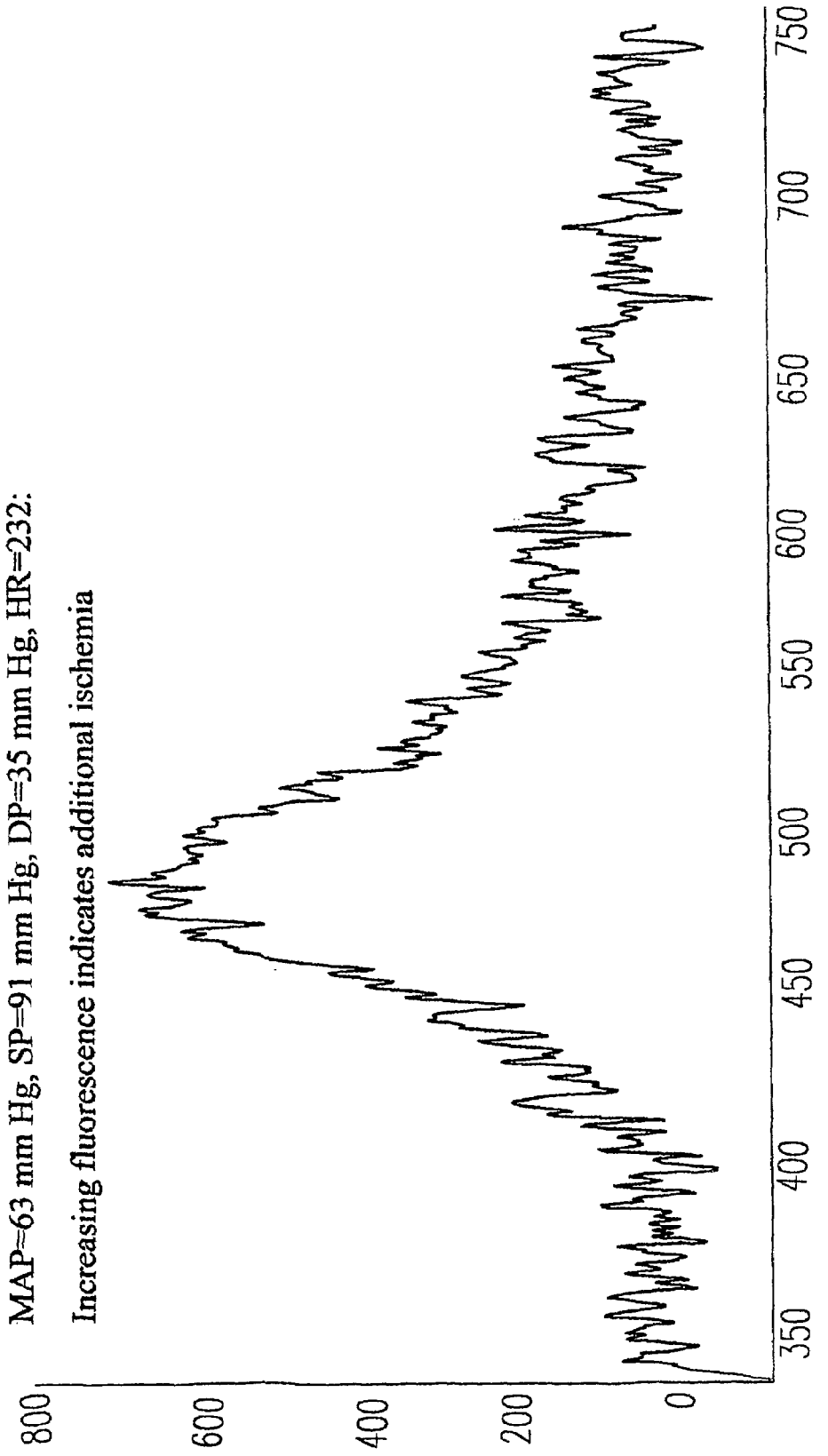
MAP=63 mm Hg, SP=91 mm Hg, DP=35 mm Hg, HR=232:
Increasing fluorescence indicates additional ischemia
800
600
400
200
0
350
400
450
500
550
600
650
700
750

FIG.16

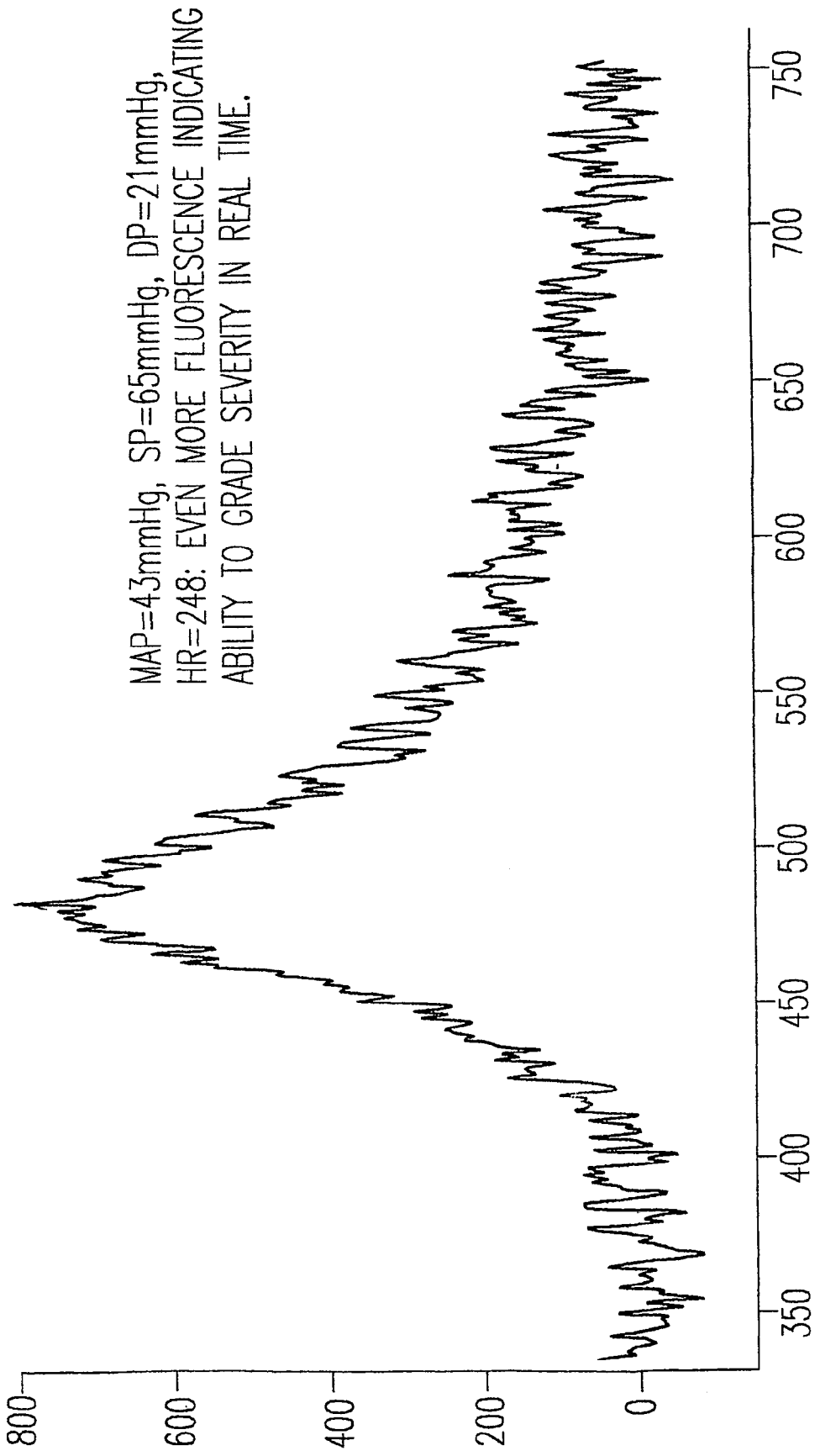
MAP=43mmHg, SP=65mmHg, DP=21mmHg,
HR=248: EVEN MORE FLUORESCENCE INDICATING
ABILITY TO GRADE SEVERITY IN REAL TIME.
800
600
400
200
0
350
400
450
500
550
600
650
700
750

FIG.17

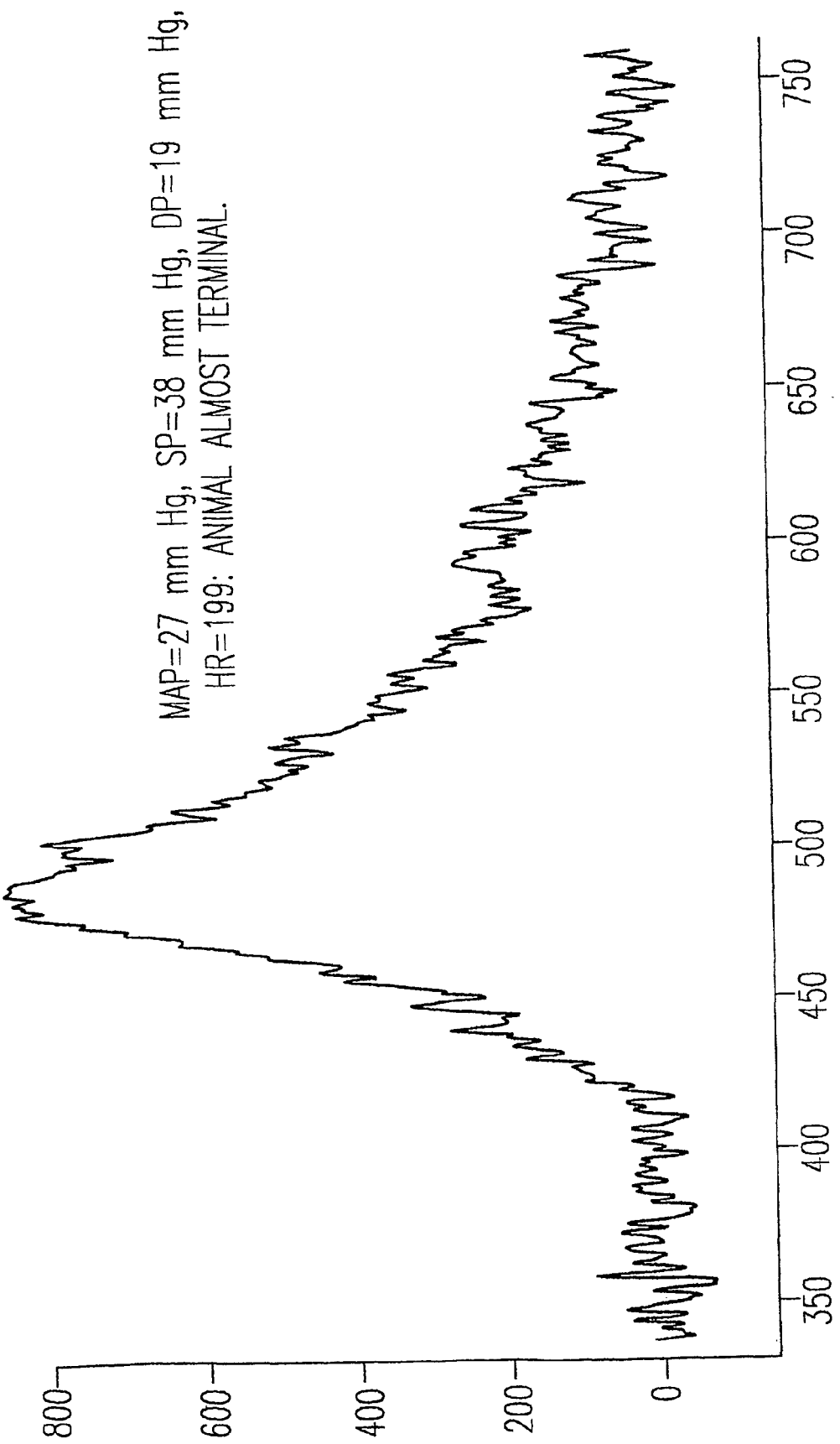
MAP=27 mm Hg, SP=38 mm Hg, DP=19 mm Hg,
HR=199: ANIMAL ALMOST TERMINAL.
800
600
400
200
0
350
400
450
500
550
600
650
700
750

FIG.18

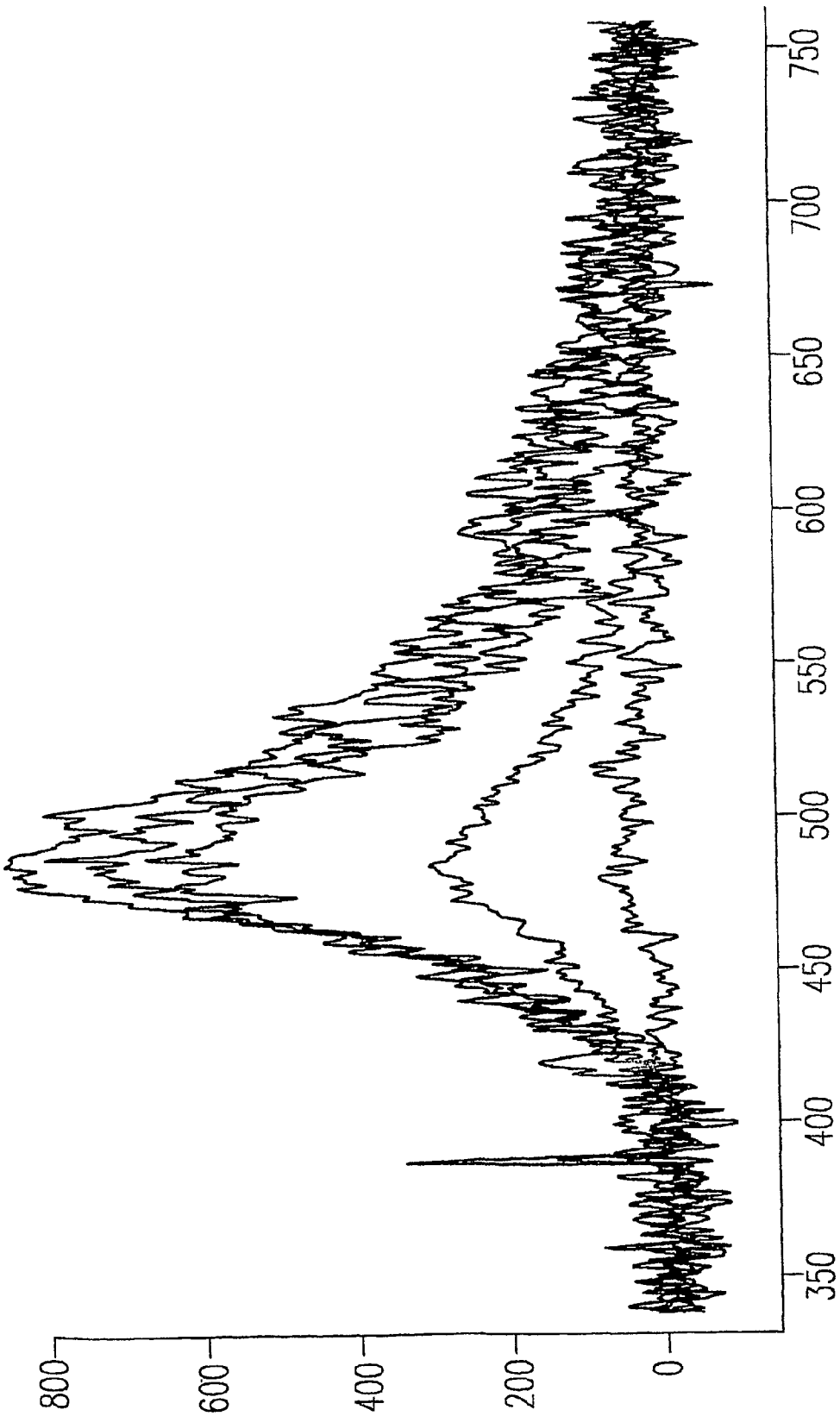

FIG.19

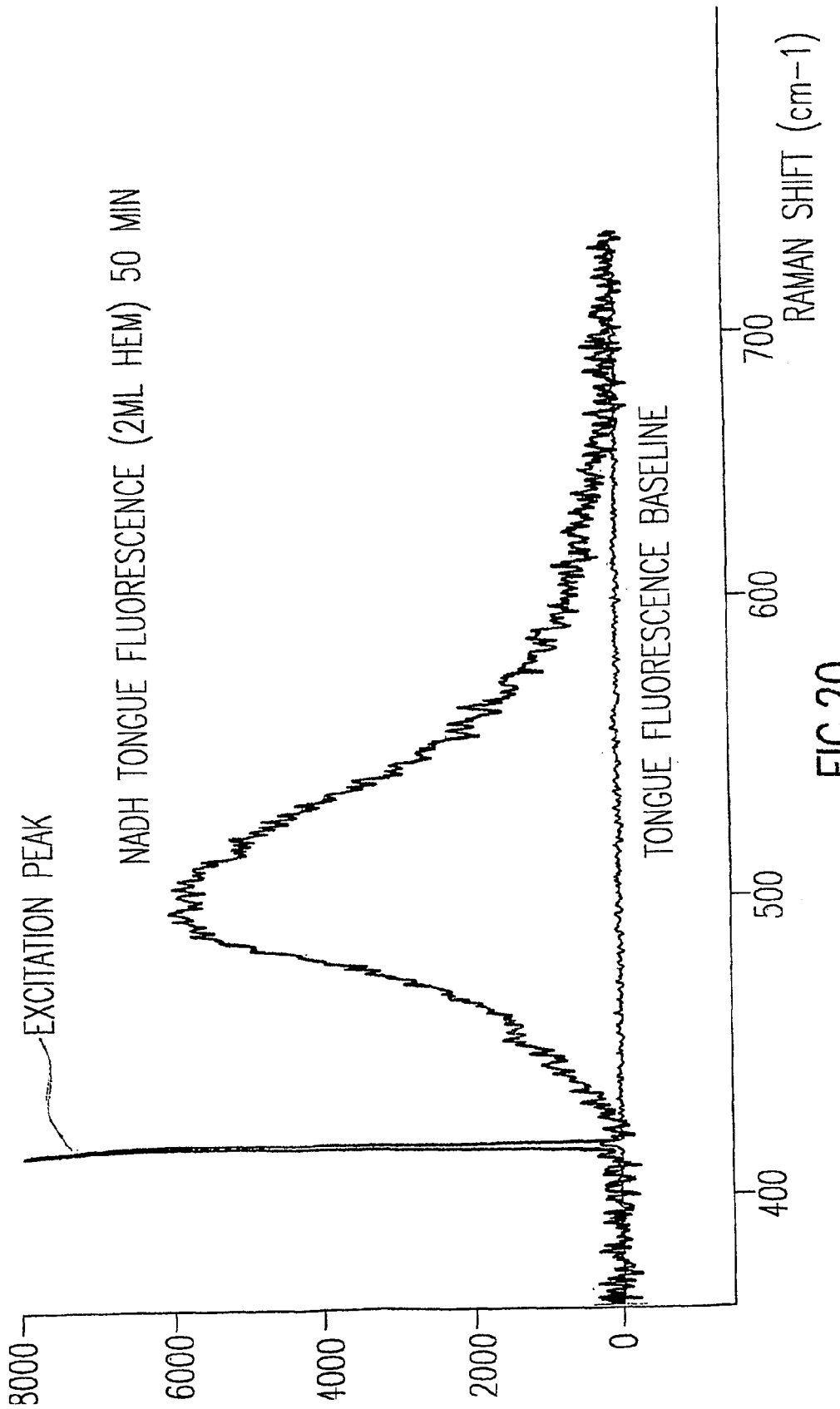
EXCITATION PEAK
NADH TONGUE FLUORESCENCE (2ML HEM) 50 MIN
TONGUE FLUORESCENCE BASELINE
8000
6000
4000
2000
0
400
500
600
700
RAMAN SHIFT (cm-1)

FIG.20

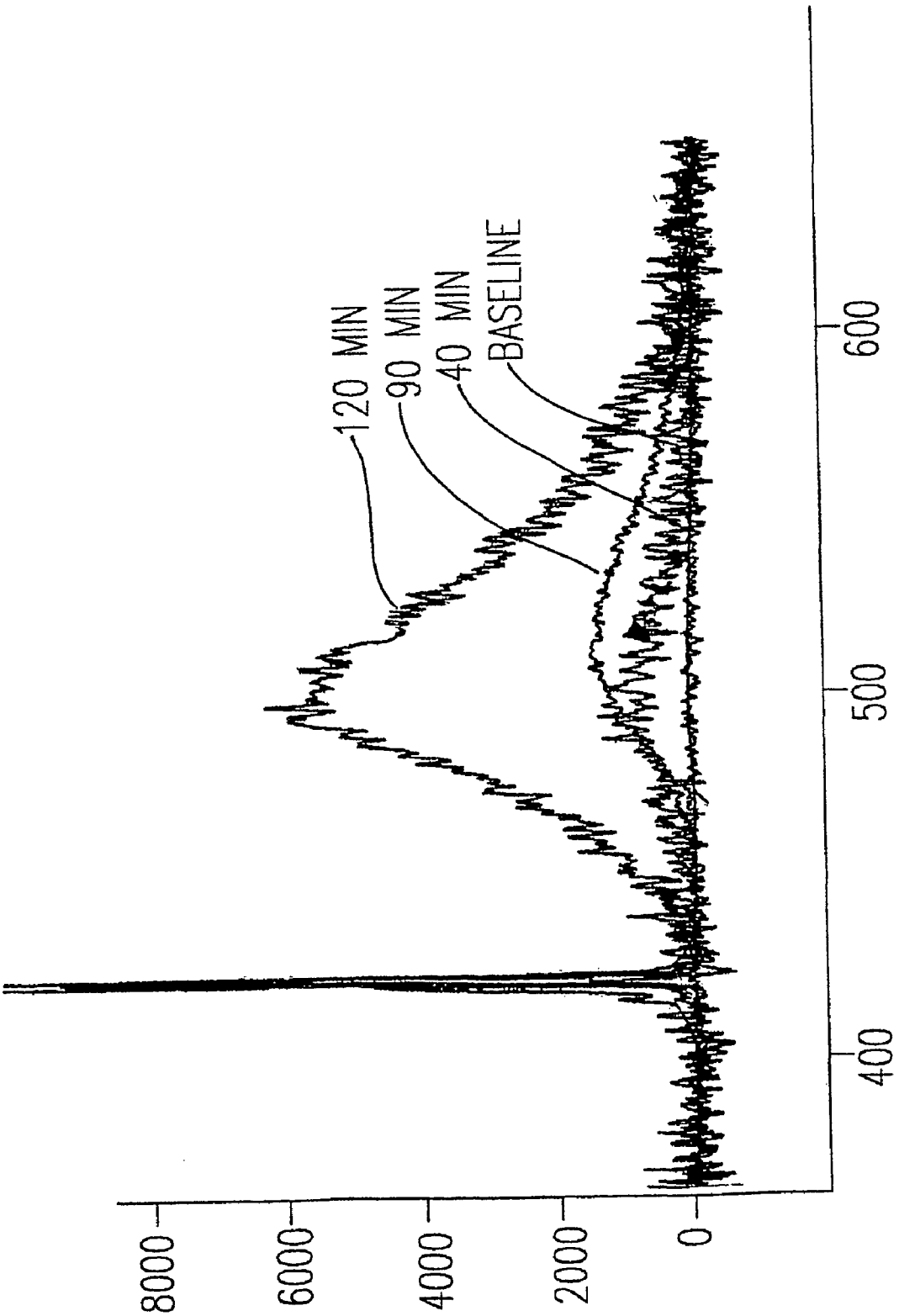
120 MIN
90 MIN
40 MIN
BASELINE
8000
6000
4000
2000
0
400
500
600

FIG.21

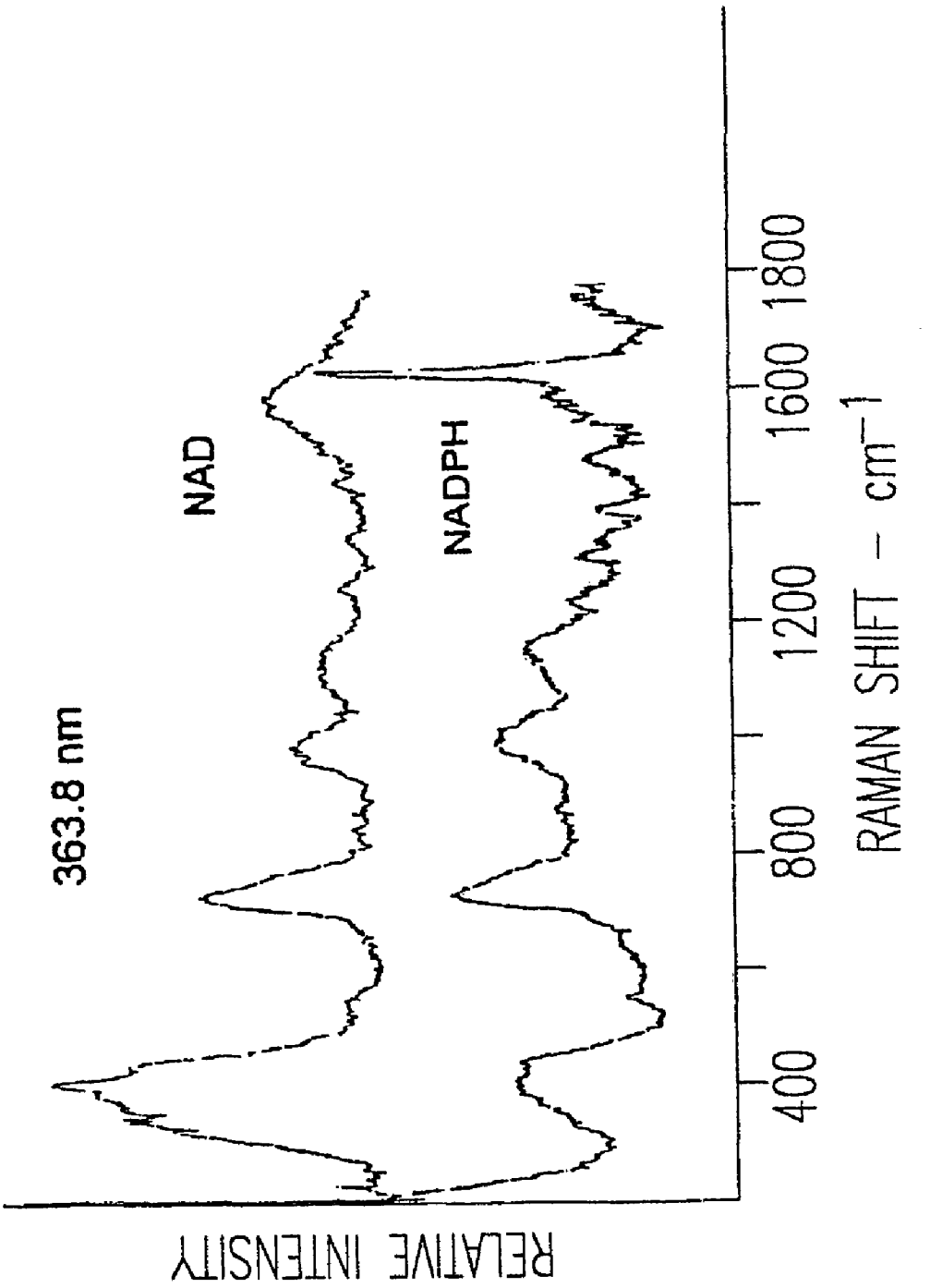
363.8 nm
NAD
NADPH
400
800
1200
1600
1800
RAMAN SHIFT – cm^{-1}
RELATIVE INTENSITY

FIG.22A

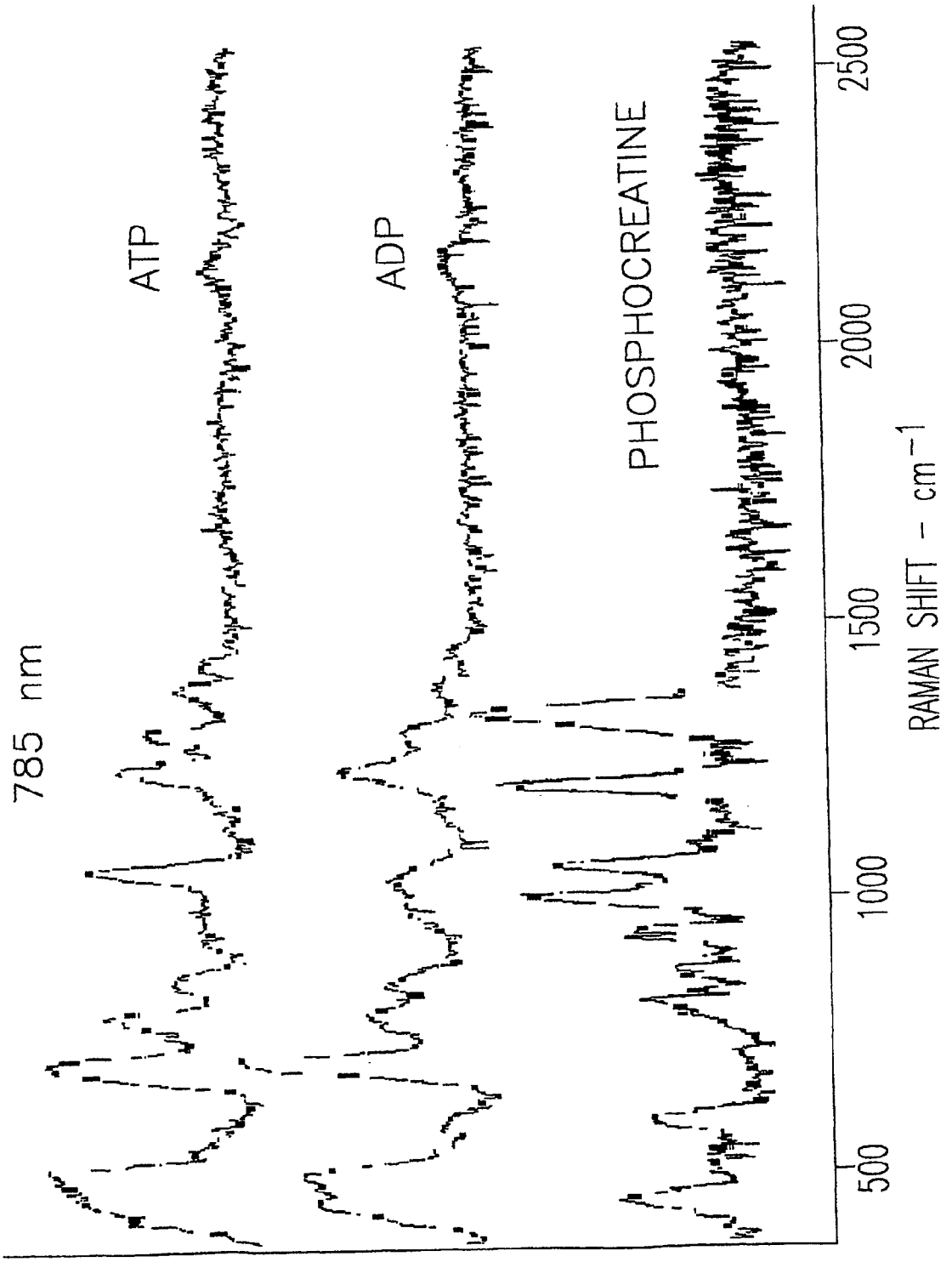
785 nm
ATP
ADP
PHOSPHOCREATINE
RELATIVE INTENSITY
500
1000
1500
2000
2500
RAMAN SHIFT - cm^{-1}

FIG.22B

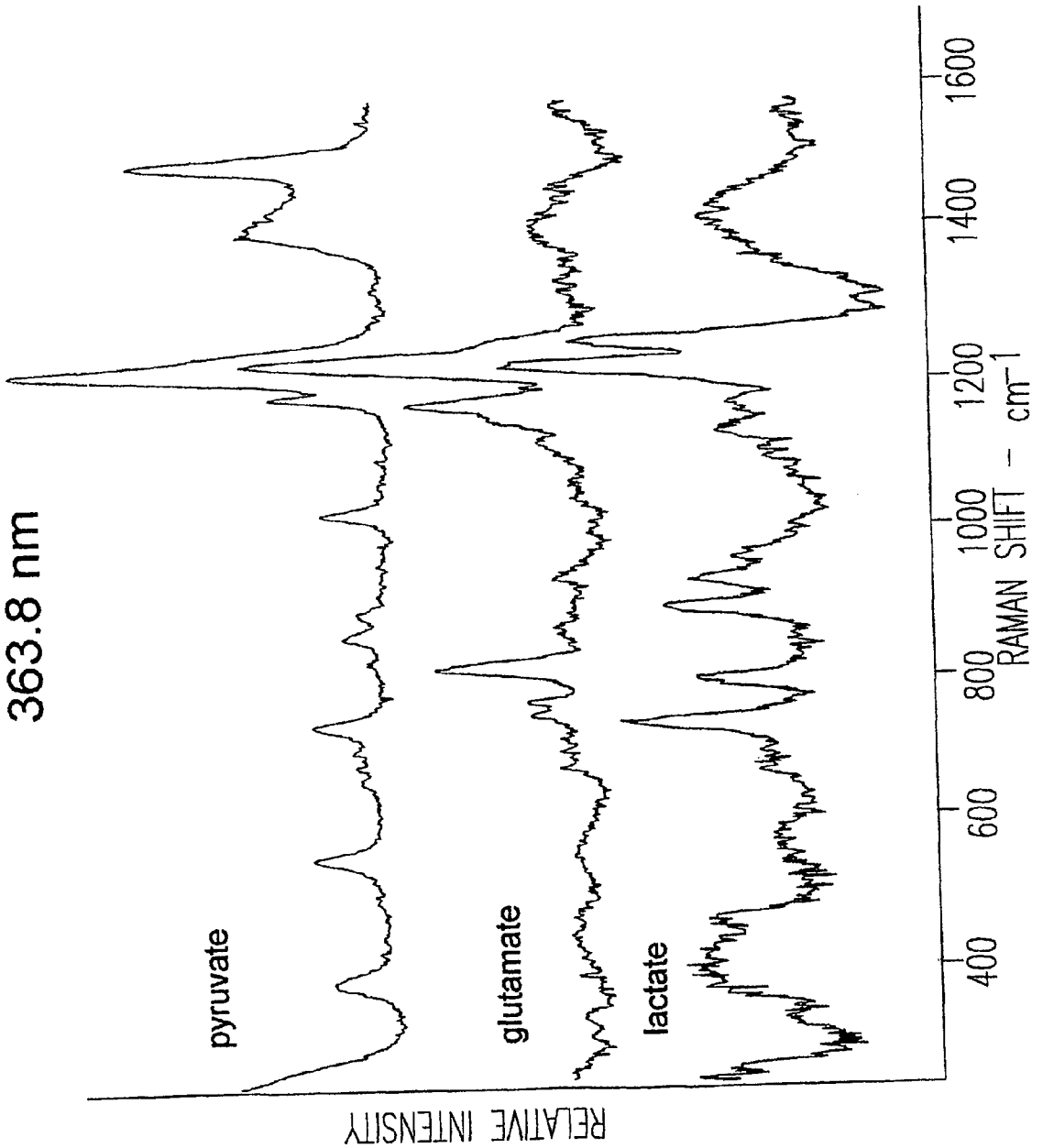
363.8 nm
pyruvate
glutamate
lactate
RELATIVE INTENSITY
400
600
800
1000
1200
1400
1600
RAMAN SHIFT - cm⁻¹

FIG.22C

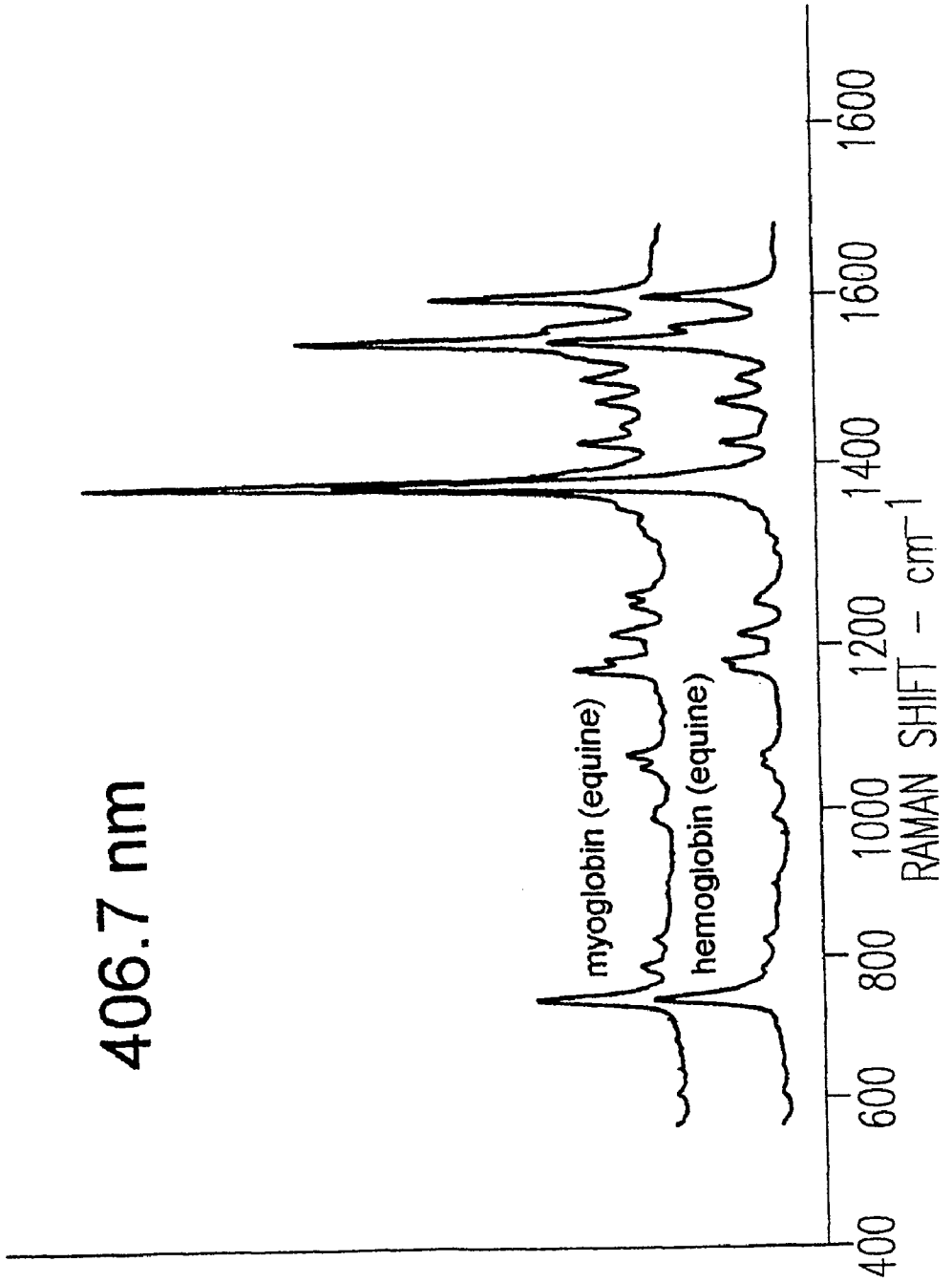
406.7 nm
myoglobin (equine)
hemoglobin (equine)
400
600
800
1000
1200
1400
1600
1600
RAMAN SHIFT – cm^{-1}

FIG.22D

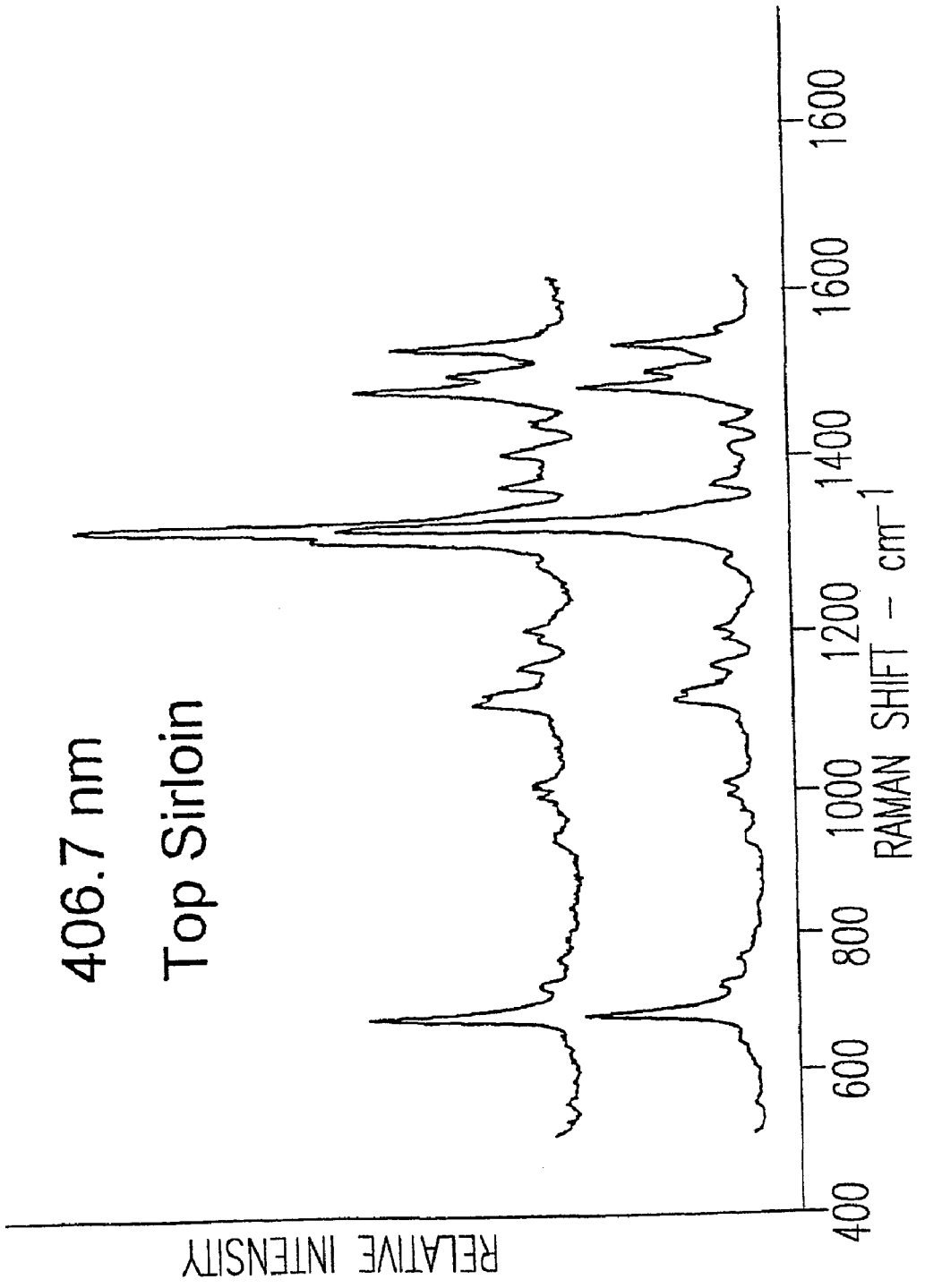
406.7 nm
Top Sirloin
RELATIVE INTENSITY
400
600
800
1000
1200
1400
1600
1600
RAMAN SHIFT - cm-1

FIG.22E

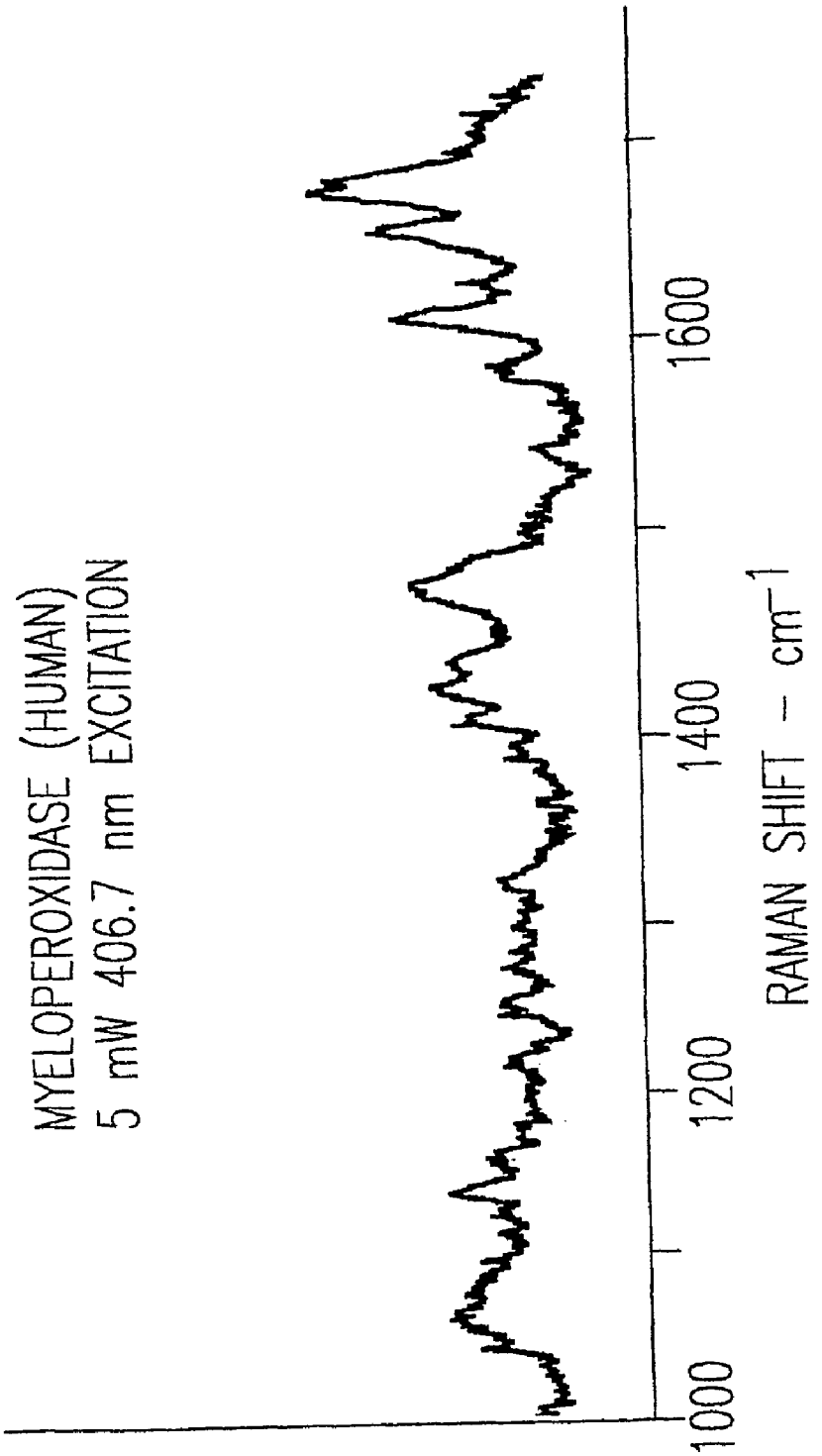
MYELOPEROXIDASE (HUMAN)
5 mW 406.7 nm EXCITATION
1000
1200
1400
1600
RAMAN SHIFT – cm^{-1}

FIG.23

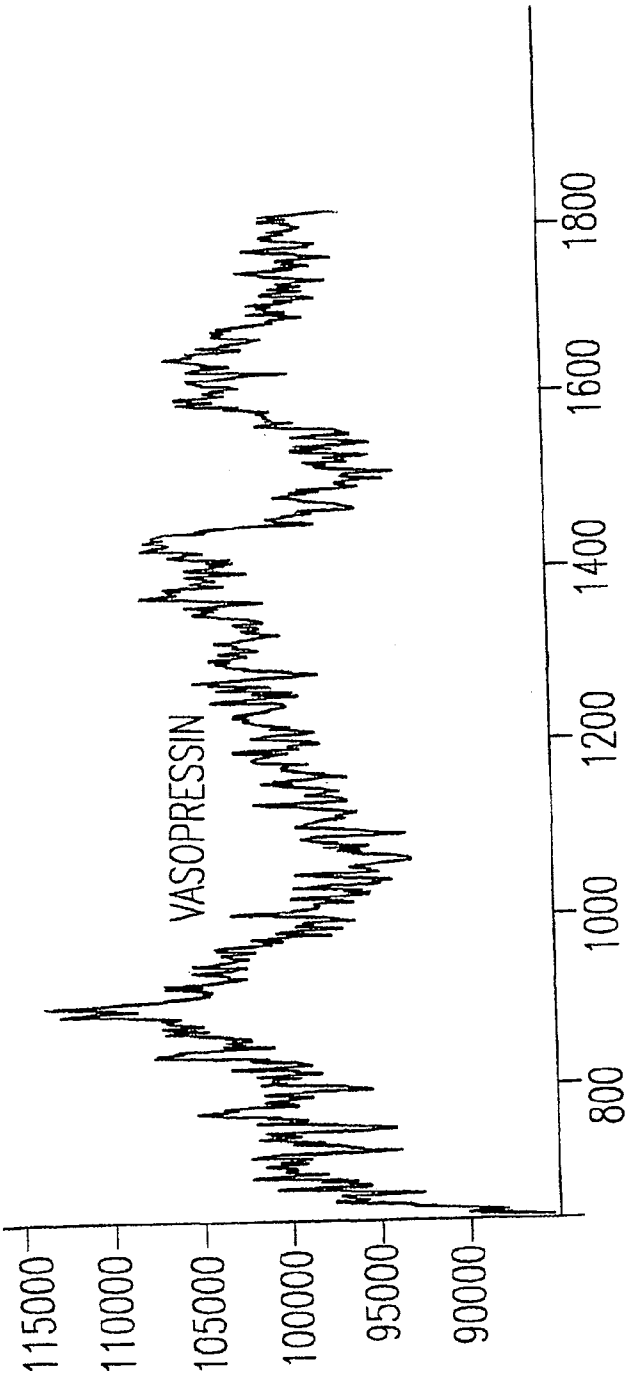
VASOPRESSIN
115000
110000
105000
100000
95000
90000
800
1000
1200
1400
1600
1800

FIG.24

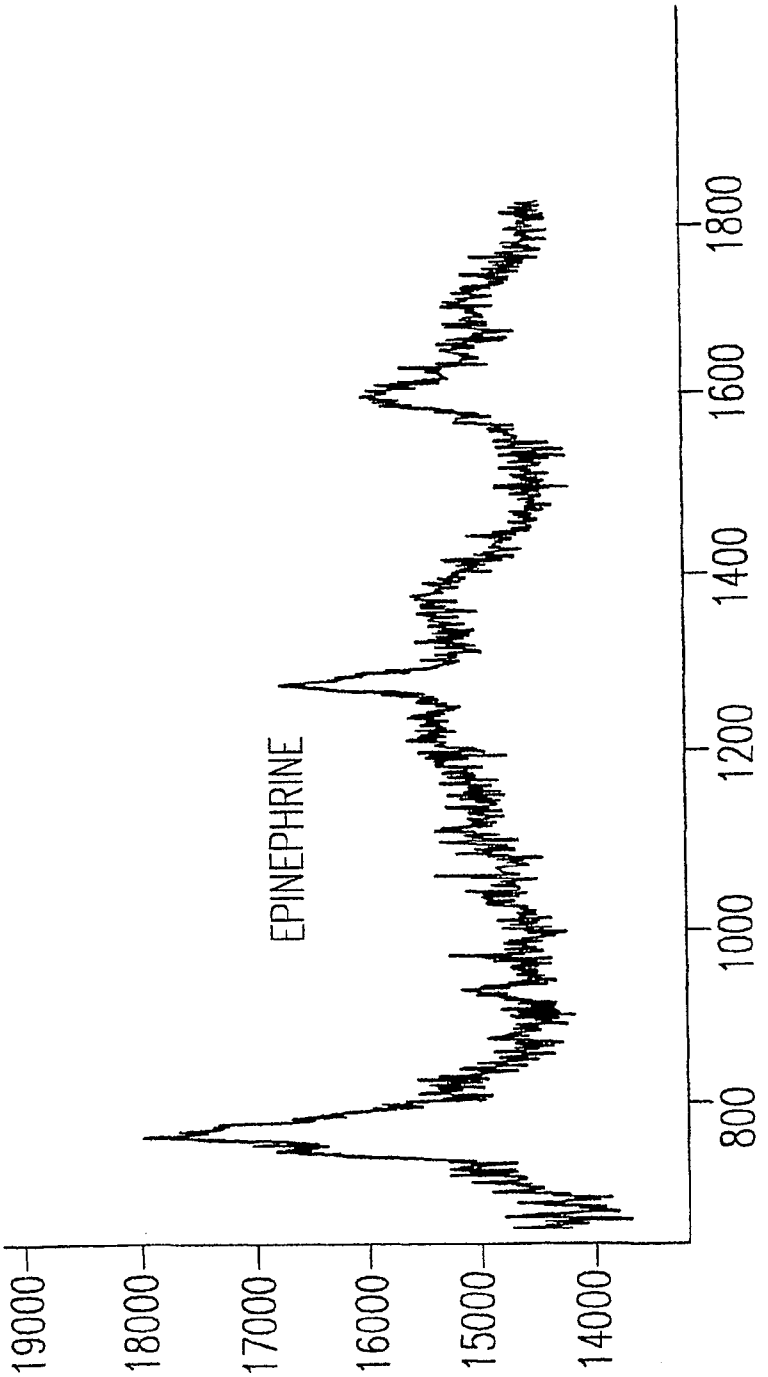
EPINEPHRINE
19000
18000
17000
16000
15000
14000
800
1000
1200
1400
1600
1800

FIG.25

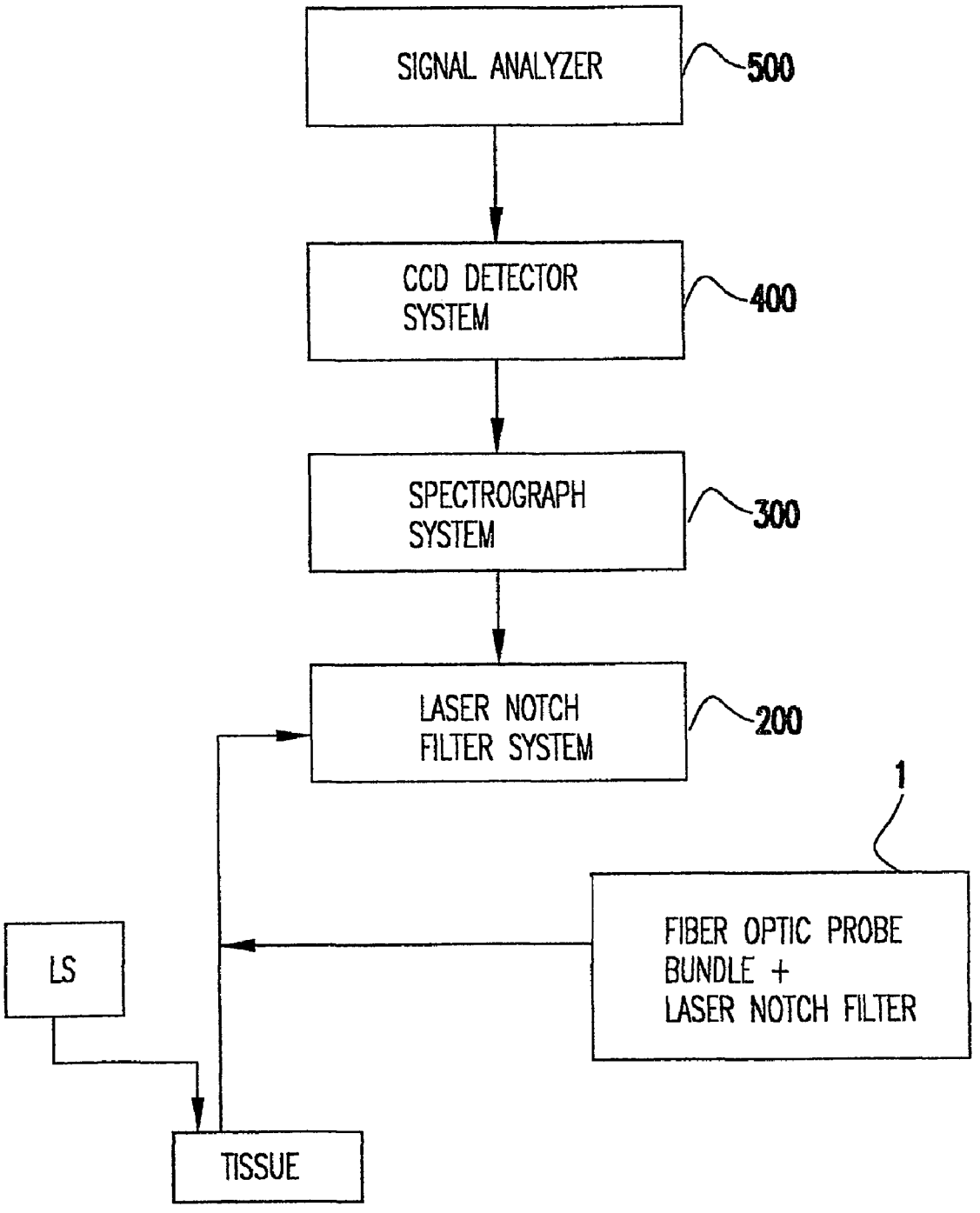
SIGNAL ANALYZER
500
CCD DETECTOR SYSTEM
400
SPECTROGRAPH SYSTEM
300
LASER NOTCH FILTER SYSTEM
200
1
FIBER OPTIC PROBE BUNDLE + LASER NOTCH FILTER
LS
TISSUE

FIG.26A

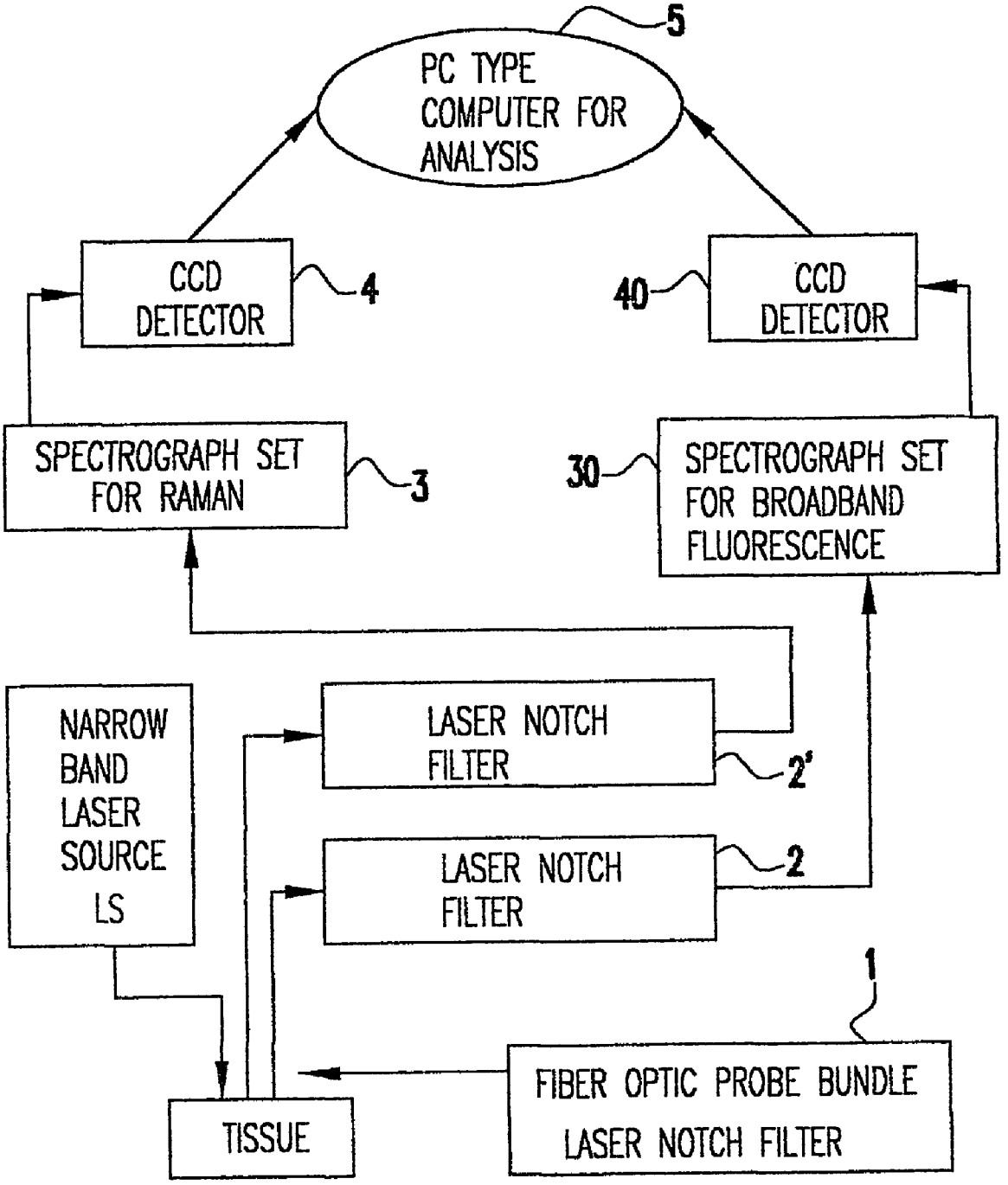
5
PC TYPE COMPUTER FOR ANALYSIS
CCD DETECTOR
4
40
CCD DETECTOR
SPECTROGRAPH SET FOR RAMAN
3
30
SPECTROGRAPH SET FOR BROADBAND FLUORESCENCE
NARROW BAND LASER SOURCE LS
LASER NOTCH FILTER
2'
LASER NOTCH FILTER
2
1
FIBER OPTIC PROBE BUNDLE LASER NOTCH FILTER
TISSUE

FIG.26B

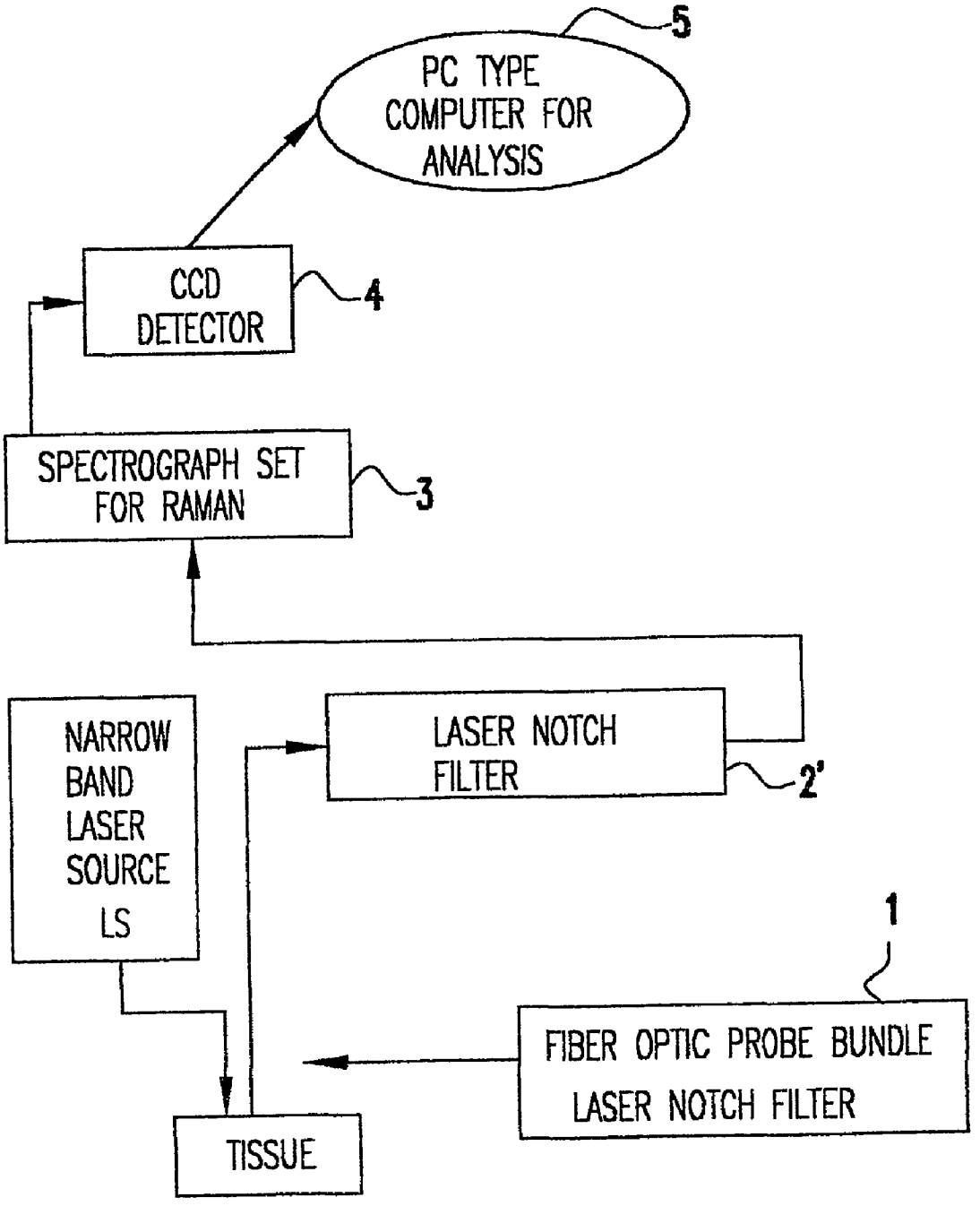
5
PC TYPE COMPUTER FOR ANALYSIS
CCD DETECTOR
4
SPECTROGRAPH SET FOR RAMAN
3
NARROW BAND LASER SOURCE LS
LASER NOTCH FILTER
2'
1
FIBER OPTIC PROBE BUNDLE
LASER NOTCH FILTER
TISSUE

FIG.26C

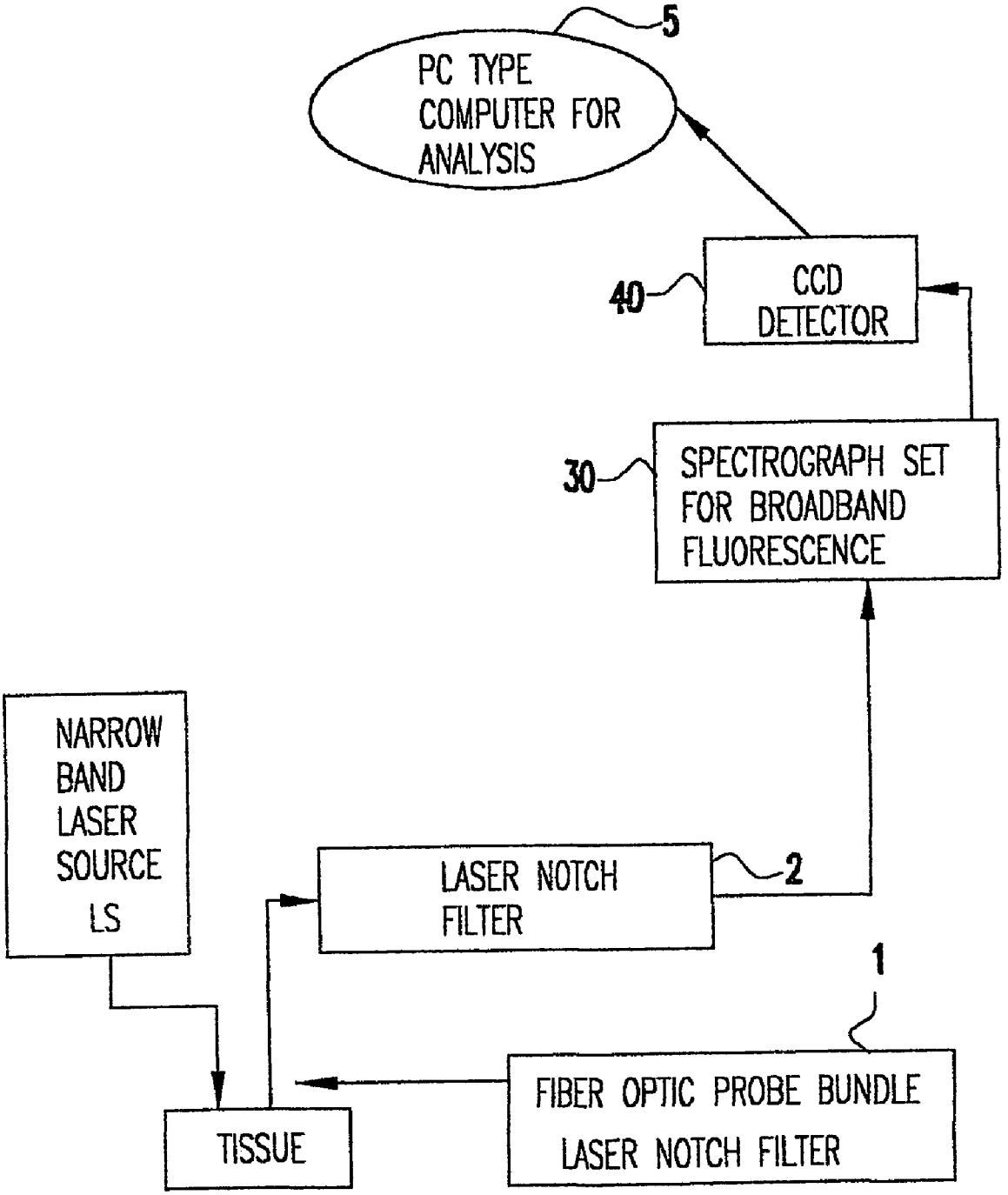
5
PC TYPE COMPUTER FOR ANALYSIS
40
CCD DETECTOR
30
SPECTROGRAPH SET FOR BROADBAND FLUORESCENCE
NARROW BAND LASER SOURCE LS
LASER NOTCH FILTER
2
1
FIBER OPTIC PROBE BUNDLE
LASER NOTCH FILTER
TISSUE

FIG.26D

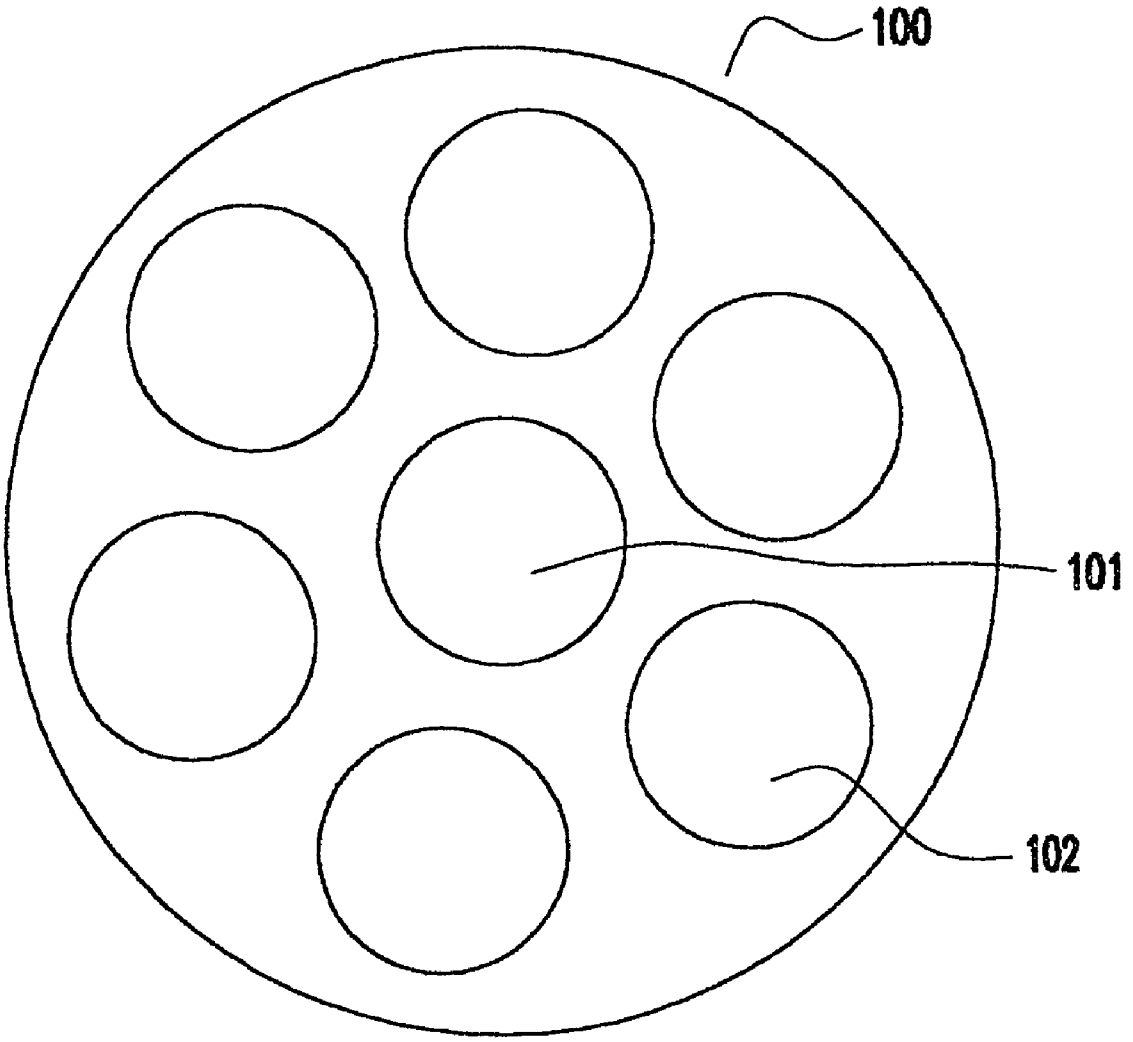

FIG.26E

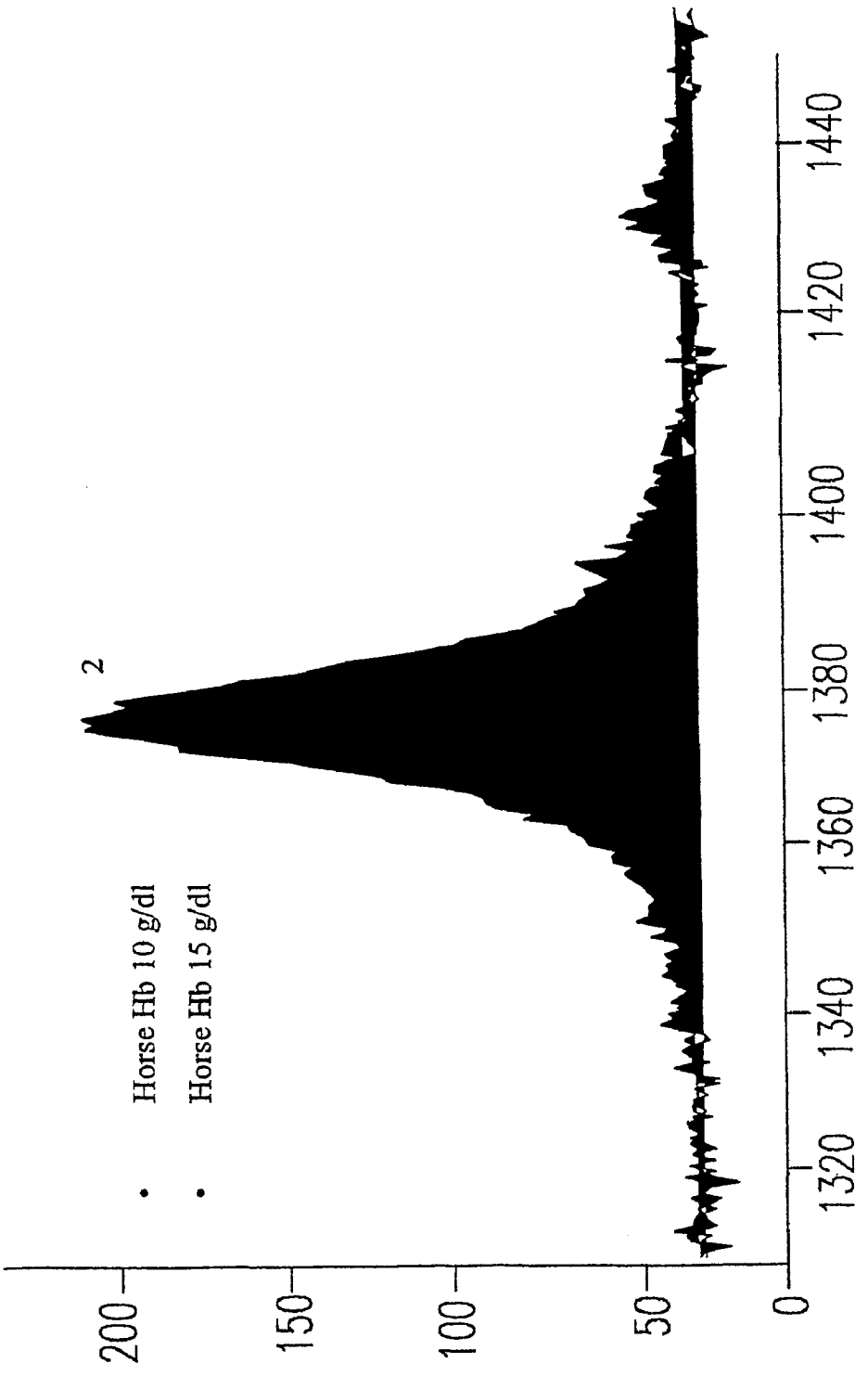
2
Horse Hb 10 g/dl
Horse Hb 15 g/dl
200
150
100
50
0
1320
1340
1360
1380
1400
1420
1440

FIG.27

TISSUE INTERROGATION SPECTROSCOPY

This application claims the benefit of Provisional Application No. 60/218,055, filed Jul. 13, 2000.

FIELD OF THE INVENTION

The invention generally relates to emergency medicine, and especially relates to shock states and critical illnesses and disease states.

BACKGROUND OF THE INVENTION

Shock is a complex entity, which traditionally has been defined as a state in which the metabolic demands of tissues are not matched by sufficient delivery of metabolic substrates, with the major substrate being oxygen. This mismatch commonly results from altered states of organ perfusion such as hemorrhage. Shock additionally involves complex inflammatory and immune mediated events which result from, and may further exacerbate, this initial metabolic mismatch. Many of these events play an important role in the development of subsequent multiorgan dysfunction, failure and death, with this latter mode responsible for over 60% of trauma deaths. Haljamae, H., "Cellular metabolic consequences of altered perfusion," in Gutierres, G., Vincent, J., eds., "Update in Intensive Care and Emergency Medicine: Tissue oxygen utilization (Springer Verlag, 1991), pp. 71–86. Despite the complexities of the inflammatory and immune components of trauma and hemorrhage, there is little debate on linking the severity of these events to the severity of initial perfusion deficits and tissue hypoxia. It is therefore essential to recognize and correct perfusion deficits at their earliest possible time. Although this seems intuitive, up to 80% of trauma patients on close monitoring continue to demonstrate evidence of tissue hypoxia secondary to perfusion deficits after what was considered to be complete resuscitation. Abou-Khalil, B., Scalea, T. M., Trooskin, S. Z., Henry, S. M., Hitchcock, R., "Hemodynamic responses to shock in young trauma patients; need for invasive monitoring," Crit. Care Med., 22:633–639 (1994).

Traditional clinical signs of tissue perfusion such as capillary refill, mental status, heart rate, pulse pressure and systemic blood pressure are very gross indicators of tissue perfusion and can only be considered to be of historic interest except at extreme values. Porter, J., Ivatury, R., "In search of optimal end points of resuscitation in trauma patients," J. Trauma, 44:908–914 (1998). Current markers of tissue perfusion include systemic lactate and base deficit measurements; transcutaneous and subcutaneous gas measurements, gastric and sublingual tonometry and spectroscopic techniques such as NIR absorption spectroscopy, fluorescence quenching, and orthogonal polarization spectral imaging. While these techniques have respective advantages, each is plagued by the relative singularity of its measure, lack of tissue specificity, inability to quantitate, or inability to easily apply or adapt for field use. Identification of any other useful markers is an important objective, and the search continues for further markers of shock states and the like. Effectively measuring and working with both known markers as well as markers being discovered would be highly beneficial to emergency medicine but is not provided in conventional technology. Information about biochemistry in shock states and disease states has not yet fully found its way and been used in practical applications. Rather, currently emergency medicine is left to rely on physical examination not much advanced by conventional, relatively limited spectroscopic measurement technology.

That is, much still turns on observation of simple vital signs. Yet, the diagnosis of shock and its severity can be difficult, and cannot be accomplished with certainty, from simple vital signs. A physical exam, including vital signs, is inadequate in detecting states of uncompensated shock. Ward, K. R., Ivatury, R. R., Barbee, R. W., "Endpoints of resuscitation for the victim of trauma," J. Intensive Care Med., 16:55–75 (2001). Dysoxia can be present despite normal vital signs. Ward et al., id.; Abou-Khalil, B., Scalea, T. M., Trooskin, S. Z., Henry, S. M., Hitchock, R., "Hemodynamic response to shock in young trauma patients: need for invasive monitoring," Crit Care Med. 22(4):633–9 (1994); Scalea, T. M., Maltz, S., Yelon, J., Trooskin, S. Z., Duncan, A. O, Scalafani, S. J., "Resuscitation of multiple trauma and head injury: role of crystalloid fluids and inotropes," Crit Care Med. 22(10):1610–5 (1994); Ivatury, R. R., Simon, R. J., Havriliak, D., Garcia, C., Greebarg, J., Stahl, W. M., "Gastric mucosal pH and oxygen delivery and oxygen consumption indices in the assessment of adequacy of resuscitation after trauma: a prospsective, randomized study," J. Trauma, 39(1):128–34; discussion 34–6 (1995).

In addition, resuscitation of victims of uncompensated shock back to "normal" vital signs is inadequate as a resuscitation endpoint. Unrecognized continued accumulation of additional oxygen debt is still possible and may contribute to later development of multisystem organ failure and death. Shoemaker, W. C., Appel, P. L., Kram, H. B., "Tissue oxygen debt as a determinant of lethal and nonlethal postoperative organ failure," Crit. Care Med., 16(11):1117–20 (1988).

Adding, to a physical exam, global measures of oxygen transport still does not ensure detection of early shock states or provide adequate information to act as sole end-points of resuscitation once shock is recognized and therapy instituted. For an outline of all of the current major technologies that have been used to detect the presence of shock and to guide its treatment, see Ward, Ivatury et al., supra. For various reasons, all have been problematic.

To better understand the difficulties in detecting shock states it is helpful to examine the biphasic relationship between oxygen delivery (DO_2) and consumption (VO_2) to understand the potential inadequacies of currently available monitoring systems. FIG. **1** demonstrates that VO_2 can remain constant over a wide range of DO_2. This is possible because cells have the ability to increase their extraction of oxygen (OER) in the face of decreased delivery. This is generally reflected by lower hemoglobin oxygen saturations in blood leaving the organ system (SvO_2), which may change before it is apparent in the physical exam. Scalea, T. M., Hartnett, R. W., Duncan, A. O., Atrweh, N. A., Phillips, T. F., Sclafani, S. J., et al., "Central venous oxygen saturation: a useful clinical tool in trauma patients," J. Trauma, 30(12):1539–43 (1990); McKinley, B. A., Marvin R. G., Cocanour, C. S., Moore, F. A., "Tissue hemoglobin O2 saturation during resuscitation of traumatic shock monitored using near infrared spectrometry," J. Trauma, 48(4):637–42 (2000). However, there is a point at which OER cannot keep pace with reductions in delivery. At this point VO_2 of the cell or organ falls (critical oxygen delivery: DO_2crit) and cells become dysoxic. This results in an increase in the oxidation-reduction (redox) value of the cell, effectively blocking the flow of electrons through the NADH-cytochrome a, a3 cascade in the mitochondria which prevents the formation of ATP. Cytochrome a,a3 (cytochrome oxidase) is the terminal electron acceptor in the mitochondrial electron transport

chain. Dysoxia can be recognized by the accumulation of a number of metabolic products such as lactate and intracellular reduced nicotinamide adenine dinucleotide (NADH). NADH offers one of the main sources of energy transfer from the TCA cycle to the respiratory chain in the mitochondria. NADH is situated on the high-energy site of the respiratory chain and during tissue dysoxia it accumulates because less NADH is oxidized to NAD+. The redox state of the mitochondria (NADH/NAD+) therefore reflects the mitochondrial energy state, which in turn is determined by the balance of oxygen availability in the cell and the metabolic rate of the cell. Siegemund, M., van Bommel, J., Ince, C., "Assessment of regional tissue oxygenation," Intensive Care Med., 25(10):1044–60 (1999). Conventional monitoring and measuring used in emergency medicine do not adequately take into account such biochemistry of shock states and the like. Knowing the biochemistry of shock states and the like but not being able to measure and monitor pertinent information thereto has been a frustrating, unresolved problem in emergency medicine.

Conventionally, a primary means of assessing tissue perfusion is through infrared (IR) or near-infrared (NIR) spectroscopy. Human skin and tissue are semi-transparent to wavelengths in this range. However, problems with IR technology arise because water strongly absorbs IR radiation. While NIR absorption spectroscopy does not suffer from water absorption as does classical IR, and NIR absorption spectroscopy is useful for the relative quantification of several specific chromophores such as hemoglobin, myoglobin, and cytochrome oxidase. Nakamoto, K., Czernuszewicz, W. S., "Infrared Spectroscopy," in: *Methods in Enzymology,* 226:259–289 (1993); Piantadisu, C., Parsons, W., Griebel, "Application of NIR Spectroscopy to problems of tissue oxygenation," in Gutierres, G., Vincent, J., eds., *Update in Intensive Care and Emergency Medicine: Tissue oxygen utilization* (Springer Verlag, 1991) pp. 41–44. Other recent work reports the ability of using NIR absorption shift of hemoglobin to measure pH. However, disadvantageously, NIR signals are so broad as to not be well-suited to quantification of overlapping species. Examples of NIR absorption spectroscopy signals being too broad to lend themselves to quantification of overlapping species include the spectra for oxy and deoxy hemoglobin and cytochrome oxidase (see FIG. **2**). Owen-Reece, H., Smith, M., Elwell, C. E., Goldstone, J. C., "Near infrared spectroscopy," Br J Anaesth, 82(3): 418–26 (1999). FIG. **2** is a graph of typical broad signals of oxy and deoxy hemoglobin and cytochrome oxidase obtained by NIR absorption spectroscopy. (In FIG. **2**, the HbO_2 and Hb signals also would include those from myoglobin.)

Conventional NADH-fluorescence techniques are more specific and quantitative than classical NIR absorption spectra but can only measure a single marker. The technique has relied on use of excitation wavelengths in the carcinogenic UV region and has not been reduced to clinical practice. Conventional noninvasive or minimally invasive measures of tissue perfusion include transcutaneous and tonometric (gastric or sublingual) monitoring of various gases such as oxygen and carbon dioxide. The major limitations of these devices are that they are limited to monitoring those specific gases and cannot provide additional information that, if provided, could be useful in diagnosis and stratification of patients. Methods such as tonometry can be cumbersome due to its invasive nature. These methods are also prone to deviations through changes either in minute ventilation or inspired oxygen concentration. Transcutaneous gas monitoring, gastric tonometry, and even sublingual tonometry are one-dimensional and are prone to non-flow related changes caused by hypo or hyper ventilation. Also, with the exception of sublingual tonometry, application of these methods in the field is problematic. Weil, M., Nakagawa, Y., Tang, W., et al., "Sublingual capnometry: A new noninvasive measurement for diagnosis and quantification of severity of circulatory shock," Crit. Care Med., 27:1225–1229 (1999).

Another concern associated with measurement of shock states, and balanced with other factors relating to measurement, is invasiveness. NIR absorption spectroscopy is being aggressively studied to use signals from these chromophores to noninvasively monitor oxygen transport at the tissue level. McKinley et al., supra. Perhaps the best-known use of this technology is in the monitoring of cerebral hemodynamics. The basis for this is that the majority of blood volume in an organ is venous and thus the tissue hemoglobin saturation should reflect the state of oxygen consumption of the tissue. Again, broad overlap of signals in addition to needing to know the pathlength of light presents challenges in quantification and differentiation of signals. For example it is difficult to distinguish hemoglobin and myoglobin making NIR use in hemorrhage problematic since myoglobin has a p50 of only 5 mmHg. Gayeski, T. E., Honig, C. R., "Direct measurement of intracellular O2 gradients; role of convection and myoglobin," Adv Exp Med Biol, 159:613–21 (1983). Because soft tissue and bone are translucent to NIR light, NIR can penetrate to significant depths, a feature with both advantages and disadvantages. Monitoring the redox state of cytochrome oxidase is also difficult unless baseline absorptions are known. There is also significant overlap between the cytochrome oxidase and hemoglobin signals. Despite this, NIR measurements of tissue saturation (StO_2) are being marketed.

Although some manufacturers of NIR absorption spectroscopy equipment claim to differentiate between the two species of oxygen hemoglobin and myoglobin, no work to this effect exists in the medical literature. In fact, evidence exists that a major portion of the NIR absorption spectroscopy signal reported from hemoglobin actually originates from myoglobin.

Another problem for NIR is that in terms of use on hollow organ systems such as the stomach, data from NIR absorption spectroscopy would likely include signals from non-stomach organs and thus not reflect data from the mucosal surface of the stomach.

Surface NADH fluorescence has been used to detect cellular dysoxia in a number of organ systems. Siegemund et al., supra. The traditional technique uses unique excitation light sources and detection filters to take advantage of the fact that NADH will fluoresce (emit light at 460 nm) when excited at a wavelength of 360 nm (near-UV). This technique has been used in video microscopy/fluorometry experiments. Van der Laan, L., Coremans, A., Ince, C., Bruining, H. A., "NADH videofluorimetry to monitor the energy state of skeletal muscle in vivo," J. Surg. Res., 74(2):155–60 (1998). However, such conventional methods do not necessarily provide optimum resolution.

Adverse effects of certain compounds (such as vasopressin and norepinephrine) on oxygen transport and the immune/inflammatory response are now beginning to be appreciated with manipulation of their actions being studied as therapeutic strategies. Kincaid, E. H., Miller, P. R., Meredith, J. W., Chang, M. C., "Enalaprilat improves gut perfusion in critically injured patients," Shock, 9(2):79–83 (1998); Catania, R. A., Chaudry, I. H., "Immunological consequences of trauma and shock," Ann. Acad. Med. Singapore, 28(1):120–32 (1999). However, satisfactory

measurement of such compounds in vivo without invasive probing has not yet been provided.

Thus, current technology includes pulmonary artery catheters, repetitive measures of lactate and base deficit, splanchnic tonometry, sublingual tonometry, NIR absorption spectroscopy, transcutaneous gas monitoring, phosphorescence quenching and fluorescence technology (indwelling blood gas/pH catheters). No such technology is without a substantial disadvantage. Civilian prehospital emergency medical services systems, emergency physicians, trauma surgeons, intensive care physicians, cardiologists, anethesiologists, and military medical personnel continue to be plagued by the insensitivity of the physical exam, lack of readily available physiologic and metabolic markers to judge the presence and severity of shock states, and lack of real-time relevant measurement approaches. In addition, it has been difficult to use singular measures to guide treatment or predict outcome. These problems are greatly magnified as the scale of the wounded population increases (such as on the battlefield and the various pre-definitive echelons of care provided to wounded soldiers or in a natural disaster). To the inventors' knowledge, currently no conventional techniques are available for real-time monitoring of a broad range of potentially valuable emergency medicine markers of shock, tissue ischemia, tissue injury, tissue inflammation, or tissue immune dysfunction.

SUMMARY OF THE INVENTION

The invention realizes methods, profiles, medical measurement devices, and other products for accurate measurement of change or lack thereof from non-shock, non-ischemic, non-inflammation, non-tissue injury, non-immune dysfunction conditions which are referred to herein as "baseline conditions". In attention to advantageous accuracy in such measurement, the invention provides practical, real-time approaches for accurately characterizing a patient's condition with respect to baseline conditions. With Raman and/or fluorescence spectroscopy according to the invention, change from baseline conditions is measured, characterized, monitored, identified and/or followed with a high degree of accuracy with measurement times on the order of seconds. Such high-accuracy measurement is achieved with Raman spectroscopy (such as resonance Raman spectroscopy) interrogation of tissue, optionally with simultaneous interrogation by fluorescence spectroscopy of compounds such as NADH. The tissue interrogation advantageously may be non-invasive to minimally-invasive to totally invasive. With methods and products according to the present invention, advantageously preclinical (ultra-early) states of shock, tissue ischemia, tissue injury, and tissue inflammation can be detected, severity can be determined, and the effectiveness of various treatments aimed at resolving the shock state can be determined, and other beneficial effects for patient care can be achieved.

In order to accomplish these and other objects of the invention, the present invention in a preferred embodiment provides a tissue analysis method, comprising interrogating a biological material (such as a biological tissue or a bodily fluid) with Raman spectroscopy and fluorescence spectroscopy to obtain spectroscopy results.

In another preferred embodiment, the invention provides a method of diagnosing shock, tissue ischemia, tissue inflammation, or tissue immune dysfunction, comprising: (A) for a target molecule population, taking a sample Raman spectroscopy, and/or fluorescence spectroscopy, profile for a patient; (B) comparing the sample spectroscopy profile with a pre-established Raman spectroscopy and/or fluorescence spectroscopy profile for the target molecule population under baseline conditions.

A further preferred embodiment provides a spectroscopy comparative profile, comprising: a pre-established Raman spectroscopy and fluorescence spectroscopy profile for a target molecule population under baseline conditions; and a sample Raman spectroscopy and fluorescence spectroscopy profile for the target molecule population.

The invention also provides for a preferred embodiment which is a method of diagnosing abnormalities in vivo and in situ, comprising: (A) for a target molecule population, taking a sample Raman spectroscopy and/or fluorescence spectroscopy profile for a patient; (B) comparing the sample Raman spectroscopy or fluorescence spectroscopy profile with a pre-established Raman spectroscopy or fluorescence spectroscopy profile for the target molecule population under baseline conditions; and (C) using differences identified in said comparing step to identify an abnormality.

In a particularly preferred embodiment of the inventive methods, simultaneous fluorescence spectroscopy probing of NADH and resonance Raman spectroscopy are performed.

Another preferred embodiment of the invention provides a medical measurement device comprising: a spectrometer with multiple wavelength settings for resonance Raman spectroscopy; and a biological probe electrically connected to the spectrometer.

Additionally, the invention in another preferred embodiment provides a spectroscopy comparative profile, comprising: a pair of Raman spectroscopy or fluorescence spectroscopy profiles for a target molecule population, wherein one profile was taken from a patient after a medical event concerning the patient.

A further preferred embodiment of the invention provides a computer system comprising: a database of stored baseline Raman spectroscopy and/or fluorescence spectroscopy profiles and a means to store patient Raman spectroscopy and/or fluorescence spectroscopy profiles.

BRIEF DESCRIPTION OF THE DRAWINGS

The foregoing and other objects, aspects and advantages will be better understood from the following detailed description of the preferred embodiments of the invention with reference to the drawings, in which:

FIG. **1** is a traditional biphasic oxygen delivery and consumption curve.

FIG. **2** is a graph of oxy and deoxy hemoglobin and cytochrome oxidase obtained by NIR absorption spectroscopy, with Δoptical density plotted versus wavelength (nm).

FIG. **3** shows near-UV resonance Raman spectroscopy according to the invention for human blood at various oxygen saturation levels.

FIG. **4** shows resonance Raman spectroscopy according to the invention of both oxygen hemoglobin and myoglobin.

FIG. **5** shows near-UV resonance Raman spectra of isolated ischemic rat skeletal muscle over time.

FIG. **6** is a baseline Resonance Raman spectrum for rat muscle, with the signal obtained in one second.

FIGS. **7**, **8**, **9** and **10** each is a Resonance Raman spectrum for the same muscle as FIG. **6**, with respective bleeding of 1 ml, 2 ml, 5 ml and 7.5 ml.

FIG. **11** is an overlay of the Raman spectra of FIGS. **6**, **7**, **8**, **9** and **10**.

FIG. **12** are resonance Raman spectra of a rat tongue.

FIG. **13** are near UV resonance Raman spectra of hemoglobin.

FIG. **14** is a spectra of baseline NADH fluorescence of the same quadricep muscle from the same animal in which NADH fluoresces after being excited with light at 406.5 nm which is the same wavelength used to produce the previous resonance Raman spectroscopy of FIGS. **5**–**10**.

FIGS. **15**, **16**, **17** and **18** each is a spectra of NADH fluorescence for the same muscle as FIG. **14**, with respective bleeding of 5 ml, 7.5 mls, 9 mls and 12 mls.

FIG. **19** is an overlay of NADH fluorescence spectra (FIGS. **14**–**18**) from the quadriceps muscle.

FIG. **20** is an overlay of NADH fluorescence spectra of a rat tongue, for baseline and after 2 cc hemorrhage for 50 minutes.

FIG. **21** is an overlay of NADH fluorescence spectra of a rat liver during graded hemorrhage over time (baseline, 40 min, 90 min and 120 min).

FIG. **22**(*a*) are preliminary Raman spectra of β-nicotinamide adenine dinucleotide in the oxidized (NAD) and reduced (NADPH or NADH) forms. FIG. **22**(*b*) are preliminary Raman spectra of the high energy phosphates ATP and ADP. FIG. **22**(*c*) are preliminary Raman spectra of the glycolytic end-products pyruvate and lactate, along with the excitatory amino acid and neurotoxin glutamate. FIG. **22**(*d*) are preliminary Raman spectra of the oxygen transporters hemoglobin (Hb) and myoglobin (Mb), from an equine. FIG. **22**(*e*) includes preliminary Raman scans of uncooked beef, with the top scan taken in a darker area, and the bottom scan taken in a lighter area with more saturated myoglobin.

FIG. **23** is a near-UV resonance Raman spectrum of myeloperoxidase.

FIG. **24** is a UV resonance Raman spectrum of vasopressin.

FIG. **25** is a UV resonance Raman spectrum of norepinephrine.

FIGS. **26**(*a*), **26**(*b*), **26**(*c*) and **26**(*d*) are schematic views of devices according to the invention. FIG. **26**(*e*) is a top view of a fiber optic bundle shown schematically in FIGS. **26**(*b*), **26**(*c*) and **26**(*d*).

FIG. **27** depicts resonant Raman spectra for horse Hb dilutions.

DETAILED DESCRIPTION OF THE PREFERRED EMBODIMENTS OF THE INVENTION

The present invention provides methods and products in which resonance Raman spectroscopy interrogates biological material (such as tissue or a bodily fluid) at near-UV excitation. The Raman spectroscopy may proceed with or without simultaneous fluorescence spectroscopy (such as NADH fluorescence spectroscopy). The interrogation advantageously may be in a non-invasive to minimally-invasive manner, but is not required to be so and if desired may be invasive. Data from interrogating tissue according to the invention may be used to detect preclinical (ultra-early) states of shock and other tissue injury and disease states, determine severity, and determine the effectiveness of various treatments aimed at resolving the shock or tissue disease/injury state of a patient.

In a preferred embodiment of the invention, a tissue analysis method comprises interrogating a biological tissue with Raman spectroscopy and fluorescence spectroscopy to obtain spectroscopy results. The Raman spectroscopy used in the present invention is that based on the Raman effect, which has been known for over 70 years and is caused by absorption of light leading to the transition of a molecule from the ground state to an excited state, followed by the emission of light with a different wavelength. Raman, C. V., Krishnan, K. S., "The colour of the sea," Nature (London), 121:619 (1928). The Raman effect has only recently, through the advancements and miniaturization of fiber optic, laser, and detector technology, become a practical technique for clinical use. Because each molecular species has its own characteristic molecular vibrations, a Raman spectrum provides a unique "fingerprint" useful for sample or marker identification. Hanlon, E. B., Manoharan, R., Koo, T. W., Shafer, K. E., Motz, J. T., Fitzmaurice, M., et al., "Prospects for in vivo Raman spectroscopy," Phys Med Biol, 45(2): R1–59 (2000); Diem, M., "Introduction to modern vibrational spectroscopy," New York: Wiley (1993). While any wavelength of light theoretically can be used as an excitation source to provide a Raman spectrum, visible excitation can produce strong broadband fluorescence, which undesirably can overwhelm Raman signals. Nevertheless, wavelengths can be chosen that produce resonance due to matching of the excitation wavelength and the electronic energy state of the scattering molecule. While Raman scattering is a rather low energy phenomenon requiring sensitive detectors, the signal is greatly enhanced when the molecule of interest is resonant (absorption maximum near the laser wavelength). This signal enhancement at a resonant frequency may be referred to as "resonance Raman spectroscopy" and allows for the selective detection of individual species of very low concentration within a complex mixture. Hanlon et al., supra.

If the excitation wavelength does not induce fluorescence within the wavelength region of interest, then remarkably high resolution Raman spectra can be obtained. If fluorescence does occur, this can be reduced or even eliminated in many instances by tuning of the excitation wavelength. Thus, while interfering fluorescence may occur with a particular excitation wavelength, it may not occur within the UV or NIR range where one could detect signals either above or below the fluorescing region, as the case may be. Hanlon, E. B., Manoharan, R., Koo, T. W., Shafer, K. E., Motz, J. T., Fitzmauric, M., Kramer, J. R., Itzkan, I, Dasari, R. R, and Feld, M. S., "Prospects for in vivo Raman spectroscopy," Phys. Med. Biol.; 45: R1–R59 (2000).

In the invention, the wavelengths for the Raman spectroscopy and/or fluorescence spectroscopy are wavelengths for which such spectroscopy equipment may be set, suitably for interrogating biological tissue in a living patient. Preferably resonance Raman spectroscopy according to the invention is performed at a deep ultraviolet wavelength, i.e., at 390 to 420 nm. Modifications of Raman spectroscopy that can be applied include Fourier Transform Raman Spectroscopy, Nonlinear Raman Spectroscopy, Raman difference spectroscopy, and Raman Optical Activity.

Examples of Raman spectra are FIGS. **3**, **4**, **5**, **6**, **7**, **8**, **9**, **10**, **11**, **12**, **13**, **22**(*a*)–(*e*), **23**, **24**, **25**. Examples of NADH fluorescence spectra are FIGS. **14**, **15**, **16**, **17**, **18**, **19**, **20**, **21**.

The inventive methods, products and profiles may include signal enhancement at a resonant frequency for a target molecule of the target molecule population. The inventive methods may include operating an electromagnetic radiation generator at a range of selectable wavelengths from about 270 nm to about 20,000 nm. Spectroscopy may be performed for multiple wavelengths. Preferably the Raman spectroscopy is resonance Raman spectroscopy at 390 to 420 nm wavelength. Because basic Raman scattering is a rather low intensity phenomenon requiring sensitive detectors, preferably Resonance Raman Spectroscopy (RRS) techniques are used, to enhance the signal when the mol-

ecule of interest is resonant (absorption maximum near the laser wavelength). The signal strength of Raman can be boosted by several orders of magnitude by providing areas of resonance. Also, use of resonant wavelengths will allow limiting laser power density to a minimum (well below the skin damage threshold of 4 watts/cm^2). Fluorescence can be avoided by choosing wavelengths not prone to this phenomenon, and through fluorescence quenching. Conversely, fluorescence may be advantageously used for quantification if a particular target is found to have identifiable Raman spectra in one light range such as the NIR but fluoresces at another light range such as the UV. Use of near UV wavelengths (violet, ~406 nm) will avoid the mutagenic potential of UV radiation, while insuring a strong Raman signal.

The use of Raman spectroscopy in the near-UV range within the clinical settings according to the invention has several advantages with respect to other optical techniques such as IR and NIR absorption spectroscopy. Use of resonance Raman spectroscopy in the near-UV range (406.7 nm) may overcome many problems associated with NIR absorbance spectroscopy and other markers of tissue perfusion. Raman spectroscopy in the NIR takes advantage of the remark transparency of tissue at these wavelengths, while at the same time providing high-resolution vibrational signals. Spiro, T. G., "Resonance Raman spectroscopy: A new structure probe for biological chromophores," Accts. Chem. Res., 7:339–344 (1974); Terner, J., El-Saye, M. A., "Time-resolved resonance Raman spectroscopy of photobiological and photochemical systems," Accts. Chem. Res., 18:331–338 (1985). Hemoglobin has strong absorption and resonance properties in the near-UV range. FIG. **3** depicts data from human blood samples in the laboratory demonstrating the sharp peaks of oxy and deoxy human hemoglobin samples. (The area under the curve (AUC) in FIG. **3** of the Raman spectra produce oxygen saturations comparable to that from a multiwavelength co-oximeter.) Comparison of area under the curves of the oxy-peak and blood gas saturations yielded a correlation coefficient of 0.997. These sharp peaks should be compared to the broad overlapping peaks of oxy and deoxy hemoglobin obtained by NIR absorption spectroscopy in FIG. **2**. Furthermore, the resonance Raman effect for hemoglobin is so specific that it can be differentiated from the resonance Raman effect of myoglobin (see FIG. **4**). FIG. **4** shows resonance Raman spectroscopy of both oxygen hemoglobin and myoglobin, demonstrating an ability to distinguish between the two.

Analyzing the spectroscopy data by computing the AUC has been mentioned. Alternately to computing area, peak height analysis may be performed. For example, tissue hemoglobin oxgyen saturation (StO_2) may be determined by either comparing area under the curve of the spectra for both oxyhemoglobin and deoxyhemoglobin and/or comparison of the peak heights between the two species. Each computation provides a percentage. The latter technique is likely to be preferable.

A characteristic of near-UV light is that it can only penetrate tissue to a depth of 1–2 mm and is noncarcinogenic. Although at first thought, depth of penetration might seem to be a disadvantage, actually there is not such a disadvantage. Pathlength becomes less important in this case in terms of quantification issue. Probe contact may be unnecessary, and fiber optics may be simplified. In terms of shock states, blood flow to the surface of any organ is compromised first. In terms of use on hollow organ systems such as the stomach, signals from near-UV resonance Raman spectroscopy would be only from the mucosal surface (an advantage over data from NIR absorption spectroscopy which would likely include signals from non-stomach organs and thus not reflect data from the mucosal surface of the stomach.)

While taking the Raman spectroscopy profile and the fluorescence spectroscopy measurement on the patient at the same time is a preferred embodiment, it will be appreciated that in other embodiments the invention does not require using both Raman and fluorescence spectroscopy.

The fluorescence spectroscopy (such as broadband fluorescence spectroscopy) of the present invention, is performed at between 390 and 800 nm. A most preferred example of fluorescence spectroscopy according to the invention is NADH surface-subsurface fluorescence spectroscopy.

As examples of the biological tissue according to the invention may be the brain, heart, lung, liver, blood, tongue or other oral mucosa, eye (such as the cornea or retina), the esophagus and stomach, peripheral skeletal muscle, skin, intestines, pancreas, kidney, bladder, urethra, skin, nailbed, cervix, uterus, oropharynx, nasopharynx, esophagus, blood etc. Probing on the tongue/oral mucosal, skin, or cornea/retina optionally may be totally noninvasive, without the requirement for probe contact with tissue. For probing the esophagus or stomach, simple fiber optics are constructed into a nasogastric tube for measurements at the level of the esophageal or stomach mucosa. Fiber optics also can be used in urinary catheters for monitoring of substances in the urine or for interrogation of the bladder mucosa. Skeletal muscle or dermis can be assessed with fiber optics of a size insertible through small needles, inserted into a muscle belly such as the deltoid or quadriceps.

The inventive methods may include monitoring a specific tissue bed (brain, heart, lung, liver, eye, blood, etc.) in the patient; placing a probe on or near any mucosal or epithelial covered surface of a body or an organ; detecting exhaled markers or mediators of organ injury (such as by placing a detector at the airway of the patient). Examples of exhaled markers or mediators are isoprostanes and/or myeloperoxidase.

Markers also may be present in a biological material according to the present wherein the markers are contained in urine, saliva, wound exudates, vitreous humor, aqueous humor, tissue exudate, gastric contents, fecal matter, or other biological materials.

The interrogating of biological material such as tissue according to the invention may be, but is not required to be, noninvasive. To maximize the number of markers and mediators that can be measured, a minimally invasive approach is preferred. Interrogating may be intermittently or continuously. A preferred example of minimally invasive probing is by minimally invasively probing the patient by a fiber optic probe or probe array inserted into a tissue bed. The tissue may be in vivo and in situ, but is not required to be. Alternately, the tissue may be removed from a patient before the tissue interrogation. As examples of interrogating tissue are mentioned inserting a probe or probe array into a muscle. Preferably interrogation is by a minimally invasive probe approach, with muscle and interstitium being interrogated directly. Such a minimally invasive approach is preferred for several reasons. UV light does not significantly penetrate epidermis. NIR light can penetrate several centimeters of tissue and can thus probe epidermis, dermis, and muscle. The inability to know the path length of light and to separate the signal of myoglobin from hemoglobin make interpretation of data for the noninvasive use of NIR absorption spectroscopy at any site other than the brain to be

conventionally difficult, and a drawback to be avoided. The large number of valuable markers, which can be detected in the UV and NIR range by Raman spectroscopy, more than outweigh any drawback to placing a small probe intramuscularly. Bench experiments have allowed measures to be made of such substances as hemoglobin within cells in the UV range. (See J. Terner, T. G. Spiro, M. Nagumo, M. F. Nicol, and M. A. El-Sayed, "Resonance Raman spectroscopy in the picosecond timescale: the CO hemoglobin photo-intermediate," J. Amer. Chem. Soc., 102: 3238–3239 (1980); J. Terner, J. D. Stong, T. G. Spiro, M. Nagumo, M. F. Nicol, and M. A. El-Sayed (1980), "Picosecond resonance Raman spectroscopic evidence for excited state spin conversion in carbonmonoxy-hemoglobin photolysis," Proc. Natl. Acad. Sci. USA, 78: 1313–1317; J. Terner, T. G. Spiro, D. F. Voss, C. Paddock and R. B. Miles, "Picosecond resonance Raman spectroscopy of oxyhemoglobin photolysis," J. Phys. Chem., 86: 859–861 (1982)). Such results indicate that cell penetration of the near-UV wavelength in the interstitium will not pose a major problem.

In the inventive methods and products, the obtained spectroscopy results preferably may be for at least one mediator or marker associated with a shock state and/or tissue injury; tissue ischemia, tissue inflammation and/or tissue immune dysfunction; for presence and/or proportions for the at least one shock state and/or tissue injury mediator or marker; for at least one mediator associated with a shock state and/or tissue injury or tissue ischemia, inflammation or immune dysfunction and/or for at least one marker of tissue perfusion or injury.

A marker and/or mediator according to the present invention may be within intracellular, interstitial or intravascular space or within exhaled air from a patient. The marker and/or mediator may be selected from the group consisting of lactate, pyruvate, ATP, PCr, AMP, ADP, Pi, NAD, NADH, albumin, endotoxin, exotoxin, microbes, cytokines-chemokines, procalcitonin, hormones, myeloperoxidase, elastase, xanthine oxidase, xanthine dehydrogenase, fatty acid binding proteins, catecholamines and vasoactive peptides. The marker or mediator may be a metabolic or pro or anti-inflammatory marker or mediator. Cardiac biomarkers, GI markers, cerebral markers, skin markers, lung markers, blood markers, and/or eye markers, etc. are mentioned as examples.

Examples of spectroscopy results according to the invention may be, e.g., data relating to diagnosing and/or following progression or resolution of shock states and/or tissue injury (such as inflammatory or immune dysfunction), and/or tissue ischemia; determining whether the tissue has insufficient oxygen delivery to meet metabolic demands of the tissue while simultaneously determining whether mitochondrial dysfunction or injury exists; monitoring for appearance of one or more tissue markers specific for a specific disease state; determining tissue viability; diagnosing tissue injury, tissue inflammation or tissue immune dysfunction; and/or continuously interrogating the patient for appearance of abnormal tissue markers specific for a suspected disease state. A preferred example of spectroscopy results are results relating to diagnosing shock.

As examples of spectroscopy results according to the present invention may be given data for tissue hemoglobin oxygen saturation including amount of oxyhemoglobin and deoxyhemoglobin by Raman spectroscopy; data for NADH presence and/or accumulation by fluorescence spectroscopy; data for oxygenated hemoglobin, deoxygenated hemoglobin and/or NADH; data for myoglobin oxygenation saturation; data for cytochrome oxidase redox status; data for pH of the tissue. A most preferred example of spectroscopy results is data for tissue hemoglobin oxygen saturation by Raman spectroscopy combined with data for NADH presence and/or accumulation by fluorescence spectroscopy.

The spectroscopy results according to the invention may be for absolute concentration (such as absolute concentration of hemoglobin in the tissue) or for relative concentration. Examples of relative concentrations are NAD/NADH; lactate/pyruvate; Pcr-ATP; ATP-ADP; Pcr-Pi; oxidized cytochrome oxidase to reduced cytochrome oxidase, and/or oxyhemoglobin with deoxyhemoglobin.

The spectroscopy results according to the invention advantageously are available on the order of seconds. Signal processing and computer algorithms may be used to process the spectroscopy data.

Another preferred embodiment of the invention provides a medical measurement device comprising: a spectrometer with multiple wavelength settings for resonance Raman spectroscopy; and a biological probe electrically connected to the spectrometer. Inventive medical measurement devices optionally may include a fluorescence spectrometer electrically connected to the biological probe; a laser source (such as a laser tunable to multiple wavelengths) and a charge coupled device. By using a laser tunable to multiple wavelengths, multiple target molecules may be detected. Such multiple target molecules may have useful detectable absorption, resonance Raman and fluorescence spectra at differing wavelengths. Exemplary devices according to the invention may be seen with regard to FIG. **26**(*a*)–(*e*).

With reference to FIG. **26**(*a*), a fixed frequency laser (preferably such as a laser LS including, but not limited to, wavelengths of approximately 290 to 420 nm) is piped **1** through one leg of a fiber optic bundle. An example of fiber optic bundle **100** is seen in further detail in FIG. **26**(*e*), shown in a configuration of one emitting fiber optic **101** (in the center) surrounded by eight collecting bundles **102**. A fiber optic bundle **100** is only one example, and the fiber optic bundle may be otherwise configured, such as containing one emitter and one or several sensor fibers, in a ratio of one emitter to one sensor up to one emitter to twelve sensors. The number of emitters could be increased and the spaces between emitters and detectors changed. The emitters and detectors might also be placed along the length of the probe as opposed to its end. The fiber optic bundle **100** may be positioned on or within a tissue sample. Re-emission from the tissue sample is collected in back-scattering configuration by the same fiber optic bundle. The end of the fiber optic bundle preferably is placeable directly onto the surface of a tissue such as the oral mucosal or heart. Alternatively, the fiber optic bundle is placeable directly into a tissue such as the brain or liver. The fiber optic arrangement does not require contact with the tissue especially when extraneous light (ambient light) is prevented from entering the fiber optic sensor.

A preferred example of an invasive fiber optic probe is one that is less than 0.2 mm, and which can be rapidly placed singularly or in an array in a muscle bed through a small gauge hypodermic needle. When such a needle is used to place a probe, after insertion the needle may then be removed and the probe secured in place such as by medical tape.

Again referring to FIG. **26**(*a*), the light collected by the fiber optic is notch filtered by a laser notch filter system **200** (comprising at least one and preferably two laser notch filters) and then distributed to a spectrograph system **300** (preferably such as a spectrograph system comprising a Raman spectrograph system and a fluorescence spec-

trograph system). The spectrograph system **300** has a respective CCD detector system **400** associated with it. The CCD detector system preferably comprises a CCD detector for each spectrograph system, i.e., when using a Raman spectrograph system with a fluorescence system, the Raman spectrograph system has an associated CCD detector and the fluorescence system has an associated CCD detector. The CCD detector system **400** provides signals to a signal analyzer **500** (such as a PC type computer). It will be appreciated that respective systems **200**, **300** and **400** each respectively may include one, two, three or more components, with some examples of such systems being given in FIGS. **26**(*b*), **26**(*c*) and **26**(*d*). Preferably, laser notch filter system **200** comprises at least one laser notch filter, spectograph **300** comprises at least one spectrometer and CCD detector system **400** comprises at least one CCD detector.

In a particularly preferred embodiment of the invention, an exemplary device is provided incorporating both Raman spectroscopy and fluorescence spectroscopy. The exemplary device according to FIG. **26**(*b*) is an example of such an inventive device combining Raman and fluorescence spectroscopy. With reference to FIG. **26**(*b*), the light collected by the fiber optic is notch filtered **2**, **2'***b* and distributed to spectrometers such a spectrograph system set for Raman **3** and a spectrograph set for broadband fluorescence **30**. An example of the Raman spectroscopy system **3** may include two spectrometers containing high groove density gratings, one set to collect Raman scattering between 300 and 3700 cm^{-1} from the laser line (collecting the Raman signal of water to use as an intensity standard) and one set to collect Raman scattering between 1200 and 1700 cm^{-1} (heme vibrations). An example of the fluorescence spectroscopy system **30** contains a low groove density grating and is set to collect broadband fluorescence emission within the region 200 to 800 nm. The Raman spectrograph system **3** has a respective CCD detector system **4** associated with it, and the fluorescence spectroscopy system **30** has a respective CCD detector system **40** associated with it. The CCD detector systems **4**, **40** provide signals to an analysis system, such as a PC type computer **5**.

With an equipment set-up according to FIG. **26**(*b*), levels of oxyhemoglobin, deoxyhemoglobin (and thus tissue hemoglobin saturation), and NADH accumulation, may be determined. Information necessary to determine blood pH within the tissue as well as the absolute concentration of hemoglobin within the tissue may be obtained. As for computing concentration, an example may be appreciated with reference to FIG. **27**, demonstrating that the resonant Raman spectroscopy technique can detect differences in the amount of hemoglobin present. Hemoglobin levels (in absolute terms) may be determined in tissue, by examining the intensity of the signals (y-axis in FIG. **27**). The more hemoglobin present in the tissue, the higher the resulting signal intensity. These intensities may be compared to known standards for the determination of hemoglobin amount.

Another example of an exemplary inventive device is one comprising an electromagnetic radiation generator (such as a laser) with a wide range of selectable wavelengths (such as deep ultraviolet, less than 270 nm to shortwave infrared all the way to 20,000 nm), filters, lenses, fiber optics, a charge coupled device (CCD), a spectrograph, and the software necessary to interpret the Raman shifts. The device can obtain resonance Raman spectra at a variety of wavelengths corresponding to the "fingerprint" or "signature" of molecules associated with tissue oxygen metabolism (such as hemoglobin (Hb), myoglobin (Mb), cytochrome oxidase (cyt a, a3), dissolved or free gases (i.e., O_2, CO_2, CO, NO, etc. in tissues, exhaled respiratory gas or intraluminal gastrointestinal gas), glucose, lactate, pyruvate, and bicarbonate. Various mediators associated with shock such as tumor necrosis factor (TNF) and other pro and anti-inflammatory cytokines, catecholamines (epinephrine, norepinephrine and dopamine), general and destructive proteins such as albumin and myeloperoxidase respectively, high energy phosphates (ATP, PCr, ADP, Pi), metabolic energy intermediates (NAD, NADH), excitatory amino acids (glutamate, aspartate), and vasocative peptides (vasopressin, angiotensin II, natriuretic peptides, etc.) can also be measured with such a technique.

Devices according to the invention may be used in a multiparametric system for non-invasive or minimally invasive monitoring of tissue perfusion and metabolism in critically ill or injured patients. Because the technique permits identification of an almost unlimited number of target compounds, ultra-early detection may be provided, as well as complete characterization and differentiation of various pathologic states. The invention provides also for determining when treatment is complete. The inventive methods and devices may be applied with regard to various shock states, and ischemia of various organ or organ systems such as the heart, brain, and gastrointestinal tract. Probes for the device may be placed within any tissue bed to monitor the state of a specific tissue. The probes and techniques also may be used to reflect the state of the organism as a whole. Probes may be constructed for intravascular placement as well as placement into other devices such as urinary catheters, gastrointestinal tubes and endoscopes, heart catheterization equipment, brain and other tissue monitoring devices.

Devices may used in the operating room to examine target molecules and the status of various organs such as the liver, GI tract, brain or heart or other tissues of interest. Implantable probes may be placed in transplanted tissues to allow for their interrogation at subsequent time points to monitor for rejection.

In another preferred embodiment, the invention provides a method of diagnosing shock, tissue ischemia, tissue inflammation, or tissue immune dysfunction, comprising: (A) for a target molecule population, taking a sample Raman spectroscopy, and/or fluorescence spectroscopy, profile for a patient; (B) comparing the sample spectroscopy profile with a pre-established Raman spectroscopy and/or fluorescence spectroscopy profile for the target molecule population under baseline conditions. A further preferred embodiment provides a spectroscopy comparative profile, comprising: a pre-established Raman spectroscopy and fluorescence spectroscopy profile for a target molecule population under baseline conditions; and a sample Raman spectroscopy and fluorescence spectroscopy profile for the target molecule population.

The profiles according to the invention may be of relative amounts, or of absolute amounts. The sample profile may be taken from a tissue or a space in a body, or taken from a tissue or a space out of the body. The respective profiles are not required to be from the same species. The comparative profiles in a preferred example include a pre-established fluorescence spectroscopy profile for NADH under baseline conditions and a sample fluorescence profile for NADH. In another preferred example, a spectroscopy comparative profile includes a pair of Raman spectroscopy profiles and a pair of fluorescence spectroscopy profiles (such as one Raman spectroscopy profile and one fluorescence spectroscopy profile taken from a patient after a medical event concerning the patient).

Preferred examples of target molecule populations are NAD/NADH; lactate/pyruvate; PCr-ATP; ATP-ADP; PCr-Pi; oxidized cytochrome oxidase to reduced cytochrome oxidase, and/or oxyhemoglobin with deoxyhemoglobin. However, it will be appreciated that further potential target molecule populations may be screened and selected as target molecule populations according to the invention.

Desired features of a marker(s) of tissue perfusion are its early change after injury; and, that its normalization would indicate that resuscitation is complete. This would help to ensure that shock is detected at its earliest possible time point and that resuscitation would not be prematurely stopped. In addition, the marker(s) would not be subject to misinterpretation from factors such as changes in minute ventilation, pain, etc.

Experimentation: Markers

Using lab bench versions with diode array detection, Raman spectroscopy was used in the UV and NIR in both reflectance and transmission mode to identify several compounds having utility as markers of hemorrhage severity and its sequelae. The first group are oxygen sensitive markers of ischemia and include hemoglobin (Hb), myoglobin (Mb) and cytochrome oxidase (Cyt aa_3). The second group is of exquisitely sensitive oxygen-related metabolic markers of shock including lactate, pyruvate, nicoteinamide adenine dinucleotide phosphate (NAD) and NAD reduced form (NADH). A third group includes the high-energy phosphates phosphocreatine (PCr), adenosine-5'-triphosphate (ATP) and adenosine-5'-diphosphate (ADP). The fourth group includes the vasoactive chemicals epinephrine and norepinephrine.

Raman spectra were obtained of post-hemorrhage markers in inflammation such as lipopolysaccharide (LPS) and cytokines such as tumor necrosis factor-alpha (TNF-α). Sample spectra of lactate, pyruvate NADH, NAD, PCr, and ATP are shown in FIGS. **27**(*a*), **27**(*b*) and **27**(*c*). Lactate and pyruvate can be easily discriminated by comparing the intensities measured at 1625 cm^{-1}. NAD/NADH can be discriminated by examining the peak around 1690 1625 cm^{-1}. PCr can be separated from other high-energy phosphates with the intensity at 1475 cm^{-1} while ATP and ADP can be separated with the peaks at 1100 and 1400 cm^{-1}.

Of particular interest in detecting the presence and severity of hemorrhagic shock are lactate/puruvate, NADH/NAD, PCr/ATP ratios and the redox status of cytochrome oxidase in skeletal muscle. In addition, hemoglobin concentration, oxygen saturation, and potentially myoglobin oxygen saturation may be obtained. The lactate/pyruvate ratio provides information on the coupling of glycolysis to oxidative phosphorylation, the NADH/NAD ratio provides information concerning the mitochondrial energy state, and the PCr/ATP ratio provides information concerning utilization of high-energy phosphate stores. Haljamae, H., "Cellular metabolic consequences of altered perfusion," in Gutierres, G., Vincent, J., eds., "Update in Intensive Care and Emergency Medicine: Tissue oxygen utilization (Springer Verlag, 1991), pp. 71–86. These indices are considered significantly more sensitive than the redox status of cytochrome oxidase or the local level of hemoglobin concentration, oxygen saturation or pH. Even so, monitoring of current NIR absorption spectroscopy derived parameters such as the redox status of cytochrome oxidase and hemoglobin concentration and saturation may be obtained with Raman spectroscopy and can be performed with greater confidence for potential quantification. One of the major advantages of the use of Raman spectroscopy over NIR absorption spectroscopy is its potential to differentiate the signal of hemoglobin from myoglobin.

Measuring lactate alone is known to be problematic because of the contribution of increased aerobic glycolysis on lactate production secondary to elevations in systemic catecholamine levels. This may occur in the absence of continuing tissue hypoxia. Luchette, F., Roboinson, B., Friend, L., McCarter, F., Frame, S. B., James, J. H., "Adrenergic antagonist reduce lactic acidosis in response to hemorrhagic shock," J. Trauma, 46:873–880 (1999). However, knowing the lactate/pyruvate ratio along with NADH/NAD and PCr/ATP ratios will provide the operator clear insight into whether true tissue hypoxia is occurring and its severity. In addition, because there is a definite lag in metabolism of lactate, restoration of adequate perfusion will likely result in return of the above ratios before normalization of lactate, thus informing the operator that instituted therapies are working or failing. Additional sensitivity could be added by external stimulation of a few muscle fibers to examine the rate of degradation and restoration of the above metabolic intermediates. Failure to normalize these values in a timely manner indicates a state of intractable shock.

The use of Raman in the near-UV and NIR has additional advantages of allowing caretakers to detect the progression of hermorrhagic shock to more complex forms of shock such as sepsis. Spectra have been obtained for inflammatory markers such as myeloperoxidase and cytokines such as TNF-α. In addition, spectra have been obtained on lipopolysaccharide, and d-lactate, which are markers indicative of intestinal barrier breakdown. Spectra on the catecholamines epinephrine and norepinephrine have been obtained. These vasocactive substances are now being recognized as sensitive markers of the level of hypoperfusion and stress caused in various shock states. These observations may be extended to vasocative peptides such as vasopressin and angiotensin, which have been measured in rat pheochromocytoma cells by Schulze et al. Schulze, H. G., Greek, L. S., Barbosa, C. J., Blades, M. W., Gorzalka, B. B., Turner, R. F. B., "Measurement of some small-molecule and peptide neurotransmitters in-vitro using a fiber-optic probe with pulsed ultraviolet resonance ultraviolet resonance Raman spectroscopy," J. Neurosci. Meth., 92:15–24 (1999).

Thus, markers mentioned herein have remarkable utility when examined in a manner of ratios. Also, absolute quantification can be obtained using embedded standards in probes placed in parallel with other emitting and sensing probes, from which can be determined an exact path length of light. The markers mentioned in this experiment were found to be detected by UV and NIR Raman spectroscopy in both the reflectance and transmission mode gives flexibility of design of methods and products according to the invention.

In Vivo Spectroscopic Experimentation

Techniques according to the invention have been successfully applied to several tissue sites in animals, demonstrating feasibility. Techniques according to the invention require no probe contact (although probe contact with tissue can take place if desired) with tissue and acquisition times are on the order of seconds.

FIG. **5** represents near UV resonance Raman signals taken from skeletal muscle subjected to isolated tourniquet ischemia. Signals were obtained in one minute (i.e., scans were acquired in one minute segments). The oxyhemoglobin signal (1375) decreases simultaneous to the increase in the deoxy hemoglobin signal (1357).

FIGS. **6**–**11** represent near UV-resonance Raman spectroscopy data of oxy and deoxy hemoglobin (with only gross signal processing) from the exposed quadriceps muscle from a rat during hemorrhage. Using area under the curve and

peak height comparison analysis, tissue saturations are demonstrated to decrease during hemorrhage. Of importance is that significant tissue desaturation occurs despite the maintenance of normal vital signs. These values for oxyhemoglobin are very similar to those reported with NIR absorption spectroscopy.

FIG. **7** is for 1 ml bleeding of the same muscle as FIG. **6**, which is the baseline spectrum. At 1 ml bleeding, no change in the oxy or deoxy peak was observed, and there was no change in vital signs. FIG. **8** is for 2 ml bleeding of the same muscle as FIGS. **6** and **7**. At 2 ml bleeding, an evolving deoxy peak is to be noted, while the animal maintained normal vital signs. At 5 ml bleeding (FIG. **9**) for the same muscle as FIGS. **6–8**, a progressively greater deoxy signal is observed, and, although vital signs (MAP decreasing) are still within the normal range. Where 7.5 ml of bleeding (FIG. **10**) has occurred for the same muscle as FIGS. **6–9**, the animal demonstrated physical evidence of decompensate shock; however, Raman spectroscopy indicates greater severity than the vital signs might predict. Results from FIGS. **6–10** are summarized in Table 1 below.

TABLE 1

	OxyHb	DeoxyHb
Baseline (FIG. 6)	69%	31%
1 ml bleed (FIG. 7)	68%	32%
2 ml bleed (FIG. 8)	53%	47%
5 ml bleed (FIG. 9)	30%	70%
7.5 ml bleed (FIG. 10)	14%	86%

A similar experiment to that of FIGS. **6–11** was performed using the tongue as the target organ, as seen with reference to FIG. **12**, which shows resonance Raman spectra demonstrating saturation changes during 3 cc hemorrhage. The signal was obtained in 5 seconds. Again, changes in tissue saturation occurred prior to changes in vital signs, demonstrating that the use of Raman spectroscopy according to the invention can be totally noninvasive.

FIG. **13** demonstrates that near-UV resonance Raman spectroscopy of hemoglobin may be used to monitor tissue pH in a manner similar to that of NIRS. The spectra of FIG. **13** are from pure oxyhemoglobin samples at different pH levels. Subtraction of the two scans provides clear evidence for a difference indicating that pH alone was responsible for the effect. FIG. **13** is for Horse Hb. Near UV resonance Raman spectra of hemoglobin are shown at pH of 8 (scan 1) and 6 (scan 2) with a subsequent subtraction scan (scan 3) demonstrating the likelihood of pH sensitive changes in the spectra.

Another important finding according to the present invention is that at this same near-UV wavelength, NADH demonstrates significant fluorescence. The present inventors have observed significant fluorescence from tissue excited in the near-UV range (406.7 nm) using a portable spectrometer. Exciting tissue in the near-UV range (406.7 nm) according to the invention provides better resolution than traditional filtering in which unique excitation light sources and detection filters are used for the conventional set-up relying on NADH fluorescing (emiting light at 460 nm) when excited at a wavelength of 360 nm (near-UV).

Based on the importance of NADH in cellular oxygen utilization (as set forth above), from this aspect of the invention may be determined the point of tissue dysoxia or critical DO_2 (ischemia) prior to being able to note increases in systemic lactate. Although NADH also exists in the cytoplasm, it does so in insignificant amounts compared to those produced within the mitochondria during states of dysoxia. In conjunction with the tissue saturation experiments above, NADH fluorescence from quadriceps (FIGS. **14–19**), tongue (FIG. **20**) and additionally liver (FIG. **21**) was obtained during graded hemorrhage.

FIG. **14** is a baseline, and FIG. **15** reports spectra after 5 mls bleeding for the same quadriceps muscle. Significant NADH fluorescence is observed after 5 ml hemorrhage. Although the animal has relatively normal vital signs, fluorescence indicated that critical dysoxia has occurred. (FIG. **15**.) At 7.5 mls of bleeding (FIG. **16**) for the same muscle, increasing fluorescence indicates additional ischemia. At 9 mls of bleeding (FIG. **17**), even more fluorescence is observed, indicating the ability to grade severity in real time. At 12 mls of bleeding (FIG. **18**), the animal is almost terminal.

In the experiment in which blood pressure was monitored, significant fluorescence occurred prior to and after changes in vital signs. With equipment according to the present invention, tissue oxygen saturation and NADH fluorescence may be simultaneously obtained. Again, the depth of tissue interrogated is the same as that for tissue oxygen saturation. Thus may be determined the point at which critical oxygen delivery (dysoxia) occurs. Significant warning prior to this time will occur as reflected in reductions in tissue oxygen saturation.

Continued NADH fluorescence after restoration of oxygen delivery indicates ongoing dysoxia despite the potential for normalization of tissue oxygen saturation. The normal heart shows little or no NADH surface fluorescence. The beginning of ischemia and maximum ischemia may e observed. Continued patch fluorescence may be observed after reperfusion. Thus, NADH fluorescence data has value in monitoring tissue even after perfusion has been restored.

Because of the kinetics of lactate production and transport, it is very likely dysoxia detected by NADH accumulation and fluorescence will occur significantly earlier than with detection of regional or systemic lactate or even CO_2. In short, the combined use of near-UV resonance Raman spectroscopy and near-UV NADH fluorescence serve as an exquisitely sensitive early warning system for pending defects in tissue perfusion and in ensuring the completeness of resuscitation.

Other heme proteins, which have importance in ischemia-reperfusion diseases can be detected using resonance Raman spectroscopy at the same near-UV wavelength (406.7 nm). These include myeloperoxidase, which is an injurious enzyme produced and released by neutrophils, and xanthine oxidase, which is converted from xanthine dehydrogenase after reperfusion of ischemia and is responsible for the production of free radicals. Hayward, R., Lefer, A. M., "Time course of endothelial-neutrophil interaction in splanchnic artery ischemia-reperfusion," Am J Physiol 275 (6 Pt 2): H2080–6 (1998); Tan, S., Yokoyama, Y., Dickens, E., Cash, T. G., Freeman, B. A., Parks, D. A., "Xanthine oxidase activity in the circulation of rats following hemorrhagic shock," Free Radic Biol Med, 15(4):407–14 (1993).

A resonance Raman spectroscopy spectrum taken for a human is shown for myeloperoxidase (FIG. **23**). The ability to detect myeloperoxidase would be helpful in evaluation of wounds and systemic reperfusion injury and sepsis.

Another group of potentially useful markers of preclinical shock secondary to hypovolemia are endogenously produced catecholamines such as epinephrine and norepinephrine and the vasoactive peptides such as angiotensin, vasopressin, endothelin, and adrenomedullin, all of which are known to be significantly elevated in the setting of hypov-

olemia and other shock states. Jakschik, B. A., Marshall, G. R., Kourik, J. L. Needleman, P., "profile of circulating vasoactive substances in hemorrhagic shock and their pharmacologic manipulation," J Clin Invest, 54(4):842–52 (1974); Lanza, V., Palazzadriano, M., Scardulla, C., Mercadante, S., Valdes, L., Bellanca, G., "Hemodynamics, prolactin and categchloamine levels during hemorrhagic shock in dogs pretreated with ap prolactin inhibitor (bromocriptine)," Pharmacol Res Commun., 19(4):307–18 (1987); Yilmazlar, A., Yilmazlar, T., Ozcan, B., Kutlay, O., "Vasopressin, renin, and adrenocorticotropic hormone levels during the resuscitation of hemorrhagic shock in dogs," J Emerg Med, 18(4):405–8 (2000); Kitajima, T., Tani, K., Yamaguchi, T., Kubota, Y., Okuhira, M., Mizuno, T., et al., "Role of endogenous endothelin in gastric mucosal injury induced by hemorrhagic shock in rats," Digestion, 56(2): 111–6 (1995); Fujioka, S., Ono, Y, Kangawa, K., Okada, K., "Plasma concentration of adrenomedullin is increased in hemorrhagic shock in dogs," Anesth Analg, 88(2):326–8 (1999); Lindner, K. H. Strohmenger, H. U., Ensinger, H., Hetzel, W. D., Ahnefeld, F. W., Georgieff, M., "Stress hormone response during and after cardiopulmonary resuscitation," Anesthesiology, 77(4):662–8 (1992); Lindner, K. H., Haak, T., Keller, A., Bothner, U., Lurie, K. G., "Release of endogenous vasopressors during and after cardiopulmonary resuscitation," Heart, 75(2):145–50 (1996).

Raman spectra of vasopressin in the UV spectrum at 350 nm is shown at FIG. **24**, and for norepinephrine in the same UV spectrum at FIG. **25**. Ability to detect, quantitate, and trend these markers can be used with regard to evaluating and treating numerous disease states such as shock, congestive heart failure, pain states, burns, etc. These and other similar mediators can be detected and quantitated using resonance Raman spectroscopy. Schulze, H. G., Greek, L. S., Barbosa, C. J., Blades, M. W., Gorzalka, B. B., Turner, R. F., "Measurement of some small-molecule and peptide neurotransmitters in-vitro using a fiber-optic probe with pulsed ultraviolet resonance Raman spectroscopy," J. Neurosci Methods, 92(1–2):15–24 (1999).

The ability to detect dysoxia and ensure its resolution at the earliest possible time has great value for the triage of ill or injured patients. Therapy and resources can be better allocated and victim's progress better monitored, reducing the incidence of under-resuscitation as well as provision of needless resuscitation. Based on the biphasic relationship of oxygen delivery and consumption of a tissue, the present invention measures hemoglobin saturation in conjunction with NADH as a reflection of the oxygen dependent bioenergetic state of the cell.

Based on experimental results herein, it is seen that near UV excitation can be exploited to simultaneously perform Raman resonance spectroscopy of oxy and deoxyhemoglobin, and surface-subsurface fluorescence of NADH. Also, UV and NIR RRS have been obtained from a number of compounds (including high-energy phosphates PCr, ATP and ADP, NAD, NADH, the glycolytic metabolites pyruvate and lactate, and the excitatory amino acid glutamate) in solid and aqueous states.

From the experimental data set forth above, it may be seen that with the use of combined UV, near UV and NIR Raman spectroscopy, identification and monitoring of a large number of useful target compounds may be accomplished, for detecting and monitoring the presence and severity of hemorrhagic shock and development or resolution of its sequelae such as sepsis. The present inventors have successfully shown that the various compounds discussed above are amenable to detection by UV, near UV and NIR Raman.

It has recently been demonstrated that NIR absorption spectroscopy can be used to determine tissue pH by examining shifts in the broad bands of hemoglobin. This is based on the known fact that histadine residues of hemoglobin are pH sensitive. NIR absorption spectroscopy is being examined to determine hematorcrit in a similar manner. Because pH sensitive shift is observed in all of the oxy and deoxy bands of the resonance Raman spectra and hemoglobin concentration differences in the heights of the bands, it may be concluded (by such techniques as partial least squares) that tissue pH and hematorcit/hemoglobin levels may be determined using resonance Raman spectroscopy.

Of recent importance has been the development of the concept of cytopathic hypoxia as an explanation for the oxygen transport abnormalities, which exist during sepsis. This theory suggests that such inflammatory compounds as tumor necrosis factor and endotoxin damage mitochondria. This damage prevents the mitochondria from utilizing oxygen. Data for studies using NIR absorption spectroscopy appear to support this theory. The combination of near-UV resonance Raman spectroscopy of hemoglobin tissue saturation and NADH fluorescence would help detect this if it existed. In such a setting, tissue saturation would be normal or elevated but NADH fluorescence would be significant. This entity of cytopathic hypoxia may be one factor which confounds the use of other monitoring modalities such as splanchnic tonometry and monitoring of mixed venous oxygen saturation.

Methods and devices according to the invention may be used in various manners, such as to exploit shifts in the spectra of molecules such as hemoglobin and myoglobin to calculate blood and tissue pH as well as detect and determine the actual hemoglobin and myoglobin oxygen saturation. Spectroscopy equipment may be coupled with probe(s) and sensor(s) to construct a device to interrogate the perfusion and metabolic status of individual tissues as well as the organism as a whole, advantageously in a noninvasive or minimally invasive manner. For instance, the invention provides a minimally invasive fiber optic probe or arrays of probes (each probe less than 0.2 mm) which are insertible into a muscle or other tissue bed with a small gauge needle. Resonance Raman spectroscopy in the deep ultraviolet wavelength (less than 270 nm) is used for interstitial fluid analysis (micron level penetration), while longer UV or near UV wavelengths are used for cellular analysis, due to slightly longer wavelengths that could penetrate to levels near 1 mm. Both the deep and near UV wavelengths also may be used with a probe placed on the oral cheek mucosal epithelium. NIR Raman spectroscopy may be used with non-invasive optical fibers placed on the skin or within tissue beds. Surface Raman spectroscopy is used to interrogate standards of detected substances for quantification.

When spectroscopy according to the present invention operates at multiple wavelengths, additional valuable metabolic and humoral targets may be selected for identification and tracking. The one-dimensionality problem of conventional emergency medical measurement technology is avoided. As has been mentioned above, for conventional IR or NIR technology, problems arise because water strongly absorbs IR radiation, and thus presents strong interference to the use of IR absorption spectroscopy in the clinical setting. The present invention is not burdened with such problems because water is a rather weak Raman scatterer. Raman spectroscopy can be used to provide the same vibrational information as the more common NIR absorption spectroscopy with no significant interference from water. In addition, the use of Raman allows one to take advantage of the

resonance Raman enhancement effect, plus polarization effects, neither of which have parallels in IR absorption spectroscopy. Thus, a principal advantage of the invention is that Raman spectroscopy does not suffer the same problems with water as normal IR spectroscopy, and, additionally, Raman spectroscopy is not limited to a single wavelength but can use a variety of wavelengths to interrogate molecules of interest at different tissue depths (skin, muscle, etc). Normal and transmission spectroscopy may be used to complement Raman spectroscopy for calibration, determination of tissue depth, and other enhancement of obtained information. Issues such as weakness of signal, potential tissue damage, and interference from fluorescence can be managed.

The ability to target multiple compounds in real-time provided by the present invention is a substantial advantage for detection and treatment of certain disease states and shock states. For example, the ability to monitor levels of catecholamines and vasoactive peptides may prove to be more sensitive of early shock states or states of intractable shock. Elevations of these compounds may indicate the severity of such states as acute sickle cell pain crises. Thus, resuscitation and treatment of such states using markers such as catecholaimnes or vasoactive peptides as endpoints may provide a relatively objective means to determine treatment efficacy.

Another example of methods according to the invention are uses in conjunction with maneuvers such as simple muscle contraction or use of a tourniquet. Monitoring rates of high-energy phosopahte degradation and regeneration or intermediary compound ratios such as lactate-pyruvate or NAD-NADH in disease states may provide relatively sensitive information concerning the state of the microvasculature.

Outpatient applications also are provided. Depending on the sensitivity of the device, the technology of the invention may be used in the outpatient setting for determination of various target compounds such as hemoglobin. The device may be used to diagnose certain precancerous or cancerous lesions (such as skin melanoma, etc.) in vivo. Point of care or continuous real-time tissue monitoring is provided with the inventive method and its components.

Because probes may be relatively small, patients may be continuously interrogated for the appearance of abnormal tissue markers specific for a suspected disease state. Examples of such markers are cardiac biomarkers such as troponin or myocardial fatty acid binding protein, GI markers of ischemia scuh as D-lactate and intestinal fatty acid-binding protein, and cerebral markers such as neuronal enolase.

Combining resonance Raman spectroscopy of tissue hemoglobin saturation and NADH fluorescence of the same region provides for detecting ultra-early perfusion deficits and determining adequacy of resuscitation. The present invention provides at least the following advantages: 1) little or no tissue contact (point and click technology); 2) rapid acquisition (such as acquisition times on the order of 1 second); 3) data (tissue saturation and point of critical oxygen delivery) that is not confounded by hypo or hypercarbia; 4) differentiation of sepsis (cytopathic hypoxia) from flow dependent dysoxia; 5) true data from mucosa (oral or other points in the GI or GU tract); 6) pH and hemaglobin (on a par with NIR absorption technology); and 7) other important markers of tissue injury such as myeloperoxidase, xanthine oxidase, vasocative substances, etc.

The present invention may be applied to known markers and also to markers as newly reported, because of the nature of resonance Raman spectroscopy. As a new marker (such as procalcitonin, etc.) is reported, the present invention provides for its study by resonance Raman spectroscopy.

The inventive methods and devices may be used for evaluation of any general shock state (trauma, cardiogenic, septic). Applications include hypoxic-hypoxia, hemorrhagic shock, cardiogenic shock, septic shock, and isolated organ ischemia (including wounds).

The inventive methods and devices may be used to evaluate the oxygen status of any organ during surgery (e.g., the heart during cardiopulmonary bypass surgery, the brain during neurosurgery, and various organs during transplant); to evaluate donor organs prior to transplant; to include in devices such as pacemakers to interrogate areas of myocardium at risk of injury; to evaluate a patient with congestive heart failure (such as at the hospital, office, home, etc.) to determine symptom etiology (such as fluid overload versus deterioration in heart function); to determine if a patient requires blood transfusion; to care for wounds.

The invention fills the current void of no universally accepted way of determining when a patient requires blood transfusion. Because each patient may have a different requirement based on past medical history and the current event, the invention is highly advantageous in allowing repetitive noninvasive measures of a sensitive tissue.

The invention benefits wound care (chronic and acute), by providing information about the oxygenation status of wounds. Care of chronic wounds is improved by the present invention providing the ability to determine oxygenation status of wounds. The use of near-UV resonance Raman spectroscopy determines tissue oxygen saturation at multiple points within the wound (within seconds) with tissue contact being unnecessary. In conjunction with the Raman spectroscopy, NADH fluorescence may be used to determine if the wound is becoming necrotic. The wound may be sampled for injurious substances interfering with wound-healing, such as myeloperoxidase.

The methods and products of the present invention have civilian and military uses. Using UV, near UV or NIR Raman spectroscopy according to the present invention provides for real-time monitoring of a broad range of valuable markers. An operator (such as a combat medic) may use a portable probe according to the invention, with the probe being pluggable into a hand held UV-NIR Raman spectrometer (such as a device the size of a hand held palm PC device). The Raman spectrometer before use on a patient may be programmed to perform V, near UV and NIR Raman spectroscopy for the markers of interest and to report them in a manner readily interpretable to indicate the presence and degree of shock. In the case of a combat medic using such a portable probe that plugs into a Raman spectrometer, the medic may then institute or order appropriate therapy while instrumenting and interrogating the next soldier using the same hand held spectrometer. In this manner, the medic can move back and forth between patients to determine the effect of the instituted therapy and to make triage decisions. When a marker or a combination of markers indicates intractable shock, an appropriate triage decision may be more readily reached than without the measurement information according to the present invention, and thus other more salvageable patients may be more likely to have access to resources and have increased chances of survival.

Data collected according to the present invention may be stored and/or transmitted. For example, data collected by a hand held device (such as a combat medic device) may be transmitted to a remote data bank. As the patient is transported, medics and physicians taking over care may use their

own devices (which may be hand held devices) to hook into the previously implanted fiber optic probe. Data measured during a new hook-up may be compared to data previously collected on the patient (such as data transmitted earlier from the field). New or additional probes optionally may be placed during surgery. The same devices, once placed, may be maintained in place and used to continuously interrogate tissue to monitor the efficacy of ongoing resuscitative efforts and to detect the development of post-hemorrhagic shock and surgical sequelae such as early sepsis. Multiple tissues beds may be interrogated, especially by using small, disposable probes.

While an operator has been referred to hereinabove, it will be appreciated that the inventive methods do not necessarily require a human operator, and that the invention may include partly and entirely automatic, such as computer-assisted, methods and devices. Such automatic and semi-automatic methods and devices may include those in which, upon measurement of ratios or amounts in a certain pre-determined adverse range, pre-formulated reactive therapies are applied. The invention provides for an optional computer system, such as a computer system comprising a database of stored baseline Raman spectroscopy and/or fluorescence spectroscopy profiles and a means to store patient Raman spectroscopy and/or fluorescence spectroscopy profiles. Such a computer system preferably includes a computing system for comparing patient profiles to baseline profiles.

While the invention has been described in terms of its preferred embodiments, those skilled in the art will recognize that the invention can be practiced with modification within the spirit and scope of the appended claims.

We claim:

1. A tissue analysis method, comprising:

interrogating a biological tissue with Raman spectroscopy and fluorescence spectroscopy to obtain spectroscopy results; analyzing the obtained spectroscopy results for at least one mediator or marker associated with a shock state.

2. The method of claim **1**, wherein the tissue interrogating is noninvasive.

3. The method of claim **1**, wherein the tissue is in vivo and in situ.

4. The method of claim **1**, wherein the tissue is removed from a patient before the tissue interrogation.

5. The method of claim **1**, including measuring NADH presence and/or accumulation by fluorescence spectroscopy.

6. The method of claim **1**, including measuring tissue hemoglobin oxygen saturation by Raman spectroscopy and measuring NADH presence and/or accumulation by fluorescence spectroscopy.

7. The method of claim **1**, including determining whether the tissue has insufficient oxygen delivery to meet metabolic demands of the tissue while simultaneously determining whether mitochondrial dysfunction or injury exists.

8. The method of claim **1**, including measuring myoglobin oxygenation saturation.

9. The method of claim **1**, including determining cytochrome oxidase redox status.

10. The method of claim **1**, including determining absolute concentration of hemoglobin in the tissue.

11. The method of claim **1**, including determining pH of the tissue.

12. The method of claim **1**, including intermittently or continuously interrogating the tissue of a patient.

13. The method of claim **1**, including determining tissue viability.

14. The method of claim **1**, including diagnosing shock.

15. A tissue analysis method, comprising:

interrogating a biological tissue with Raman spectroscopy and fluorescence spectroscopy to obtain spectroscopy results, including:

measuring tissue hemoglobin oxygen saturation including amount of oxyhemoglobin and deoxyhemoglobin by Raman spectroscopy; and/or

measuring tissue hemoglobin oxygen saturation by Raman spectroscopy and measuring NADH presence and/or accumulation by fluorescence spectroscopy; and/or

determining whether the tissue has insufficient oxygen delivery to meet metabolic demands of the tissue while simultaneously determining whether mitochondrial dysfunction or injury exists.

16. The tissue analysis method of claim **15**, wherein the obtained spectroscopy results are for at least one mediator or marker associated with a shock state and/or tissue injury.

17. The method of claim **16**, wherein the obtained spectroscopy results are for presence and/or proportions for the at least one shock state and/or tissue injury mediator or marker.

18. The method of claim **16** including determining the concentration of at least one mediator or marker.

19. The method of claim **18**, including determining absolute concentration.

20. The method of claim **18**, including determining relative concentration.

21. The method of claim **16** including determining the presence of at least one mediator or marker.

22. The method of claim **16**, wherein the obtained spectroscopy results are selected from the group consisting of at least one mediator associated with a shock state, tissue injury or tissue ischemia, inflammation or immune dysfunction, and at least one marker of tissue perfusion or injury.

23. The method of claim **22**, wherein the marker may be within intracellular, interstitial or intravascular space or within exhaled air from a patient.

24. The method of claim **22**, wherein the marker is selected from the group consisting of lactate, pyruvate, ATP, Pcr, AMP, ADP, Pi, NAD, NADH, albumin, endotoxin, exotoxin, microbes, cytokines-chemokines, procalcitonin, hormones, myeloperoxidase, elastase, xanthine oxidase, xanthine dehydrogenase, fatty acid binding proteins, catecholamines and vasoactive peptides.

25. The method of claim **22**, wherein the marker or mediator is a metabolic or pro or anti-inflammatory marker or mediator.

26. The method of claim **16**, including monitoring for appearance of one or more tissue markers specific for a specific disease state.

27. The method of claim **16**, including diagnosing tissue injury, tissue inflammation or tissue immune dysfunction.

28. The method of claim **15**, including diagnosing and/or following progression or resolution of shock states and/or tissue injury, and/or tissue ischemia.

29. The method of claim **28**, wherein the tissue injury includes inflammatory or immune dysfunction.

30. The method of claim **15**, including determining absolute concentration of hemoglobin in the tissue.

31. The method of claim **15**, including determining pH of the tissue.

32. The method of claim **15**, including continuously interrogating the patient for appearance of abnormal tissue markers specific for a suspected disease state.

33. The method of claim 32, wherein the markers are cardiac biomarkers, GI markers, cerebral markers, skin markers, lung markers, blood markers, and/or eye markers.

34. The tissue analysis method of claim 15, including measuring tissue hemoglobin oxygen saturation including amount of oxyhemoglobin and deoxyhemoglobin by Raman spectroscopy.

35. The tissue analysis method of claim 15, including measuring tissue hemoglobin oxygen saturation by Rama spectroscopy and measuring NADH presence and/or accumulation by fluorscence spectroscopy.

36. The tissue analysis method of claim 15, including determining whether the tissue has insufficient oxygen delivery to meet metabolic mends of the tissue while simultaneously determining whether mitochondrial dysfunction or injury exists.

37. A method of diagnosing shock, comprising:

(A) for a target molecule population, taking a sample Raman spectroscopy, and/or fluorescence spectroscopy, profile for a patient;

(B) comparing the sample spectroscopy profile with a pre-established Raman spectroscopy and/or fluorescence spectroscopy profile for the target molecule population under baseline conditions; and,

(C) diagnosing shock based on results of the comparing step.

38. The method of claim 37, wherein the method is non-invasive.

39. The method of claim 37, wherein the target molecule population comprises oxygenated hemoglobin, deoxygenated hemoglobin and/or NADH.

40. The method of claim 37, wherein the profiles are of relative amounts.

41. The method of claim 40, including operating an electromagnetic radiation generator at a range of selectable wavelengths from about 270 mm to about 30,000 nm.

42. The method of claim 37, wherein the profiles are of absolute amounts.

43. The method of claim 37, including taking the profiles by Raman spectroscopy.

44. The method of claim 43, including signal enhancement at a resonant frequency for a target molecule of the target molecule population.

45. The method of claim 37, including monitoring a specific tissue bed in the patient.

46. The method of claim 45, wherein the specific tissue bed is a brain, heart, lung, liver, eye, intestines, stomach, pancreas, kidney, bladder, urethra, skin, nailbed, cervix, uterus, oropharynx, nasopharynx, eosphagus or blood.

47. The method of claim 37, including calculating pH of blood and/or tissue.

48. The method of claim 37, including minimally invasively probing the patient by a fiber optic probe or probe array inserted into a tissue bed.

49. The method of claim 48, wherein the probe or probe array is inserted into a muscle.

50. The method of claim 37, including analysis of interstitial fluid.

51. The method of claim 32, including resonance Raman spectroscopy at 390 to 420 nm wavelength.

52. The method of claim 51, wherein the sample profile is taken from a tissue or a space in a body.

53. The method of claim 51, wherein the sample profile is taken from a tissue or a space out of the body.

54. The method of claim 37, including cellular analysis.

55. The method of claim 37, including placing a probe on or near any mucosal or epithelial covered surface of a body or an organ.

56. The method of claim 37, including simultaneously performing fluorescence spectroscopy probing of NADH while performing Raman spectroscopy.

57. The method of claim 37, wherein spectroscopy is performed for multiple wavelengths.

58. A method of diagnosing shock, tissue ischemia, tissue injury, tissue inflammation, or tissue immune dysfunction, comprising:

(A) for a target molecule population, taking a sample Raman spectroscopy, and/or fluorescence spectroscopy, profile for a patient;

(B) comparing the sample spectroscopy profile with a pre-established Raman spectroscopy and/or fluorescence spectroscopy profile for the target molecule population under baseline conditions, wherein the profiles are of relative amounts of NAD/NADH; lactate/pyruvate; Pcr-ATP; ATP-ADP; Pcr-Pi; oxidized cytochrome oxidase to reduced cytochrome oxidase, and/or oxyhemoglobin with deoxyhemoglobin.

59. A method of diagnosing shock, tissue ischemia, tissue injury, tissue inflammation, or tissue immune dysfunction, comprising:

(A) for a target molecule population, taking a sample Raman spectroscopy, and/or fluorescence spectroscopy, profile for a patient;

(B) comparing the sample spectroscopy profile with a pre-established Raman spectroscopy and/or fluorescence spectroscopy profile for the target molecule population under baseline conditions, including detecting exhaled markers or mediators of organ injury.

60. The method of claim 59, wherein exhaled markers or mediators of lung injury are detected.

61. The method of claim 59, wherein a detector is placed at the airway of the patient.

62. The method of claim 59, wherein the exhaled markers indicate organ injury.

63. The method of claim 59, wherein the exhaled markers or mediators are isoprostanes and/or myeloperoxidase.

64. A method of diagnosing abnormalities in vivo and in situ, comprising:

(A) for a target molecule population, taking a sample Raman spectroscopy and/or fluorescence spectroscopy profile for a patient;

(B) comparing the sample Raman spectroscopy or fluorescence spectroscopy profile with a pre-established Raman spectroscopy or fluorescence spectroscopy profile for the target molecule population under baseline conditions;

(C) using differences identified in said comparing step to identify an abnormality associated with a shock state.

65. The method of claim 64, including, while taking the Raman spectroscopy profile, also performing fluorescence spectroscopy measurement on the patient.

66. A computer system comprising:

a database of stored baseline Raman spectroscopy and/or fluorescence spectroscopy profiles and

a means to store patient Raman spectroscopy and/or fluorescence spectroscopy profiles;

including a computing system for comparing patient profiles to baseline profiles with regard to a shock state.

67. A biological material analysis method, comprising:

interrogating a biological material with Raman spectroscopy and

fluorescence spectroscopy to obtain spectroscopy results;

analyzing the obtained spectroscopy results for at least one mediator or marker associated with a shock state.

68. The biological material analysis method of claim **67**, wherein the biological material is bodily fluid.

69. The biological material analysis method of claim **67**, wherein the biological material is tissue.

70. The method of claim **67**, wherein the marker is contained in a biological material selected from the group consisting of urine, saliva, wound exudates, vitreous humor, aqueous humor, tissue exudate, gastric contents, and fecal matter.

* * * * *

UNITED STATES PATENT AND TRADEMARK OFFICE

CERTIFICATE OF CORRECTION

PATENT NO. : 7,113,814 B2
APPLICATION NO. : 10/332613
DATED : September 26, 2006
INVENTOR(S) : Kevin R. Ward et al.

It is certified that error appears in the above-identified patent and that said Letters Patent is hereby corrected as shown below:

In the Specification

At Column 1, line 5, please insert the following:

--STATEMENT OF GOVERNMENT INTEREST

This invention was made with government support under contract number GM57042 awarded by the National Institutes of Health. The government has certain rights in the invention.--

Signed and Sealed this
Twenty-third Day of December, 2014

Michelle K. Lee

Michelle K. Lee
Deputy Director of the United States Patent and Trademark Office

US 20150031966A1

(19) **United States**

(12) **Patent Application Publication**

(10) **Pub. No.: US 2015/0031966 A1**

(43) **Pub. Date: Jan. 29, 2015**

Ward et al.

(54) **EVALUTATING CARDIOVASCULAR HEALTH USING INTRAVASCULAR VOLUME**

(71) Applicant: **THE REGENTS OF THE UNIVERSITY OF MICHIGAN**, Ann Arbor, MI (US)

(72) Inventors: **Kevin Ward**, Superior Twp., MI (US); **Mohamad Hakam Tiba**, Ann Arbor, MI (US); **James M. Blum**, Ann Arbor, MI (US)

(21) Appl. No.: **14/445,926**

(22) Filed: **Jul. 29, 2014**

Related U.S. Application Data

(60) Provisional application No. 61/859,615, filed on Jul. 29, 2013.

Publication Classification

(51) **Int. Cl.**

A61B 5/00	(2006.01)
A61B 8/06	(2006.01)
A61B 5/026	(2006.01)
A61B 5/0295	(2006.01)
A61B 5/0205	(2006.01)

(52) **U.S. Cl.**

CPC ***A61B 5/4836*** (2013.01); ***A61B 5/0295*** (2013.01); ***A61B 5/0205*** (2013.01); ***A61B 5/0261*** (2013.01); ***A61B 5/7282*** (2013.01); ***A61B 8/06*** (2013.01); ***A61B 5/0075*** (2013.01); *A61B 5/02108* (2013.01)

USPC **600/301**; 600/506; 600/484

(57) **ABSTRACT**

Non-invasive monitoring of cardiovascular health is performed by monitoring changes in the volume of blood in the venous side of the vascular system. The blood volume changes are determined from measurements of bioimpedance of limbs or neck, in particular changes in bioimpedance in response to blood modulating events performed on the limbs or neck, where bioimpedance is measured and compared before and after such events.

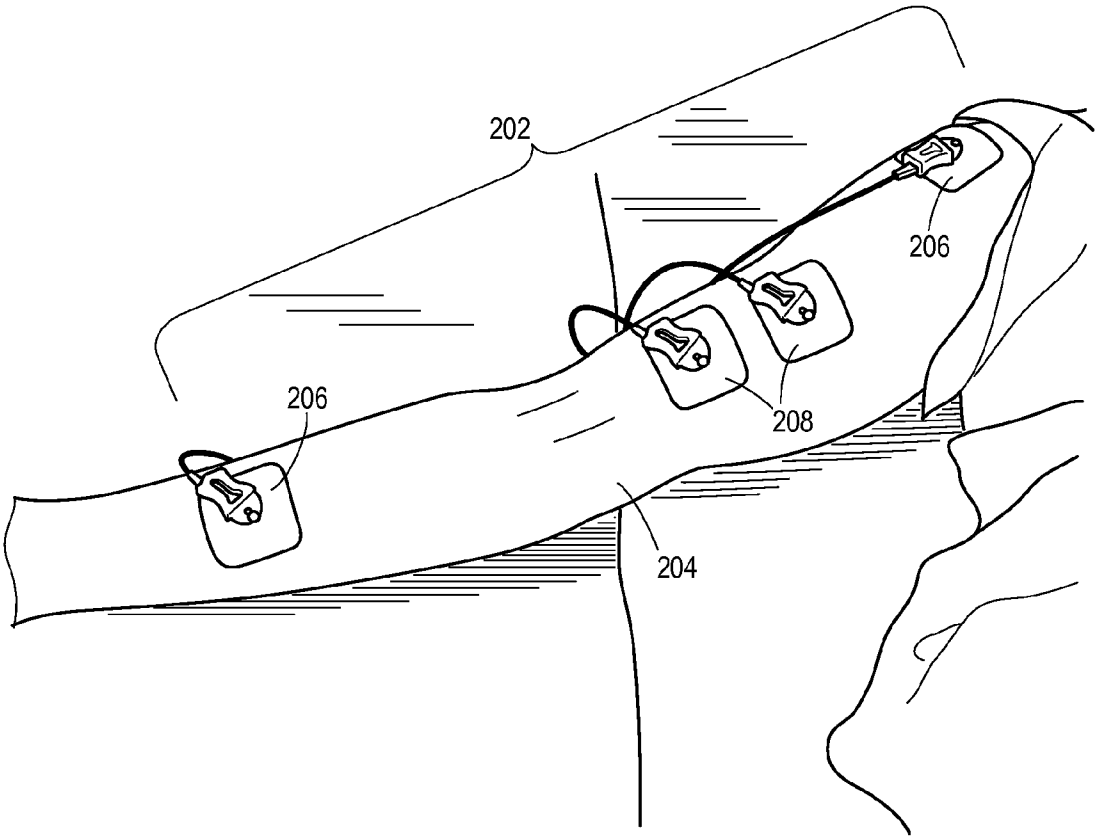

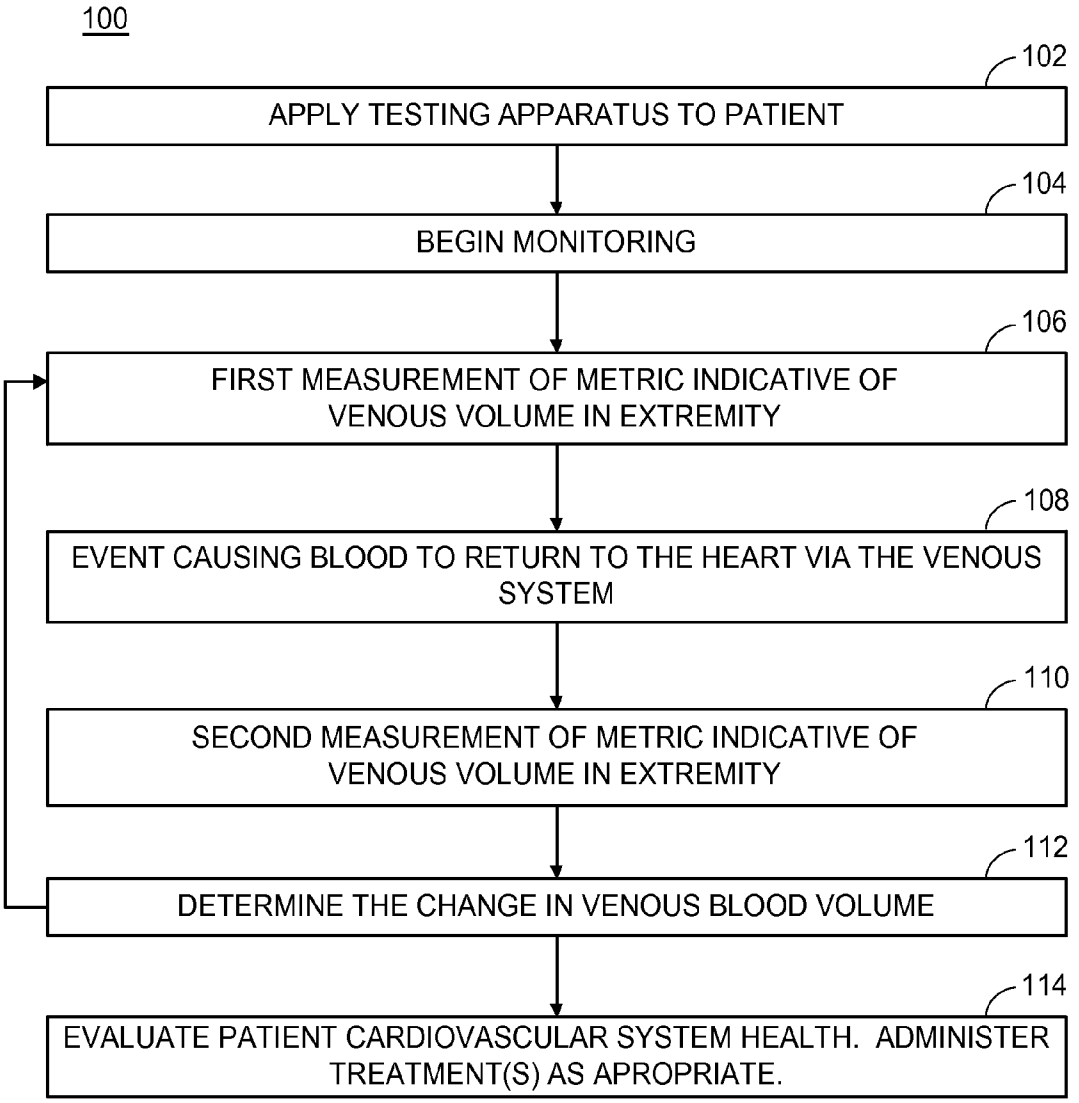
100
102
APPLY TESTING APPARATUS TO PATIENT
104
BEGIN MONITORING
106
FIRST MEASUREMENT OF METRIC INDICATIVE OF VENOUS VOLUME IN EXTREMITY
108
EVENT CAUSING BLOOD TO RETURN TO THE HEART VIA THE VENOUS SYSTEM
110
SECOND MEASUREMENT OF METRIC INDICATIVE OF VENOUS VOLUME IN EXTREMITY
112
DETERMINE THE CHANGE IN VENOUS BLOOD VOLUME
114
EVALUATE PATIENT CARDIOVASCULAR SYSTEM HEALTH. ADMINISTER TREATMENT(S) AS APROPRIATE.

FIG. 1

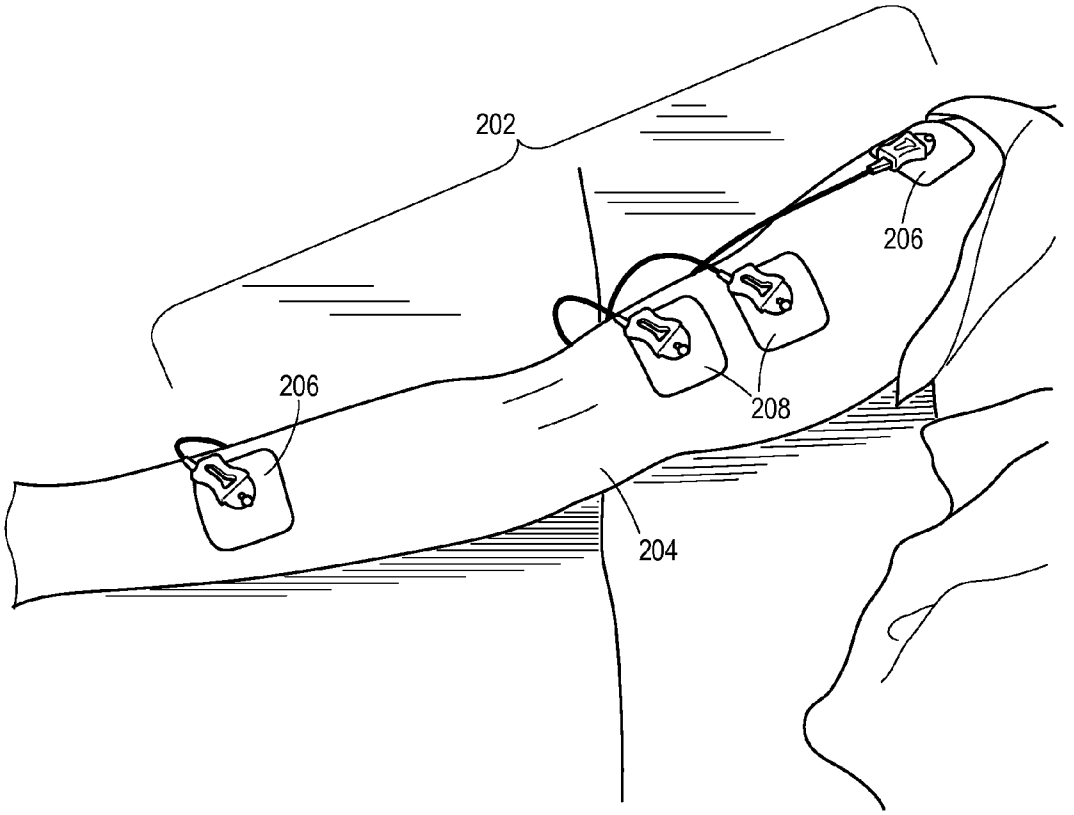

FIG. 2

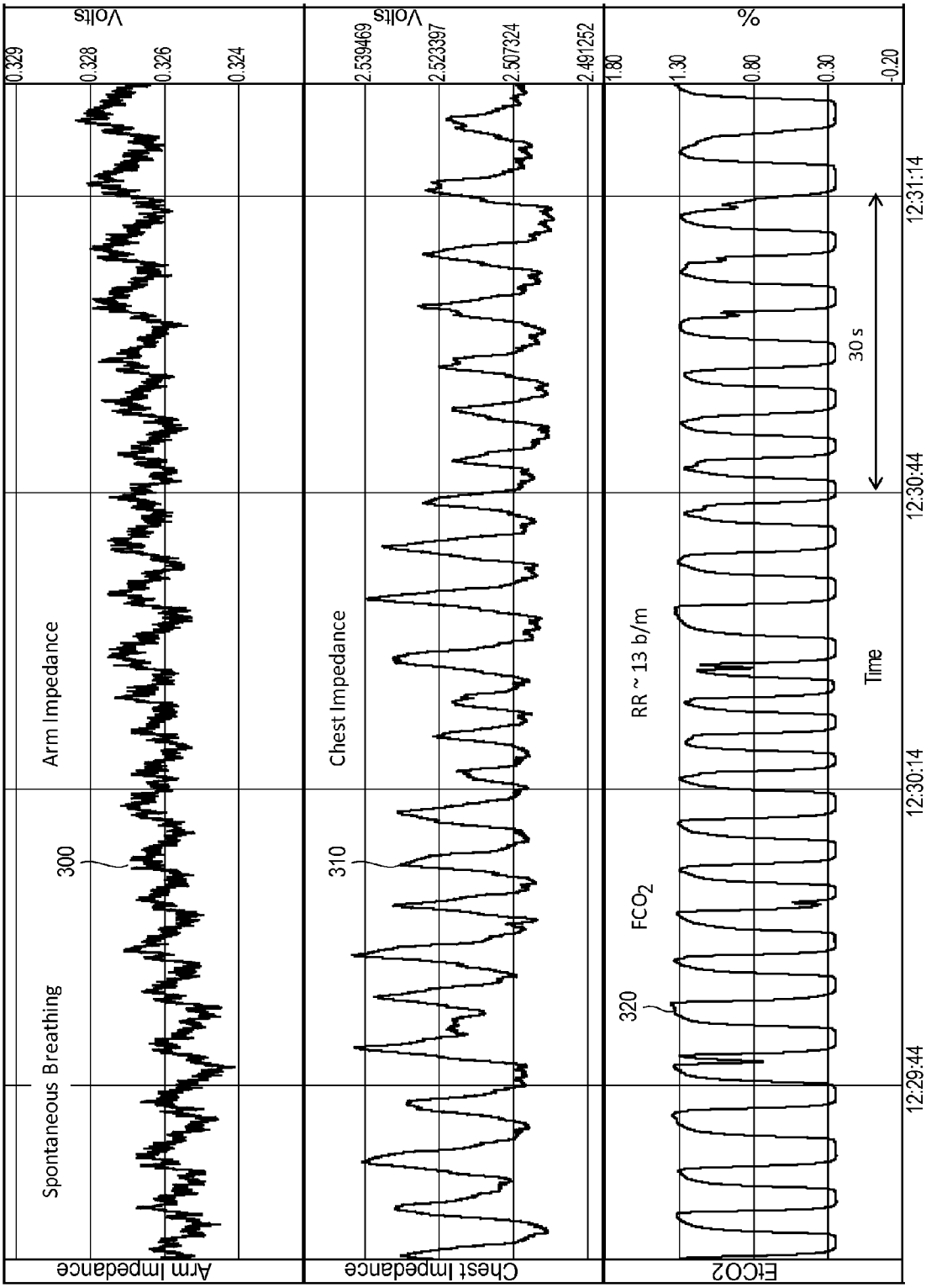
Arm Impedance
Volts
0.329
0.328
0.326
0.324
Spontaneous Breathing
300
Arm Impedance
Chest Impedance
Volts
2.539469
2.523397
2.507324
2.491252
310
Chest Impedance
EtCO2
%
1.80
1.30
0.80
0.30
-0.20
320
FCO2
RR ~ 13 b/m
30 s
Time
12:29:44
12:30:14
12:30:44
12:31:14

FIG. 3

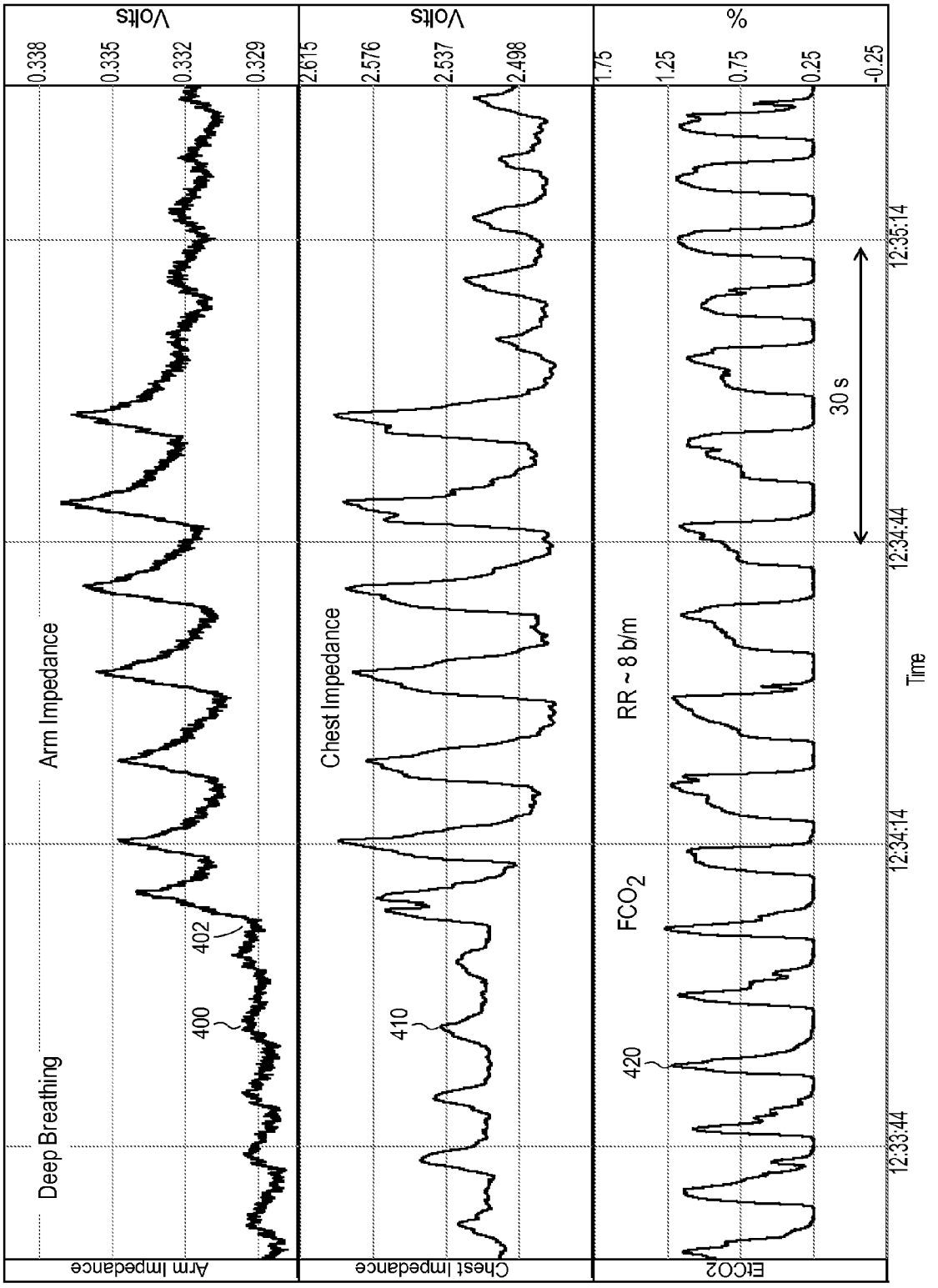
Arm Impedance
Volts
0.338
0.335
0.332
0.329
Deep Breathing
400
402
Chest Impedance
Volts
2.615
2.576
2.537
2.498
410
ETCO2
%
1.75
1.25
0.75
0.25
-0.25
RR ~ 8 b/m
FCO2
420
30 s
12:33:44
12:34:14
12:34:44
12:35:14
Time

FIG. 4

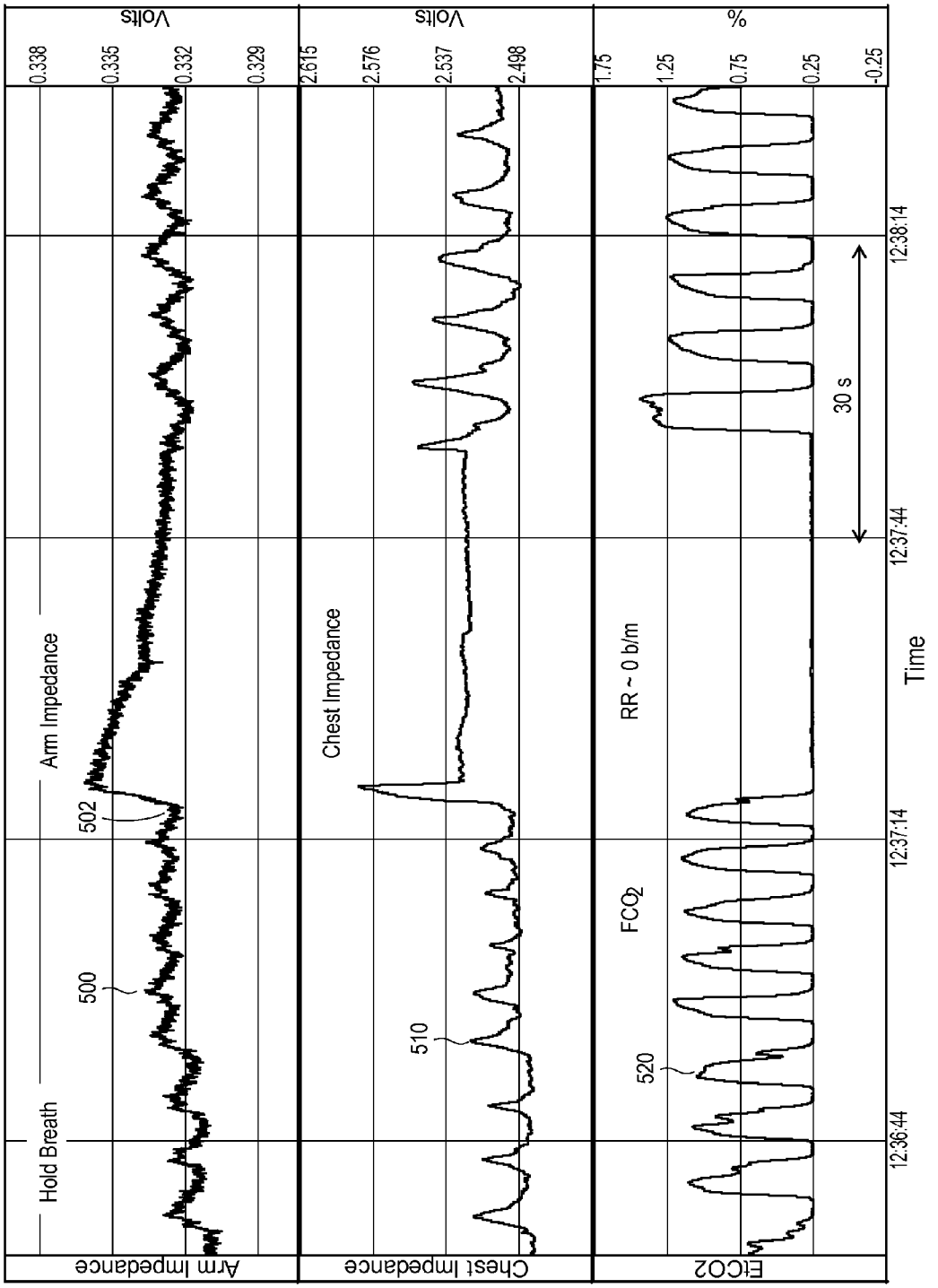
Arm Impedance
Volts
0.338
0.335
0.332
0.329
Hold Breath
Arm Impedance
500
502
Chest Impedance
Volts
2.615
2.576
2.537
2.498
Chest Impedance
510
EtCO2
%
1.75
1.25
0.75
0.25
-0.25
RR ~ 0 b/m
FCO2
520
30 s
12:36:44
12:37:14
12:37:44
12:38:14
Time

FIG. 5

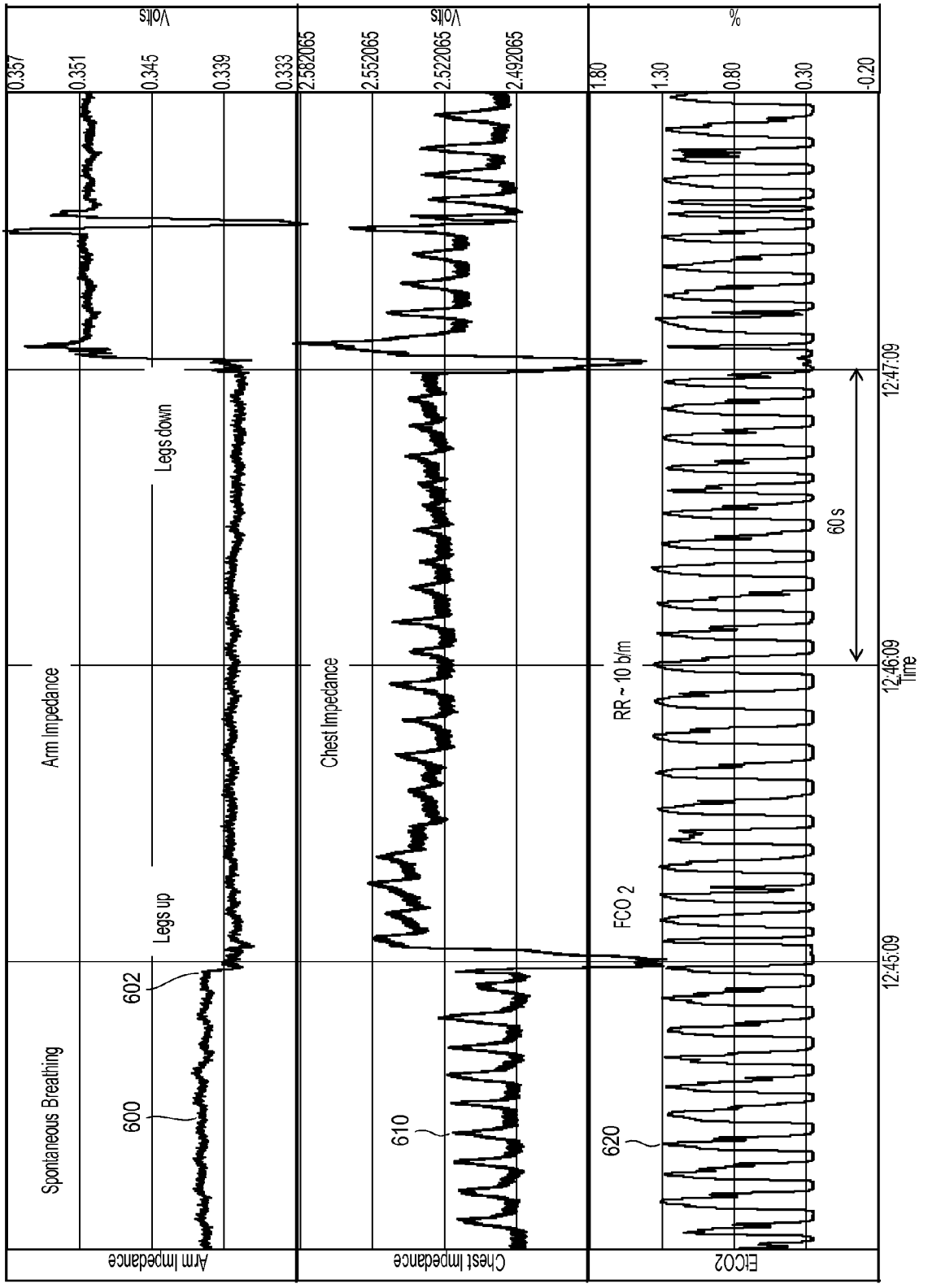
Arm Impedance
Volts
0.357
0.351
0.345
0.339
0.333
Spontaneous Breathing
Arm Impedance
Legs up
Legs down
600
602
Chest Impedance
Volts
2.582065
2.552065
2.522065
2.492065
Chest Impedance
610
EtCO2
%
1.80
1.30
0.80
0.30
-0.20
FCO 2
RR ~ 10 b/m
620
60 s
12:45:09
12:46:09
12:47:09
Time

FIG. 6

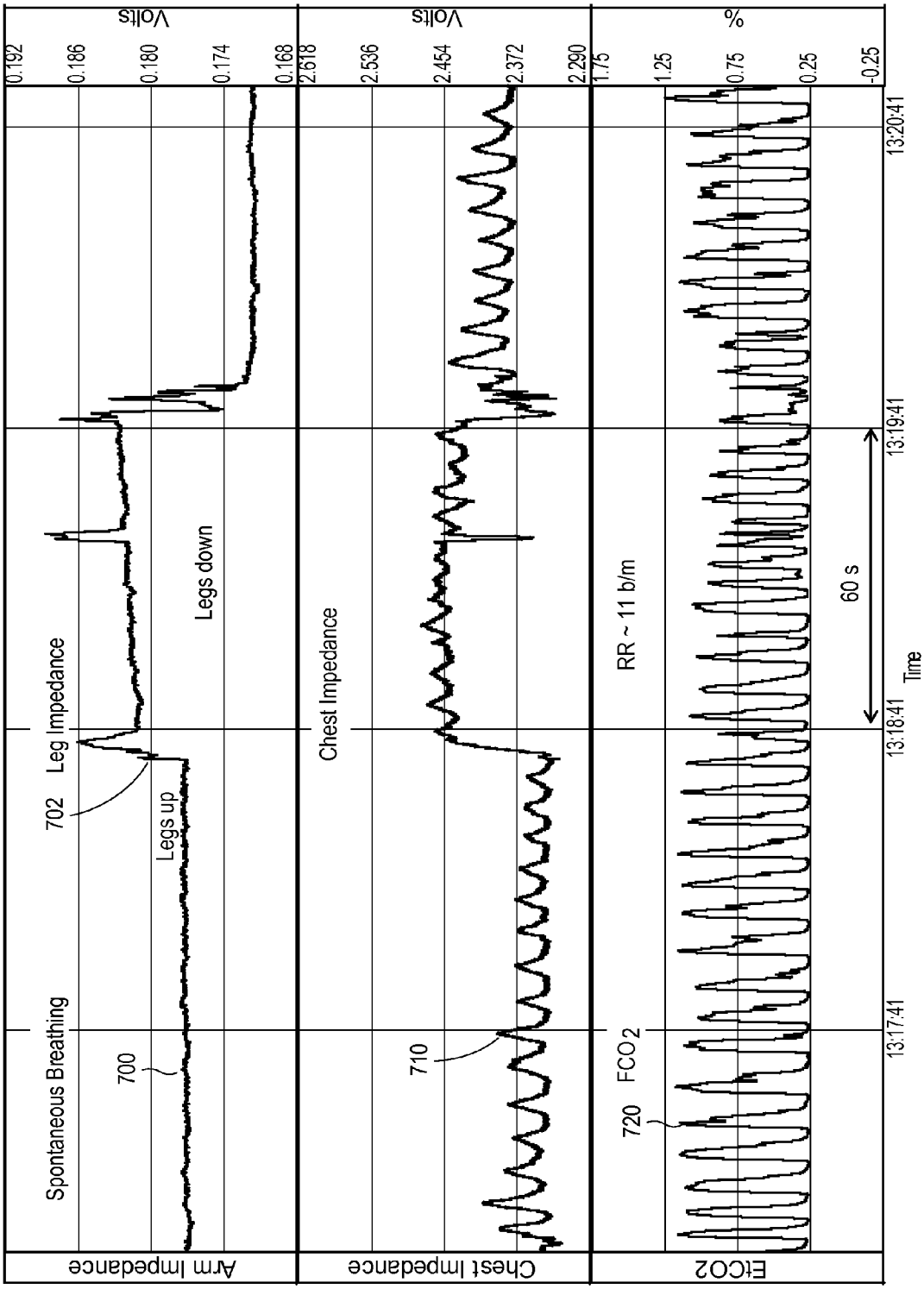
Arm Impedance
Volts
0.192
0.186
0.180
0.174
0.168
Spontaneous Breathing
700
Leg Impedance
702
Legs up
Legs down
Chest Impedance
Volts
2.618
2.536
2.454
2.372
2.290
710
EtCO2
%
1.75
1.25
0.75
0.25
-0.25
720
FCO2
RR ~ 11 b/m
60 s
13:17:41
13:18:41
13:19:41
13:20:41
Time

FIG. 7

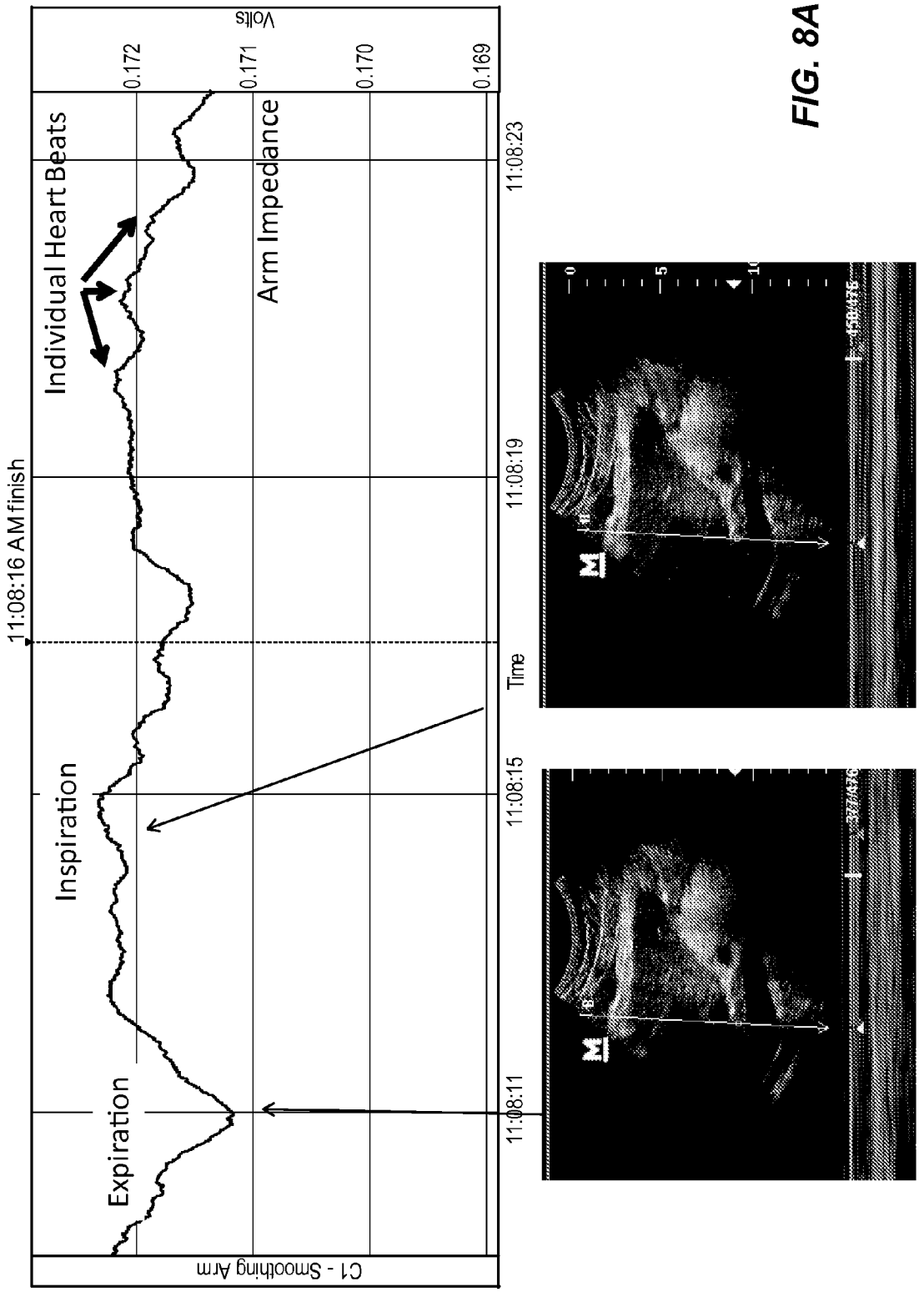
Volts
0.172
0.171
0.170
0.169
Individual Heart Beats
Arm Impedance
11:08:16 AM finish
Inspiration
Expiration
C1 - Smoothing Arm
11:08:11
11:08:15
Time
11:08:19
11:08:23

FIG. 8A

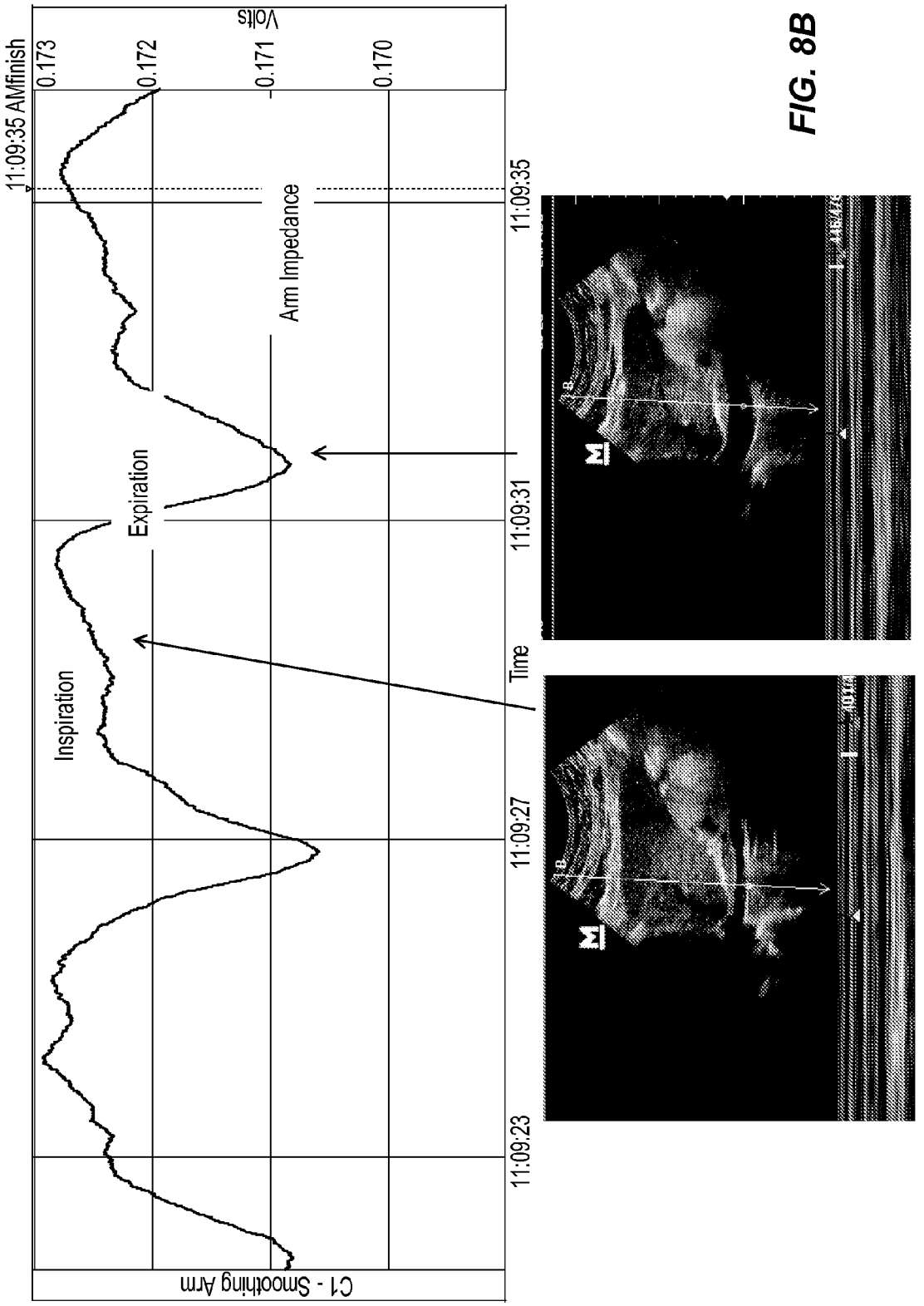
C1 - Smoothing Arm
Volts
0.173
0.172
0.171
0.170
11:09:35 AMfinish
Inspiration
Expiration
Arm Impedance
11:09:23
11:09:27
11:09:31
11:09:35
Time

FIG. 8B

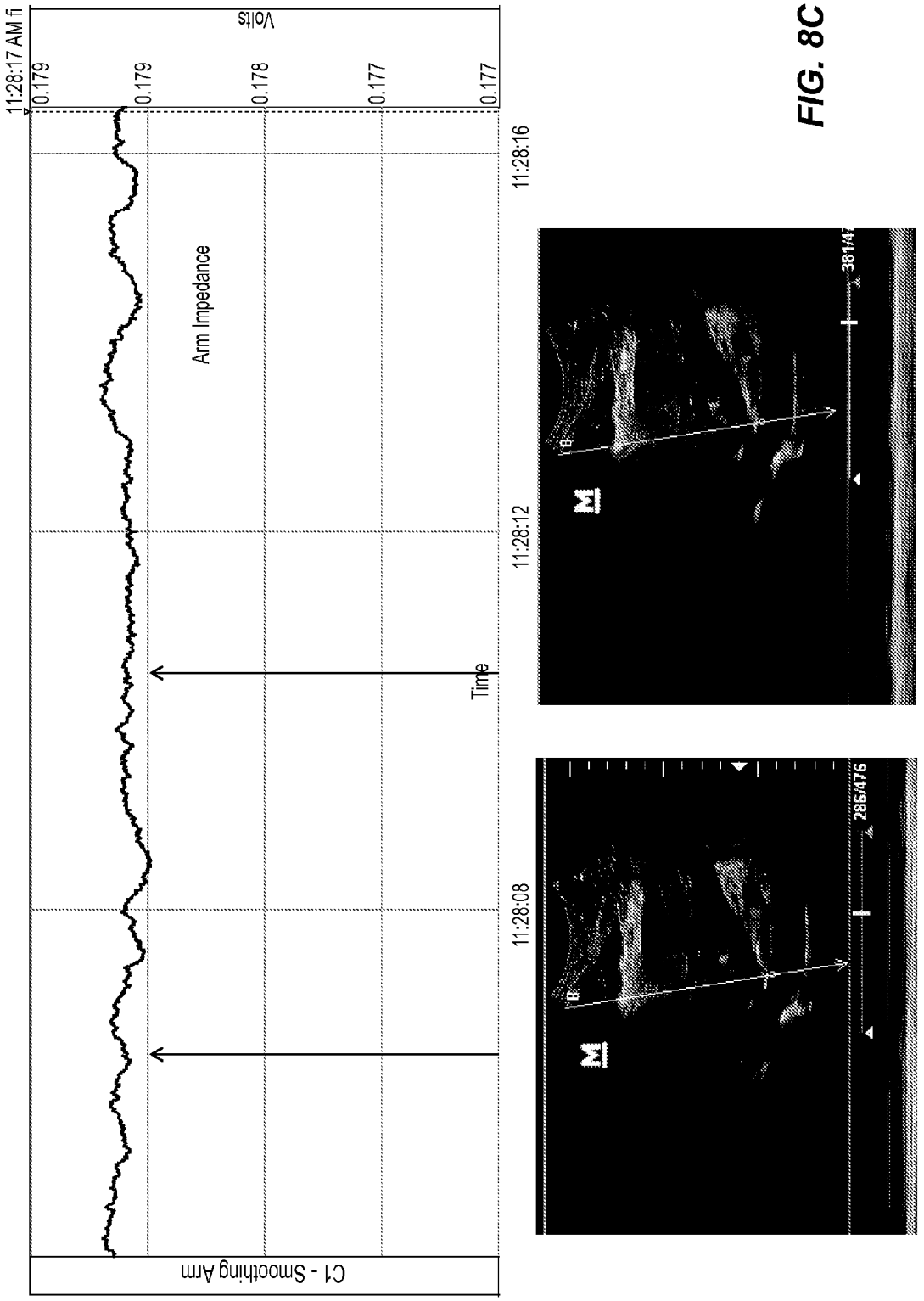
C1 - Smoothing Arm
11:28:17 AM fi
0.179
0.179
0.178
0.177
0.177
Volts
Arm Impedance
Time
11:28:08
11:28:12
11:28:16

FIG. 8C

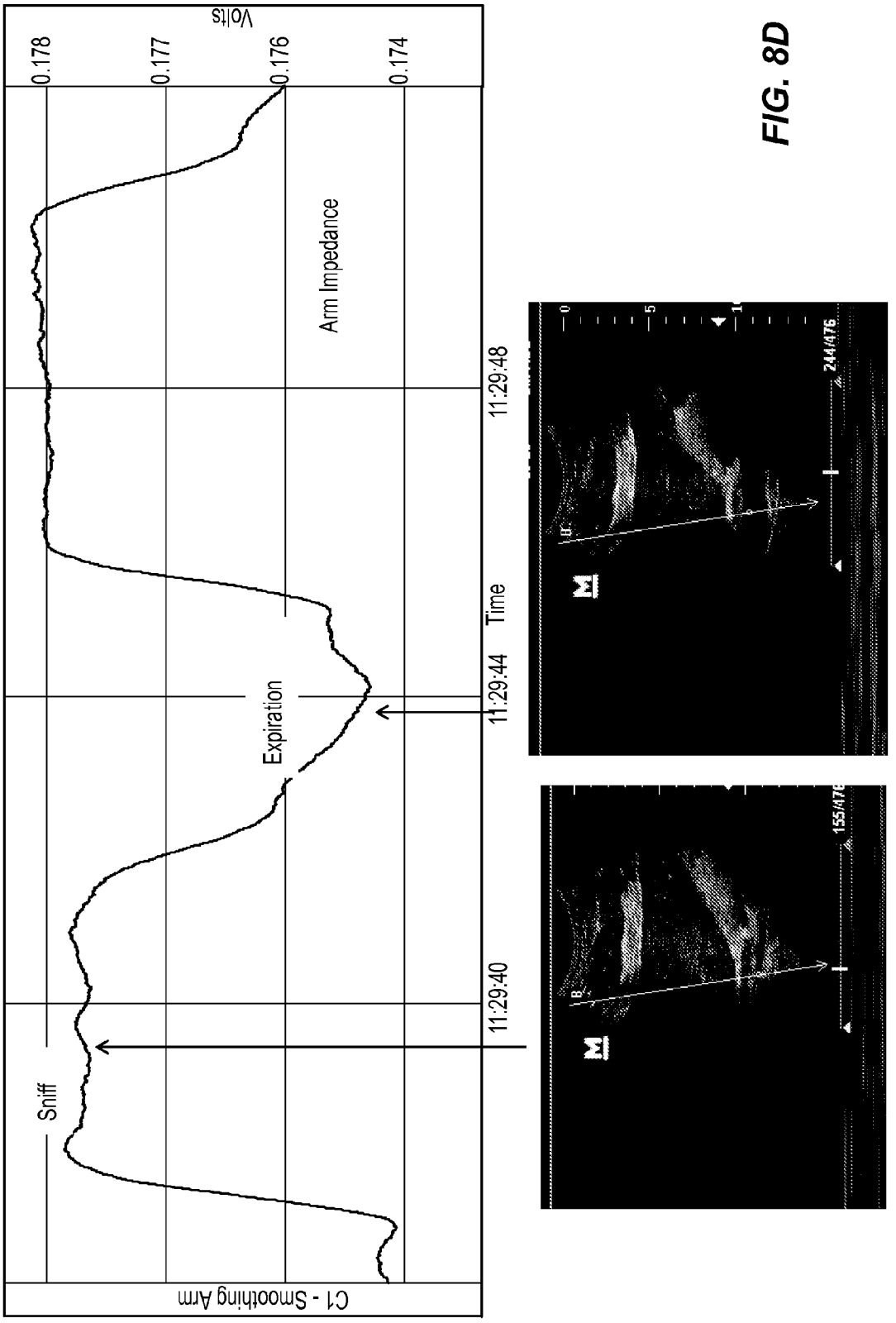
Volts
0.178
0.177
0.176
0.174
Arm Impedance
Sniff
Expiration
11:29:40
11:29:44
Time
11:29:48
C1 - Smoothing Arm

FIG. 8D

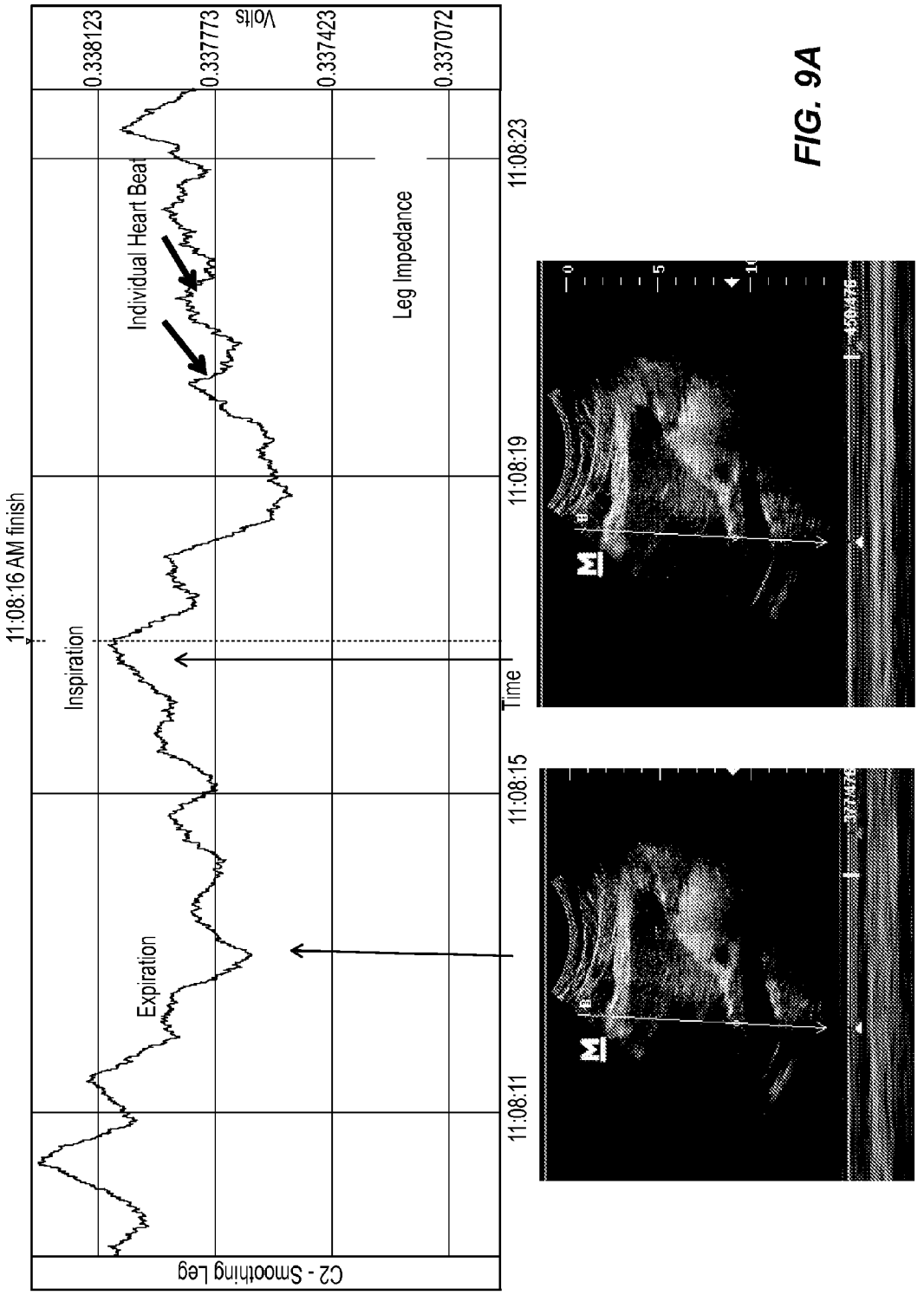
C2 - Smoothing Leg
Volts
0.338123
0.337773
0.337423
0.337072
11:08:16 AM finish
Inspiration
Expiration
Individual Heart Beat
Leg Impedance
Time
11:08:11
11:08:15
11:08:19
11:08:23

FIG. 9A

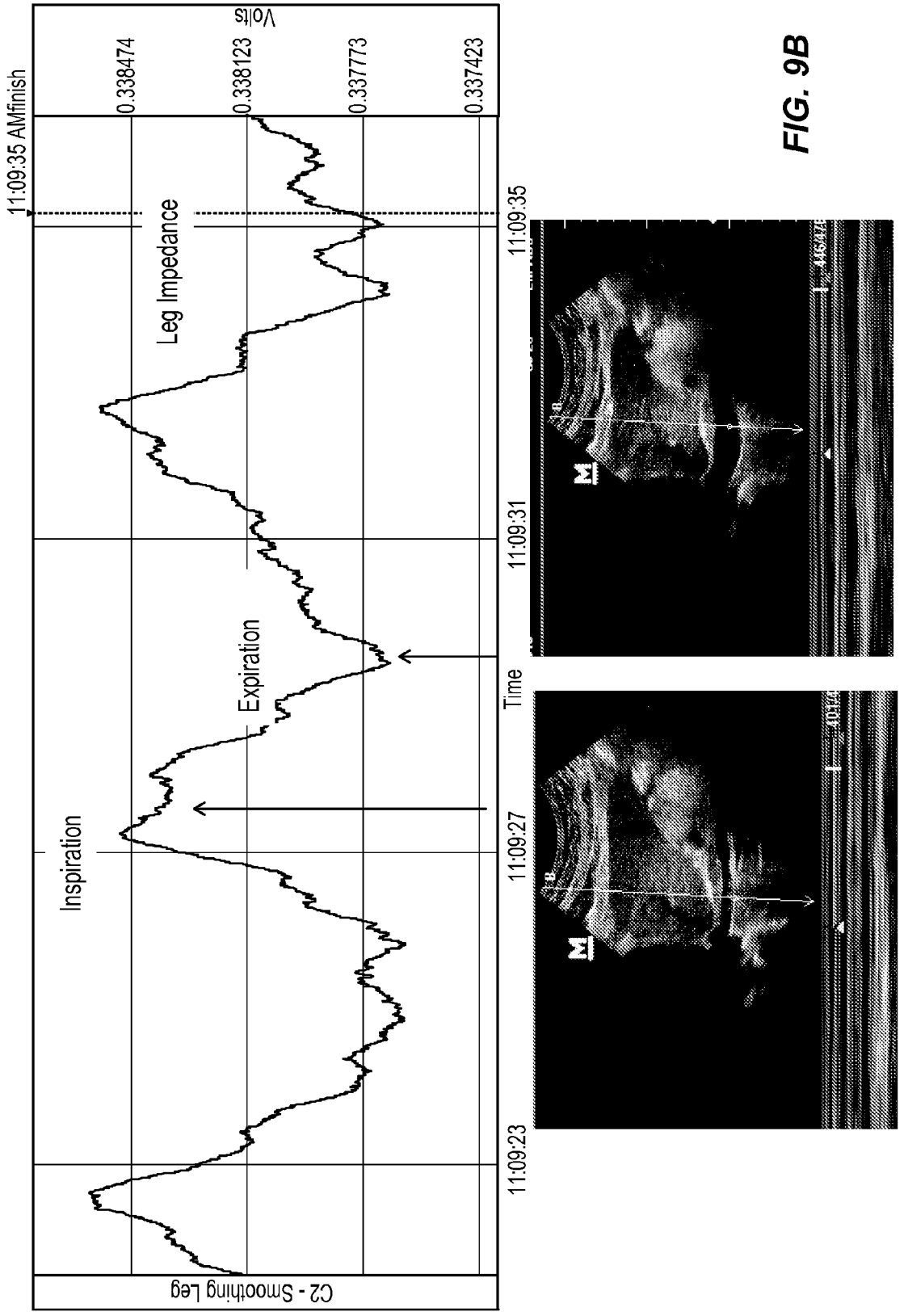
11:09:35 AMfinish
Volts
0.338474
0.338123
0.337773
0.337423
Leg Impedance
Inspiration
Expiration
C2 - Smoothing Leg
Time
11:09:23
11:09:27
11:09:31
11:09:35

FIG. 9B

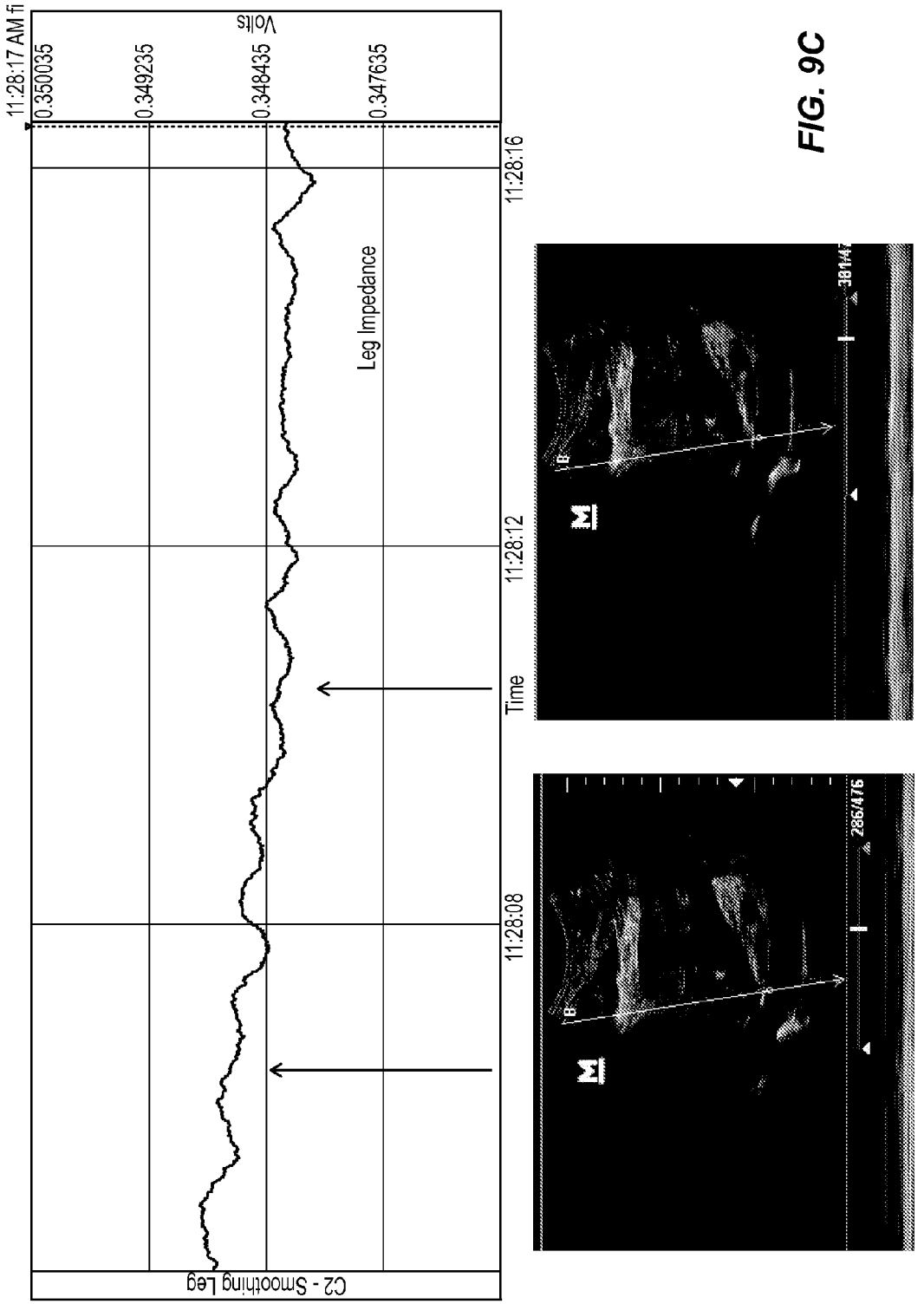
11:28:17 AM fi
0.350035
0.349235
0.348435
0.347635
Volts
Leg Impedance
11:28:16
11:28:12
11:28:08
Time
C2 - Smoothing Leg
M
B
286/476

FIG. 9C

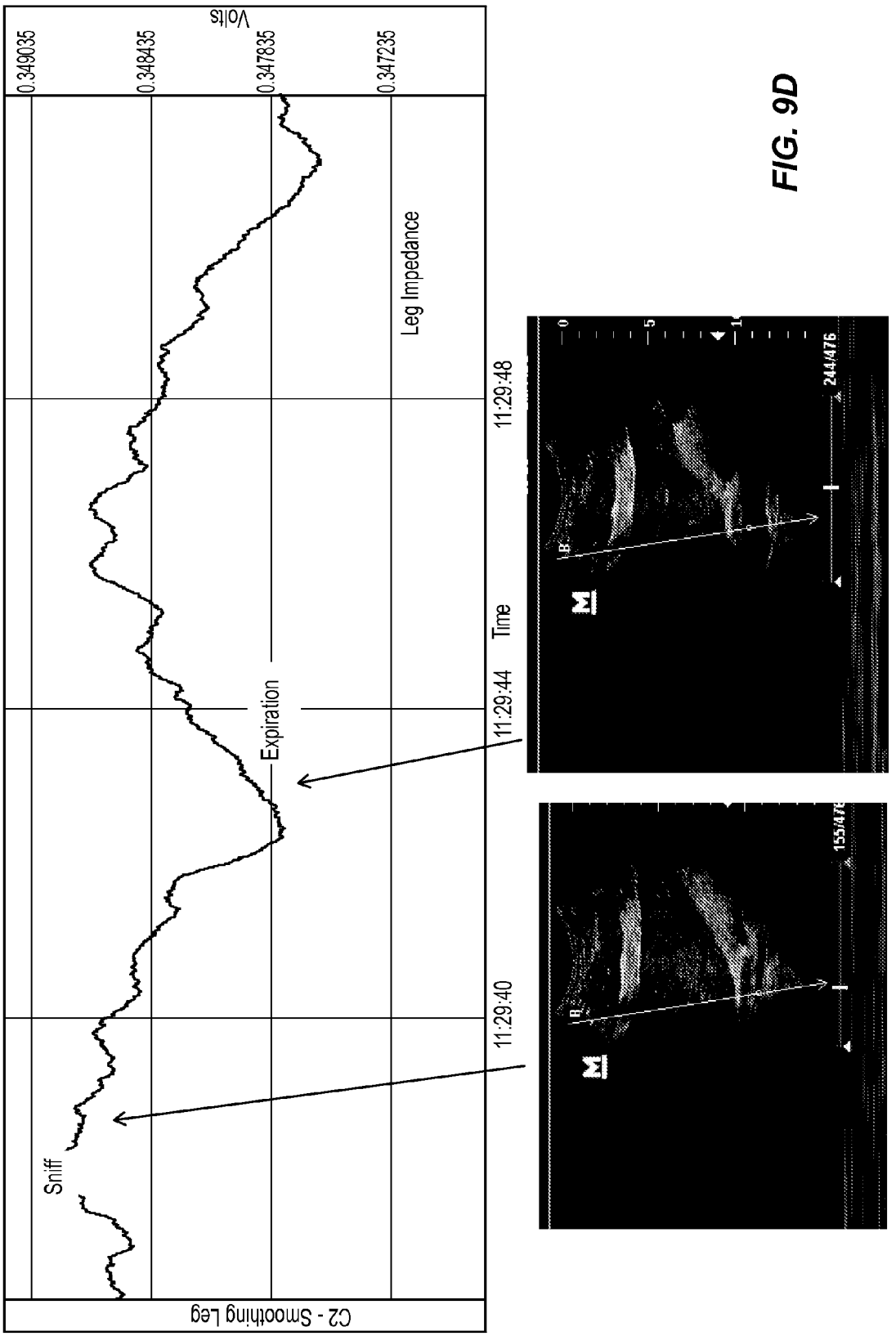
C2 - Smoothing Leg
Volts
0.349035
0.348435
0.347835
0.347235
Leg Impedance
Sniff
Expiration
11:29:40
11:29:44
Time
11:29:48

FIG. 9D

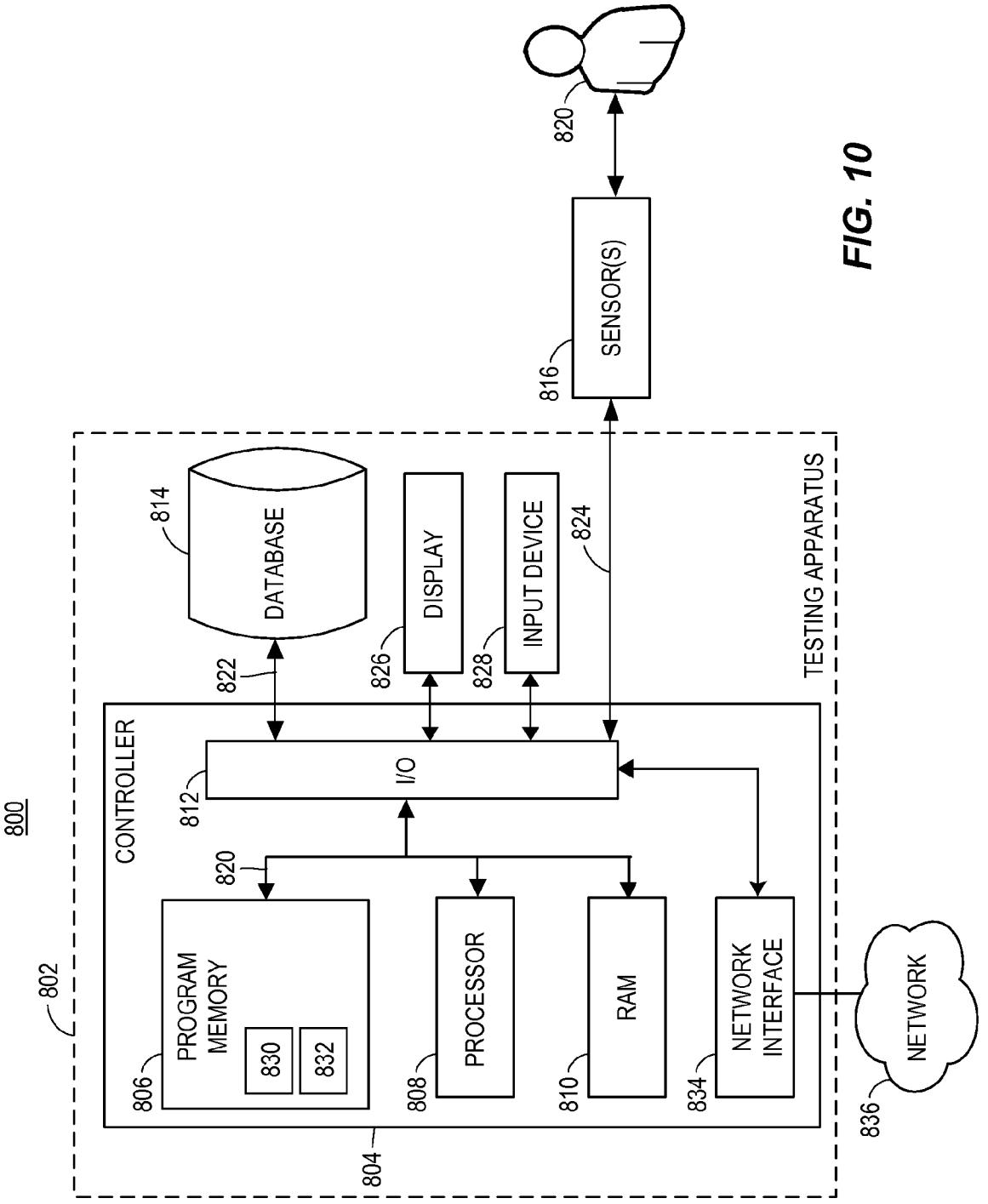
800
802
804
TESTING APPARATUS
CONTROLLER
I/O
812
820
PROGRAM MEMORY
806
830
832
PROCESSOR
808
RAM
810
NETWORK INTERFACE
834
NETWORK
836
DATABASE
814
DISPLAY
826
INPUT DEVICE
828
822
824
SENSOR(S)
816
820

FIG. 10

EVALUTATING CARDIOVASCULAR HEALTH USING INTRAVASCULAR VOLUME

CROSS-REFERENCE TO RELATED APPLICATIONS

[0001] The present application claims the benefit of U.S. Provisional Application No. 61/859,615, entitled "Evaluating Cardiovascular Health Using Intravascular Volume," filed on Jul. 29, 2013, which is hereby incorporated by reference herein in its entirety.

FIELD OF INVENTION

[0002] The present disclosure generally relates to a system and a method for evaluating a patient's cardiovascular health and, more particularly, to a non-invasive method for determining a patient's intravascular volume status by measuring the change in peripheral venous volume in response to an event causing blood to return to the heart via the venous system.

BACKGROUND

[0003] For patients suffering from a variety of injuries or disease states such as cardiac arrest, burns, trauma, heart failure, sepsis, dehydration from any cause, renal failure, or dialysis, it is important to monitor the relationship between the volume of circulating blood and the patient's ability to circulate that volume of blood. Further, in many medical conditions, it is important to know if patients will hemodynamically respond in a favorable manner to providing intravenous fluids and/or if they are volume overloaded. This is especially important in complex states such as sepsis and cardiogenic shock.

[0004] However, determination of a patient's intravascular volume status in a noninvasive manner has been problematic. Methods of monitoring cardiac output are commonly used to assess the condition of patient's suffering from a variety of conditions. However, many of the methods that are non-invasive fail to quantify the volume of blood circulating within the patient relative to the patient's ability to circulate that volume. These parameters are important because ideally the physician could adjust the volume of circulating blood (for example via intravenous fluids) in order to achieve optimum cardiovascular circulation or output. Recently, impedance cardiography has been used to measure changes in cardiac output (and thus stroke volume) in response to temporary central fluid provision by raising of the lower extremities. This approach, however, is expensive, generally does not provide sufficient measurement sensitivity or accuracy, and may not be an option to some patients. In particular, impedance cardiography may necessitate that a patient's lower extremities be raised by a health care provider and many further necessitate repetitive raising if used as an endpoint measure. In many instances, raising of the legs will not be possible due to lower extremity injury, pelvic fracture or in situations where the patient may have limb amputation. In addition, passive leg lifting, as a provocative volume challenge maneuver may be ill suited since limb volume will greatly vary between individuals and even potentially within an individual if it is used repetitively when impedance cardiography is used as the end-point of the maneuver. Further, impedance cardiography has not been used to guide a reduction of intravascular volume. Thus, a passive extremity lift when used in conjunction with impedance cardiography as a hemodynamic endpoint cannot be used as a continuous measure to guide therapy.

[0005] Another approach, using ultrasound of the inferior and superior vena cava, has been used to look at the changes in these large venous vessels in response to spontaneous and mechanical ventilation with great accuracy. The collapsibility of these large vessels during respiration is indicative of volume status including right atrial pressure and whether or not the patient will increase their cardiac output in response to intravenous fluid administration. However, despite its utility such monitoring is prohibitively cumbersome and expensive and requires an experienced ultrasound operator. Furthermore, ultrasonic measurement of the inferior and superior vena cava cannot be performed continuously for a relatively long period of time. Other technologies like pulse pressure variation and stroke volume variation have been used to examine arterial changes produced by volume induced changes in cardiac output caused by respiration. However, measuring the volume variation of the arterial system has been problematic for various reasons (e.g., various pharmaceuticals may alter arterial vascular stiffness and volume largely independent of total intravascular volume). Additionally, it is unknown whether such a technique will work in patients with very stiff arterial systems from calcific and chronic hypertension conditions. Also such techniques may also require that the tidal volume of the patient be carefully controlled.

SUMMARY

[0006] The present application describes techniques to non-invasively monitor cardiovascular system health by monitoring changes in the volume of blood in the venous system of the arms, legs, or neck of patients by using one or more methods of determining tissue volume and/or volume changes of an extremity such as an arm, leg, or neck of the patient. The volume or volume changes may be determined using impedance plethysmography, near infrared spectroscopy, photoplethysmography, galvanic skin response, laser Doppler flowmetry, or ultrasound; although in the illustrated examples techniques using impedance measurements and changes in impedance are detailed.

[0007] In an example, a method for evaluating the cardiovascular condition of a patient, the method includes: (a) recording a first impedance of a limb or extremity of the patient at a first time in response to receiving a first impedance reading from a plurality of sensors on a limb or extremity or neck; (b) after the occurrence of an event modulating blood return to the heart via the venous system of the patient, recording a second impedance of the limb or extremity or neck at a second time in response to receiving a second impedance reading from a plurality of sensors on a limb or extremity or neck, wherein the first impedance and the second impedance each correspond to a volume of blood flowing within the limb or extremity or neck; and (c) determining a change in venous blood volume between the first time and the second time by comparing the first impedance and the second impedance to determine a change in volume of blood.

[0008] In accordance with another example, a testing apparatus for evaluating the cardiovascular condition of a patient, the testing apparatus includes: one or more electrodes; one or more processors; a computer-readable memory storing non-transient instructions that when executed by the one or more processors cause the testing apparatus to: (a) use the one or

more electrodes to record a first impedance of a limb or extremity or neck of the patient at a first time in response to receiving a first impedance reading from a plurality of sensors on a limb or extremity or neck; (b) after the occurrence of an event modulating blood return to the heart via the venous system of the patient, use the one or more electrodes to record a second impedance of the limb or extremity or neck at a second time in response to receiving a second impedance reading from a plurality of sensors on a limb or extremity or neck, wherein the first impedance and the second impedance each correspond to a volume of blood flowing within the limb or extremity or neck; and (c) determine a change in venous blood volume between the first time and the second time by comparing the first impedance and the second impedance to determine a change in volume of blood.

[0009] In accordance with yet another example, a closed-loop cardiovascular condition evaluation system including: a testing apparatus; and a processor and a memory, the memory storing instructions that when executed by the processor, cause the processor to evaluate a cardiovascular condition of a subject in response to determining the change in the venous blood volume between the first time and the second time determined by comparing the first impedance and the second impedance, for different treatment cycles.

[0010] In accordance with yet another example, a method for evaluating the cardiovascular condition of a patient, the method includes: (a) determining a first volume of blood of a limb or extremity or neck of the patient at a first time; (b) after the occurrence of an event causing blood to return to the heart via the venous system of the patient, determining a second volume of blood of the limb or extremity or neck at a second time; (c) determining a change in venous blood volume between the first time and the second time by comparing the first volume of blood and the second volume of blood; and (d) determining one or more of: (1) how the patient will hemodynamically respond to one or more of an addition of cardiovascular fluid or removal of cardiovascular fluid, (2) how the patient will hemodynamically respond to one or more cardiovascular drugs which promote changes in cardiac output, changes in cardiovascular preload, and changes in cardiovascular afterload, or (3) determining how the patient will response to changes in mechanical or noninvasive ventilation.

BRIEF DESCRIPTION OF THE DRAWINGS

[0011] The figures described below depict various aspects of the system and methods disclosed herein. It should be understood that each figure depicts an embodiment of a particular aspect of the disclosed system and methods, and that each of the figures is intended to accord with a possible embodiment thereof. Further, wherever possible, the following description refers to the reference numerals included in the following figures, in which features depicted in multiple figures are designated with consistent reference numerals.

[0012] FIG. **1** depicts an example intravascular volume status monitoring process for implementing the intravascular volume status monitor in accordance with an example;

[0013] FIG. **2** depicts example placement of an impedance measuring device on an extremity of a patient (e.g., an arm), in accordance with an example application of the monitoring process of FIG. **1**;

[0014] FIGS. **3-7** depict example graphs of impedance measured from an arm of a patient, impedance measured from the chest wall of the patient, and end-tidal carbon dioxide (CO_2) measured from the nose of a patient as functions of time;

[0015] FIGS. **8A-8D** depict graphs of arm impedance measurements measured under different breathing conditions, specifically, normal breathing (FIG. **8A**), deep breathing (FIG. **8B**), holding breath (FIG. **8C**), and sniff breathing against a partially closed glottis (FIG. **8D**). Simultaneous changes in IVC diameter are also noted.

[0016] FIGS. **9A-9D** depict graphs of leg impedance measurements measured under different breathing conditions, specifically, normal breathing (FIG. **9A**), deep breathing (FIG. **9B**), holding breath (FIG. **9C**), and sniff breathing against a partially closed glottis (FIG. **9D**). Simultaneous changes in IVC diameter are also noted.

[0017] FIG. **10** depicts an example block diagram illustrating the various components used in implementing an exemplary embodiment of the intravascular volume monitoring method.

DETAILED DESCRIPTION

[0018] Although the following text sets forth a detailed description of numerous different embodiments, it should be understood that the legal scope of the invention is defined by the words of the claims set forth at the end of this patent. The detailed description is to be construed as exemplary only and does not describe every possible embodiment, as describing every possible embodiment would be impractical, if not impossible. One could implement numerous alternate embodiments, using either current technology or technology developed after the filing date of this patent, which would still fall within the scope of the claims.

[0019] It should also be understood that, unless a term is expressly defined in this patent using the sentence "As used herein, the term '_____' is hereby defined to mean . . . " or a similar sentence, there is no intent to limit the meaning of that term, either expressly or by implication, beyond its plain or ordinary meaning, and such term should not be interpreted to be limited in scope based on any statement made in any section of this patent (other than the language of the claims). To the extent that any term recited in the claims at the end of this patent is referred to in this patent in a manner consistent with a single meaning, that is done for sake of clarity only so as to not confuse the reader, and it is not intended that such claim term be limited, by implication or otherwise, to that single meaning. Finally, unless a claim element is defined by reciting the word "means" and a function without the recital of any structure, it is not intended that the scope of any claim element be interpreted based on the application of 35 U.S.C. §112, sixth paragraph.

[0020] FIG. **1** is a flow diagram depicting an example embodiment of an intravascular volume status monitoring process **100**. It may be advantageous to monitor the intravascular volume status of a patient for any of a number of injuries or diseases such as cardiac arrest, burns, trauma including combat trauma, heart failure, sepsis, dehydration from any cause, renal failure, dialysis, etc. Further, it may also be advantageous to conduct general status monitoring including respiratory rate and respiratory quality monitoring as discussed herein. Further still, a longer term use of the process **100** may be to monitor the status of a patient suffering from edema. Prior to commencing monitoring, the testing apparatus, such as the testing apparatus **802** illustrated in FIG. **10** discussed below, would be applied to the patient (block **102**).

As described herein, the testing apparatus **802** may be any of a number of devices and sensors used to gather the venous volume and other data used to evaluate the patient's intravascular volume status.

[0021] FIG. **2** is an illustration of how the testing apparatus **802** and the sensor(s) **816** operatively connected thereto may be used to measure impedance (and thus measure venous volume changes as discussed below). The testing apparatus **802** and the sensors **816** (not shown in FIG. **2**) may collectively be referred to as an impedance measuring device **202**. In some embodiments, the impedance measuring device is an impedance plethysmograph. The impedance measuring device **202** may be coupled to the patient via electrodes **206** and **208**. As shown in FIG. **2**, the electrodes **206** and **208** may be placed on the arm **204** of a patient. The impedance measuring device **202** may include two sets of electrodes. A first set of electrodes **206** are used to inject electrical current (e.g., 1 mA of alternating current) into the arm **204**. A second set of electrodes **208** is used to monitor the impedance of the arm **204**. Of course it will be appreciated that more than or less than four electrodes may be used to measure impedance. Further, different placement patterns for the electrodes **206** and **208** may be used (e.g., a circumferential pattern around the arm **204**). Additionally, instead of placing the electrodes **206** and **208** on the arm **204**, it will be understood that electrodes could be placed on the leg or neck of the patient to measure impedance as discussed herein. It will be appreciated that the electrodes **206** and **208** are placed peripherally (i.e., on the arm, neck, or legs) in order to take advantage of the venous volume modulation that will be produced through ventilation that will be reflected in relative blood volume changes in these peripheral sites. These sites are also insulated by distance so that they are not affected by motion of the chest. Traditional chest wall impedance used to measure respiratory rate use the impedance changes produced by small distance changes between impedance electrodes to make the respiratory rate measure. These changes in impedance at the chest are independent of cyclical blood volume changes. It will also be appreciated that the electrodes **206** and **208** do not have to be aligned along a vein. Volume changes are being made across a segment of tissue at the periphery which is dominated by movement of venous blood at that site. Accordingly, the testing apparatus **802** may be used to provide information about the relationship between ventilation, venous return, and heart function as described herein.

[0022] In another embodiment, the testing apparatus **802** may include any of a number of apparatuses useful for determining the volume of blood in one or more of the patient's extremities. For example, the testing apparatus may be a photoplethysmograph, a galvanic skin response monitor, a near infrared spectroscopy device, a laser Doppler device with our without speckle tracking, or an ultrasound device with or without speckle tracking. The present techniques, which focus on venous-side blood volume assessment, can be combined with other vascular techniques, including arterial-side measurement devices. As such, the testing apparatus **802** could be a device that also provides impedance cardiography, pulse pressure variation measurements, and stroke volume variation measurements, or the testing apparatus **802** could be a device coupled to one or more such devices (not shown), through a network, where such devices are coupled to a subject. Coordinating the present venous-side techniques with arterial-side measurements can provide additional information on vascular condition, such as preload, venous return, cardiac output, afterload, and vascular compliance.

[0023] As shown in FIG. **1**, with the testing apparatus **802** in place, the monitoring of the patient's intravascular volume status may commence (block **104**). Monitoring may be conducted at any of a number of physical locations (e.g., an intensive care unit, an operating room, a dialysis clinic, emergency department, ambulance, home health care, etc.). Once monitoring has begun, the testing apparatus **802** may take a first measurement of the extremity (block **106**), that measurement being of a physical metric indicative of venous volume in the extremity. For example, if the testing apparatus **802** is an impedance measuring device such as the one illustrated in FIG. **2**, the testing apparatus **802** may take a first impedance measurement of the extremity as the physical metric indicative of venous volume. The impedance of the extremity is based in large part on the blood volume within the extremity. Because blood is a good electrical conductor, impedance will decrease or increase if more or less blood volume, respectively, exists in the extremity. The first measurement may be a single data point, but the first measurement may also include multiple data points taken over a first period of time. Further, the first measurement may include a series of data points taken over a first period of time to establish a baseline measurement of the patient's intravascular volume cycle over the course of a plurality of respirations. As discussed herein, such respirations may be spontaneous and/or mechanically induced.

[0024] Subsequent to the first measurement of the extremity, an event causing blood to return to the heart via the venous system may occur (block **108**). These events causing blood to return to the heart via the venous system may also be referred to as "respiratory challenges" herein. For example, taking a deep breath produces a larger negative intrathoracic pressure thus pulling more blood from the extremity. Spontaneous respiration creates negative pressure in the thorax which in turn creates a pressure gradient between the chest and the limbs/abdomen. This negative pressure gradient sucks blood into the large veins of the abdomen and chest which then empty this volume into the heart. Because spontaneous inspiration pulls blood from the extremities, the degree to which this will happen will depend on how full the right heart is and how forcefully the patient inspires. The degree to which spontaneous or negative pressure ventilation enhances venous return as it relates to central venous volume has been shown to be reflected by ultrasound imaging in the diameter of the inferior and superior vena cava and their ability to collapse. Similar but converse changes will be noted for patients undergoing positive pressure mechanical ventilation. In particular, the increase in intrathoracic pressure may cause the blood flow returning from the limbs and abdomen to slow, which may be detected by monitoring the change in volume as discussed herein. Centrally, this has been demonstrated using ultrasound imaging to change the diameter of the superior and inferior vena cava. It will be appreciated that such changes may be caused by higher intrathoracic pressures which in turn may cause expansion or collapse of the inferior and superior vena cava. Such expansion or collapse may change the volume of the inferior and superior vena cava and this in return will be manifest by volume changes peripherally. Because of this, the process **100** may be used to optimize vascular volume and even mechanical ventilation parameters by understanding the effects of mechanical ventilation on the central cardiovascular system's venous component. Additionally,

changing the elevation of the extremities also may result in both local and remote blood volume changes that can be detected and are likely reflective of the patient's cardiovascular status as discussed herein. Raising the extremity will cause blood to flow into the central circulatory system, but the volume of blood flow will be dependent on the volume of blood already present in the central circulation system as well as the height of the extremity. Further, blood volume in the extremities may be affected by applying pressure to the patient's chest or abdomen. Accordingly, in an attempt to cause blood to return to the heart via the venous system, the patient may be instructed to take a deep breath, the patient may be instructed to inspire or expire against an impedance valve which produces a set negative inspiratory or positive expiratory pressure respectively, one or more of the patient's limbs may be raised or to a particular height, pressure (positive or negative) may be applied to the patient's chest or abdomen, and/or the parameters of positive pressure mechanical ventilation may be adjusted. The change in the volume of blood in the extremity being monitored may be used to determine the patient's intravascular health similar to changes in IVC diameter. In fact changes in IVC diameter as measured by ultrasound during respiration (spontaneous and mechanical ventilation) have been accurately correlated with right atrial or central venous pressure. FIGS. **8** and **9** demonstrate quantifiable changes in limb impedance and changes in vena cava diameter. In essence the limbs or neck would be treated as extensions of the vena cava, such that one can determine changes in blood volume in the limbs or neck as well as the volume and diameter changes in the vena cava, from changes in impedance in limbs or neck. These determinations can be explicit, e.g., with actual volumetric or length units, or inferred, e.g., maintaining units as impedance units. In this way, measure of changes in impedance, or other physical metric, may be used to determine changes in changes in blood volume on the heretofore unmeasured venous-side of the vascular system. Moreover, the changes in blood volume may be determined, explicitly from the impedance data or inferentially as represented by the impedance data. Moreover still, the changes in limb or neck volume, as measured by impedance or other method, also correlate with changes in right atrial pressure and central venous pressure.

[0025] During and/or after the occurrence of the event causing modulation of blood return to the heart via the venous system, the testing apparatus **802** may take a second measurement of the extremity (block **110**), for example, of the same physical metric indicative of venous volume in the extremity as first measured (block **106**). For example, if the testing apparatus **802** is an impedance measuring device such as the one illustrated in FIG. **2**, the testing apparatus **802** may take a second impedance measurement of the extremity. As with the first measurement, the second measurement may include a series of data points taken during a second period of time. Using the first measurement and the second measurement, the process **100** may then determine the change in venous volume in the extremity (e.g., by subtracting the mean value of the first measurement from the mean value second measurement) (block **112**). The block **112** may determine the change in venous volume from the values of the physical metric (e.g., impedance) taken at the first (block **106**) and the second (block **110**) points in time. When impedance (also termed bioimpedance) is used as the physical metric, then the changes in impedance will provide a relatively linear correlation to the changes in volume when compared to the changes in the diameter of the vena cava. In some examples, the actual change in blood volume is determined from the changes in impedance, i.e., calculated, while in other examples, the change is determined inferentially. Thus, in these ways, the present techniques are, in some implementations, able to determine changes in venous blood volume without needing to measure absolute values for the physical metric, e.g., without needing to measure absolute impedance. Instead changes in the physical metric, e.g., changes in impedance, can be measured.

[0026] In some examples, the blocks **106** and **110** may take the first and second measurements, respectively, over a period of time and determine a local peak value of the physical metric over those periods of time value, and provide those local peak values to the block **112**. In some examples, the blocks **106** and **110** may take the first and second measurements, respectively, over a period of time and determine a peak-to-peak value for the physical metric over those periods of time, and provide those peak-to-peak values to the block **112**. In any of these examples, the first and second measurements may be normalized to each individual's breathing baseline. In some examples, the normalization can occur from plotting this data versus changes in the diameter of an individual's inferior vena cava. In an example experimental implementation using control subjects and patients who were critically ill, an exponential model was fit to measured impedance data and was shown to have high predictive value of impedance changes on both a per individual basis (e.g., R^2=0.91±0.05 and R^2=0.96±0.03 for control subjects and patients, respectively) and a per subject group basis.

[0027] Referring again to FIG. **1**, the process of taking measurements of volume before and after a blood moving event and calculating the change in volume may be repeated one or more times. That is, the processes for blocks **106-112** may be repeated numerous times to monitor and assess the effects of different events on blood volume. Additionally various types of blood moving events may occur during monitoring. For example, a patient may be instructed to breathe normally for several cycles, instructed to take several deep breaths, and then have a limb be raised and/or lowered as discussed herein. By monitoring the patient's intravascular volume status before and after several occurrences of events causing blood to return to the heart via the venous system, a healthcare provider may assess whether the addition or subtraction of intravascular fluid would be advantageous to the patient's health as discussed below. The length of time the patient may be monitored may vary and may depend in part on (a) how ill or injured the patient is and (b) what treatments are being undertaken to optimize the patient's cardiovascular system and how the patient's cardiovascular system responds to this treatment discussed below. Accordingly, the patient may be monitored for minutes, hours, or days. Further, it may be advantageous to continuously monitor the extremity to detect changes in circulating volume over time in order to detect hydration states and continuing blood loss.

[0028] The event(s) modulating blood return may result from direct or indirect instruction from health care personnel, and as part of a treatment efficacy determination. Example events include spontaneous inspiration, positive pressure mechanical ventilation, raising a limb or extremity or neck of the patient, applying negative or positive pressure to the abdomen or chest, inspiration against a negative impedance valve, or discrete maneuvers performed with mechanical ventilation. Those discrete maneuvers performed with mechanical

ventilation may include, by way of example, adjusting positive pressure ventilation, negative pressure ventilation, maintaining inspiratory or expiratory pause, or a combination thereof.

[0029] Personnel may instruct patients to engage in events modulating blood return, at, before, or during a diagnosis test or administration of treatment. The change in venous blood volume is then determined based on changes in measured impedance before and after the events. The personnel may instruct the patient to engage in one event or in a protocol of events, e.g., performing different breathing exercises in a prescribed manner (such as, rapid breaths followed by deep expiration and deep inspiration breaths, different types of breaths taken at different limb positions, etc.). For example, an administering physician may instruct a patient to perform a blood-modulating event, from which changes in venous blood volume is determined between different time points, to determine how the patient will hemodynamically respond to treatment by a cardiovascular fluid, or how the patient will respond to the removal of a cardiovascular fluid. The physician thus uses the blood-modulating events to assist in determining patient's likely responsiveness a treatment. From here, the physician can assess which treatments will be most effective. The technique can be used to determine responsiveness to any number of conditions, including hemodynamic responsiveness to administration or removal of one or more cardiovascular drugs, such as drugs intended to promote cardiac output, changes in cardiovascular preload, changes in cardiovascular afterload, etc. In yet other examples, the blood modulating events may be used to determine how a patient will respond to changes in mechanical or noninvasive ventilation.

[0030] Mechanical ventilation may be from adjusting positive pressure ventilation, negative pressure ventilation, maintaining inspiratory or expiratory pause, or a combination thereof.

[0031] In some examples, instructions for performing blood modulating events may be supplied to the patient automatically by a system **800**, for example, using a display **826**, and under instruction by instructions executed by a processor **808** and stored in a program memory **806**, described further hereinbelow.

[0032] The instructions can be provided to a patient that is remote from a medical facility connected to the testing apparatus through a network, such as at the patient's home. Whether at a medical facility or remotely, the technique may be performed on a patient undergoing a general examination or undergoing a specific treatment, such as treatment for cardiac arrest, edema, burns, trauma, heart failure, sepsis, dehydration, renal failure, or dialysis.

[0033] FIGS. **3-7** illustrate graphs of the impedance measured in an extremity before, during, and after the occurrence of the event causing blood to return to the heart via the venous system (e.g., spontaneous respiration, moving one or more limbs, etc.). Each of FIGS. **3-7** includes three graphs. As discussed below, the top graph in each of FIGS. **3-7** is a graph of the impedance measured at an extremity of the patient (e.g., arm, leg, etc.). The middle graph in each of FIGS. **3-7** is a graph of the impedance measured at the chest wall of the patient. The electrodes were placed in a pattern similar to patterns used in known in-hospital respiratory monitoring. However, unlike the impedance measured at the patient's extremity, the changes in impedance in the chest level does not represent blood volume changes in the chest but rather changes in the distance between the electrodes in response to chest expansion. It will be appreciated by one of ordinary skill in the art that in each of FIGS. **3-7**, a comparison of the top graph of impedance measured at an extremity to the middle graph of impedance measured at the chest wall shows the greater sensitivity conferred by the methods discussed herein. In particular, the top graph may illustrate a more pronounced response to respiratory challenges relative to regular, spontaneous breaths. The bottom graph in each of FIGS. **3-7** is a graph of the end-tidal CO_2 monitoring from the nose. End-tidal CO_2 is a direct measurement of respiration, however the measuring apparatus used to generate FIGS. **3-7** introduced a slight delay in registering the measurements, which caused the bottom graph to be slightly out of phase with the top and middle graphs due to the side-stream sampling nature of the CO_2 measurement. However, because the amplitude and frequency of the top graph of impedance track with the peaks and troughs of the bottom graph of end-tidal CO_2, it will be appreciated by one of ordinary skill in the art that measuring impedance at an extremity can serve as an indirect measurement of respiratory rate and the degree of respiratory effort. The performance of impedance in this aspect is improved over end-tidal CO_2 monitoring.

[0034] FIG. **3** includes an illustration of a graph **300** of the impedance measured in a patient's arm while the patient engages in normal, spontaneous breaths. FIG. **3** also includes a graph **310** of chest impedance and a graph **320** of end-tidal CO_2. It will be appreciated that each of the graphs **300**, **310**, and **320** track one another and exhibit a substantially-regular amplitude and frequency as the patient breathes. FIG. **4** is an illustration of a graph **400** of the impedance measured in a patient's arm while the patient engages in deep, spontaneous breaths starting at point **402**. FIG. **4** also includes a graph **410** of chest impedance and a graph **420** of end-tidal CO_2. It will be appreciated that amplitude of waveform of the graphs **400** and **410** increase after point **402** while the patient is taking deep breaths, however the rate of breathing has not substantially increased. Additionally, it will be appreciated that the frequency of the graphs **400**, **410**, and **420** have not increased. Additionally, FIG. **5** is an illustration of a graph **500** of the impedance measured in a patient's arm while the patient takes and holds a deep breath at point **502**, with a characteristic spike and gradual tapering of impedance. FIG. **5** also includes a graph **510** of chest impedance and a graph **520** of end-tidal CO_2. As discussed herein, the relatively larger change in impedance may indicate a greater flow of blood toward the heart caused by greater negative intrathoracic pressure caused by a deep breath. The differences between FIG. **3** and FIGS. **4** and **5** will be appreciated by one of ordinary skill in the art. In particular, it will be noted that the change in impedance in FIG. **4** and FIG. **5** while the patient was taking deep breaths or taking and holding a deep breath, respectively, are larger relative to the change in impedance in FIG. **3**.

[0035] FIG. **6** is an illustration of a graph **600** of the impedance measured in a patient's arm while the patient's legs are raised and lowered while the patient is taking spontaneous breaths. At point **602**, the patient's legs are raised, causing the impedance measured in the arm to decrease slightly as more blood is present in the patient's arm. Then, at point **604**, the patient's legs are lowered, causing impedance in the arm to spike as less blood is present in the patient's arm. FIG. **6** also includes a graph **610** of chest impedance and a graph **620** of end-tidal CO_2. FIG. **7** is an illustration of a graph **700** of the impedance measured in a patient's leg as the patient's legs are

raised and lowered while the patient is taking spontaneous breaths. At point **702**, the patient's legs are raised, causing the impedance measured in the leg to increase as less blood is present in the leg. Then, at point **704**, the patient's legs are lowered, causing the impedance measured in the leg to decrease as more blood is present in the patient's leg. FIG. **7** also includes a graph **710** of chest impedance and a graph **720** of end-tidal CO_2.

[0036] Referring again to FIG. **1**, after calculating the change in venous volume at the extremity, the cardiovascular health of the patient can be evaluated and appropriate treatments or interventions may be planned and applied (block **114**). A healthcare provider may use the process **100** to assess the condition of the patient to determine whether it may be beneficial to increase the volume of circulating blood in order to achieve optimum cardiovascular circulation or output. If the patient is volume deficient, the volume of circulating blood may be increased, for example, by a blood transfusion, administering intravenous (IV) fluids, or other known ways of administering fluids. If the patient is hypervolemic, the volume of circulating blood may be decreased, for example, by diuresis or other known ways of decreasing fluids. In the past, a healthcare provider might hypothesize that a patient is volume depleted based merely on the patient's injury or illness (e.g., severe burns) and administer IV fluids without having the capability of determining whether such fluids may be beneficial beforehand. However, using the disclosed embodiments, if a healthcare provider initially believes that a patient has a condition that would be respond favorably to the addition of IV fluids, but the change in volume (e.g., as determine by measuring the change in impedance as discussed herein) is small in response to various respiratory challenges (e.g., deep breaths, manipulation of limbs, etc.), then the healthcare provider may determine that the patient will not respond to being given additional IV fluids. Conversely, if the change in volume is large, then the healthcare provider may determine that the patient will respond favorably to fluids. Similarly, if the healthcare provider hypothesizes that the patient's condition may be improved by removing fluids, the healthcare provider may use the example process **100** to determine that the change in volume is small, indicating that removing fluids may be beneficial. Additionally, the process **100** may be used to titrate positive pressure or negative pressure ventilation and the administration of either pharmaceuticals or mechanical maneuvers that increase blood flow dependent or independent of making the heart pump more efficiently.

[0037] Further, it is possible to use the technology as a respiratory monitor to determine not only the respiratory rate but also the degree of respiratory effort. Accordingly, the process **100** may be used to estimate central venous pressure (CVP) levels noninvasively similar to how Ultrasound of the superior or inferior vena cava have been used, as well as to detect changes in the cardiorespiratory system which may signal the deterioration or improvement of a patient's condition. Because there are no valves in the proximal large veins in the neck and limbs, the geometric changes in these vessels in response to the respiratory challenges discussed above may parallel those of the superior and inferior vena cava. Accordingly, the volume measuring techniques discussed above may be useful for indirectly measuring the volume of blood in the superior and inferior vena cava.

[0038] FIG. **10** is an example block diagram **800** illustrating the various components used in implementing an example embodiment of the intravascular volume monitoring process **100** discussed herein. A testing apparatus **802** may be coupled to a patient **820** via sensors **816** in accordance with executing the functions of the disclosed embodiments. The testing apparatus **802** may have a controller **804** operatively connected to the database **814** via a link **822** connected to an input/output (I/O) circuit **812**. It should be noted that, while not shown, additional databases may be linked to the controller **804** in a known manner. The controller **804** includes a program memory **806**, the processor **808** (may be called a microcontroller or a microprocessor), a random-access memory (RAM) **810**, and the input/output (I/O) circuit **812**, all of which are interconnected via an address/data bus **820**. It should be appreciated that although only one microprocessor **808** is shown, the controller **804** may include multiple microprocessors **808**. Similarly, the memory of the controller **804** may include multiple RAMs **810** and multiple program memories **806**. Although the I/O circuit **812** is shown as a single block, it should be appreciated that the I/O circuit **812** may include a number of different types of I/O circuits. The RAM(s) **810** and the program memories **806** may be implemented as semiconductor memories, magnetically readable memories, and/or optically readable memories, for example. A link **824** may operatively connect the controller **804** to a sensor **816** through the I/O circuit **812**. The sensor **816** may be operatively connected to the patient **820**. The sensor **816** may include the impedance measuring device **202** and electrodes **206** and **208** discussed in connection to FIG. **2**.

[0039] The program memory **806** and/or the RAM **810** may store various applications (i.e., machine readable instructions) for execution by the microprocessor **808**. For example, an operating system **830** may generally control the operation of the testing apparatus **802** and provide a user interface to the testing apparatus **802** to implement the process **100** described herein. The program memory **806** and/or the RAM **810** may also store a variety of subroutines **832** for accessing specific functions of the testing apparatus **802**. By way of example, and without limitation, the subroutines **832** may include, among other things: a subroutine for taking measurements with the sensor **816** and other subroutines, for example, implementing software keyboard functionality, interfacing with other hardware in the testing apparatus **802**, etc. For example, the process **100** of FIG. **1** (and instructions elsewhere described herein) may be stored on the program memory **806** for execution by the processor **808**. The program memory **806** and/or the RAM **810** may further store data related to the configuration and/or operation of the testing apparatus **802**, and/or related to the operation of one or more subroutines **252**. For example, the data may be data gathered by the sensor **816**, data determined and/or calculated by the processor **808**, etc. In addition to the controller **804**, the testing apparatus **802** may include other hardware resources. The testing apparatus **802** may also include various types of input/output hardware such as a visual display **826** and input device(s) **828** (e.g., keypad, keyboard, etc.). In an embodiment, the display **826** is touch-sensitive, and may cooperate with a software keyboard routine as one of the software routines **832** to accept user input. It may be advantageous for the testing apparatus to communicate with a broader medical treatment network (not shown) through any of a number of known networking devices and techniques (e.g., through a commuter network such as a hospital or clinic intranet, the Internet, etc.). For example, the testing apparatus may be connected to a medical records database, hospital management processing system, health care professional terminals

(e.g., doctor stations, nurse stations), patient monitoring systems, automated drug delivery systems such as smart pumps, smart infusion systems, automated drug delivery systems, etc. Accordingly, the disclosed embodiments may be used as part of an automated closed loop system or as part of a decision assist system. By way of example, a network interface **834** is coupled to the I/O interface **812** for connecting the testing apparatus **802** to a network **836**, through a wired or wireless connection.

[0040] In this way, the system **800** may be used to determine the cardiovascular condition of the patient and whether that condition has improved or deteriorated over the period of time, e.g., by measuring changes in venous blood volume over time, and in response to procedures performed by the patient and in response to different treatments provided to the patient. Ventilatory effort of the patient can be determined, e.g., how much effort does it take for a patient to reach a desired volume of inspiration or expiration as measured by impedance and as that correlates to venous blood volume. The cardiovascular condition of a patient can be monitored over time to determine if the condition has improved or deteriorated, e.g., by determining a baseline impedance pattern for a patient and then comparing subsequent impedance measures to that baseline do determine variations from the baseline.

[0041] The system **800** may be used to further determine, from the impedance measurements and determined changes in venous blood volume, a central venous pressure or right atrial venous pressure. The system **800** may be further used to determine respiratory rate and respiratory effort, from the change in venous blood volume data. The change in venous blood volume, the respiratory rate, and respiratory effort may be monitored over time to determine if the patient's condition has improved or deteriorated, for example, in response to different treatment cycles and different treatment conditions. In some examples, the system **800** may detect patterns in the changes in volume of blood over a period of time and detect outlines in changes in volume of blood over that time, as indicators of various conditions. In any of these cases, the memory **806** may store the appropriate instructions that are executed by the processor **808** to automatically affect such monitoring and determinations.

[0042] Throughout this specification, plural instances may implement components, operations, or structures described as a single instance. Although individual operations of one or more methods are illustrated and described as separate operations, one or more of the individual operations may be performed concurrently, and nothing requires that the operations be performed in the order illustrated. Structures and functionality presented as separate components in example configurations may be implemented as a combined structure or component. Similarly, structures and functionality presented as a single component may be implemented as separate components. These and other variations, modifications, additions, and improvements fall within the scope of the subject matter herein.

[0043] Additionally, certain embodiments are described herein as including logic or a number of routines, subroutines, applications, or instructions. These may constitute either software (e.g., code embodied on a non-transitory, machine-readable medium) or hardware. In hardware, the routines, etc., are tangible units capable of performing certain operations and may be configured or arranged in a certain manner. In example embodiments, one or more computer systems (e.g., a standalone, client or server computer system) or one or more hardware modules of a computer system (e.g., a processor or a group of processors) may be configured by software (e.g., an application or application portion) as a hardware module that operates to perform certain operations as described herein.

[0044] In various embodiments, a hardware module may be implemented mechanically or electronically. For example, a hardware module may comprise dedicated circuitry or logic that is permanently configured (e.g., as a special-purpose processor, such as a field programmable gate array (FPGA) or an application-specific integrated circuit (ASIC)) to perform certain operations. A hardware module may also comprise programmable logic or circuitry (e.g., as encompassed within a general-purpose processor or other programmable processor) that is temporarily configured by software to perform certain operations. It will be appreciated that the decision to implement a hardware module mechanically, in dedicated and permanently configured circuitry, or in temporarily configured circuitry (e.g., configured by software) may be driven by cost and time considerations.

[0045] Accordingly, the term "hardware module" should be understood to encompass a tangible entity, be that an entity that is physically constructed, permanently configured (e.g., hardwired), or temporarily configured (e.g., programmed) to operate in a certain manner or to perform certain operations described herein. Considering embodiments in which hardware modules are temporarily configured (e.g., programmed), each of the hardware modules need not be configured or instantiated at any one instance in time. For example, where the hardware modules comprise a general-purpose processor configured using software, the general-purpose processor may be configured as respective different hardware modules at different times. Software may accordingly configure a processor, for example, to constitute a particular hardware module at one instance of time and to constitute a different hardware module at a different instance of time.

[0046] Hardware modules can provide information to, and receive information from, other hardware modules. Accordingly, the described hardware modules may be regarded as being communicatively coupled. Where multiple of such hardware modules exist contemporaneously, communications may be achieved through signal transmission (e.g., over appropriate circuits and buses) that connect the hardware modules. In embodiments in which multiple hardware modules are configured or instantiated at different times, communications between such hardware modules may be achieved, for example, through the storage and retrieval of information in memory structures to which the multiple hardware modules have access. For example, one hardware module may perform an operation and store the output of that operation in a memory device to which it is communicatively coupled. A further hardware module may then, at a later time, access the memory device to retrieve and process the stored output. Hardware modules may also initiate communications with input or output devices, and can operate on a resource (e.g., a collection of information).

[0047] The various operations of example methods described herein may be performed, at least partially, by one or more processors that are temporarily configured (e.g., by software) or permanently configured to perform the relevant operations. Whether temporarily or permanently configured, such processors may constitute processor-implemented modules that operate to perform one or more operations or func-

tions. The modules referred to herein may, in some example embodiments, comprise processor-implemented modules.

[0048] Similarly, the methods or routines described herein may be at least partially processor-implemented. For example, at least some of the operations of a method may be performed by one or more processors or processor-implemented hardware modules. The performance of certain of the operations may be distributed among the one or more processors, not only residing within a single machine, but deployed across a number of machines. In some example embodiments, the processor or processors may be located in a single location (e.g., within a home environment, an office environment or as a server farm), while in other embodiments the processors may be distributed across a number of locations.

[0049] The performance of certain of the operations may be distributed among the one or more processors, not only residing within a single machine, but deployed across a number of machines. In some example embodiments, the one or more processors or processor-implemented modules may be located in a single geographic location (e.g., within a home environment, an office environment, or a server farm). In other example embodiments, the one or more processors or processor-implemented modules may be distributed across a number of geographic locations.

[0050] Unless specifically stated otherwise, discussions herein using words such as "processing," "computing," "calculating," "determining," "presenting," "displaying," or the like may refer to actions or processes of a machine (e.g., a computer) that manipulates or transforms data represented as physical (e.g., electronic, magnetic, or optical) quantities within one or more memories (e.g., volatile memory, non-volatile memory, or a combination thereof), registers, or other machine components that receive, store, transmit, or display information.

[0051] As used herein any reference to "one embodiment" or "an embodiment" means that a particular element, feature, structure, or characteristic described in connection with the embodiment is included in at least one embodiment. The appearances of the phrase "in one embodiment" in various places in the specification are not necessarily all referring to the same embodiment.

[0052] Some embodiments may be described using the expression "coupled" and "connected" along with their derivatives. For example, some embodiments may be described using the term "coupled" to indicate that two or more elements are in direct physical or electrical contact. The term "coupled," however, may also mean that two or more elements are not in direct contact with each other, but yet still co-operate or interact with each other. The embodiments are not limited in this context.

[0053] As used herein, the terms "comprises," "comprising," "includes," "including," "has," "having" or any other variation thereof, are intended to cover a non-exclusive inclusion. For example, a process, method, article, or apparatus that comprises a list of elements is not necessarily limited to only those elements but may include other elements not expressly listed or inherent to such process, method, article, or apparatus. Further, unless expressly stated to the contrary, "or" refers to an inclusive or and not to an exclusive or. For example, a condition A or B is satisfied by any one of the following: A is true (or present) and B is false (or not present), A is false (or not present) and B is true (or present), and both A and B are true (or present).

[0054] In addition, use of the "a" or "an" are employed to describe elements and components of the embodiments herein. This is done merely for convenience and to give a general sense of the description. This description, and the claims that follow, should be read to include one or at least one and the singular also includes the plural unless it is obvious that it is meant otherwise.

[0055] This detailed description is to be construed as examples and does not describe every possible embodiment, as describing every possible embodiment would be impractical, if not impossible. One could implement numerous alternate embodiments, using either current technology or technology developed after the filing date of this application.

What is claimed:

1. A method for evaluating cardiovascular condition of a patient, the method comprising:

(a) recording a first impedance of a limb or extremity or neck of the patient at a first time in response to receiving a first impedance reading from a plurality of sensors on a limb or extremity or neck;

(b) after the occurrence of an event modulating blood return to the heart via the venous system of the patient, recording a second impedance of the limb or extremity or neck at a second time in response to receiving a second impedance reading from a plurality of sensors on a limb or extremity or neck, wherein the first impedance and the second impedance each correspond to a volume of blood flowing within the limb or extremity or neck; and

(c) determining a change in venous blood volume between the first time and the second time by comparing the first impedance and the second impedance to determine a change in volume of blood.

2. The method of claim **1**, wherein (a)-(c) are performed repeatedly over a period of time, the method further comprising:

(d) determining whether the cardiovascular condition of the patient has improved or deteriorated over the period of time.

3. The method of claim **2**, wherein determining whether the cardiovascular condition of the patient has improved or deteriorated over the period of time includes monitoring the ventilatory effort of the patient and ventilatory dynamics of the patient.

4. The method of claim **2**, wherein determining whether the cardiovascular condition of the patient has improved or deteriorated over the period of time includes:

(1) using a first portion of the recorded impedances to determine a baseline impedance pattern for the patient, and

(2) comparing a second portion of the recorded impedances to the baseline impedance pattern to detect deviations from the baseline impedance pattern.

5. The method of claim **1**, wherein placing electrodes on one of a limb or extremity or neck to monitor the impedance of the limb or extremity or neck includes placing two electrodes to inject electrical current and two electrodes to measure impedance.

6. The method of claim **1**, wherein the event modulating blood return to the heart includes one or more of spontaneous inspiration, positive pressure mechanical ventilation, raising a limb or extremity or neck of the patient, applying negative or

positive pressure to the abdomen or chest, inspiration against a negative impedance valve, or discrete maneuvers performed with mechanical ventilation.

7. The method of claim **6**, wherein the discrete maneuvers performed with mechanical ventilation comprise adjusting positive pressure ventilation, negative pressure ventilation, maintaining inspiratory or expiratory pause, or a combination thereof.

8. The method of claim **1**, wherein (a) and (b) are performed outside a medical facility.

9. The method of claim **1**, wherein the patient is undergoing treatment for one or more of cardiac arrest, edema, burns, trauma, heart failure, sepsis, dehydration, renal failure, or dialysis.

10. The method of claim **1**, further comprising:

(d) determining one or more of:

(1) how the patient will hemodynamically respond to one or more of an addition of cardiovascular fluid or removal of cardiovascular fluid,

(2) how the patient will hemodynamically respond to one or more cardiovascular drugs which promote changes in cardiac output, changes in cardiovascular preload, and changes in cardiovascular afterload, or

(3) determining how the patient will respond hemodynamically to changes in mechanical or noninvasive ventilation.

11. The method of claim **1**, further comprising: determining changes in vena cava diameter, central venous pressure, or right atrial venous pressure from the change in venous blood volume.

12. The method of claim **1**, further comprising: determining respiratory rate and effort from the change in venous blood volume.

13. A testing apparatus for evaluating cardiovascular condition of a patient, the testing apparatus comprising:

one or more electrodes;

one or more processors;

a computer-readable memory storing non-transient instructions that when executed by the one or more processors cause the testing apparatus to:

(a) use the one or more electrodes to record a first impedance of a limb or extremity or neck of the patient at a first time in response to receiving a first impedance reading from a plurality of sensors on a limb or extremity or neck;

(b) after the occurrence of an event modulating blood return to the heart via the venous system of the patient, use the one or more electrodes to record a second impedance of the limb or extremity or neck at a second time in response to receiving a second impedance reading from a plurality of sensors on a limb or extremity or neck, wherein the first impedance and the second impedance each correspond to a volume of blood flowing within the limb or extremity or neck; and

(c) determine a change in venous blood volume between the first time and the second time by comparing the first impedance and the second impedance to determine a change in volume of blood.

14. The testing apparatus of claim **13**, wherein the non-transient instructions include instructions that when executed by the one or more processors cause the testing apparatus to determine whether the cardiovascular condition of the patient has improved or deteriorated over the period of time.

15. The testing apparatus of method of claim **14**, wherein the instructions to determine whether the cardiovascular condition of the patient has improved or deteriorated over the period of time includes instructions to monitor a respiratory rate of the patient and a respiratory effort of the patient.

16. The method of claim **15**, wherein the instructions to determine whether the cardiovascular condition of the patient has improved or deteriorated over the period of time includes instructions to:

(1) use a first portion of the recorded impedances to determine a baseline impedance pattern for the patient, and

(2) compare a second portion of the recorded impedances to the baseline impedance pattern to detect deviations from the baseline impedance pattern.

17. The testing apparatus of claim **13**, wherein the one or more electrodes include two electrodes to inject electrical current and two electrodes to measure impedance.

18. The testing apparatus of claim **13**, wherein the event modulating blood to return to the heart includes one or more of spontaneous inspiration; positive pressure mechanical ventilation, negative pressure ventilation, or raising a limb or extremity or neck of the patient.

19. The testing apparatus of claim **13**, further comprising a photoplethysmograph, a galvanic skin response monitor, a near infrared spectroscopy device, a laser Doppler device with or without speckle tracking, or an ultrasound device with or without speckle tracking.

20. The testing apparatus of claim **13**, further comprising impedance cardiography measurement, pulse pressure variation measurement, or stroke volume variation measurement.

21. A closed-loop cardiovascular condition evaluation system comprising:

the testing apparatus of claim **13**; and

a processor and a memory, the memory storing instructions that when executed by the processor, cause the processor to evaluate a cardiovascular condition of a subject in response to determining the change in the venous blood volume between the first time and the second time determined by comparing the first impedance and the second impedance, for different treatment cycles.

22. The closed-loop system of claim **21**, wherein the different treatment cycles comprising, determining the change in venous blood volume under a first treatment condition and under a second treatment condition.

23. The closed-loop system of claim **22**, wherein the first treatment condition is a pre-cardiovascular treatment condition and the second treatment condition is after a cardiovascular treatment has been applied.

24. The closed-loop system of claim **21**, wherein the memory stores instructions that when executed by the processor, cause the processor to adjust a cardiovascular treatment in response to the determination in the change of venous blood volume.

25. A method for evaluating the cardiovascular condition of a patient, the method comprising:

(a) determining a first volume of blood of a limb or extremity or neck of the patient at a first time;

(b) after the occurrence of an event causing blood to return to the heart via the venous system of the patient, determining a second volume of blood of the limb or extremity or neck at a second time;

(c) determining a change in venous blood volume between the first time and the second time by comparing the first volume of blood and the second volume of blood; and

(d) determining one or more of,

(1) how the patient will hemodynamically respond to one or more of an addition of cardiovascular fluid or removal of cardiovascular fluid,

(2) how the patient will hemodynamically respond to one or more cardiovascular drugs which promote changes in cardiac output, changes in cardiovascular preload, and changes in cardiovascular afterload,

(3) determining how the patient will response to changes in mechanical or noninvasive ventilation, or

(4) determining respiratory rate and magnitude of respiratory effort.

26. The method of claim **25**, wherein the first and second volume of blood in a limb is determined by measuring the diameter of a major vein in the limb or extremity or neck using ultrasonic imagery with our without speckle tracking, or laser Doppler Flowmetry with or without speckle tracking, or near infrared spectroscopy, or photoplethysmography, or galvanic skin response.

27. The method of claim **26**, wherein (a)-(c) are performed repeatedly over a period of time, the method further comprising:

(e) determining whether the cardiovascular condition of the patient has improved or deteriorated over the period of time.

28. The method of claim **27**, wherein determining whether the cardiovascular condition of the patient has improved or deteriorated over the period of time includes using a learning algorithm to

(1) detect a pattern in the changes of volume of blood over the period of time, and

(2) detect outliers in the changes of volume of blood over the period of time.

* * * * *